Regulation of clathrin-coated vesicle nucleation

by

James R. Thieman

B.S., Bucknell University, 2005

Submitted to the Graduate Faculty of

the School of Medicine in partial fulfillment

of the requirements for the degree of

Doctor of Philosophy

University of Pittsburgh

2011

UNIVERSITY OF PITTSBURGH

SCHOOL OF MEDICINE

This thesis was presented

by

James R. Thieman

It was defended on

June 9th, 2011

and approved by

Dr. Meir Aridor
Committee Chair
Department of Cell Biology and Physiology

Dr. Gerard L. Apodaca
Department of Medicine, Renal-Electrolyte Division

Dr. Simon C. Watkins
Department of Cell Biology and Physiology

Dr. Alessandro Bisello
Department of Pharmacology and Chemical Biology

Dr. Linton M. Traub
Dissertation Advisor
Department of Cell Biology and Physiology

Regulation of clathrin-coated vesicle nucleation

James R. Thieman, PhD

University of Pittsburgh, 2011

Clathrin-mediated endocytosis is a selective pathway for the entry of transmembrane proteins into the cell through the generation of a short-lived vesicular intermediate. Cells and tissues depend on this process for obtaining nutrients, modulation of signaling and cell migration. The clathrin-coated structure intermediate is assembled on the plasma membrane from a cohort of 20-30 distinct proteins that aid in cargo selection, scaffolding, membrane bending and scission of the vesicle. Exactly how these complex assemblies are nucleated at the plasma membrane remains unclear although the lipid phosphatidylinositol-4,5-bisphosphate (PtdIns(4,5)P_2) plays an important role by anchoring many of the endocytic components. The work in this thesis helps to clarify the nucleation phase by describing the molecular details of the interaction between a PtdIns(4,5)P_2-generating lipid kinase PIPKIγ and the heterotetrameric clathrin adaptor AP-2. By engaging a subdomain on the AP-2 β2 subunit appendage, the kinase is strategically positioned at assembly sites to generate PtdIns(4,5)P_2 and drive coat assembly forward. Clathrin binds to the same subdomain on the β2 appendage but with a higher apparent affinity. I therefore invoke a model in which PtdIns(4,5)P_2 production for nucleation is negatively regulated by PIPKIγ displacement from AP-2 by clathrin at later stages of assembly. I also demonstrate that a cargo-sorting alternate adaptor that binds to the other subsite on the AP-2 β2 appendage is not subject to displacement by clathrin during clathrin-coated vesicle budding, ensuring non-competitive cargo incorporation into the vesicle. Finally, the PtdIns(4,5)P_2-binding EFC domain proteins

FCHO1 and FCHO2 have been proposed to act as dedicated nucleators of clathrin-coated structures on the plasma membrane. I demonstrate in multiple cell lines that these proteins are not invariantly required for placement of clathrin-coated assemblies on the plasma membrane despite being early arriving components themselves. FCHO1/2 are involved in the regulation of the size and number of these assemblies in some cellular contexts. My data support the model of PtdIns(4,5)P_2 regulated, not protein regulated, nucleation of clathrin-coated structures; however multiple parallel pathways may contribute to initiation of endocytic buds.

TABLE OF CONTENTS

LIST OF TABLES

LIST OF FIGURES

PREFACE

With sincerest gratitude, I would like to thank my thesis advisor Dr. Linton Traub for his personal investment in my training. Linton has profoundly affected the way I think, write and speak, has sparked my curiosity and has taught me the value of questioning my assumptions. He is a gifted and modest scientist and I am fortunate to have his friendship. I would like to thank the members of my committee for their support during my studies, especially Dr. Simon Watkins. Simon has helped me discover my passion for biological imaging, has provided invaluable career advice and opportunities and has acted as a second mentor. Dr. Gerry Apodaca has been instrumental in solidifying my interest in science by inviting me into his lab for two summers as an undergraduate student. Dr. Meir Aridor has challenged me to think more deeply about my project. Dr. Sandro Bisello has provided me with exceptional training during my rotation in his lab and has provided insightful advice through the years.

I am thankful for the friendship and assistance of all Traub laboratory members, past and present: Dr. Sanjay Mishra for teaching me much of what I know of biochemistry, Amie Steinhauser, Peter Keyel and Matthew Hawryluk for their friendship, Drs. S. Sanker, P.K. Umasankar and Souvik Chakraborty for making the lab an enjoyable and dynamic place in recent years, and

Anupma Jha for sharing in the trials and tribulations of graduate school. Thank you also to Andrew and Annie Steiner, for making my time during my graduate work unforgettable.

I would especially like to thank my family. I have been blessed to have wonderful parents, Jim and Gail Thieman, who have put my education, personal growth and faith before their own needs. They have taught me the importance of hard work and integrity and I love them dearly. Thank you to my sister Annie and her family for their love and support and reminding me about the important things in life. Last and certainly not least, thank you to my wife and best friend Jackie. She has pulled me through the toughest of times in graduate school and given me the confidence to face my challenges. Thank you for understanding me and all the happiness you have brought me.

ABBREVIATIONS

AAK1	Adaptor-associated kinase 1
Alk2	Activin receptor-like kinase 2
ANTH	AP180 N-terminal homology
APs	Associated proteins/Assembly polypeptides
AP-2	Adaptor protein 2
Arf	ADP-ribosylation factor
ARH	Autosomal recessive hypercholesterolemia
BAR	Bin/Amphiphysin/Rvs167
BSA	Bovine serum albumin
CALM	Clathrin assembly lymphoid myeloid leukemia protein
CCS	Clathrin-coated structure
CCP	Clathrin-coated pit
CCV	Clathrin-coated vesicle
CIE	Clathrin-independent endocytosis
CLASP	Clathrin-associated sorting protein
CLIC	Clathrin and dynamin-independent carrier
CME	Clathrin-mediated endocytosis
Dab2	Disabled 2

DAG	Diacylglycerol
DGK	Diacylglycerol kinase
EFC	Extended FER/CIP4 homology
EGF/EGFR	Epidermal growth factor/epidermal growth factor receptor
EH	eps15 homology
ENTH	Epsin N-terminal homology
eps15	Epidermal growth factor receptor substrate 15
ER	Endoplasmic reticulum
FCHO	Fes/CIP4 homology only
GAK	Cyclin G associated kinase
GEF	Guanine nucleotide exchange factor
GFP	Green fluorescent protein
GGA	Golgi-localized gamma adaptin ear homology
GST	Glutathione-S-transferase
GTP	Guanosine triphosphate
HIP1/Hip1R	Huntington interacting protein 1/Related
His_6	Hexahistidine
Hrb	HIV-1 Rev binding protein
LDL/LDLR	Low density lipoprotein/low density lipoprotein receptor
μHD	Mu homology domain
Muniscin	Mu homology domain and meniscus shaped
NPF	Nucleation promoting factor
PH	Pleckstrin homology

PIP	Phosphatidylinositol phosphate
PIPKI	Type I Phosphatidylinositol-4-phosphate 5-Kinase
PLD	Phospholipase D
PtdIns(4)P	Phosphatidylinositol-4-phosphate
PtdIns(4,5)P_2	Phosphatidylinositol-4,5-bisphosphate
PtdIns(5)P	Phosphatidylinositol-5-phosphate
PtdOH	Phosphatidic acid
PTB	Phosphotyrosine binding
RT-PCR	Reverse-Transcriptase Polymerase Chain Reaction
SHIP2	SH2 domain-containing inositol phosphatase 2
siRNA	Small interfering ribonucleic acid
SNARE	Soluble NSF attachment protein receptor
SV	Synaptic vesicle
Syt	Synaptotagmin
tdRFP	Tandem dimer tomato red fluorescent protein
Tf/TfR	Transferrin/transferrin receptor
TIR-FM	Total internal reflection fluorescence microscopy
TGN	*trans*-Golgi network
UIM	Ubiquitin-interacting motif
VSV-G	Vesicular stomatitis virus G-protein
WASP/N-WASP	Wiskott-Aldrich syndrome protein/Neural-WASP
YFP	Yellow fluorescent protein

1.0 INTRODUCTION

1.1 INTRACELLULAR TRANSPORT

1.1.1 Vesicular transport

Central to the classification and diversification of life on earth are the inherent differences between eukaryotic and prokaryotic cells. Eukaryotic cells have evolved a cohort of membrane-bound organelles that facilitate numerous biochemical reactions and serve to separate these reactions in space and time, while prokaryotes have not (Alberts *et al.*, 2002). These organelles contain three-dimensional aqueous reaction vessel lumens of varying molarities and pH and an encompassing two-dimensional lipid membrane scaffold. This type of static representation of eukaryotic cell structure fails to convey the immense effort cells make in order to maintain homeostasis. Continual energy expenditure must be made to target proteins and lipids to the correct sub-cellular location and to prevent passive transport of inappropriate molecules, as well as to retrieve membrane that prevents organelle contraction and expansion. Not surprisingly, complex and conserved mechanisms have evolved to control intracellular traffic.

The existence of sub-cellular organelles has been known since the 19th century, however our understanding of communication between these organelles only began to take shape in the 1960s through the work of George Palade. Working with pancreatic exocrine cells, Palade

showed that newly synthesized proteins destined for secretion are first translocated into the endoplasmic reticulum (ER) and then sequentially transit through the Golgi complex, secretory granules and finally the extracellular space (Palade, 1975). Non-secreted proteins that reside at the plasma membrane, endosomes and lysosome also pass through some of these common compartments. Palade noted that the compartments maintain their identity over time and postulated that secretory proteins shuttle between them in transport vesicles. In time, Palade's work gave rise to the generalized vesicle transport hypothesis (Bonifacino and Glick, 2004): A donor membrane generates a small (~50-100 nm) vesicle into which proteins (soluble and membrane-bound) are packaged, the vesicle travels to a target membrane and fusion of the two lipid bilayers releases the contents into the target.

Further substantiating the vesicle transport model and initiating the molecular characterization of this process was work by the Schekman and Rothman laboratories. A screen for *Saccharomyces cerevisiae* secretion or *sec* mutants by Schekman's group revealed 23 complementation groups that displayed morphologic phenotypes associated with altered vesicular transport: 1. accumulation of small vesicles, 2. an enlarged ER network and 3. an abnormal Golgi complex (Novick *et al.*, 1980). Over the following two decades the *sec* proteins were identified and characterized as components of the vesicle generation and fusion machinery (Schekman and Novick, 2004). In a different *in vitro* approach by Rothman's laboratory, donor membrane Golgi fractions lacking an enzyme necessary for the synthesis of complex oligosaccharides generation on the viral glycoprotein (G protein) from Vesicular Stomatitis Virus (VSV-G) infected cells were mixed with a wild-type acceptor membrane Golgi fraction. The further processing of viral glycoprotein N-linked sugars was monitored to follow transport between Golgi cisternae (Balch *et al.*, 1984a; Balch *et al.*, 1984b; Braell *et al.*, 1984). VSV-G,

starting in the donor Golgi became fully processed despite the seemingly maintained integrity of the Golgi fractions. These experiments strongly suggested that cellular proteins are shuttled by vesicles to their destination.

1.1.2 Coated vesicles

Working in the same years as Palade, Thomas Roth and Keith Porter discovered a common theme in vesicular transport: generation of trafficking vesicles occurs through a coated vesicle intermediate. As will become apparent in later sections, protein coats fulfill three main functions during vesicle formation: 1. assistance in deforming the membrane, 2. uniformity in size of generated vesicles and 3. selection of integral membrane proteins destined for transport, hereafter referred to as ‘cargo’.

1.1.2.1 Clathrin-coated vesicles

Roth and Porter were interested in how circulating proteins within female mosquito hemolymph were deposited as yolk inside developing oocytes (Roth and Porter, 1964). They noticed that shortly following a blood meal, a proliferation of “bristle-coated pits and vesicles” on the cytoplasmic surface of the mosquito oocyte plasma membrane occurs. These pits and vesicles contained three distinguishable layers by electron microscopy: an inner, extracellular/luminal layer corresponding to massed yolk protein, a middle layer of ~75-Å corresponding to the bilayer membrane, and an outer layer ~200-Å thick that resembled a coat of fibrous bristles in the thin sections. Most remarkably, they correctly predicted from static images that these coated pits likely operated as a shuttle by concentrating yolk, budding from the surface, uncoating and fusing to form the large mature yolk bodies seen in mosquito oocytes. Coated vesicles are not

restricted to the endocytic pathway and were subsequently observed on the Golgi complex (Friend and Farquhar, 1967) where they are involved in anterograde biosynthetic traffic.

The ensuing decade was dedicated to isolating coated vesicles and biochemically characterizing them. Fractionation of guinea pig brain and electron microscopic observation revealed that coated vesicles were ~50 nm diameter vesicles surrounded by a ~100 nm diameter cage of pentagonal and hexagonal facets (Kanaseki and Kadota, 1969). By purifying these vesicles biochemically, Barbara Pearse identified the main proteinaceous component of coated vesicles as a ~180 kDa protein that she named clathrin (Pearse, 1975, 1976). Trimerization of clathrin heavy chain molecules into a three-legged triskelion that also contains three 25-29 kDa associated clathrin light chain polypeptides was found to be the basic structural unit of these coated vesicle cages (Ungewickell and Branton, 1981). Less abundant, and initially overlooked, associated proteins (APs) of ~110, 50 and 16 kDa isolated with coated vesicles were subsequently shown to promote clathrin triskelion polymerization *in vitro* (Keen *et al.*, 1979) and were re-dubbed ‘assembly polypeptides’ for APs (Keen, 1987). Clathrin-coated vesicles (CCVs) are now known to coordinate trafficking of cargo both from the plasma membrane during endocytosis and in biosynthetic traffic out of the *trans*-Golgi network (TGN) and on endosomes in endocytic trafficking. The molecular details of coat-directed vesicle assembly will be discussed below.

1.1.2.2 COPI coated vesicles

The generality of the use of protein coats for vesicle formation was extended when ultrastructural examination of the Golgi revealed coated buds that were not immunoreactive for clathrin (Griffiths *et al.*, 1985; Orci *et al.*, 1985). Closer analysis demonstrated these coats were morphologically different from clathrin and appeared as ‘obtuse spikes’ (Orci *et al.*, 1986).

Biochemical purification of protein components of this coat gave rise to the name Golgi coat promoter or Coatomer (Waters *et al.*, 1991) and later COPI coats. COPI coats are now known to be important in the early secretory pathway where they mediate retrograde transport between Golgi cisternae, from the Golgi to the ER and also, possibly, in anterograde transport from the ER-Golgi Intermediate Complex to the Golgi (Beck *et al.*, 2009). It was likely the transport of oligosaccharide-processing enzymes between Golgi fractions in COPI vesicles that allowed VSV-G to mature in the Rothman experiments (Balch *et al.*, 1984a; Balch *et al.*, 1984b). The COPI coat recognizes specific amino-acid tracts or sorting signals within cargo, in this case typically ER resident proteins, for inclusion into budding vesicles. This process is termed cargo selection and is another common theme of vesicular transport as discussed below.

1.1.2.3 COPII coated vesicles

In contrast to the purely morphological initial discovery of clathrin and COPI coats, a third, ER-derived coated vesicle was discovered as a result of its *in vitro* reconstitution (Barlowe *et al.*, 1994). COPII coated vesicles are formed at distinct ER exit sites from the progressive assembly of the Sar1 Guanosine triphosphate (GTP)ase, the Sec23/24 inner coat, and Sec13/31 outer coat (Miller and Barlowe, 2010) that culminates in the release of small (~60 nm) vesicles (Barlowe *et al.*, 1994). Many of the *sec* mutants possess mutations in genes for the COPII coat or its regulatory factors (Schekman and Novick, 2004). Assembling COPII buds segregate cargo for export from resident ER proteins through the recognition of diacidic and dihydrophobic sorting signals in the cytosolic portion of transmembrane cargo or soluble cargo receptors (Aridor *et al.*, 1998; Barlowe, 2003).

1.2 THE ENDOCYTIC PATHWAY

Cells, both in multicellular organisms and free-living unicellular organisms, do not operate in complete isolation but must interact with their environment. The plasma membrane represents a barrier between the potentially harsh surroundings and the cell's controlled cytosol. The cell must continually respond to its environment and can accomplish this in part by actively adjusting the protein and lipid composition of the plasma membrane. This is often handled by endocytosis, the invagination and vesiculation/tubulation of a region of plasma membrane entrapping a volume of extracellular fluid and integral membrane proteins in the immediate region. Delivery of the vesicle/tubule to internal membranes then allows degradation or recycling of the internalized contents. Because of the complexity of cell-cell, cell-tissue and cell-organism communication, mammalian cells have evolved a multitude of endocytic pathways each with different functions to effectively interact with and respond to their environment.

1.2.1 Clathrin-independent endocytosis

Endocytic pathways are first characterized by their dependence on or independence of a clathrin coat. Within the clathrin-independent endocytosis (CIE) branch, internalization is further classified by size (Mayor and Pagano, 2007). Macropinocytosis is the internalization of large volumes of extracellular fluid through membrane extensions that fuse with each other or back onto the plasma membrane producing vesicles on the order of >1 μm (Kerr and Teasdale, 2009). Macropinocytosis is tied to the formation of circular dorsal ruffles, can be stimulated by various growth factors, and requires the actin cytoskeleton and the Rho family GTPase Rac1 (Doherty and McMahon, 2009). One natural function of macropinocytosis is fluid-phase sampling of the

environment for antigen presentation by immune cells, though a variety of pathogens can induce macropinosome formation for their host entry (Kerr and Teasdale, 2009).

Phagocytosis is an endocytic pathway for the internalization of large (>1 μm) solid particles into cells. Professional phagocytic cells, including macrophages, monocytes and neutrophils in mammals, engulf opsonized pathogens or apoptotic cell bodies through actin-enriched membrane protrusions (Doherty and McMahon, 2009). There appears to be at least two distinct phagocytic pathways: internalization of IgG opsonized particles ligated to its receptor FcγR in a mainly Rac1 and Cdc42 GTPase dependent pathway and uptake of C3bi-coated particles by the complement receptor CR3 in a mainly RhoA GTPase dependent manner (Groves *et al.*, 2008).

There also exist multiple clathrin-independent pathways for generating trafficking vesicles on a smaller order (< 1μm) and pinocytic (fluid-phase) in nature (Mayor and Pagano, 2007). The best characterized of these is caveolar endocytosis. Caveolae are 50-80 nm flask-shaped plasma membrane invaginations that are enriched in cholesterol and sphingolipids (Hansen and Nichols, 2010). One of the primary functions of caveolae is in transcytosis of serum factors in endothelial cells (Oh *et al.*, 2007) such as albumin (Schubert *et al.*, 2001). Caveolae are also subverted for simian virus 40 entry (Anderson *et al.*, 1996). Caveolae have a striated coat by electron microscopy formed by the proteins caveolins and cavins, but how these structures contribute to function or endocytosis is not clear (Hansen and Nichols, 2010). New data suggest caveolae are membrane reservoirs to regulate surface tension (Sinha *et al.*, 2011).

Finally, there are a number of other clathrin and caveolin-independent endocytic pathways that appear to operate in the absence of a morphologically discernable coat and require Rho/ADP ribosylation factor (Arf) family GTPases. For example, tubular and ring-like plasma

membrane invaginations called Clathrin- and Dynamin-independent Carriers (CLICs) endocytose glycosylphosphatidylinositol-anchored proteins and Cholera toxin B in a process dependent on Cdc42 GTPase (Kirkham *et al.*, 2005; Mayor and Pagano, 2007). The variability in mechanisms to generate non-clathrin endocytic vesicles/phagosomes/macropinosomes may reflect the unique challenges or range of cargo encountered at the interface between various cell types and their environment. Many questions pertaining to the mechanics and cargo selection of CIE pathways remain.

1.2.2 Clathrin-mediated endocytosis

By far the best-characterized endocytic pathway at the morphological, biochemical, structural and mechanistic levels is that generating CCVs. Clathrin-mediated endocytosis (CME) plays critical roles in nutrient absorption such as for the transferrin (Tf) receptor (TfR) and low density lipoprotein receptor (LDLR) (Orci *et al.*, 1978; Booth and Wilson, 1981), modulation of signal transduction through downregulation of surface receptors (Le Roy and Wrana, 2005), cell migration (Nishimura and Kaibuchi, 2007) and neurotransmission (Smith *et al.*, 2008). In the standard textbook model, clathrin-coated pits (CCPs), or more appropriately clathrin-coated structures (CCSs), are generated anew from the progressive accumulation of adaptors and clathrin from a soluble pool on a region of the plasma membrane (Alberts *et al.*, 2002). A layered assembly is created with the cargo-laden plasma membrane on the inside, a middle adaptor layer bound to cargo and an outer clathrin coat layer attached to the adaptor layer. Increasing curvature of the nascent bud is accompanied by concentration of cargo molecules (Figure 1.1). Finally the GTPase dynamin oligomerizes at the neck and promotes scission of the vesicle followed shortly by uncoating and recycling of the endocytic components.

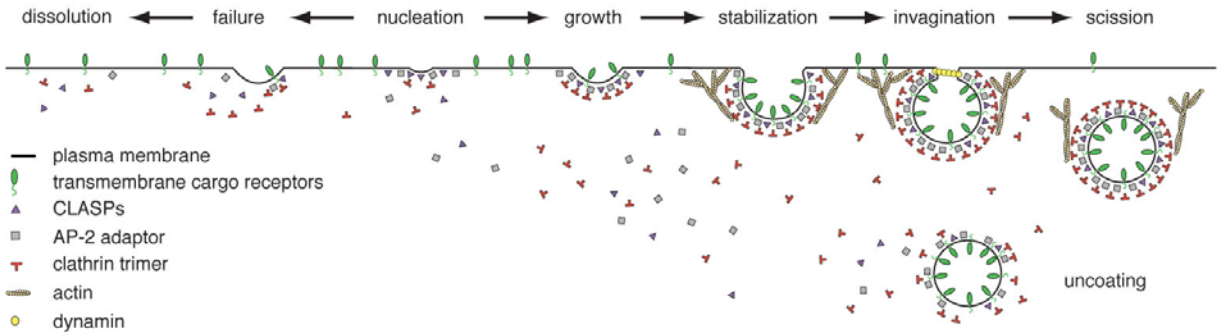

Figure 1.1: Clathrin-coated pit and vesicle formation.
Clathrin-coated pits form through successive steps. On a patch of the plasma membrane, AP-2 adaptors and clathrin-associated sorting proteins (CLASPs) are recruited during the nucleation phase. If the assembly fails to stabilize the components are released and dissolution occurs. If the components are stabilized through binding transmembrane cargo receptors, the assembly continues through a growth phase during which more cargo is concentrated and clathrin trimers are polymerized into a coat. When the assembly is deeply invaginated, Dynamin GTPase assembles at the neck to promote scission with the help of actin-mediated tension. After budding the coat is disassembled and coat components are recycled for further rounds of endocytosis. Image modified from (Traub, 2009).

1.3 COMPONENTS AND ASSEMBLY OF CLATHRIN-COATED STRUCTURES

1.3.1 Clathrin

As described above, clathrin is a trimer of three heavy chains with three associated light chains forming a triskelion. The triskelion contains three-fold rotational symmetry about the heavy chain C-terminal trimerization domain (Ungewickell and Branton, 1981). Each heavy chain leg is kinked and contains a straight, helical proximal segment, a flexible knee, a straight, helical distal segment, a straight, helical ankle segment and an N-terminal, β-propeller fold terminal domain (Figure 1.2A) (Edeling *et al.*, 2006b).

In an assembled clathrin lattice, a single triskelion vertex is present at each corner between adjacent hexagon–hexagon or hexagon–pentagon facets. Triskelion self-assembly is accomplished through anti-parallel binding of proximal and distal leg segments (Fotin *et al.*, 2004). In this configuration many terminal domains are clustered beneath the polygonal lattice specifically below vertices (see Figure 1.6) (Edeling *et al.*, 2006b). This architecture is important as clathrin has no inherent affinity for the plasma membrane and binds via interactions with the adaptor layer through its terminal domains (Unanue *et al.*, 1981).

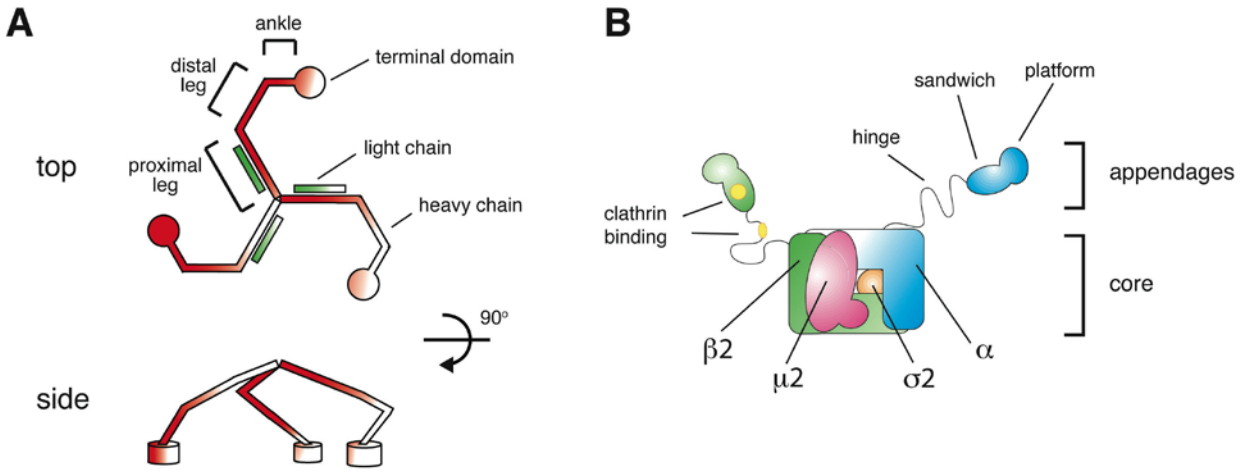

Figure 1.2: Organization of clathrin and AP-2.
(A) Clathrin heavy chains (red) trimerize at their C-termini to form a triskelion. A straight segment adjacent to the trimerization domain is the proximal leg, followed by the knee, distal leg, ankle and the terminal domain. One clathrin light chain (green) binds to one heavy chain along the proximal leg. The triskelion is curved, projecting the terminal domains down. (B) AP-2 is a heterotetramer composed of two large subunits, α (blue) and β2 (green), a medium subunit μ2 (magenta) and a small subunit σ2 (orange). All four subunits fold compactly into a brick-like core. The large subunits have an unstructured C-terminus (hinge) that ends in an independently folded appendage domain. Regions on the β2 subunit that bind clathrin are denoted by gold circles.

1.3.2 The heterotetrameric adaptor AP-2

In order to act as a mechanical scaffold for vesicle formation, clathrin binds to adaptors that themselves bind to the membrane as well as cargo molecules. For this reason, the originally named 'assembly polypeptides' (Keen, 1987) have more commonly assumed the name 'adaptor proteins' as they can link clathrin assembly to cargo selection. The AP family is composed of four heterotetrameric protein complexes (AP-1–4) that are ubiquitously expressed (Boehm and Bonifacino, 2001). The APs each contain two large (~100-140 kDa) subunits: γ, α, δ, ε and β1-4, one medium (~50 kDa) subunit: μ1-4 and one small (~20 kDa) subunit: σ1-4 for AP-1 through AP-4, respectively. These adaptors regulate CCV formation (AP-1 and AP-2) or vesicle formation (AP-3 and AP-4) at different subcellular domains: AP-2 at the plasma membrane and AP-1, AP-3 and AP-4 at the TGN and endosomes (Nakatsu and Ohno, 2003). Further discussion will focus on how AP-2 coordinates endocytosis at the plasma membrane.

Biochemical and structural studies have greatly advanced our knowledge of how AP-2 functions in CCV assembly. AP-2 (as well as AP-1, -3 and -4) consists of a brick-like core domain with two independently folded appendages connected by flexible, unstructured chains called the hinge domains (Figure 1.2B) (Heuser and Keen, 1988). The AP-2 core is assembled from all four subunits: the α and β2 N-termini, the μ2 and the σ2. The α and β2 subunit N-termini each have an alpha-solenoid fold with a sharp ~90° turn that creates a curved rectangle (Collins *et al.*, 2002). Tucked into the large subunit turns are the structurally analogous σ2 for α and the μ2 N-terminus for β2. The μ2 subunit has a middle unstructured domain and C-terminal curved β-sheet domain. This μ2 C-terminus fits neatly into the remaining space of the α/β2 'bowl' (Collins *et al.*, 2002).

Projecting off at the C-termini of α and β2 are the unstructured hinge domains that end in the folded 'appendage' domains. Despite a low primary sequence conservation between the α and β2 appendages, they share a similar tertiary structure (Traub *et al.*, 1999; Owen *et al.*, 2000), Both appendages can be further divided into an amino terminal sandwich subdomain, comprised of a β-sandwich fold, and a carboxyl terminal platform subdomain, formed by a combination of β-sheet and α helices. The AP-2 appendage domains are critical to proper CME as they coordinate interactions with ~20-30 endocytic proteins including clathrin (Mishra *et al.*, 2004; Edeling *et al.*, 2006a) and antibodies that bind the α appendage (AP.6) interfere with Tf uptake when microinjected into cells (Chin *et al.*, 1989). The appendages will be discussed in greater detail below.

Cargo molecules contain linear amino-acid sequences in their cytosolic aspects, known as sorting signals, for their positive-selection and incorporation into forming CCVs. As the most prominent component of CCVs after clathrin, AP-2 is the prototypical adaptor for cargo selection. The μ2 subunit of AP-2 specifically recognizes tyrosine-based sorting signals of the consensus YXXØ (where X is any amino acid and Ø is a bulky hydrophobic residue) (Ohno *et al.*, 1995; Owen and Evans, 1998). AP-2 can coordinate the simultaneous internalization of multiple sorting signal type containing cargo (Table 1.1). It also recognizes the consensus [DE]XXXL[LI] (brackets indicate one of the contained residues) through the σ2 and α hemicomplex (Doray *et al.*, 2007; Kelly *et al.*, 2008). These different signals allow the non-competitive (Warren *et al.*, 1997) constitutive endocytosis of a variety of receptors. Interestingly in the 'closed' conformation the μ2 C-terminal domain and σ2/α hemicomplex cargo sites are blocked by the β2 subunit (Collins *et al.*, 2002) and must undergo rearrangement to accommodate cargo. This suggests recognition of sorting signals is not what recruits AP-2 to the

plasma membrane and agrees with failure of AP-2 to bind to endosomes that are rich in TfR and LDLR.

1.3.3 Monomeric adaptors

1.3.3.1 Clathrin-associated sorting proteins

The AP-2 centric model of cargo sorting has been expanded in recent years with the observations that distinct cargo with different sorting signals do not compete with each other for entry through CCPs (Warren *et al.*, 1998) and that short interfering RNA (siRNA) depletion of AP-2 in cell culture only minimally affects internalizaton of some cargo such as LDLR (Hinrichsen *et al.*, 2003; Motley *et al.*, 2003). An array of alternate adaptors or clathrin-associated sorting proteins (CLASPs), that increase the sorting repertoire of CCSs beyond AP-2-bound cargo, and their recognized sorting signals have been identified (Traub, 2009).

β-arrestin 1 and 2 were the first recognized CLASPs. Following stimulation of G protein-coupled receptors (GPCRs) with an appropriate ligand, multiple serine and threonine residues within the cytosolic loops of these receptors are phosphorylated by the G protein-coupled receptor kinase (GRK) family members (Ritter and Hall, 2009). β-arrestins contain an N-terminal bilobed arrestin fold that simultaneously recognizes this three dimensional array of receptor-attached phosphates and receptor loops (Marchese *et al.*, 2003) and phosphoinositides (Gaidarov *et al.*, 1999). This interaction rapidly desensitizes signal propagation by uncoupling heterotrimeric G proteins from the receptor. β-arrestin is usually soluble in the basal state as the largely unstructured C-terminus is bound back on the arrestin fold as an inhibitory clamp. Upon receptor engagement, electrostatic associations with the receptor-attached phosphates discharge the C-terminus revealing AP-2 appendage and clathrin binding motifs (Edeling *et al.*, 2006a;

Burtey *et al.*, 2007). The revealed clathrin coat interaction motifs target β-arrestin and the associated desensitized receptor to pre-existing clathrin-coated pits for endocytosis and downregulation (Scott *et al.*, 2002). In contrast to the YXXØ and [DE]XXXL[LI] sorting signals constitutively recognized by AP-2, β-arrestin recognition of phosphate signals and coupling to the endocytic machinery constitutes a regulated form of endocytosis. As there are roughly 1000 GPCRs encoded in the human genome (Takeda *et al.*, 2002) making them the largest receptor family, and many but not all utilize β-arrestins and clathrin, this endocytic regulation is critical to homeostasis and adaptation.

Table 1.1: Sorting signals for clathrin-mediated endocytosis

Sorting Signal/Type	Recognition Protein or Domain	Example of Cargo
YXXØ*	AP-2 μ2	Transferrin receptor
[DE]XXXL[LI]	AP-2 σ2/α	CD4
[FY]XNPX[YF]	Dab2 and ARH PTB domain	LDL receptor
phospho-Ser/Thr	β-arrestin 1 and 2	GPCRs
Ubiquitin	epsin and eps15 UIM	EGF receptor

* ∅ indicates a bulky hydrophobic residue: Leu, Met, Ile, Phe

The CLASPs autosomal recessive hypercholesterolemia (ARH) and Disabled-2 (Dab2) recognize sorting signals of the consensus sequence [FY]XNPX[YF] (Traub, 2009). Coincidentally, this tyrosine-based sorting signal was discovered by Joseph Goldstein and Michael Brown (Anderson *et al.*, 1977; Chen *et al.*, 1990) prior to the characterization of AP-2 or knowledge of alternative adaptors. Mutations in this sequence prevent endocytosis of low density lipoprotein particles by LDLR giving rise to familial hypercholesterolemia. In these proteins, the N-terminal phosphotyrosine binding (PTB) domain (a misnomer because it binds unphosphorylated tyrosine) simultaneously binds the [FY]XNPX[YF] signal and the inositol

headgroup of the lipid phosphatidylinositol-4,5-bisphosphate (PtdIns(4,5)P_2) (Figure 1.3), coordinating cargo sorting and membrane localization (Stolt and Bock, 2006). The ARH and Dab2 C-termini are unstructured and bind to AP-2 and clathrin, similar to β-arrestin.

In mammals, many cell surface molecules destined for CME contain primary sequence encoded sorting signals, however in the yeast *S. cerevisiae* the primary endocytic signal is appended ubiquitin molecules (Lauwers *et al.*, 2010). Three ubiquitin binding proteins, Ent1p, Ent2p, and Ede1p function redundantly in yeast to sort ubiquitinated cargo (Shih *et al.*, 2002). The mammalian orthologues epsin 1, epsin 2, and epidermal growth factor receptor substrate 15 (eps15), respectively function in a similar manner (Wendland, 2002; Sorkina *et al.*, 2006). To target to the plasma membrane, epsin 1 contains an epsin N-terminal homology (ENTH) domain and eps15 contains three N-terminal eps15 homology (EH) domains that both bind to PtdIns(4,5)P_2 (Figure 1.3) (Traub, 2009). The C-terminal regions of both epsin 1 and eps15 are unstructured. Immediately downstream of the ENTH domain in epsin 1 are three ubiquitin-interacting motifs (UIM) while eps15 contains two UIMs at its extreme C-terminus that bind polyubiquitin (Hawryluk *et al.*, 2006) by conforming to α-helices (Sims and Cohen, 2009). Epsin contains multiple NPF motifs (Asp-Pro-Phe) that allow it to bind the eps15 EH domains, and in fact the name epsin comes from its identification as an eps15 interacting protein (Chen *et al.*, 1998). The remaining regions of unstructured polypeptide contain motifs for binding AP-2 and clathrin (epsin 1) or solely AP-2 (eps15) and will be described in detail below. Similar to post-translational phosphorylation for β-arrestins, ubiquitination of cargo following activation such as for the epidermal growth factor receptor (EGFR) promotes regulated endocytosis through epsin/eps15 (Traub, 2009). A common theme begins to emerge that many, but not all, CLASPs

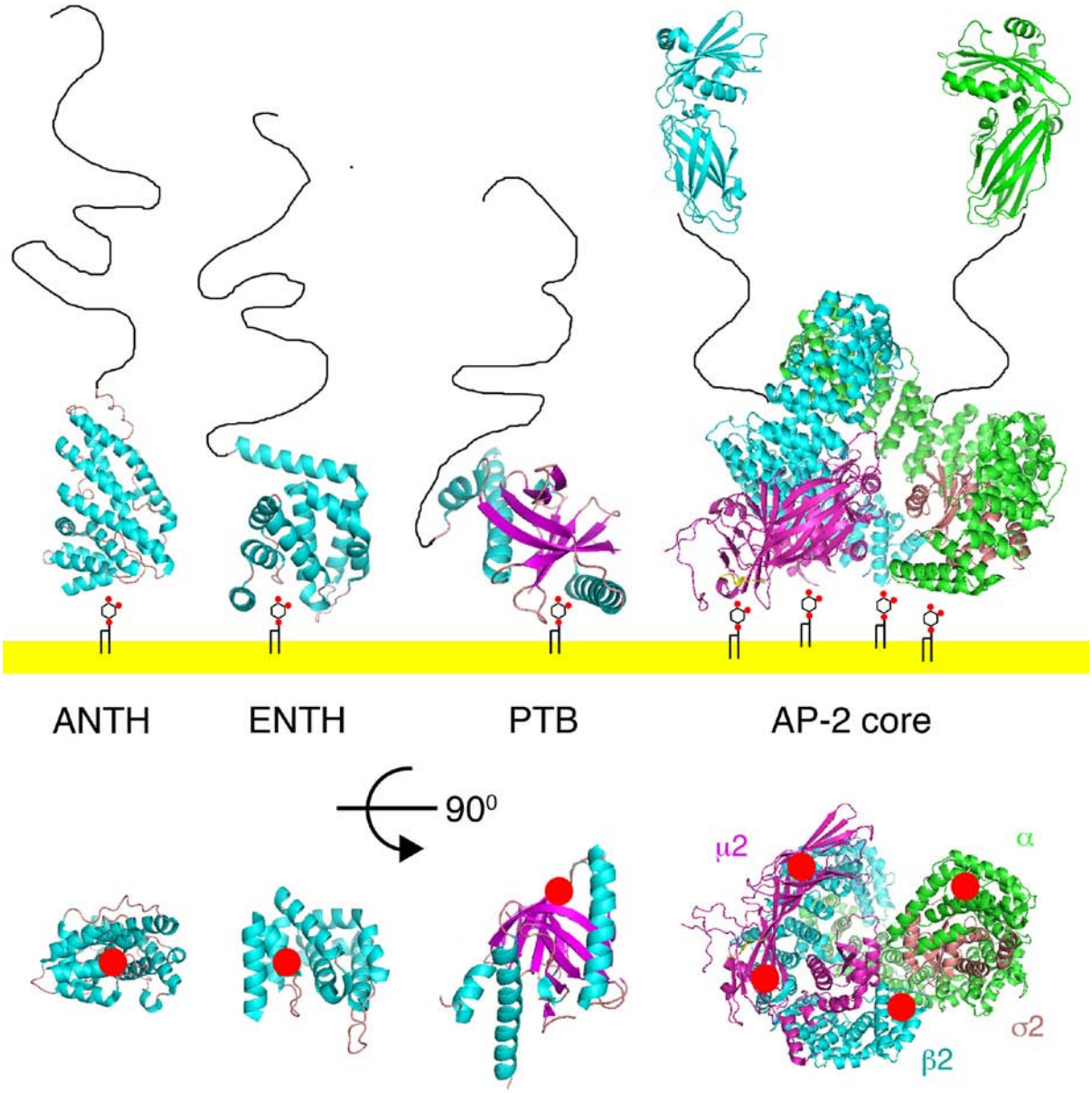

Figure 1.3. Endocytic protein domains for plasma membrane association.
Crystal structures of domains of significant tertiary structure of adaptors involved in CME. The AP180 N-terminal homology (ANTH) domain from AP180 (PDB# 1HG5), epsin N-terminal homology (ENTH) domain from epsin (PDB# 1H0A), a phosphotyrosine binding (PTB) domain from Dab2 (PDB# 1M7E) and the open conformation of the AP-2 core (PDB# 2XA7) are depicted. These domains display affinity for the lipid PtdIns(4,5)P_2. The plasma membrane is represented by the yellow line and individual PtdIns(4,5)P_2 molecules are represented by six-member rings with red dots at the 1, 4 and 5 positions embedded in the plasma membrane. PtdIns(4,5)P_2 coordinates with specific residues in these domains. AP-2 binds four molecules of PtdIns(4,5)P_2: two through the μ2 subunit, one through the β2 and one through the α subunit. By rotating the structures 90° the PtdIns(4,5)P_2 contact sites are more clearly seen (red spots, bottom). The unstructured C-termini of AP180, epsin and Dab2 are depicted as black lines. The AP-2 appendages (PDB# 1E42 and 1QTS) are shown connected by unstructured hinge domains. Structures were rendered in PyMOL.

sort cargo and recognize the plasma membrane through folded N-terminal domains and interact with the endocytic machinery through interaction motifs within unstructured C-terminal regions.

1.3.3.2 Endocytic Accessory factors

CCPs are highly regulated protein assemblies both in time and space. As such they contain a multitude of additional structural and enzymatic factors, termed accessory factors, that control assembly. For example, the neuronal specific protein AP180 and its ubiquitously expressed homolog clathrin assembly lymphoid myeloid leukemia protein (CALM) may act as CLASPs for soluble NSF attachment protein receptors (SNAREs) (Harel *et al.*, 2008), they also function to promote AP-2 and clathrin assembly at the plasma membrane (Ahle and Ungewickell, 1986). AP180 and CALM accomplish these functions through the typical modular architecture: a PtdIns(4,5)P_2 binding AP180 N-terminal homology (ANTH) domain (Figure 1.3), structurally related to the epsin ENTH domain, and an unstructured C-terminus with multiple AP-2 and clathrin binding motifs (Kalthoff *et al.*, 2002). Intersectin is a CCP structural protein that does not bind cargo. It appears to scaffold assembly/CLASP proteins such as the epsins and eps15 to later acting scission (dynamins), actin-related (neural Wiskott-Aldrich Syndrome Protein, N-WASP), and lipid phosphatase (synaptojanin, SHIP2) proteins (Pechstein *et al.*, 2010b).

The energetic cost of generating a spherical vesicle from a flat membrane of typical biological composition is a membrane-bending free energy of ~250-600 k_BT and reactions of thermal energy >100 k_BT do not occur spontaneously (Hurley *et al.*, 2010). Clathrin polymerization is absolutely required for generating membrane curvature (Hinrichsen *et al.*, 2006) and could potentially supply some of this energy. Further membrane bending and/or stabilization may come from members of the Bin/Amphiphysin/Rvs167 (BAR) domain family (Suetsugu *et al.*, 2010). BAR domains are α-helical obligate anti-parallel homodimers that have

a crescent shape. Through numerous Lys/Arg residues on the concave domain surface that interact with negative phospholipids and the propensity of these domains to oligomerize, BAR domain proteins influence membrane curvature in various locations throughout the endocytic and biosynthetic pathways. The BAR domain proteins endophilin and amphiphysin bind indirectly (endophilin) or directly (amphiphysin) to AP-2 and clathrin (Slepnev *et al.*, 2000) and both bind directly to dynamin through their C-terminal SH3 domains (Simpson *et al.*, 1999). By preferentially binding curved membranes with a circular diameter of ~22 nm, endophilin and amphiphysin couple constriction of the neck of deeply invaginated CCPs to dynamin recruitment for scission (Brett and Traub, 2006).

The terminal stages of CCV formation are characterized by vesicle scission, propulsion and uncoating. The dynamin GTPase plays a critical role in liberating the forming vesicle from the plasma membrane. Though the mechanistic details are still being worked out, dynamin self-assembly at the neck of deeply invaginated CCPs and its GTP hydrolysis induce conformational changes that promote membrane scission (Mettlen *et al.*, 2009). Actin nucleation may provide tensile force for scission (Ferguson *et al.*, 2009) and transport for movement of the vesicle away from the membrane (Galletta *et al.*, 2010). In 3T3 cells, actin is apparently used at all buds (Taylor *et al.*, 2011). Finally, CCVs must uncoat to allow fusion of the vesicle with endosomes. This is accomplished by targeting the chaperone Hsc70 to clathrin triskelions on the vesicle after budding through an interaction with the co-chaperone auxilin (neuron specific) or cyclin G-associated kinase (GAK, ubiquitous), two adaptors that directly engage the clathrin trimerization domain (Eisenberg and Greene, 2007). ATP hydrolysis by Hsc70 promotes triskelion disengagement and this step in conjunction with dynamin-mediated GTP hydrolysis are the only

direct energy inputs into the system. This raises the issue of how a complex assembly process proceeds forward favorably without frequent failure.

1.4 NUCLEATION OF CLATHRIN-COATED STRUCTURES

The formation of CCPs at the plasma membrane is a constitutive process. The biochemical and biophysical reactions that govern the earliest phase of CCP construction, i.e. the process of going from a naked patch of plasma membrane to a nascent assembly of AP-2, clathrin and cargo, is termed nucleation. Despite active research in the CME field for the past four and a half decades, it is only within the last 10 years that a clearer molecular understanding of this dynamic process has begun to take shape.

Purified AP-1 and AP-2 promote clathrin cage assembly *in vitro* at physiological pH (Keen, 1987) and early on were expected to precede clathrin deposition on membranes. At the TGN, recruitment of AP-1 is dictated by the Arf1 GTPase (Stamnes and Rothman, 1993; Traub *et al.*, 1993) working in concert with cargo (Le Borgne *et al.*, 1996; Salamero *et al.*, 1996). Nucleation of AP-1-positive CCVs is initiated when a guanine nucleotide exchange factor (GEF) for Arf1 stimulates GTP binding by Arf1. The GTP bound active form of Arf1 extends a myristol group to anchor itself to the membrane. Through coincidence detection, AP-1 recognizes Arf1-GTP and cargo on the TGN for its correct placement. Coatomer utilizes Arf1 in a mechanistically similar manner to nucleate COPI coats and Sar1 GTPase stimulates COPII coat production. Thus coat nucleation in these instances is directly dependent on an energy input (GTP).

To date, no evidence implicates an obligatory GTPase in the nucleation of AP-2-positive CCVs at the plasma membrane. Some *in vitro* experiments have shown that recombinant GTP-loaded Arf6 can increase the recruitment of purified AP-2 to liposome membranes (Paleotti *et al.*, 2005). A second study showed that Arf6 may be important in the specific internalization of the angiotensin receptor through CCPs (Poupart *et al.*, 2007). However neither study demonstrated a strict dependence of CCSs distribution on Arf6, though a regulatory role for this protein is within reason. Recently, it was demonstrated that Arf6 is loaded into CCVs in preparation for its function in recycling from endosomes (Montagnac *et al.*, 2011). Therefore unlike other coated-vesicle pathways, CME is not dependent on an Arf GTPase.

1.4.1 An AP-2 docking complex and synaptotagmins

The earliest models for CCP initiation at the plasma membrane posited that receptor tails promoted AP-2 recruitment to the membrane with subsequent clathrin assembly (Pearse and Crowther, 1987). The attractiveness of this model aside from its simplicity is that CCVs would only be generated when cargo was available. This model was further supported by reconstitution experiments in which purified AP-2 and clathrin were used to generate CCPs on isolated fibroblast ventral membranes. Treatment of AP-2/clathrin stripped membranes with elastase prior to addition of purified components abolished AP-2 binding (Mahaffey *et al.*, 1990). Also the elastase-cleaved membrane-derived fragments purified over an AP affinity column were dominated by a 45 kDa fragment that could inhibit AP-2 binding to membranes (Peeler *et al.*, 1993). This gave rise to the idea that there was a specific AP-2 receptor or “docking complex” responsible for nucleating CCPs that would then be available for cargo concentration (Kirchhausen *et al.*, 1997).

The process of CME is perhaps most robust in neurons and in particular at presynaptic boutons where it serves the function of compensatory endocytosis for replenishment of synaptic vesicles (SV) (Rizzoli and Jahn, 2007). The hypothesis that a SV protein could act as an AP-2 docking factor, because many proteins found in SVs are directly retrieved by CCVs without an endosomal intermediate, lead to the finding that Synaptotagmin I (Syt I) could bind AP-2 (Zhang *et al.*, 1994). Syts are integral membrane and Ca^{2+} binding proteins that act as a molecular trigger for Ca^{2+} induced exocytosis (Pang and Sudhof, 2010). As Syt I is a neuronal protein, this finding could not explain how AP-2 was recruited in somatic cells. This was followed by a second study by the same group that showed a variety of Syts with wider tissue expression profiles also bound AP-2 (Li *et al.*, 1995).

Further research into this model for CCV nucleation showed that tyrosine sorting signal-containing peptides increased AP-2 binding to Syt I, suggesting cargo enhances recruitment of AP-2 (Haucke and De Camilli, 1999). AP-2 binding of the Syt Ca^{2+}-binding C2 domain, C2B, occurs through the μ2 subunit at a region distinct from YXXØ-recognition (Haucke *et al.*, 2000), so perhaps the excess peptide biased the AP-2 core toward the open conformation so that it can recognize Syt. Finally, in a cell culture model, a truncated version of the more ubiquitous Syt VII oligomerizes with endogenous Syt of HeLa cells and inhibits LDL uptake as a dominant negative (von Poser *et al.*, 2000). These lines of evidence were interpreted as to label Syt a nucleating protein for CME.

However the function of Syt as a dedicated docking protein for AP-2 has been called into question for the following reasons: 1. Neurotransmission phenotypes of Syt-null *Drosophila* have provided contradictory results, either being modest (DiAntonio *et al.*, 1993) or severe (Littleton *et al.*, 1993), whereas AP-2α mutant alleles are lethal (Gonzalez-Gaitan and Jackle,

1997), 2. Proteomics of liver-derived CCVs failed to detect a Syt isoform (Girard *et al.*, 2005), and 3. Research along these lines have not been followed up on in more recent years. For these reasons, Syts may be cargoes for CCPs but are not likely to be the nucleating complex in all budding reactions; Syts have a well established biochemical role in regulating membrane fusion (Pang and Sudhof, 2010).

1.4.2 Phosphatidylinositol lipids and associated lipid kinases

How then is AP-2 selectively deposited at the plasma membrane to promote CCS assembly? Phosphatidylinositol is a relatively minor lipid present in the cytosolic leaflets of eukaryotic cell membrane, constituting just ~15% of total phospholipids (Di Paolo and De Camilli, 2006). Reversible phosphorylation of three hydroxyl groups (C-3, C-4 and C-5) on the 6-member inositol ring gives rise to seven different phosphatidylinositol phosphate (PIP) moieties or phosphoinositides (Figure 1.4A,B). A subset of these phosphoinositides has specific cellular distributions on various organelles. Phosphatidylinositol-4,5-bisphosphate (PtdIns(4,5)P_2) is concentrated almost exclusively at the plasma membrane. Therefore PtdIns(4,5)P_2 could act as a compartmental cue to regulate AP-2 and clathrin assembly (Figure 1.4C).

Purified AP-2 binds to protein-extracted vesicles and membranes (Virshup and Bennett, 1988) (though integral membrane receptors are likely present and may have contributed), which initially implicated AP-2-membrane interactions as important for CCP formation. In fact, clathrin has no affinity for membranes (Unanue *et al.*, 1981) and so AP-2 is required to link clathrin to the budding vesicle and the cargo. This is accomplished through four PtdIns(4,5)P_2-recognizing basic side chain residue patches within the AP-2 core that coordinate with the lipid phosphate groups: one each upon the α subunit (Gaidarov and Keen, 1999; Collins *et al.*, 2002)

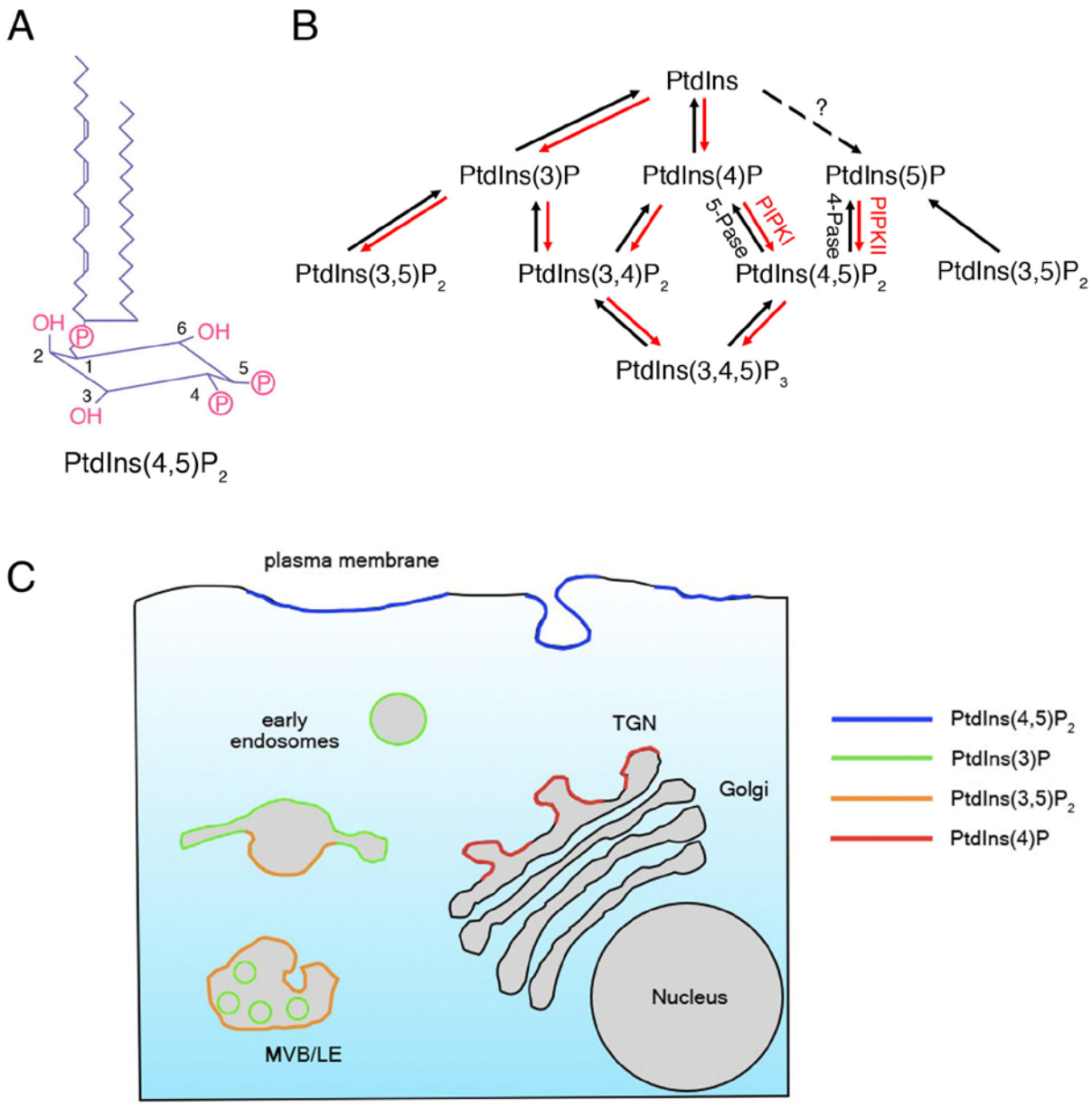

Figure 1.4: Phosphoinositide species generation and subcellular distribution.
(A) The inositol ring of phosphatidylinositol (PtdIns) can be reversibly phosphorylated at the C-3, C-4 and C-5 positions. Phosphatidylinositol-4,5-bisphosphate (PtdIns(4,5)P_2) is shown. (B) Reversible phosphorylation of PtdIns yields seven different phosphoinositides. These reactions are carried out by many unique and some overlapping lipid kinases (red) and phosphatases (black). Only relevant lipid enzymes are labeled for simplicity. (C) Subcellular distribution of phosphoinositides. MVB/LE, multivesicular body/late endosome; TGN, trans-Golgi network. (B) and (C) are modified from (Vicinanza *et al.*, 2008).

and β2 subunit (Jackson *et al.*, 2010) and two at the distal C-terminus of the μ2 subunit (Collins *et al.*, 2002; Rohde *et al.*, 2002; Jackson *et al.*, 2010). Mutation of these critical residues in the AP-2 α subunit prevent recruitment of the AP-2 complex to the plasma membrane in cells (Gaidarov and Keen, 1999) and inhibits Tf endocytosis (Motley *et al.*, 2006) while the β2 site is also important for binding to membranes (Jackson *et al.*, 2010). The importance of PtdIns(4,5)P_2 in CCP assembly extends to nearly all adaptors as their modular domains, including the ENTH (Itoh *et al.*, 2001), ANTH (Ford *et al.*, 2001), EH (Naslavsky *et al.*, 2007) and PTB (Mishra *et al.*, 2002a) domains, bind this lipid (Figure 1.3).

Cell culture assays have allowed careful perturbation of lipids to assess the effects on CCP nucleation. The earliest demonstration for a direct role of PtdIns(4,5)P_2 in nucleation involved the inhibition of TfR sequestration in perforated cells by the addition of the PtdIns(4,5)P_2-binding pleckstrin homology domain from phospholipase C δ (Jost *et al.*, 1998). More recently, an expression system consisting of rapamycin-inducible protein domain heterodimerization leading to membrane recruitment of a phosphatidylinositol 5-phosphatase, convincingly shows that acute PtdIns(4,5)P_2 depletion causes a dramatic loss of fluorescently-tagged AP-2 from the plasma membrane (Zoncu *et al.*, 2007) and disruption of Tf uptake (Varnai *et al.*, 2006). The reproducibility of this experiment has strengthened this model of nucleation (Abe *et al.*, 2008). Furthermore, pharmacological inhibition of phospholipase D, an enzyme that produces phosphatidic acid (PtdOH) that can stimulate PtdIns(4,5)P_2-producing lipid kinases, causes reversible loss of endocytic structures on the plasma membrane (Boucrot *et al.*, 2006), though the specificity of PtdOH inhibition by this method has been called into question (Antonescu *et al.*, 2010). That currently no similar observations of complete loss of AP-2

structures upon Arf6 or Syt depletion have been reported indicates that, currently, PtdIns(4,5)P_2 is the most likely candidate for facilitating CCP nucleation.

PtdIns(4,5)P_2 in mammals is produced by the type I and type II PIP kinases (PIPKI and PIPKII) (Heck *et al.*, 2007). Though originally thought to both use phosphatidylinositol-4-phosphate (PtdIns(4)P) as a substrate, it is now known that PIPKIs utilize PtdIns(4)P and phosphorylate the C-5 position while PIPKIIs utilize phosphatidylinositol-5-phosphate (PtdIns(5)P) and phosphorylate the C-4 position to generate the same product. PIPKIs produce the majority of PtdIns(4,5)P_2 in cells and this family is further divided into three isoforms: PIPKIα, PIPKIβ (Ishihara *et al.*, 1996; Loijens and Anderson, 1996), and PIPKIγ (Ishihara *et al.*, 1998). In addition PIPKIγ is alternatively spliced at its C-terminus producing PIPKIγ661 (PIPKIγa), PIPKIγ635 (PIPKIγb) and PIPKIγ688 (PIPKIγc) (mouse terminal residues 661 and 635, rat terminal residue 688) (Giudici *et al.*, 2004).

Direct modulation of PtdIns(4,5)P_2 generating and consuming enzymes have also highlighted the importance of lipid metabolism in CCP nucleation and regulation of endocytosis. Knockout of PIPKIγ in mice is postnatally lethal by 24 hours. However in isolated neurons from these animals, a defect in compensatory endocytosis and reduction in generation of clathrin-coated bud profiles following depolarization is observed (Di Paolo *et al.*, 2004). The pups appeared anatomically normal after birth and are thought to have died from synaptic defects, underscoring the importance of PtdIns(4,5)P_2 for CME in neurotransmission. In *Drosophila*, hypomorphic alleles of the type I PIPK Skittles greatly reduces yolk protein endocytosis in oocytes (Compagnon *et al.*, 2009). By contrast, knockout of synaptojanin 1 in mice, a polyphosphoinositide phosphatase, results in the accumulation of clathrin-coated vesicle profiles (~6x greater than wildtype) in nerve terminals of neurons in culture (Cremona *et al.*, 1999).

These results and others have given rise to a phosphoinositide phosphorylation-dephosphorylation cycle model in which a wave of PtdIns(4,5)P_2 production promotes CME and its hydrolysis promotes uncoating (Cremona and De Camilli, 2001). This model gained support recently when live-cell imaging studies of fluorescent PtdIns(4,5)P_2-binding domains expressed at low-levels in yeast, where CME shares many mechanistic parallels with vertebrate CME, indicated that PtdIns(4,5)P_2 levels rise and fall during endocytic actin patch progression (Sun *et al.*, 2007a).

An important question for the regulation of CCP nucleation and turnover is whether the steady-state levels of PtdIns(4,5)P_2 at the plasma membrane are sufficient for CCP generation or whether local generation of PtdIns(4,5)P_2 is needed in addition? Three lines of evidence suggest that direct binding of PIPKIs to the endocytic machinery could prime nascent assembly zones for PtdIns(4,5)P_2 production and drive the budding reaction forward. In one, a putative YXXØ sorting signal (YSPL) in the C-terminus of PIPKIγ engages the AP-2 μ2 subunit via the YXXØ recognition region (Bairstow *et al.*, 2006). Forced expression of PIPKIγ in MDCK cells increased Tf endocytosis without detectably altering global PtdIns(4,5)P_2 levels, while PIPKIγ knockdown in HeLa cells reduced Tf uptake. Similarly, another group found that the AP-2 μ2 subunit can bind the core of PIPKIα, β or γ but at a region distinct from the YXXØ sorting signal recognition domain (Krauss *et al.*, 2006). Simultaneous binding of YXXØ sorting signal-containing cargo stimulates PIPKI enzymatic activity. In a completely different study, the C-terminus of PIPKIγ was found to interact with the AP-2 β2 subunit appendage domain (Nakano-Kobayashi *et al.*, 2007). In neurons, depolarization results in dephosphorylation of the PIPKIγ C-terminus, allowing its interaction with AP-2 and in turn stimulates kinase activity. At least for

CME in the brain, where PIPKIγ is highly concentrated, one or a combination of these modes of interaction may be important for rapidly nucleating CCPs.

These summarized findings on PtdIns(4,5)P_2 can be combined with a role for cargo in synthesizing a general mechanism of CCP nucleation. The presence of cargo, and the cytosolic sorting signals contained within, by itself does not drive recruitment of AP-2 to membranes to nucleate CCPs as determined by overexpression studies (Santini *et al.*, 1998; Loerke *et al.*, 2009). In fact there is a cooperativity between PtdIns(4,5)P_2 binding by the α/β2/μ2 subunits and sorting signal recognition by the AP-2 core (Höning *et al.*, 2005). Structural studies reveal that the AP-2 core is likely in a 'closed' conformation in the cytosol and a conformational change stabilized by PtdIns(4,5)P_2 binding to α/β2/μ2 allows cargo access to the sorting subunits (Collins *et al.*, 2002; Jackson *et al.*, 2010). This conformational change is catalyzed by μ2 Thr156 phosphorylation by adaptor-associated kinase 1 (AAK1) (Ricotta *et al.*, 2002) biasing the μ2 subunit to extend and expose the PtdIns(4,5)P_2 and YXXØ-binding regions (Jackson *et al.*, 2010). Therefore cargo likely stabilizes nucleating clathrin structures and is incorporated into budding vesicles during assembly (Ehrlich *et al.*, 2004; Loerke *et al.*, 2009). Coincidence detection of PtdIns(4,5)P_2 and cargo restrict AP-2 deposition to the plasma membrane.

1.4.3 The EFC domain proteins FCHO1 and FCHO2

The BAR domain proteins are intimately tied to membrane curvature generation/sensing throughout the endocytic and biosynthetic pathways (Suetsugu *et al.*, 2010). BAR domains themselves are obligate anti-parallel homodimers that form a crescent shape. The N-BAR subfamily consists of members such as amphiphysin with an N-terminal BAR domain containing

an amphipathic helix that may insert into the membrane during protein assembly. The extended FER/CIP4 homology (EFC) domain (also known as F-BAR) subfamily has sequence similarity to N-BAR proteins as well as overall conservation of tertiary structure (Roberts-Galbraith and Gould, 2010). The majority of EFC domain proteins have the EFC domain at the N-terminus and one or more SH3 domains at the C-terminus, similar to N-BAR proteins. The main difference between EFC and N-BAR proteins is that EFC domain proteins typically have a larger radius of curvature associated with the crescent-shaped EFC domain and some EFC domain proteins form end-to-end oligomers, a property not yet demonstrated for N-BAR proteins (Roberts-Galbraith and Gould, 2010).

A recently discovered subfamily within the EFC domain proteins is the muniscin proteins (mu homology domain and meniscus shaped) that include FCHO1, FCHO2 and Syp1p (Reider *et al.*, 2009). The Fes/CIP4 homology only (FCHO) proteins were discovered as lacking a C-terminal SH3 domain unlike other EFC domain proteins but now, in addition to the *S. cerevisiae* protein Syp1p, are known to have a C-terminal μ homology domain (μHD). The μHD has sequence and structural homology to the cargo sorting AP-2 μ2 subunit (Reider *et al.*, 2009). This property makes the muniscins a unique group of proteins within the EFC subfamily whose cellular functions are largely unknown. In yeast, Syp1p (FCHO homolog) and Ede1p (eps15 homolog) are early arriving proteins at cortical actin patches (endocytic sites in yeast) where they regulate patch turnover and polarized endocytic placement at the bud neck (Stimpson *et al.*, 2009). Syp1 binds Ede1p through its μHD and may also act as a cargo-specific adaptor for the endocytosis of the yeast transmembrane protein Mid2p (Reider *et al.*, 2009).

In mammals, FCHO1 and FCHO2 have been proposed to act as nucleators of CCPs (Henne *et al.*, 2010). FCHO1/2 like Syp1p bind to PtdIns(4,5)P_2-enriched membranes and can

promote tubulation *in vitro* (Reider *et al.*, 2009; Henne *et al.*, 2010). FCHO1/2 and eps15 are early components of mammalian CCPs, preceding clathrin and other endocytic proteins. This is a property that would be expected for a nucleating factor. Most striking is that the levels of FCHO proteins are reported to control the rate of AP-2 appearance/disappearance at the plasma membrane: FCHO1 + 2 knockdown completely eliminates fluorescently labeled AP-2 appearance at spots on the membrane while overexpression of FCHO2 increased the number and fluctuations of AP-2 spots (Henne *et al.*, 2010). This property of FCHO1/2 is attributed to the binding of the adaptors eps15 and intersectin to the μHD which could then bind AP-2 for tethering and recruiting it to the plasma membrane. Early recruitment of FCHO1/2 could then begin an assembly chain to construct CCPs. In this model, nucleation and assembly are therefore tied to initiation of membrane curvature. These findings and conjectures remain to be independently validated.

1.5 PROGRESSION OF CLATHRIN-COATED STRUCTURES

1.5.1 Clathrin-assembly interaction motifs

Following the nucleation phase, or the placement of a few molecules of AP-2 and clathrin on the plasma membrane, a growth or assembly phase must occur as the nascent bud grows to the appropriate size to incorporate cargo and promote membrane invagination. CCPs are complex protein assemblies built from a large number of protein-protein interactions (see web diagram in (Traub, 2011)). On the order of 30 proteins are implicated in or are present at some time in

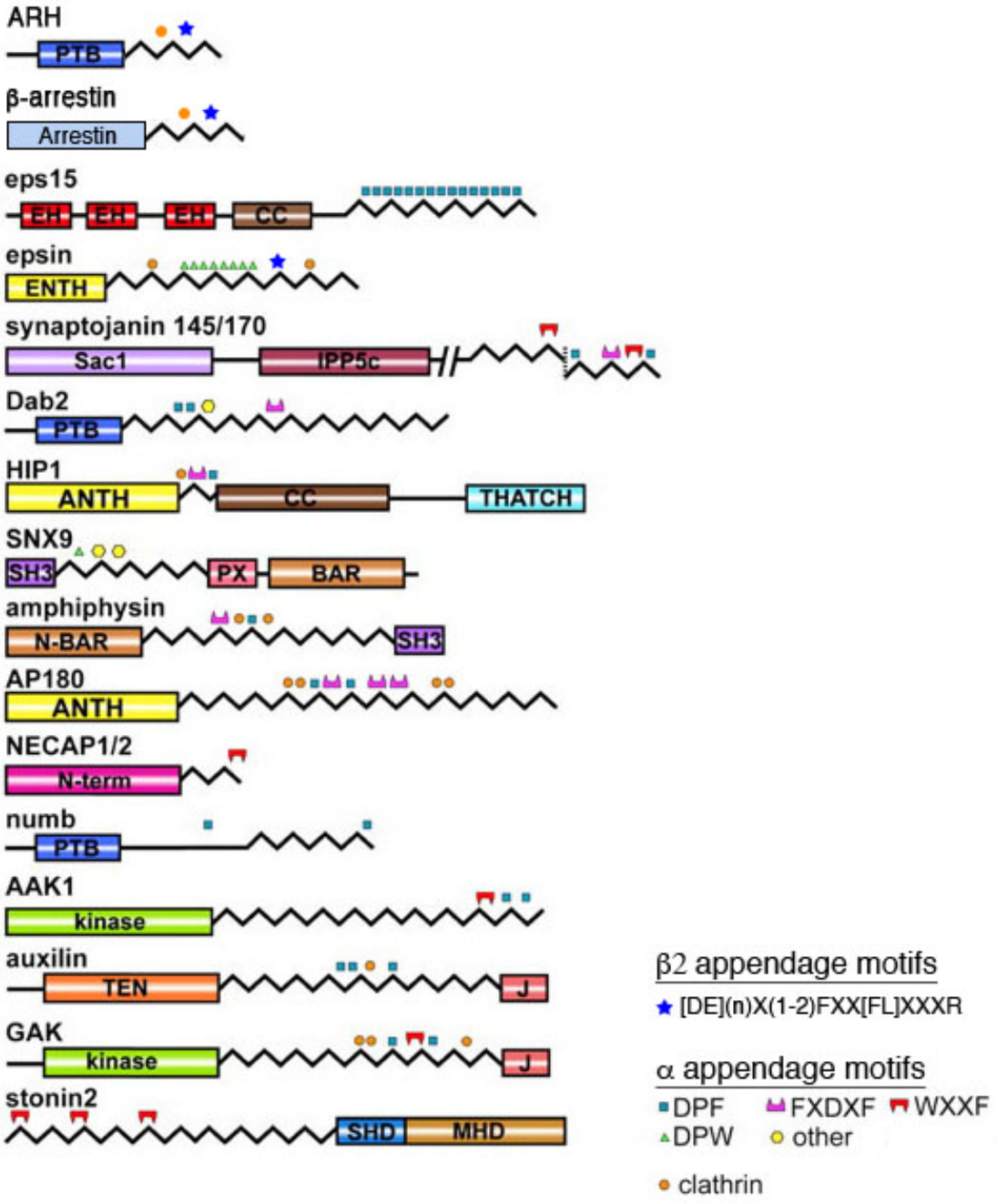

Figure 1.5: General architecture of endocytic adaptors and accessory factors.
The modular structure of many endocytic proteins comprised of one or more folded domains (colored boxes) and regions for which secondary structure cannot be predicted (zigzags, Jpred2) containing motifs for AP-2 and/or clathrin. Regions not corresponding to known domains are represented by straight lines. ANTH, AP180 N-terminal homology; BAR, BIN-amphiphysin-RVS; CC, coiled coil; EH, eps15 homology; ENTH, epsin-N-terminal homology; IPP5c, inositol 5-phosphatase catalytic domain; J, DNA J domain; MHD, μ subunit homology domain; PTB, phosphotyrosine-binding domain; PX, Phox domain; Sac1, suppressor of actin 1; SH3, Src homology 3, SHD, stonin homology domain; TEN, tensin homology; THATCH, talin-HIP1/1R actin-tethering C-terminal homology. Figure modified from (Mishra *et al.*, 2004).

assembling clathrin lattices. Work over the past two decades has attempted to characterize the molecular details of these interactions and how they are organized in space and time (Traub, 2005; Schmid and McMahon, 2007; Reider and Wendland, 2011). A common theme has emerged that unstructured primary sequence motifs in adaptors, accessory factors and regulatory enzymes bind to folded hub domains in AP-2 and clathrin (Figure 1.5).

As introduced earlier, the core of AP-2 is primarily responsible for binding to PtdIns(4,5)P_2- enriched membranes via the α and β2 (Jackson *et al.*, 2010) and μ2 (Rohde *et al.*, 2002) subunits and to YXXØ and [DE]XXXL[LI] sorting signals through the μ2 and σ2/α, respectively. The α and β2 appendage domains in contrast act as hubs and coordinate interactions with a majority of proteins involved in CME (Traub *et al.*, 1999; Owen *et al.*, 2000). Typically hydrophobic residue side chains with specific spacing between residues in the unstructured region of the appendage binding partner bury themselves in the binding pocket of

Table 1.2: Clathrin assembly interaction motifs

Consensus Sequence	Example Proteins	Binding Site
DP[FW]	eps15, epsin, Dab2	AP-2 α appendage platform
FXDXF	amphiphysin, AP180	AP-2 α appendage platform
WXX[FW]X[DE]	Synaptojanin 1, AAK1, NECAP	AP-2 α appendage sandwich
$[DE]_nX_{1-2}$FXX[FL]XXXR	β-arrestin 1/2, ARH, epsin 1	AP-2 β2 appendage platform
F rich	eps15, AP180, amphiphysin	AP-2 β2 appendage sandwich
L∅[DEN] ∅[DEN]	AP-2, epsin, Dab2, ARH, β-arrestin	clathrin HC terminal domain
PWXXW	amphiphysin	clathrin HC terminal domain
NPF	epsin 1, Dab2	eps15 EH domain

* X denotes any amino acid; ∅ indicates a bulky hydrophobic residue: Leu, Met, Ile, Phe

either the α or β2 appendage platform (C-terminal) subdomain or sandwich (N-terminal) subdomain (Table 1.2). The interaction of a single motif is relatively weak, k_D 10-100 mM, however low affinity is often compensated for by high avidity with the presence of multiple motifs (Edeling *et al.*, 2006b).

The α appendage binding sites were fully characterized first by structural and biochemical studies and accommodate three different interaction motifs. The α appendage platform binds DP[FW] and FXDXF motifs in partially overlapping sites (Benmerah *et al.*, 1996; Owen *et al.*, 1999; Brett *et al.*, 2002). These motifs are present in a large number of endocytic proteins including eps15, epsin, Dab2, synaptojanin and AP180 (Mishra *et al.*, 2004). The binding site upon the α appendage sandwich subdomain binds the motif of consensus WXX[FW]X[DE] (Mishra *et al.*, 2004; Praefcke *et al.*, 2004; Ritter *et al.*, 2004; Walther *et al.*, 2004). The presence of this motif is more restricted than DP[FW] and FXDXF and is found in proteins such as synaptojanin 1, AAK1 and GAK. Also, proteins that have both platform and sandwich binding motifs such as synaptojanin 1 can engage both simultaneously (Mishra *et al.*, 2004). The presence of multiple and varied motifs likely allows these proteins to cross-link AP-2 molecules and stabilize the assembly.

While the α appendage binds endocytic motifs in extended, unstructured conformations, the AP-2 β2 appendage platform subdomain induces unstructured motifs to adopt an α-helical secondary structure (Mishra *et al.*, 2005; Edeling *et al.*, 2006a; Schmid *et al.*, 2006). Sequences of the consensus $[DE]_nX_{1-2}FXX[FL]XXXR$ in the CLASPs ARH, β-arrestin and epsin facilitate binding to this domain (Edeling *et al.*, 2006a; Schmid *et al.*, 2006). The key anchoring Phe and Arg residues are spaced as to align on one side of the induced α-helix. The β2 appendage also harbors a sandwich site for binding endocytic proteins. Though not as fully characterized as

other sites, it appears that Phe side chains of a sequence in eps15, AP180 and amphiphysin are important for burrowing in this binding pocket during engagement (Edeling *et al.*, 2006a; Schmid *et al.*, 2006).

The clathrin heavy chain terminal domain is also a hub during assembly. The terminal domain is a seven-bladed β-propellar fold that projects down into the adaptor layer of CCPs and CCVs. Many adaptors including AP-2, epsin, Dab2, ARH and β-arrestins contain a clathrin box motif of the consensus LØ[DEN]Ø[DEN] that binds in a linear conformation between blades 1 and 2 of the terminal domain (ter Haar *et al.*, 2000; Traub, 2005). Often a clathrin box motif will accompany one or more AP-2 interaction motifs. A less common W box motif (PWXXW) found in amphiphysins may also contribute to assembly and binds to the center of the terminal domain (Miele *et al.*, 2004). Clathrin and W box motifs allow adaptors and AP-2 to capture soluble

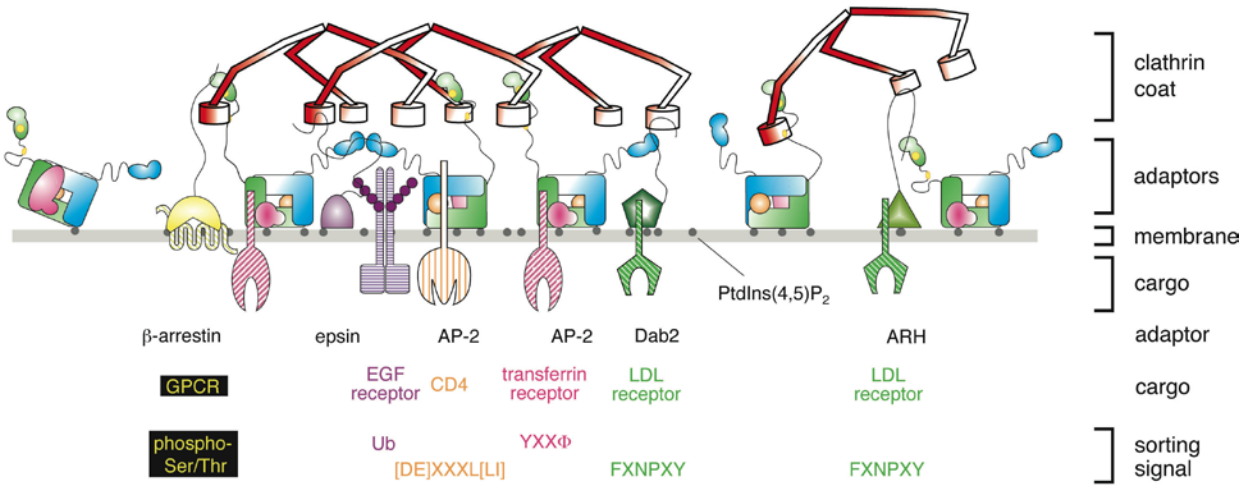

Figure 1.6: Molecular assembly of clathrin-coated structures.
This figure illustrates the initial placement of adaptors and clathrin on the plasma membrane prior to membrane invagination. AP-2 molecules are transiently recruited by binding PtdIns(4,5)P_2 through the α subunit (far left) and are stabilized by μ2 rearrangement (far right). This promotes receptor binding (center). Clustering of AP-2 and CLASPs promotes clathrin binding through AP-2 appendages and clathrin box motifs in the AP-2 hinge (yellow ellipse) and monomeric adaptors. FCHO1/2 and eps15 and intersectin are not depicted. Sorting signals or tags within cargo molecules are labeled below the figure, as are the adaptors that recognize these signals. Adaptors and cargo are color-coded. This flat clathrin assembly will proceed to a spherical coat such as that seen in Figure 1.1.

clathrin triskelions and promote their polymerization. Clearly the multiplicity of binding partners and four spatially separate interaction surfaces of the AP-2 appendages permit many binding possibilities. How these are managed during assembly is not clear but seems crucial to the successful budding of a CCV.

1.5.2 Chronology of assembly

Combining the information from adaptor-AP-2-clathrin binding and recent data from time-resolved imaging of transiently expressed accessory factor lifetimes at productive CCPs (Taylor *et al.*, 2011), we can begin to construct a clearer picture of how CCPs assemble. An 'early adaptor module' (based on peak time and recruitment profile) consists of FCHO1, FCHO2, eps15 and AP-2 and peaks early (Taylor *et al.*, 2011). Binding of FCHO1/2 to PtdIns(4,5)P_2 may allow the simultaneous binding of eps15 and intersectin to the FCHO μHD and PtdIns(4,5)P_2 or vise versa (Henne *et al.*, 2010). A nascent bud site so constructed may then be set for the recruitment of AP-2 (which appears after FCHO and eps15), through binding to a DPF array (Mishra *et al.*, 2004) and Phe rich β2 appendage sandwich binding site (Schmid *et al.*, 2006) at the eps15 C-terminus and/or α/β2 sandwich binding motifs in intersectin (Pechstein *et al.*, 2010a). Co-recognition of AP-2 appendage interaction motifs and PtdIns(4,5)P_2-enriched membranes through the α/β2 subunits would transiently dock 'closed' AP-2 molecules. AAK1 recruited by the AP-2 α appendage then would mediate phosphorylation of Thr156 on AP-2 μ2 (Ricotta *et al.*, 2002) and PtdIns(4,5)P_2 and cargo sorting would stabilize the open AP-2

conformation. AAK1 activity is increased by assembled clathrin, ensuring sorting competent AP-2 in CCSs while simultaneously regulating AAK1 kinase activity (Conner *et al.*, 2003).

A 'later adaptor module' that slowly builds and peaks at the time of vesicle scission but may start appearing during the 'early adaptor module' is composed of epsin, CALM (the ubiquitous AP180 homolog), and clathrin (Taylor *et al.*, 2011). Epsin, by virtue of its PtdIns(4,5)P_2-binding ENTH domain, C-terminal DPW motifs, and NPF motifs that bind the eps15 EH domain (de Beer *et al.*, 2000) would be recruited. AP180/CALM would bind PtdIns(4,5)P_2 through the ANTH domain, AP-2 α and β2 appendages through an array of motifs (Ford *et al.*, 2001) and eps15 through NPF motifs. This point of assembly would be critical for clathrin recruitment and polymerization. Epsin, AP180/CALM and AP-2 contain clathrin box motifs (Morris *et al.*, 1993; Shih *et al.*, 1995; Drake *et al.*, 2000). It has been proposed that the unstructured C-termini of the monomeric adaptors/accessory factors could extend with a radius of 150-180 Å into the cytosol and create a clathrin 'capture zone' through the exposed clathrin box motifs (Ungewickell and Hinrichsen, 2007; Zhuo *et al.*, 2011). Membrane bound AP-2 molecules could potentially extend the appendage domains up to 60 Å to capture and stabilize clathrin triskelions closer to the membrane where they would begin to polymerize. AP-2 strongly binds clathrin in an anti-parallel bivalent manner through a clathrin box squence contained in the β2 hinge (Shih *et al.*, 1995) and a second binding region on the β2 appendage that recognizes the clathrin distal leg (Edeling *et al.*, 2006a; Schmid *et al.*, 2006). At this point the assembly may resemble the schematic shown in Figure 1.6.

Bud invagination requires clathrin polymerization (Hinrichsen *et al.*, 2006) but alone may be insufficient and require other factors. An amphipathic helix inserted into the membrane by the epsin ENTH domain may contribute by expanding the cytosolic membrane leaflet relative to the

extracellular leaflet (Ford *et al.*, 2002), although this remains to be shown *in vivo*. The N-BAR and EFC domain proteins likely contribute as well. Syndapin2, an EFC protein, is recruited and exits during the assembly phase and may stabilize or induce curvature along FCHO1/2 and clathrin (Taylor *et al.*, 2011). The N-BAR protein module of endophilin 2, amphiphysin 1, and BIN1 sharply peak and regress just prior to scission suggesting they function at the highly curved CCP neck where they can recruit dynamin through their SH3 domains. In accordance with this, dynamin 1 and 2 peak almost precisely at the moment of scission (Taylor *et al.*, 2011). Amphiphysin in particular is at least partially recruited through interaction with the AP-2 α and β2 appendages and clathrin terminal domains (Miele *et al.*, 2004; Edeling *et al.*, 2006a).

1.5.3 Accessory factor displacement and directionality of assembly

A currently unresolved and global question in the field is, given the number of components and complexity of their interactions, what ensures the forward progression of CCP assembly? Clearly the residency of an endocytic protein at an assembling bud is determined by the number of contacts it makes with the coat proteins, the affinity and avidity of these interactions, and availability of binding sites over time. If phases of assembly are determined by the protein content in CCPs at that time, directionality could be imparted by the addition of new protein components or removal of others.

Biochemical experiments have confirmed that some accessory factors can be displaced from AP-2 during clathrin assembly. Initial structural and functional characterization of the AP-2 β2 appendage revealed that while the α appendage has no affinity for clathrin, the β2 appendage can bind clathrin weakly (Owen *et al.*, 2000). When supplied with the β2 appendage and the

adjacent hinge domain, which contains a clathrin box motif, clathrin bound more robustly and the binding of adaptors/accessory factors including AP180, eps15 and epsin was compromised. Site-directed mutagenesis of potential binding surfaces concentrated on the platform domain as that was the only site known on the α appendage at the time. Mutation of a few residues including Tyr888, Arg879 and Trp841 on the platform of the isolated β2 appendage alone reduced or eliminated binding of clathrin as well as the adaptors/accessory factors with the exception of eps15 and suggested that adaptor and clathrin binding to the platform site was mutually exclusive (Owen *et al.*, 2000). These findings were confirmed in a later study by the same group that showed that with increased binding of clathrin to the β2 appendage and hinge, AP180 and amphiphysin binding decreased relative to binding to the appendage alone (Schmid *et al.*, 2006). However this study was fraught with inconsistencies to the first. Binding of eps15 and epsin to the β2 appendage and hinge were unaffected by the presence of clathrin. Furthermore, mutation of the β2 platform residue Tyr888 that eliminated binding of accessory factors and clathrin in pull down assays previously (Owen *et al.*, 2000), had only a minor effect on the accessory factors (Schmid *et al.*, 2006).

In contrast to these studies, two lines of evidence suggest that the distal leg of clathrin binds not to the β2 appendage platform but to the sandwich site. In pull down experiments with the β2 appendage and hinge domain, mutation of the β2 sandwich site (tyrosine-815) and the terminal domain-binding clathrin box within the hinge had a synergistic effect in the reduction of clathrin binding (Edeling *et al.*, 2006a). This site is bound by eps15, AP180 and amphiphysin. Secondly, computational modeling suggests the clathrin leg ankle domain binds to the Golgi-localized gamma-adaptin ear homology protein (GGA), an adaptor for CCV formation at the Golgi, at a site that has structural homology to the AP-2 β2 appendage sandwich subdomain

(Knuehl *et al.*, 2006). GGAs do not have a platform subdomain. Though the precise details are in conflict, the idea that clathrin binds to AP-2 in an anti-parallel manner by the clathrin terminal domain binding a clathrin box motif in the hinge and the clathrin ankle domain binding to the appendage is supported. Competition of proteins from AP-2 could remove them from the bud site unless the proteins make additional contacts such as with clathrin itself.

A variation on this idea is the "changing hubs" model (Schmid *et al.*, 2006; Schmid and McMahon, 2007). In this model, the early assembly phase is governed by the AP-2 appendage hubs. The numerous appendage binding partners are recruited and assist in recruiting and assembling clathrin. As clathrin polymerizes into the lattice around AP-2 and occupies the β2 appendage (in this model the platform site), the displaced binding partners are retained within the assembling CCP through a switch in binding to the clathrin terminal domain hub. It is proposed that this change in binding site importance can drive the process forward although the precise mechanistic details are unknown.

1.6 GOALS OF THIS DISSERTATION

Clathrin-mediated endocytosis is a complex cellular phenomenon that utilizes ~20-30 proteins to build a scaffold that efficiently selects cargo from other resident surface proteins while simultaneously invaginating the plasma membrane. Work over the past few decades has identified many of these participating components and uncovered how they interact with the coat, however a clear understanding of the initial nucleation phase of clathrin-coated pit assembly is lacking. My dissertation research seeks to define how early regulatory proteins interface with the endocytic machinery and test the function of newly identified nucleator

proteins *in vivo*. In Chapter 2, I show that the PtdIns(4,5)P_2-generating enzyme PIPKIγ, present at nerve terminals, prefers to bind to AP-2 via the β2 appendage. I also show that it specifically binds to the β2 appendage sandwich subdomain in an interaction that is mutually exclusive with clathrin. Because PIPKIγ associates with the sandwich subdomain and my model is that PtdIns(4,5)P_2 production could be finely controlled by evicting the PIPKIγ when clathrin assembly overwhelms the β2 hub, clathrin would need to engage the sandwich site to regulate protein dynamics. Therefore, in Chapter 3 I test the "changing hubs" model of clathrin-coated pit assembly and show that *in vivo* the β2 appendage platform partner β-arrestin 1 is not displaced by clathrin during endocytosis. In Chapter 4 I test the function of the recently discovered endocytic proteins FCHO1 and FCHO2 in clathrin-mediated endocytosis *in vivo*. While FCHO1/2 have been proposed to act as obligate nucleators of clathrin-coated pits, I show that they are not absolutely required for endocytic site placement in cells or for cargo internalization. Instead they appear to regulate clathrin-coated structure size and number. This thesis helps to clarify mechanistic models on how the site of clathrin assembly is initially selected and formed.

2.0 CLATHRIN REGULATES THE ASSOCIATION OF PIPKIγ661 WITH THE AP-2 ADAPTOR β2 APPENDAGE*

*Reprinted from *Journal of Biological Chemistry*, (2009, volume 284, issue 20, pp. 13924-13939), with permission from The American Society for Biochemistry and Molecular Biology

2.1 ABSTRACT

The AP-2 clathrin adaptor differs fundamentally from the related AP-1, AP-3 and AP-4 sorting complexes because membrane deposition does not depend directly on an Arf-family GTPase. Instead, phosphatidylinositiol 4,5-bisphosphate (PtdIns(4,5)P_2) appears to act as the principal compartmental cue for AP-2 placement at the plasma membrane, as well as for the docking of numerous other important clathrin-coat components at the nascent bud site. This PtdIns(4,5)P_2 dependence makes type I phosphatidylinositol 4-phosphate 5-kinases (PIPKI) lynchpin enzymes in the assembly of clathrin-coated structures at the cell surface. PIPKIγ is the chief 5-kinase at nerve terminals and here we show that the 26 amino acid, alternatively-spliced C-terminus of PIPKIγ661 is an intrinsically unstructured polypeptide that binds directly to the sandwich subdomain of the AP-2 β2 subunit appendage. An aromatic side chain-based, extended interaction motif that also includes the two bulky C-terminal residues of the short PIPKIγ635

variant is necessary for β2 appendage engagement. The clathrin heavy chain accesses the same contact surface on the AP-2 β2 appendage but, because of additional clathrin binding sites located within the unstructured hinge segment of the β2 subunit, clathrin binds the β2 chain with a higher apparent affinity than PIPKIγ661. A clathrin-regulated interaction with AP-2 could allow PIPKIγ661 to be strategically positioned for regional PtdIns(4,5)P_2 generation during clathrin-coated vesicle assembly at the synapse.

2.2 INTRODUCTION

The key regulatory activity of phosphatidylinositol 4,5-bisphosphate (PtdIns(4,5)P_2) during clathrin-mediated endocytosis is firmly established (Di Paolo and De Camilli, 2006; Krauss and Haucke, 2007). The heterotetrameric AP-2 adaptor complex and numerous clathrin-associated sorting proteins (CLASPs) display dedicated surfaces or domains that engage PtdIns(4,5)P_2 with good selectively (Maldonado-Baez and Wendland, 2006; Schmid and McMahon, 2007; Ungewickell and Hinrichsen, 2007). PtdIns(4,5)P_2, which is localized to the cell surface, thus biases the deposition and assembly of these coat components at the plasma membrane by synergizing with other low affinity interactions in a phenomenon termed coincidence detection (Di Paolo and De Camilli, 2006; Schmid and McMahon, 2007). Later acting endocytic regulatory proteins also bind to PtdIns(4,5)P_2. The large GTPase dynamin contains a pleckstrin homology (PH) domain, which engages PtdIns(4,5)P_2 and is required for vesicle scission (Vallis *et al.*, 1999). Similarly, the clathrin uncoating cofactor, auxilin, has a PTEN-homology domain that also binds to phosphoinositides and is necessary for targeting of this J-domain protein to clathrin-coated membranes (Lee *et al.*, 2006). The lipid binding features of all these endocytic

components is in full accord with PtdIns(4,5)P_2 being necessary for both early and late stages of coated vesicle production (Jost *et al.*, 1998).

PtdIns(4,5)P_2 is a general, apparently ubiquitous marker of the plasma membrane and the concept of functionally autonomous, stable PtdIns(4,5)P_2-enriched microdomains within the cytosolic leaflet of the membrane has been challenged (Brough *et al.*, 2005; van Rheenen *et al.*, 2005; Yaradanakul and Hilgemann, 2007). This raises the question of whether the prevailing PtdIns(4,5)P_2 concentration at the cell surface is simply permissive and sufficient for nucleation and sustained clathrin-coated vesicle assembly and budding, or whether, in addition to basal PtdIns(4,5)P_2 that might act as an initial compartmental cue, regional synthesis of this lipid is also necessary for clathrin-coat assembly and progression. Supporting the first possibility is the general decrease in PtdIns(4,5)P_2 levels in the brains of phosphatidylinositol phosphate kinase type Iγ (PIPKIγ) nullizygous mice that parallels major synaptic vesicle recycling aberrations in neurons of these animals, which die before (Narkis *et al.*, 2007; Wang *et al.*, 2007) or shortly after (Di Paolo *et al.*, 2004) birth. Also, activated P2Y purinergic receptors, which trigger phospholipase C-mediated cleavage of PtdIns(4,5)P_2, diminish clathrin-mediated uptake of insulin (Carvou *et al.*, 2006), suggesting that signaling and endocytic processes can utilize a common phosphoinositide pool. PtdIns(4,5)P_2 is rather uniformly dispersed over the plasma membrane of the budding yeast *Saccharomyces cerevisiae* (Stefan *et al.*, 2002; Yu *et al.*, 2004) and Mss4p, the only phosphatidylinositol 4-phosphate 5-kinase in this organism, is not localized to cortical, clathrin-containing endocytic structures (Sun *et al.*, 2007a). In mammalian cells, the subcellular positioning of PIPKI enzymes is, at least in part, dictated by substrate availability/concentration as switching the activation loop residues of a type II PIPK, which usually acts on PtdIns5P, to that of a PIPKI, induces the chimeric kinase to localize to the cell

surface (Kunz *et al.*, 2000). In addition, ectopically expressed, tailored proteins that drive rapamycin-induced consumption of bulk PtdIns(4,5)P_2 lead to a rapid and dramatic loss of the majority of surface-associated clathrin-coated structures and halt clathrin-dependent internalization (Varnai *et al.*, 2006; Zoncu *et al.*, 2007; Abe *et al.*, 2008). In fact, excess PH domain can block clathrin-mediated endocytosis in an *in vitro* reconstitution assay (Jost *et al.*, 1998).

Yet the second idea of localized PtdIns(4,5)P_2 synthesis is in accord with the subcellular localization of PIPKI isozymes depending upon more than just the location of PtdIns4P (Brough *et al.*, 2005), and with the PIPKI enzymes associating physically with the AP-2 adaptor complex (Bairstow *et al.*, 2006; Krauss *et al.*, 2006; Nakano-Kobayashi *et al.*, 2007) and with β-arrestin (Nelson *et al.*, 2008). That the interaction with AP-2 stimulates catalysis (Krauss *et al.*, 2006; Nakano-Kobayashi *et al.*, 2007) lends additional support for a feed-forward model for staged PtdIns(4,5)P_2 generation at nascent clathrin assembly zones at the cell surface. The fact that ectopic expression of PIPKI enzymes in cultured cells increases both the number of surface clathrin-coated structures and the rate of internalization (Padron *et al.*, 2003) also indicates that PtdIns(4,5)P_2 on the cell surface can be limiting. Local production of PtdIns(4,5)P_2 might counteract general competition of endocytic factors with other cell surface proteins for a limited phosphoinositide pool, and thus may be important to sustain the rapid kinetics of clathrin-mediated endocytosis. This may be particularly relevant *in vivo* during signal transmission when PtdIns(4,5)P_2 is consumed to generate diacylglycerol (DAG), Ins(1,4,5)P_3 or PtdIns(3,4,5)P_3 (Carvou *et al.*, 2006; Di Paolo and De Camilli, 2006; Krauss and Haucke, 2007).

Irrespective of precisely how PIPKI enzymes translocate to the plasma membrane, what is also clear is that temporal remodeling of PtdIns(4,5)P_2 apparently accompanies coated vesicle

biogenesis (Perera *et al.*, 2006; Sun *et al.*, 2007a). After targeted gene disruption of the phosphoinositide polyphosphatase synaptojanin 1, neurons exhibit excessive and prolonged clathrin coat associations with the membrane (Cremona *et al.*, 1999; Harris *et al.*, 2000). Somewhat analogously, *S. cerevisiae* synaptojanin null mutants display mislocalized PtdIns(4,5)P_2, the phospholipid now appearing in endosomal structures (Stefan *et al.*, 2002; Sun *et al.*, 2007a). These results show clearly that under normal conditions, PtdIns(4,5)P_2 within forming transport vesicles is dephosphorylated prior to, or rapidly following, scission from the cell surface. Recent time-resolved live-cell imaging of the two splice isoforms of synaptojanin 1, termed SJ145 and SJ170 (Ramjaun and McPherson, 1996), reveals that while SJ145 masses at the bud site around the time of the fission event, SJ170 populates the coat throughout the assembly process (Perera *et al.*, 2006). Thus molecular mechanisms appear to exist to align cycles of PtdIns(4,5)P_2 formation and hydrolysis with progression of the coated assemblage toward the final fission step. In this study, we confirm that PIPKIγ, a vital lipid kinase (Di Paolo *et al.*, 2004; Narkis *et al.*, 2007; Wang *et al.*, 2007) and the major PtdIns4P kinase at the synapse (Wenk *et al.*, 2001), binds to AP-2 chiefly through the functionally autonomous appendage domain of the large β2 chain. We show that this depends on an interaction surface positioned upon the sandwich subdomain of the β2 appendage, a site also engaged by clathrin and eps15. Binding of these proteins to the β2 appendage is mutually exclusive, leading to a model for spatial and temporal phosphoinositide remodeling managed by AP-2 appendages.

2.3 RESULTS

2.3.1 PIPKIγ661 membrane translocation and AP-2 recruitment

Synaptic plasma membranes (Figure 2.1A), purified from rat brain synaptosome preparations (Figure 2.1B) by hypotonic lysis, contain trace levels of all three PIPKI isoforms, α, β and γ (Figure 2.1C). After extracting the membranes with 1 M KCl, predominantly the ~90-kDa PIPKIγ isoforms and PIPKIα are removed, but the treatment has no effect on the membrane-associated proteins Syt 1 and SNAP-25 (Figure 2.1C). Cell-free kinase assays show that the salt-washing procedure diminishes the temperature-dependent synthesis of PtdIns(4,5)P_2 to ~67% (n = 3; Figure 2.1D, compare lane b and d), presumably due to the removal of PIPKI. By contrast, PtdIns4P synthesis changes <10% on the extracted membranes. Using the salt-washed synaptic plasma membranes as a template for *in vitro* clathrin-coat assembly assays, we find that the translocation of cytosolic clathrin, the AP-2 adaptor complex and AP180 correlates with the accumulation of PIPKIγ661on the synaptic membranes (Figure 2.1E, lane c), and an increase in PtdIns(4,5)P_2 synthesis (Figure 2.1D, compare lane d and f). The recruitment of PIPKIγ661 under these conditions suggests there may be linkage between PIPKIγ and AP-2/clathrin membrane translocation. In fact, there is evidence for PIPKI enzymes associating directly with AP-2 in three molecularly distinct manners. The long-splice isoform of PIPKIγ contains a C-terminal ^{644}YSPL sequence that can interact with the cargo-selective μ2 subunit of AP-2, akin to YXXØ-type receptor sorting signals (Bairstow *et al.*, 2006). The same general region of the 26 amino-acid C-terminal insert of PIPKIγ661 can bind to the independently folded

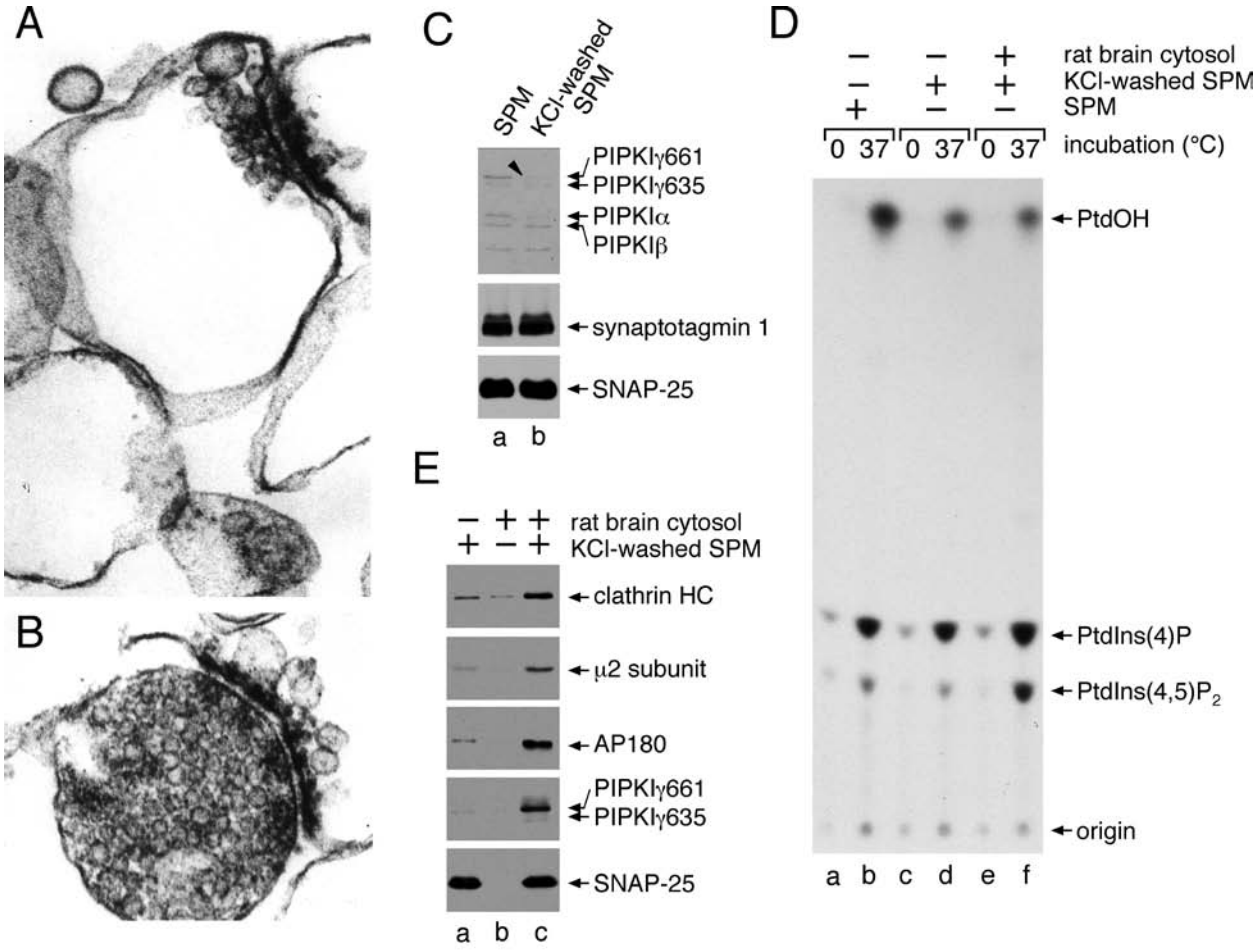

Figure 2.1: PIPKIγ661 and AP-2 are coordinately recruited to the synaptic plasma membrane.
(A) and (B), aliquots of synaptic plasma membrane (A) or synaptosomes from which they were derived (B) were fixed with 2% glutaraldehyde and processed for EM. Thin section micrographs typical of the many fields examined are shown. (C) Samples of 50 μg synaptic plasma membrane (SPM) were suspended in assay buffer alone or supplemented with 1 M KCl were sedimented after incubation on ice for 30 min. Aliquots of each resuspended membrane pellet were prepared for SDS-PAGE and immunoblotting. Portions of the blots were probed with an affinity-purified polyclonal anti-PIPKI antibody or mAbs directed against Syt 1 or SNAP-25. (D) Reactions containing 0.5 mg/ml untreated or salt-washed synaptic plasma membranes, 5 mg/ml cytosol and 500 μM [γ-^{32}P] ATP were prepared as indicated. After incubation at 37°C for 10 min the lipids were extracted and analyzed by TLC and autoradiography. A representative experiment of 3 is shown and the migration positions of authentic phospholipid standards are indicated. (E) reactions containing 50 μg/ml salt-washed synaptic plasma membranes, 5 mg/ml rat brain cytosol and an ATP regenerations system were prepared as indicated. After incubation at 37°C for 15 min, membranes were sedimented and prepared for SDS-PAGE and immunoblotting. Portions of the blots were probed with anti-clathrin-subunit heavy chain (HC) mAb TD.1, rabbit R11-29 anti-μ2 serum, or an anti-AP180, anti-PIPKIγ or anti-SNAP-25 mAb, and only relevant portions of the blots are shown.

β2 appendage of AP-2 (Nakano-Kobayashi *et al.*, 2007). In addition, the central kinase domain of all three PIPKI isoforms is proposed to associate with the μ2 subunit of AP-2, but in a manner that does not overlap with cargo binding; rather, concomitant PIPKI and YXXØ-sequence engagement by μ2 appears to stimulate the catalytic activity of the lipid kinase (Krauss *et al.*, 2006).

2.3.2 The PIPKIγ661 binding surface upon AP-2

To attempt to resolve whether the β2 or μ2 subunit of AP-2 represents a dominant interaction partner for the C-terminal 26 amino acid extension of PIPKIγ661, we used baculovirus-encoded AP-2 hemicomplexes (Figure 2.2C) (Doray *et al.*, 2007). First, we verified that the individual chains expressed in Sf9 cells associate into a macromolecular complex. Anti-FLAG immunoprecipitation shows that removal of the FLAG-tagged β2 subunit also depletes the μ2 subunit from the lysate (Figure 2.2A, compare lane a and b). The relative stoichiometry of the assembled β2·μ2 hemicomplex is seen on the Coomassie blue-stained gel (lane c). Likewise, a FLAG-tagged β2-subunit trunk, lacking the C-terminal 359 residues encoding the unstructured hinge as well as the appendage domain, immunoprecipitates along with the co-expressed μ2 (lane f). This is expected, as μ2 binds to the α-helical solenoid portion of the β2 subunit trunk (Collins *et al.*, 2002). These experiments confirm the assembly of the β2·μ2 and β2 trunk·μ2 hemicomplexes. Notably, the putative insect β subunit, recognized by the anti-β mAb, was not depleted from the lysates with the anti-FLAG mAb (lanes b and e).

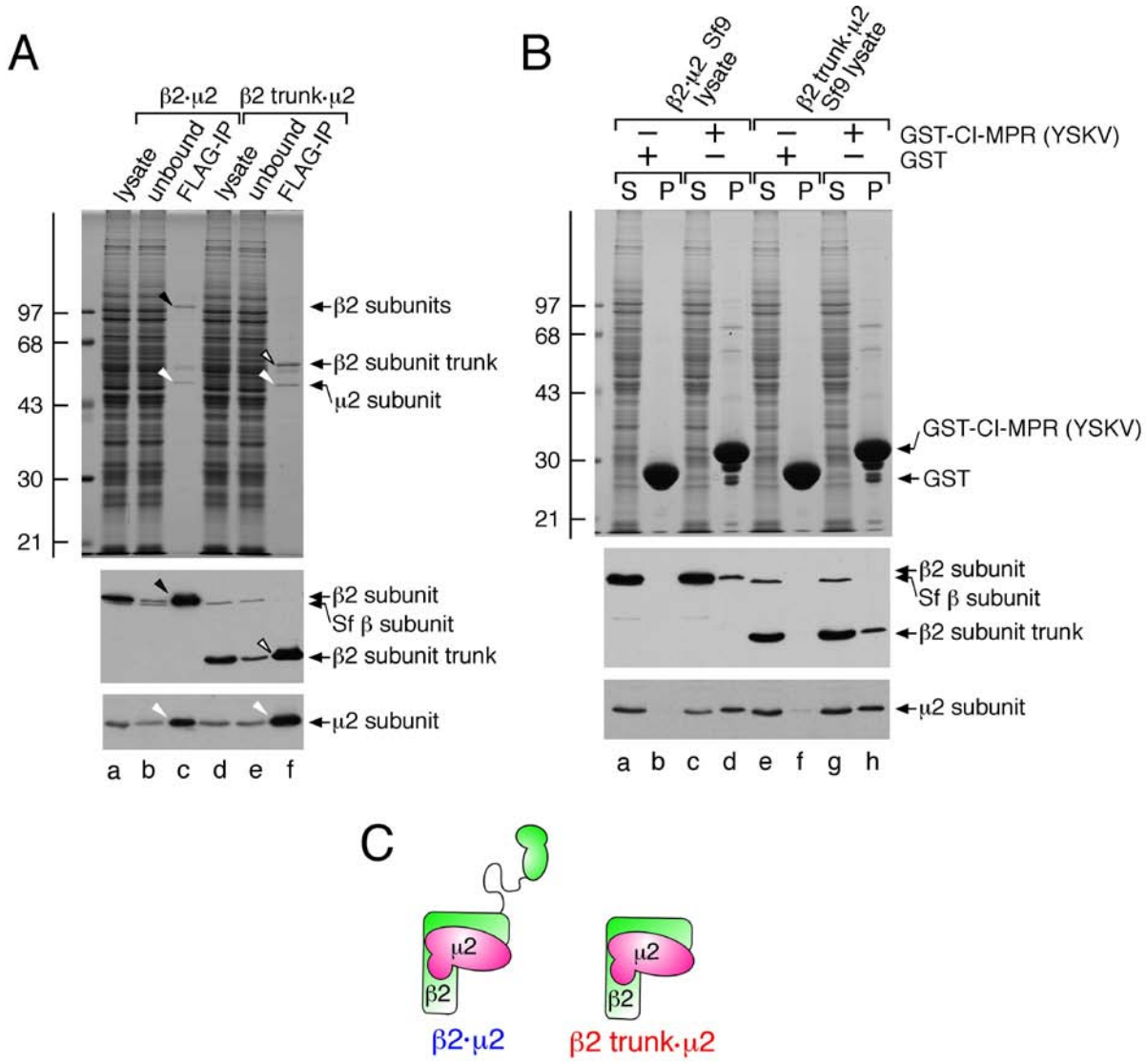

Figure 2.2: An AP-2 hemicomplex can bind YXX∅ sorting signals.
(A) Equivalent volumes of Sf9 cell lysate overexpressing either the β2·μ2 or the β2 trunk·μ2 hemicomplex before (lanes a and d) or after (lanes b and e) immunoprecipitation with agarose-coupled anti-FLAG mAb M2, and aliquots from the washed and FLAG-peptide eluted immunprecipitate pellet (lane c and f) were resolved by SDS-PAGE and either stained with Coomassie blue or transferred to nitrocellulose. Portions of the blots were probed with anti-β1/β1-subunit mAb 100/1 or anti-μ2 serum, and only the relevant portions shown. The migration position of the molecular mass standards is indicated on the left, and the location of the immuoprecipitated β2 subunit (black arrowhead), β2 trunk (open arrowhead) and μ2 subunit (white arrowheads) are shown. (B) Approximately 250 μg of GST (lanes a,b,e and f) or GST-CI-MPR (YSKV; lanes c,d,g and h) immobilized on glutathione-Sepharose was incubated with Sf9-cell lysates overexpressing either the β2·μ2 (lanes a-d) or β2 trunk·μ2 (lanes e-h) hemicomplexes as indicated. After centrifugation, aliquots of ~1.5% of each supernatant (S) and ~12.5% of each washed pellet (P) were resolved by SDS-PAGE and either stained with Coomassie blue or transferred to nitrocellulose. Portions of the blots were probed with anti-β1/β1-subunit mAb 100/1 or anti-μ2 serum, and only the relevant portions shown. (C) Schematic representation of the AP-2 β2·μ2 hemicomplex used in (A) and (B).

The capability of the two hemicomplexes to bind comparably to YXXØ-type sorting signals, which are recognized by the μ2 subunit (Ohno *et al.*, 1995; Owen and Evans, 1998), is seen with a portion of the CI-MPR cytoplasmic domain (residues 2337-2372) fused to glutathione-S-transferase (GST) (Figure 2.2B) (Doray *et al.*, 2007). While there is no association of either the FLAG-β2 subunit or μ2 with GST (lanes b and f), some of both the β2 and μ2 protein are recovered in the pellet fraction from GST-CI-MPR affinity isolations (lanes d and h). Still, none of the presumptive Sf9 AP-2 (β subunit) binds to the GST-CI-MPR (lanes f and h), and the relative stoichiometry of the bound μ2 compared with the soluble fraction is greater than either the β2 full-length or β2 trunk (lanes d and h). We interpret this to indicate that μ2 alone (uncomplexed) has the highest apparent affinity for YXXØ signals, although the strength of this interaction is still rather weak. Some of the binary β2·μ2 or β2 trunk·μ2 complexes also clearly associate with GST-CI-MPR but the failure of heterotetrameric AP-2 to bind appreciably is fully consistent with the cytosolic pool of AP-2 assuming a basal, closed conformation that blocks the YXXØ binding site on μ2 (Collins *et al.*, 2002).

Similar experiments using the C-terminal region of the PIPKIγ635 or PIPKIγ661 kinase variants (Ishihara *et al.*, 1998) show that only the long-splice isoform associates with the β2·μ2 hemicomplex (Figure 2.3, lane j). In fact, the presence of the full-length β2 subunit bound to GST-PIPKIγ(460-661) can be seen by Coomassie blue staining. By contrast, if incubated with either GST or GST-PIPKIγ(460-635), there is complete recovery of the full-length or the β2 trunk in the supernatant fraction (lanes a, c, e and g). This shows that necessary AP-2 binding information is indeed located within the terminal 26 residues of PIPKIγ661. Nevertheless, the β2 trunk·μ2 hemicomplex does not associate with the GST-PIPKIγ (460-661) like the intact β2·μ2 hemicomplex (compare lane l and j).

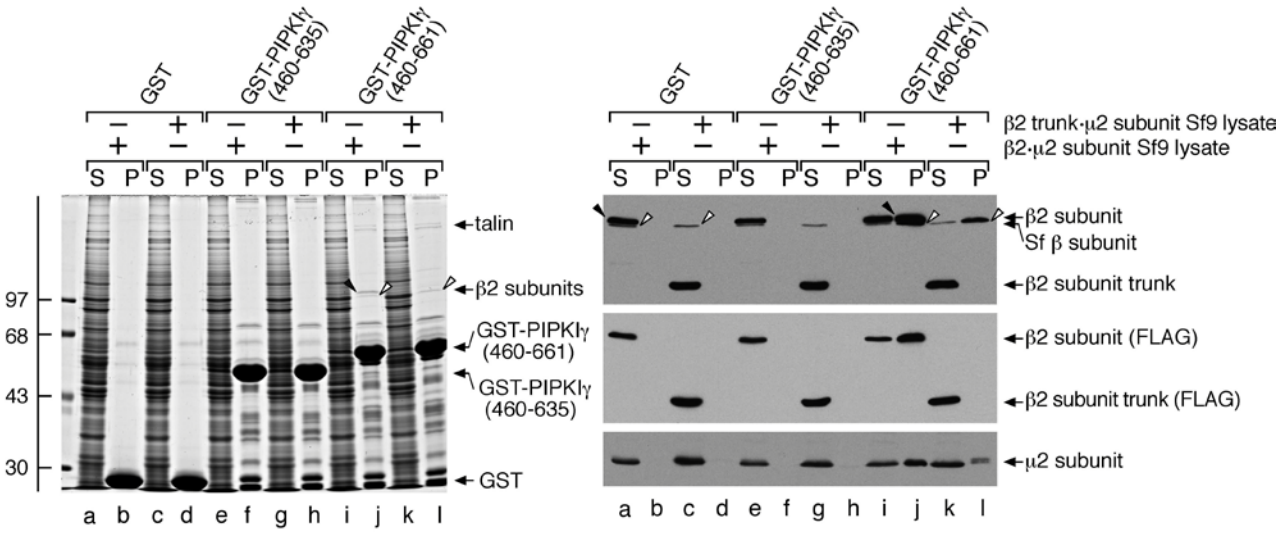

Figure 2.3: The C terminus of PIPKIγ661 but not PIPKIγ635 binds selectively to the AP-2 β2 appendage.

Approximately 200 μg of GST (lanes a-d), GST-PIPKIγ (460-635) (lanes e-h) or GST-PIPKIγ (460-661) immobilized on glutathione beads was incubated with incubated with Sf9-cell lysates overexpressing either the β2·μ2 (lanes a,b,e,f,i and j) or β2 trunk·μ2 (lanes c,d,g,h,k and l) hemicomplexes. After centrifugation, aliquots of ~1.5% of each supernatant (S) and ~15% of each washed pellet (P) were resolved by SDS-PAGE and either stained with Coomassie blue or transferred to nitrocellulose. Portions of the blots were probed with anti-β1/β1-subunit mAb 100/1, anti-FLAG mAb M1 or anti-μ2 serum, and only the relevant portions shown. The migration positions of the FLAG-tagged β2 (arrowheads) and the presumptive Sf9 cell β subunit (open arrowheads) are indicated.

There is a full-length β subunit recovered in the pull-down pellet after incubation with the β2-trunk lysate, but this chain does not contain a FLAG epitope (lane l), and the boųndμ2 migrates slightly slower than the expressed mammalian μ2 subunit (lane l). We thus conclude that although the β2 trunk·μ2 fails to bind to the immobilized GST-PIPKIγ (460-661), the endogenous Sf9 AP-2 heterotetramer specifically engages the 26 amino-acid extension of PIPKIγ661 since no binding is seen with the PIPKIγ (460-635) (lane h). This is in sharp contrast to the lack of association of the endogenous invertebrate AP-2 complex (Sf9 AP-2) with a GST-presented YXXØ sorting signal (Figure 2.2B).

In other experiments to assure that the FLAG-epitope-negative, ~100-kDa β-immunoreactive band and the slower mobility μ2 subunit are indeed constituents of the Sf9 cell AP-2, we used affinity isolation with a C-terminal segment of ARH. ARH contains a single $[DE]_nX_{1-2}FXX[FL]XXXR$ AP-2-binding motif that binds exclusively to the β2 subunit appendage (He *et al.*, 2002; Mishra *et al.*, 2002b; Edeling *et al.*, 2006a; Schmid *et al.*, 2006). The GST-ARHM2 fusion contains a 20 amino acid tract that fully contains this interaction motif (Mishra *et al.*, 2005) that quantitatively removes the presumptive Sf9 cell β subunit from the supernatant and is recovered in the pellet fraction (data not shown). Furthermore, when bound to the immobilized ARH β-subunit interaction motif, the slower mobility μ2 form is detected (data not shown). These studies reveal that the β and μ2 bands observed indeed represent the endogenous invertebrate AP-2 present in the Sf9 cell lysates.

The 26 amino acid extension of PIPKIγ661 also binds physically to the FERM domain of the integrin-associated protein talin, allowing regulated PtdIns(4,5)P_2 formation at focal adhesions (Di Paolo *et al.*, 2002; Ling *et al.*, 2002). Accordingly, the ~230-kDa insect talin in lysates of either β2·μ2 (Figure 2.3, lane j) or β2 trunk·μ2 (lane l) binds to the GST-PIPKIγ (460-

661) but not (460-635) (lanes f and h), as expected. Overall, we conclude from this series of experiments that the β2 appendage of the AP-2 complex, and not the μ2 subunit, is the major site for PIPKIγ661 interaction under these conditions. This interpretation is in full accord with a recent independent study (Nakano-Kobayashi *et al.*, 2007).

2.3.3 PIPKIγ661 appendage selectivity

The AP-2 complex has two independently folded appendages that project away from the central heterotetrameric core (see Figure 1.2). Despite only ~11% sequence identity, the α- and β2-subunit appendages have an analogous overall fold (Owen *et al.*, 2000) and share many binding partners (Edeling *et al.*, 2006a; Schmid *et al.*, 2006); therefore, the appendages could either be indiscriminately or selectively accessed by PIPKIγ661. In fact, PIPKIγ661 shows a striking selectivity for the β2 appendage over the α. Pull-down assays show that the GST-α and GST-β2 appendages bind to similar and different subsets of CLASPs and accessory factors (Figure 2.4, lanes d and f). While both bind to AP180, epsin 1, and eps15 roughly equally, only GST-β2 binds to PIPKIγ661 (Figure 2.4, lane d, right). This is reminiscent of the strict preference of ARH and β-arrestin for the β2 appendage (He *et al.*, 2002; Laporte *et al.*, 2002; Mishra *et al.*, 2002b; Edeling *et al.*, 2006a; Schmid *et al.*, 2006). Significantly, the α appendage also has distinctive interaction partners; the endocytic protein NECAP 1 binds only to GST-α, for example (Figure 2.4, lane f) (Ritter *et al.*, 2004). Cdk5 is known to phosphorylate PIPKIγ661 at Ser645 and dephosphorylation of this residue by calcineurin following calcium-induced synaptic vesicle exocytosis allows an interaction with AP-2 to promote compensatory endocytosis (Nakano-Kobayashi *et al.*, 2007). Of the two bands detected by the anti-PIPKIγ mAb,

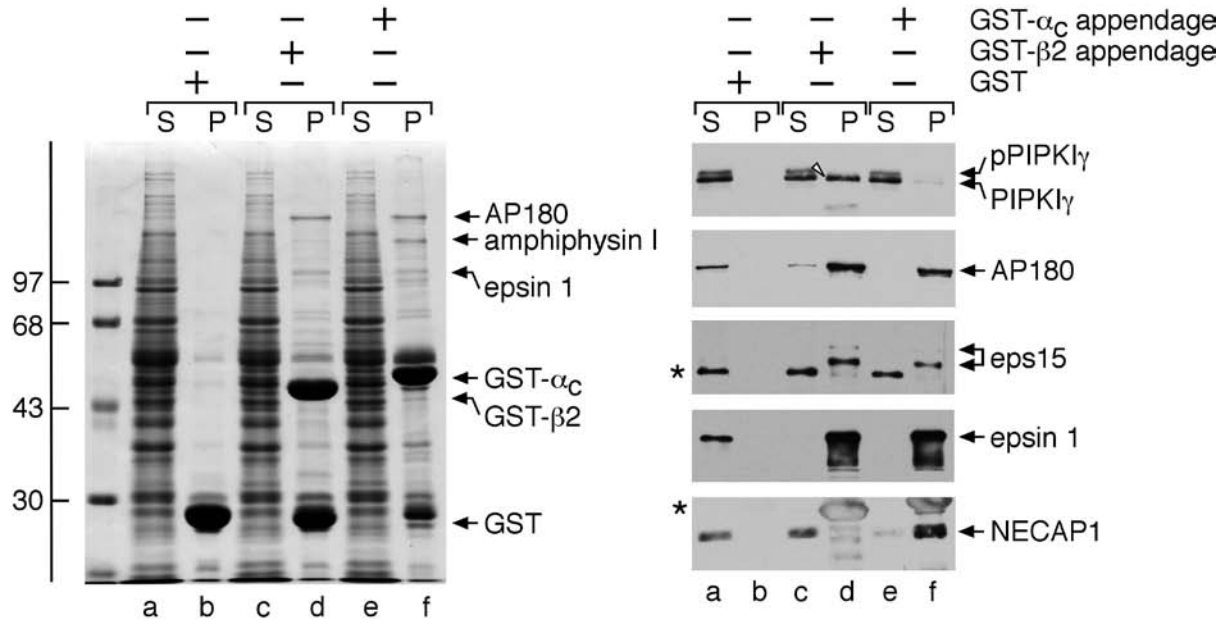

Figure 2.4: PIPKIγ661 discriminates between the AP-2 α and β2 appendages.
Approximately 100 μg of GST (lanes a and b), GST-β2 appendage (lanes c and d) or GST-α_C appendage (lanes e and f) immobilized on gluthathione-Sepharose was incubated with rat brain cytosol as indicated. After centrifugation, aliquots of ~1.5% of each supernatant (S) and ~10% of each washed pellet (P) were resolved by SDS-PAGE and either stained with Coomassie blue or transferred to nitrocellulose. Portions of the blots were probed with anti-PIPKIγ mAb clone 12, anti-AP180 mAb clone 34, or affinity-purified anti-eps15, epsin 1 or NECAP 1 antibodies, and only the relevant portions shown. The different migration of the non-phosphorylated (arrowhead) and phosphorylated (pPIPKIγ) forms of PIPKIγ is indicated.

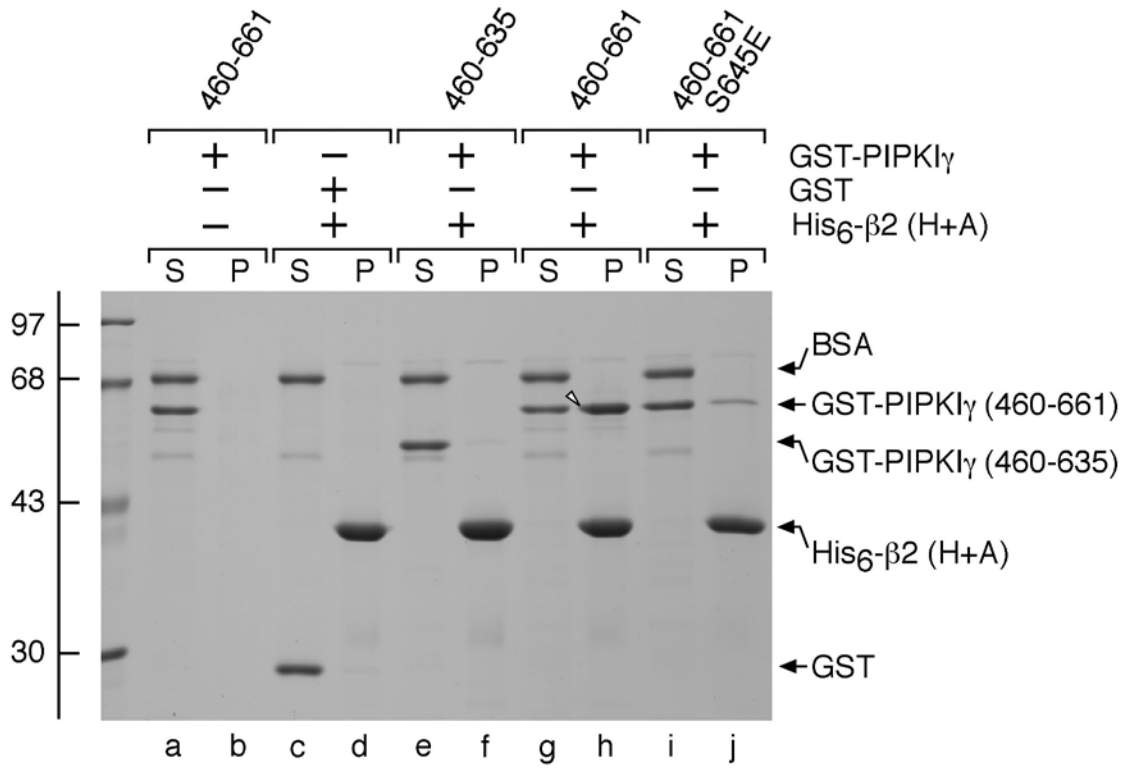

Figure 2.5: PIPKIγ661 directly engages the β2 appendage.
Approximately 5 μg of His_6-tagged β2 hinge + appendage (H +A; lanes c-) immobilized on Ni-NTA-agarose was incubated with ~25 μg GST (lanes c and d), GST-PIPKIγ (460-635) (lanes e and f), GST-PIPKIγ (460-661) (lanes g and h) or GST-PIPKIγ (460-661 with a phosphomimetic S645E mutation) (lanes i and j) as indicated in the presence of carrier BSA. GST-PIPKIγ (460-661) was also incubated with Ni-NTA-agarose alone (lanes a and b). After centrifugation, aliquots of ~2.5% of each supernatant (S) and ~25% of each washed pellet (P) were resolved by SDS-PAGE and stained with Coomassie blue.

only the lower band, which corresponds to the unphosphorylated protein, binds to β2, consistent with previous findings (Nakano-Kobayashi *et al.*, 2007).

2.3.4 PIPKIγ661 directly engages the β2 appendage

In binary interaction assays, when immobilized His_6-tagged AP-2 β2 hinge + appendage is incubated with soluble GST-PIPKIγ (460-661), the two proteins interact and PIPKIγ is recovered in the pellet with the β2 hinge + appendage (Figure 2.5, lane h). Conversely, the C-terminal segment of the PIPKIγ short-splice isoform (GST-PIPKIγ(460-635)) does not bind the β2 hinge + appendage and remains in the supernatant (Figure 2.5, lane e), as does GST (lane c). This corroborates a direct interaction between PIPKIγ661 and the β2 appendage mediated by the 26 amino acid extension of the long splice isoform. Furthermore, a phosphomimetic S645E mutant in a GST-PIPKIγ (460-661) background has a sharply reduced ability to bind β2 (Figure 2.5, lane j) in the direct interaction assay.

2.3.5 PIPKIγ661 binds the β2 appendage sandwich domain

Like the AP-2 α appendage, the β2 appendage plays an integral role in recruiting CLASPs and accessory factors to sites of endocytosis by acting as an organizational hub (Owen *et al.*, 2000; Edeling *et al.*, 2006a; Schmid *et al.*, 2006; Keyel *et al.*, 2008). The β2 appendage contains two rigidly apposed functional surfaces: an N-terminal, β-sheet-containing sandwich subdomain and a C-terminal, α-helix- and β-sheet-containing platform subdomain (Owen *et al.*, 2000). Mutation and co-crystallization studies reveal the two sites bind to discrete sets of endocytic

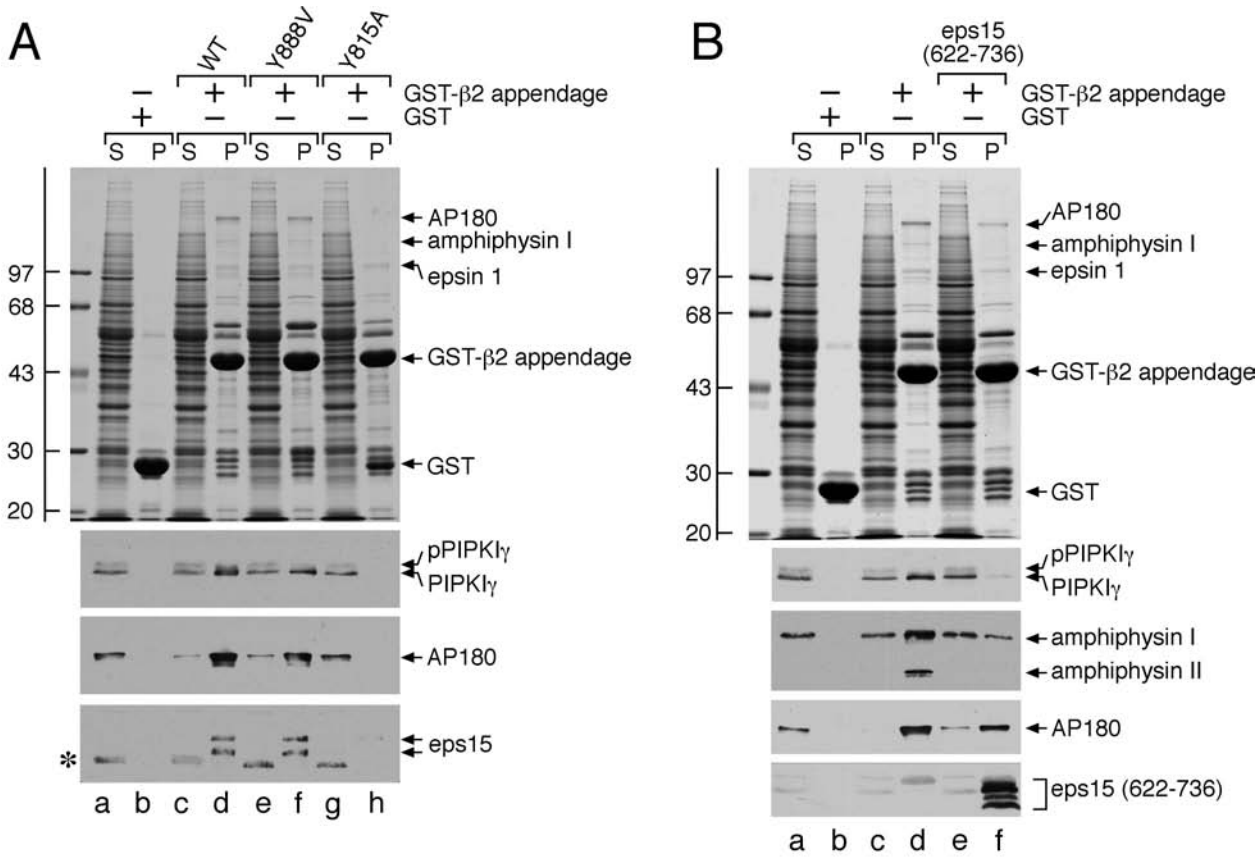

Figure 2.6: PIPKIγ661 physically contacts the sandwich subdomain of the AP-2 β2 appendage.
(A) Approximately 100 μg of GST (lanes a and b), GST-β2 appendage (lanes c and d) or GST-β2 Y888V (lanes e and f) or Y815A (lanes g and h) mutant appendage immobilized on gluthathione-Sepharose was incubated with rat brain cytosol as indicated. After centrifugation, aliquots of ~1.5% of each supernatant (S) and ~10% of each washed pellet (P) were resolved by SDS-PAGE and either stained with Coomassie blue or transferred to nitrocellulose. Portions of the blots were probed with anti-PIPKIγ mAb clone 12, anti-AP180 mAb clone 34, or affinity-purified anti-eps15 antibodies, and only the relevant portions shown. The slowed migration of the phosphorylated from of PIPKIγ (pPIPKIγ) is indicated, as is the location of the Coomassie-blue stained epsin 1 band. (B) Approximately 100 μg of GST (lane a and b) or GST-β2 appendage (lanes c-f) immobilized on glutathione-Sepharose was incubated with rat brain cytosol in the absence or presence of 2 μM eps15 (622-736) competitor polypeptide (lanes e and f) as indicated. After centrifugation, aliquots of ~1.5% of each supernatant (S) and ~10% of each washed pellet (P) were resolved by SDS-PAGE and either stained with Coomassie blue or transferred to nitrocellulose. Portions of the blots were probed with anti-PIPKIγ mAb clone 12, anti-amphiphysin mAb clone 15, anti-AP180 mAb clone 34, or anti-eps15 antibodies, and only the relevant portions shown. The slowed migration of the phosphorylated from of PIPKIγ (pPIPKIγ) is indicated, as is the location of the Coomassie-blue stained epsin 1 band.

proteins (Edeling *et al.*, 2006a; Schmid *et al.*, 2006). To determine whether PIPKIγ661 interacts with either of these sites, we mutated select residues critical for binding at each surface. A Y888V mutation in the β2 platform subdomain has no effect on the binding of PIPKIγ or the established sandwich-binding partners AP180 and eps15 (Figure 2.6A, lane d and f). This alteration does reduce epsin 1 binding (49,50). By contrast, a Y815A sandwich subdomain mutation completely eliminates the binding of PIPKIγ661, AP180, and eps15, while epsin 1 binding is essentially unaffected (Figure 2.6A, lane h). These results indicate that PIPKIγ661 associates directly with the sandwich subdomain of the β2 appendage.

Competition experiments in which the immobilized GST-β2 is incubated with cytosol and an eps15 polypeptide encompassing the region co-crystallized with β2 appendage at the sandwich site (50) confirm the contact site. Alone, the GST-β2 recovers the typical cohort of soluble endocytic proteins (Figure 2.6B, lane d). Addition of the eps15 polypeptide to the mixture substantially reduces PIPKIγ661 and amphiphysin I and -II binding (Figure 2.6B, lane f). AP180 binding is clearly reduced, although not to the same extent as the kinase (lane f).

2.3.6 Delineation of the PIPKIγ661 AP-2 interaction motif

Since the PIPKIγ (460-661) but not the -(460-635) binds to the AP-2 β2 appendage, we evaluated whether just the terminal 28 amino acids of the human PIPKIγ668 variant (also termed PIP5K Iγ90 (Di Paolo *et al.*, 2002)) are sufficient for this interaction. AP-2 binds to only the 28-residue extension considerably weaker than in the context of the 460-661 fragment in a GST pull-down assay (Figure 2.6, compare lane f and h). Yet, in the same assay, the extent of the association with talin is similar for both GST fusions (Figure 2.6). This could indicate

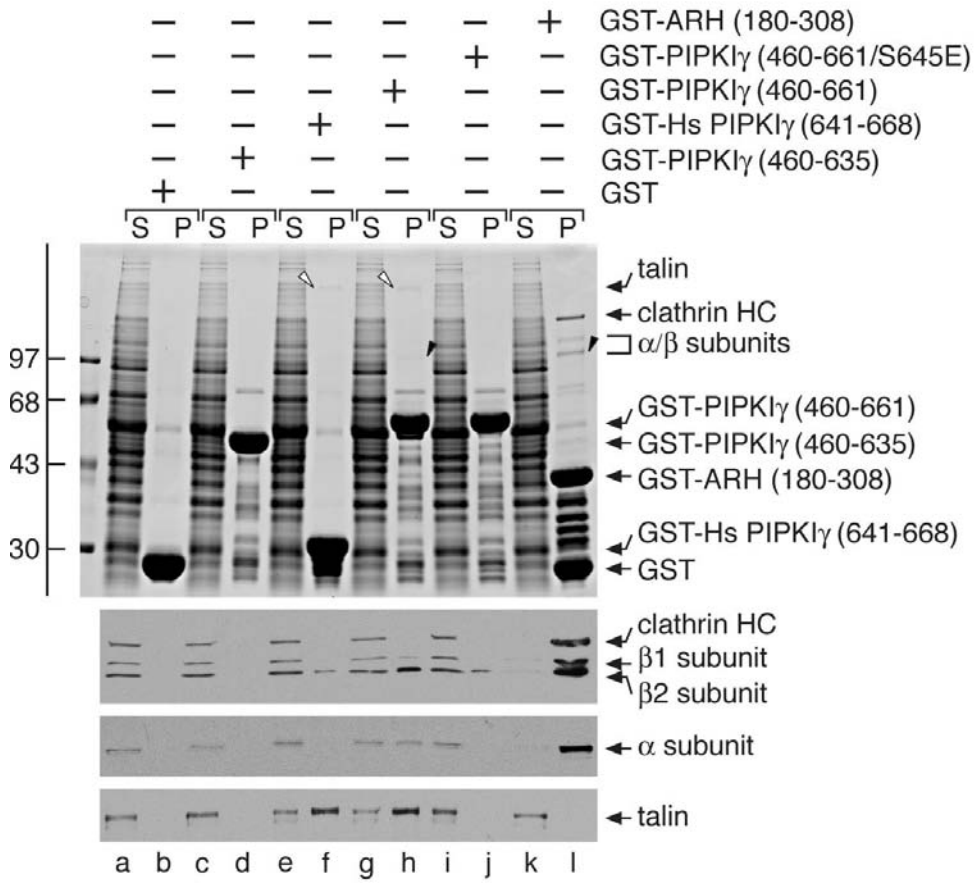

Figure 2.7: The alternatively spliced C terminus of PIPKIγ alone does not contain all the AP-2 binding information.

Approximately 200 μg of GST (lanes a and b), GST-PIPKIγ (460-635) (lanes c and d), GST-Hs PIPKIγ (641-668) (lanes e and f), GST-PIPKIγ (460-661) (lanes g and h), GST-PIPKIγ (460-661/S645E) (lanes i and j) or GST-ARH (180-308) (lanes k and l) immobilized on glutathione-Sepharose was incubated with rat brain cytosol as indicated. After centrifugation, aliquots of ~1.5% of each supernatant (S) and ~10% of each washed pellet (P) were resolved by SDS-PAGE and either stained with Coomassie blue or transferred to nitrocellulose. Portions of the blots were probed with anti-clathrin heavy chain (HC) mAb TD.1 and anti-β1/β2 subunit mAb 100/1, anti-AP-2 α subunit mAb C4, or anti-talin mAb 8d4, and only the relevant portions shown. The position of talin (red arrowhead) and the AP-2 β2 and α subunits (black arrowhead) on the stained gel is shown. Note that PIPKIγ661 clearly binds to the β2 appendage of AP-2 more weakly than ARH, which has a K_D for AP-2 of ~2 μM (Edeling *et al.*, 2006a; Schmid *et al.*, 2006).

that while talin binds only the 26/28 amino acid extension in PIPKIγ661/668, AP-2 may bind primarily to this same region but depend on a distinct secondary structural element or be stabilized by an adjacent region(s) within residues 460-635.

Using controlled tryptic proteolysis of bacterially expressed 460-635 and 460-661 polypeptides derived from PIPKIγ, a hierarchical sequence of degradation fragments is observed (Figure 2.8A). Immunoblots with either a mAb that detects both PIPKIγ635 and -661 or affinity-purified antibodies that detect the 26 amino-acid extension of PIPKIγ661 reveal that both epitopes are efficiently removed by low concentrations of trypsin. This is in contrast to the stably folded bacterial chaperone DnaK, co-purified with the PIPKIγ peptides, that is unaffected by lower trypsin concentrations (Figure 2.8A). Neither antibody reacts with the more stable PIPKIγ fragments. Additionally, circular dichroism analysis of the 460-635 and 460-661 protein segments indicate that both are essentially unstructured (Figure 2.8B). Indeed, the 460-661 polypeptide is resistant to denaturation at 100°C, as are the C-terminal portions of the natively unstructured endocytic proteins epsin 1 and AP180 (Kalthoff *et al.*, 2002). We believe the intrinsic disorder of the C-terminal region of PIPKIγ makes it unlikely that the difference in AP-2 binding between the GST-PIPKIγ (460-661) and GST-Hs PIPK1γ (641-668) (equivalent to the mouse 636-661) is due to secondary structural elements. Instead, residues at the junction of the 635 and 661 splice isoforms may contribute to AP-2 β2-appendage binding. To examine this further, we used a third rodent PIPKIγ splice variant, PIPKIγ687 (also termed PIPkin IγC (Giudici *et al.*, 2004) or PIPkin Ig93 (Giudici *et al.*, 2006)), which contains a distinct 26 amino-acid insert positioned between the C-terminus of PIPKIγ635 and the N-terminus of PIPKIγ661 26 amino-acid insert (Figure 2.9). Interestingly, separating the C-terminal end of the 635 splice isoform from the 661 insert in this configuration diminishes AP-2 binding to roughly that seen

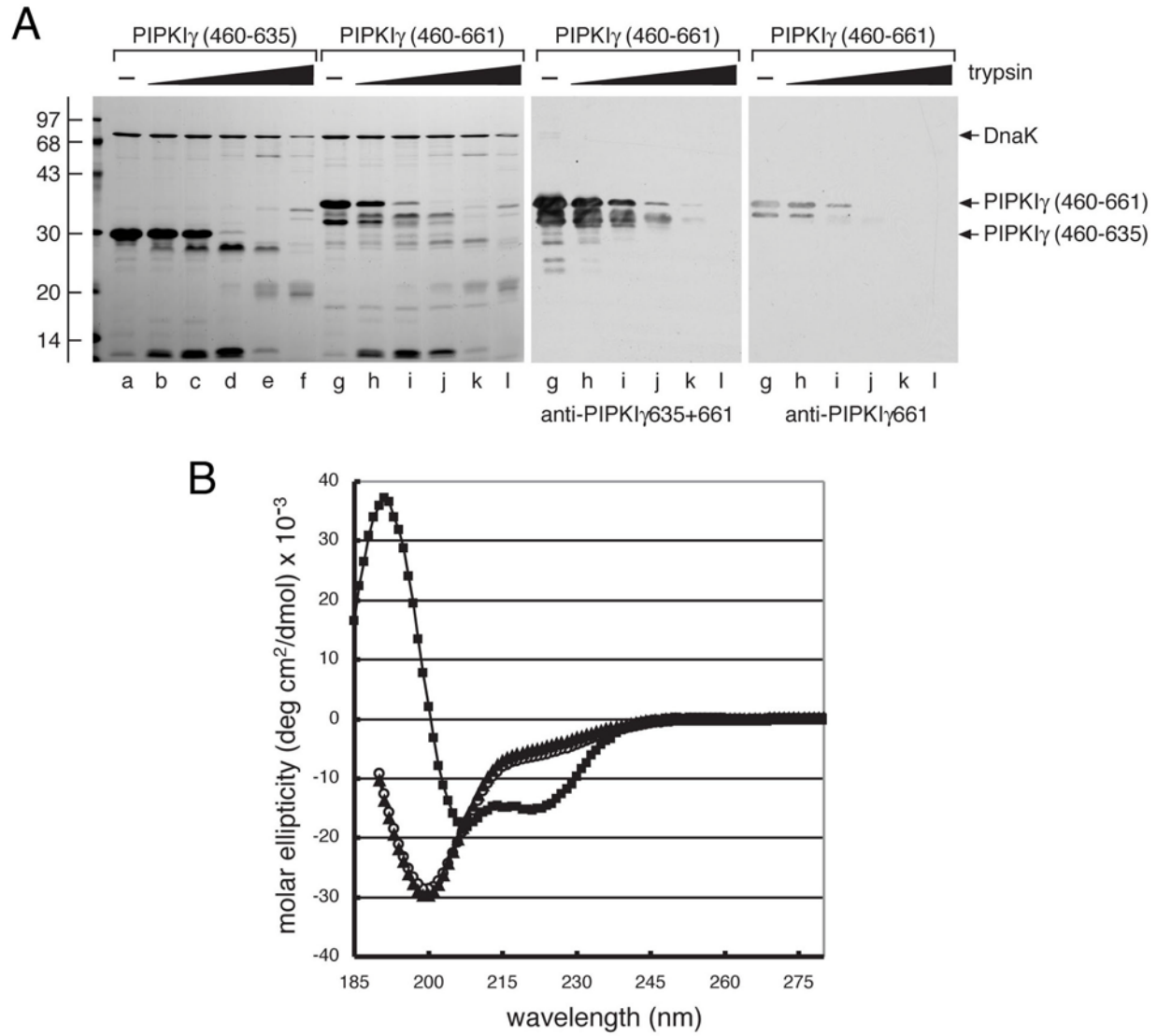

Figure 2.8: The PIPKIγ661 C terminus lacks secondary structure.
(A) Aliquots (20 μg) of PIPKIγ (460-635) (lanes a-f) or PIPKIγ (460-661) (lanes g-l) were incubated alone or with 1:5 serial fivefold dilutions of trypsin (0.6-375 ng) in 50 mM Tris pH 8.0, 150 mM NaCl, 5 mM $CaCl_2$, 1 mM DTT at 37°C for 1 hour. Proteolysis was stopped by the addition of 95°C SDS sample buffer and aliquots of 10% of each reaction resolved by SDS-PAGE either stained with Coomassie blue or transferred to nitrocellulose. The PIPKIγ (460-661) portion of the blot was probed with anti-PIPKIγ mAb clone 12 that recognizes both isoforms or with an affinity purified antibody that recognizes only the PIPKIγ661 isoform. (B) Circular dichroism spectra of PIPKIγ (460-635) (open circles), PIPKIγ (460-661) (triangles), and epsin 1 ENTH domain (squares) polypeptides were measured in 25 mM potassium phosphate + 1 mM DTT. Measurements were made from 280 nm to 185 nm at 1 nm increments and the spectra were baseline corrected and represent the average of five (PIPKIγ) or three (ENTH) runs. Note the signature α-helical features of the globular ENTH domain compared with the unstructured PIPKIγ polypeptides.

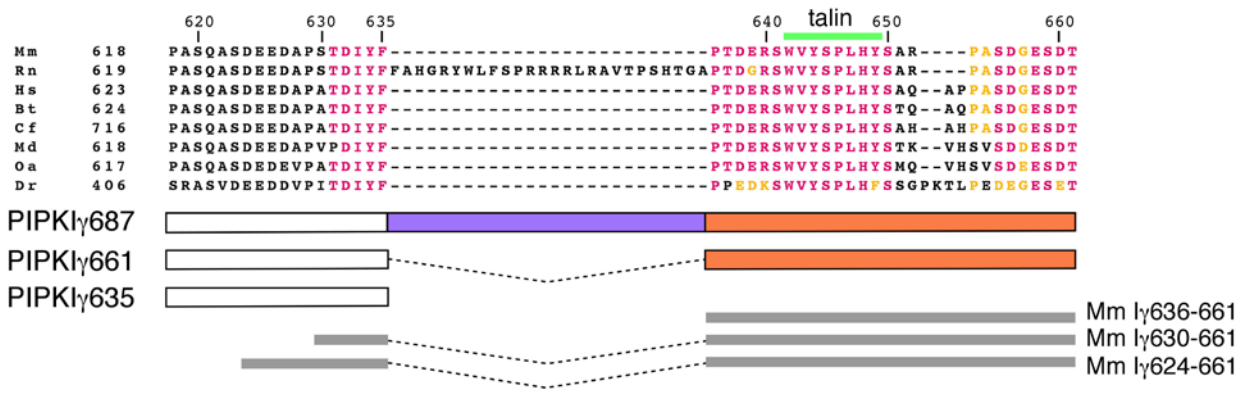

Figure 2.9: Schematic of the three PIPKIγ splice variants.
Primary sequence alignment of the C-terminal segment of PIPKIγ isoforms from various species; murine (Mm; accession number: NP_032870.1), rat (Rn; NP_001009967.2), human (Hs; NP_036530.1), bovine (Bt; XP_585653.4), feline (Cf; XP_542172.2), opossum (Md; XP_001363745.1), platypus (Oa; XP_001511349.1) and zebrafish (Dr; XP_683392.3). Identical residues colored pink and conservatively substituted residues yellow. The location of the talin-binding motif is indicated above, and the GST-fusion proteins spanning the junction between the PIPKIγ635 and -661 isoforms tested below.

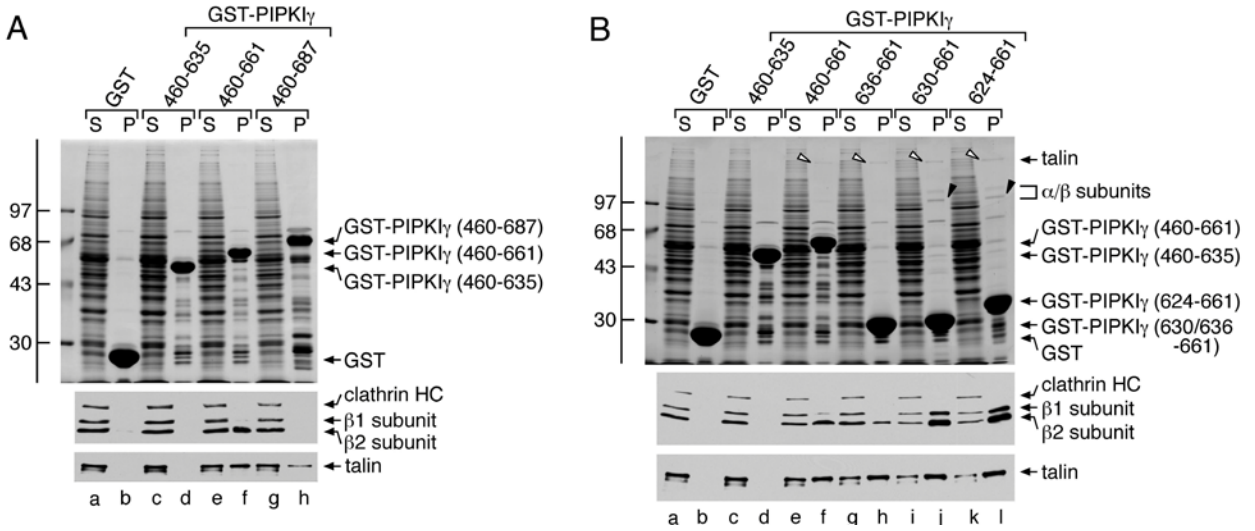

Figure 2.10: Differing partner binding properties of the three PIPKIγ splice variants.
(A) Approximately 200 μg of GST (lanes a and b), GST-PIPKIγ (460-635) (lanes c and d), GST-PIPKIγ (460-661) (lanes e and f), or GST-PIPKIγ (460-687) (lanes g and h) immobilized on glutathione-Sepharose was incubated with rat brain cytosol as indicated. After centrifugation, aliquots of 1.5% of each supernatant (S) and 10% of each washed pellet (P) were resolved by SDS-PAGE and either stained with Coomassie blue or transferred to nitrocellulose. Portions of the blots were probed with anti-clathrin heavy chain (HC) mAb TD.1 and anti-β1/β2 subunit mAb 100/1, or with anti-talin mAb 8d4 and only the relevant portions shown. (B) Approximately 200 μg of GST (lanes a and b), GST-PIPKIγ (460-635) (lanes c and d), GST-PIPKIγ (460-661) (lanes e and f), GST-PIPKIγ (636-661) (lanes g and h), GST-PIPKIγ (630-661) (lanes i and j) , or GST-PIPKIγ (624-661) (lanes k and l) immobilized on glutathione-Sepharose was incubated with rat brain cytosol as indicated. After centrifugation, aliquots of 1.5% of each supernatant (S) and 10% of each washed pellet (P) were resolved by SDS-PAGE and either stained with Coomassie blue or transferred to nitrocellulose. Portions of the blots were probed with anti-clathrin heavy chain (HC) mAb TD.1 and anti-β1/β2 subunit mAb 100/1, or anti-talin mAb 8d4, and only the relevant portions shown. The position of talin (open arrowhead) and the AP-2 β2 and α_C subunits (black arrowhead) on the stained gel is shown.

with the GST-PIPKIγ (460-635) alone (Figure 2.10A). This indicates that residues proximal to the 26 amino-acid insert may contribute to the engagement of the β2 appendage of the AP-2 adaptor. Indeed, a pair of constructs that include the last six (GST-PIPKIγ (630-661)) or twelve (GST-PIPKIγ (624-661)) residues of PIPKIγ635 have dramatically increased AP-2 binding capability compared with the mouse PIPKIγ661 C-terminus alone fused to GST (GST-PIPKIγ636-661)) (Figure 2.10B). There is little change in the interaction with talin for these fusion proteins however. These results confirm then that the extreme C-terminal region of the PIPKIγ635 splice isoform contributes to binding to the AP-2 β2 appendage but, alone, is insufficient for associating with AP-2.

2.3.7 The β2 sandwich subdomain contact surface

A yeast two-hybrid interaction screen with the PIPKIγ 630-661 peptide fused to the DNA binding domain of Gal4p corroborates that this sequence engages the sandwich subdomain of the β2 appendage. Transformed AH109 yeast grow on quadruple dropout selection plates only when expressing both the PIPKIγ (630-661) and β2 appendage but not either protein alone (Figure 2.11A). Site-directed mutagenesis of selected residues on the β2 appendage shows a Y888V mutation, which disrupts the platform interaction site (Owen *et al.*, 2000), has no effect on PIPKIγ interaction. By contrast the Y815A substitution, as well as alteration of several other side chains that contribute to the sandwich site interaction surface (Gln756, Gln804, Ala806 and Lys808; Figure 2.11B) (Edeling *et al.*, 2006a; Schmid *et al.*, 2006) strongly impede the binding to the PIPKIγ C-terminal 630-661 polypeptide (Figure 2.11A).

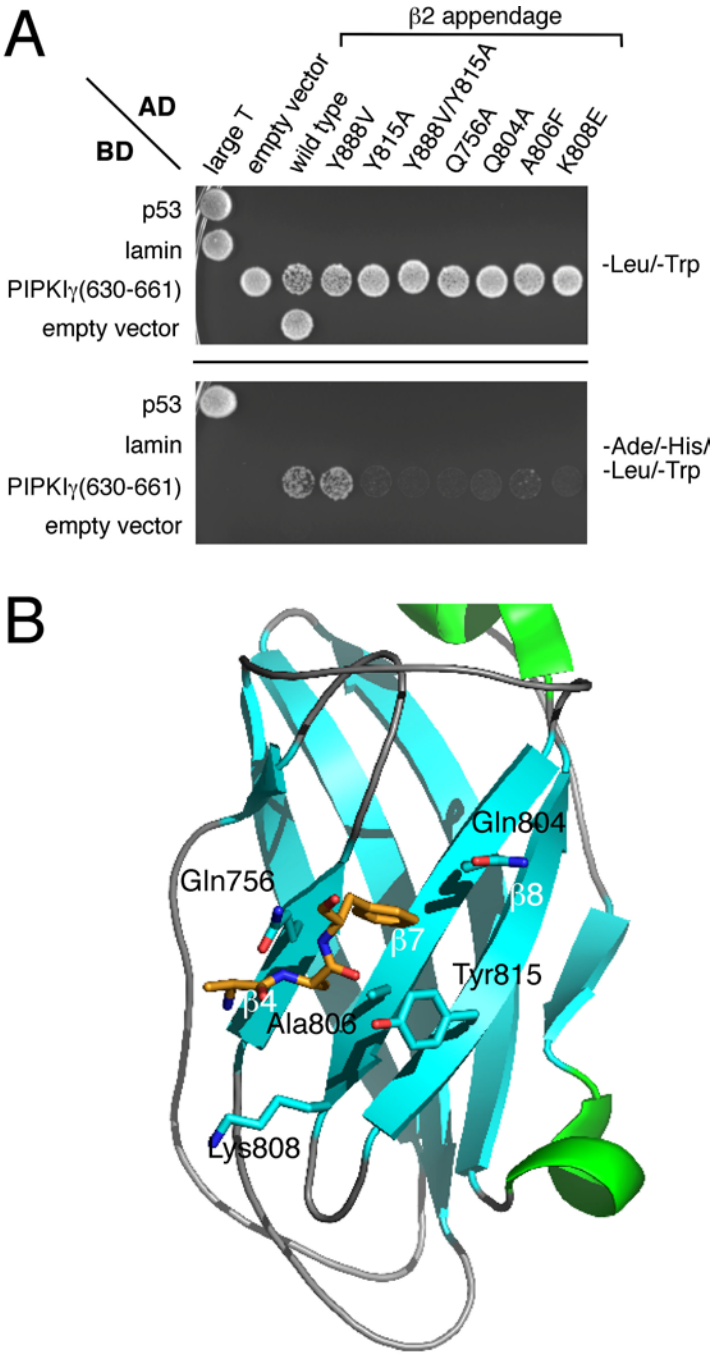

Figure 2.11: AP-2-PIPKIγ interaction in a yeast two-hybrid assay.
(A) *Saccharomyces cerevisiae* strain AH109 transformed with the indicated Gal4 pGBKT7 binding domain (*BD*) pGADT7 activation domain (*AD*) plasmid combinations were spotted onto SD minimal medium plates lacking either Leu and Trp, or Ade, His, Leu, and Trp and grown at 30°C. (B) Ribbon representation (PDB accession: 2G30) of the AP-2 β2 appendage sandwich subdomain indicating the location of important side chains (blue, nitrogen; red, oxygen) involved in accommodating the PIPKIγ661 C-terminal interaction motif. Shown in stick representation (gold) is the location of co-crystallizing AAF peptide that demarcates a portion of the binding surface upon the β2 appendage sandwich subdomain.

2.3.8 Pinpointing key anchor residues in PIPKIγ necessary for β2 appendage engagement

Having delineated the AP-2 β2 interaction motif in PIPKIγ661 to a tract of ~20 residues, we next tested the importance of selected hydrophobic side chains within this region. This is because for all characterized adaptors and accessory factors that associate with the α and β2 appendages, aromatic residue-containing motifs are critically important binding determinants, such as the DP[FW] motif in eps15 and epsin (Maldonado-Baez and Wendland, 2006), the WXX[FW]X[DE]$_n$ motif in SJ170 (Jha *et al.*, 2004), NECAP (Ritter *et al.*, 2004) and stonin 2 (Mishra *et al.*, 2004; Walther *et al.*, 2004), and the [DE]$_n$X$_{1-2}$FXX[FL]XXXR motif in ARH and β-arrestin (Edeling *et al.*, 2006a; Schmid *et al.*, 2006). There are five phylogenetically conserved aromatic residues in the mapped PIPKIγ AP-2 binding region (Figure 2.9 and 2.12A). Two, Trp642 and Tyr644, are vicinal to Ser645, which inhibits AP-2 binding when phosphorylated (Figure 2.5) (Nakano-Kobayashi *et al.*, 2007). Both a W642A mutation and a more conservative phenylalanine substitution (W642F) eliminate β2 binding (Figure 2.12B and 2.13A, lanes f and h) in either binary GST pull-down assays (Figure 2.12B) or with rat brain cytosol (Figure 2.13A). Likewise, a Y644A change eliminates β2-appendage binding (Figure 2.12B and 2.13A, lane j) but the conservative Y644F mutation reduces, but does not abolish, β2 engagement (Figure 2.12B and 2.13A, lane l). This finding is significant because alignment of the sequences that follow the C-terminal IYF of the Iγ635 isoform in either the Iγ661 or Iγ687 variants shows some obvious similarities (Figure 2.12A). The longest Iγ687 insert has a Trp positioned analogously to Trp642 in Iγ661 and a Phe at the position equivalent to Tyr644. In fact, five of the eleven N-terminal residues are identical between the two alternatively spliced proteins and two conservatively substituted (Figure 2.12A). Nevertheless, the Iγ687 protein does not bind to AP-2

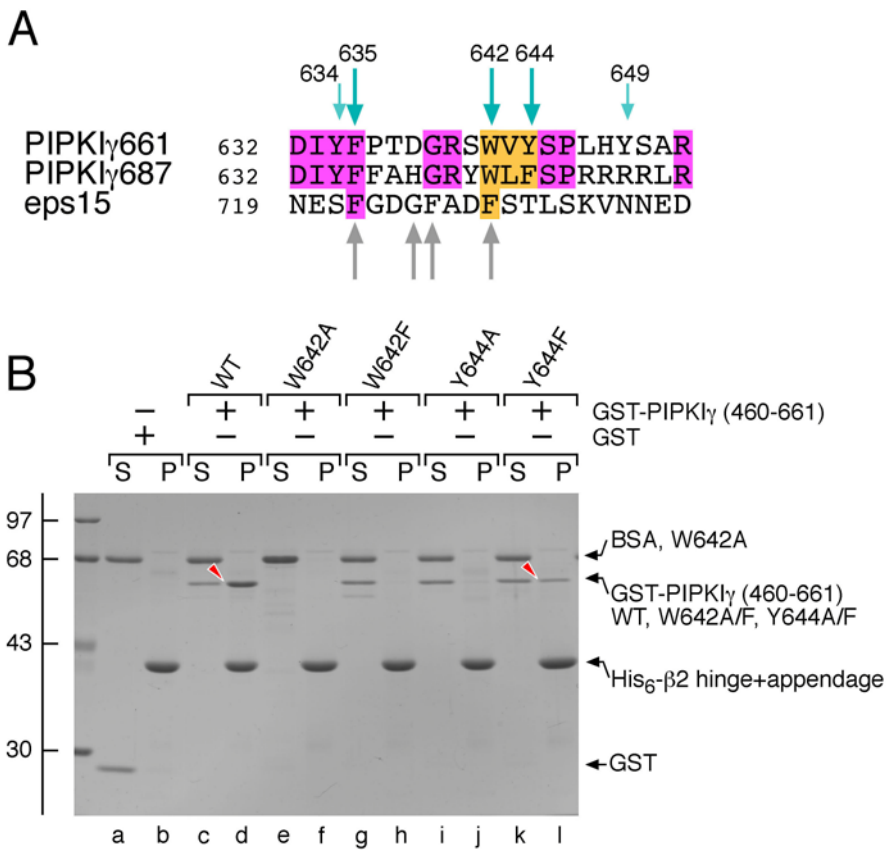

Figure 2.12: Delineation of key anchor residues that mediate PIPKIγ661 binding to the β2 appendage.

(A) Primary sequence alignment of the two PIPKIγ 26 amino acid inserts and comparison with a tract from eps15 that also bind to the AP-2 β2 appendage sandwich subdomain. (B) Approximately 40 μg of His_6-tagged β2 hinge + appendage immobilized on Ni-NTA-agarose was incubated with ~10 μg GST (lanes a and b), GST-PIPKIγ (460-661) wild type (WT, lanes c and d), or GST-PIPKIγ (460-661) containing W642A (lanes e and f), W642F (lanes g and h), Y644A (lanes i and j), or Y644F (lanes k and l) mutations in the presence of carrier BSA. After centrifugation, aliquots of ~4% of each supernatant (S) and ~25% of each washed pellet (P) were resolved by SDS-PAGE and stained with Coomassie blue.

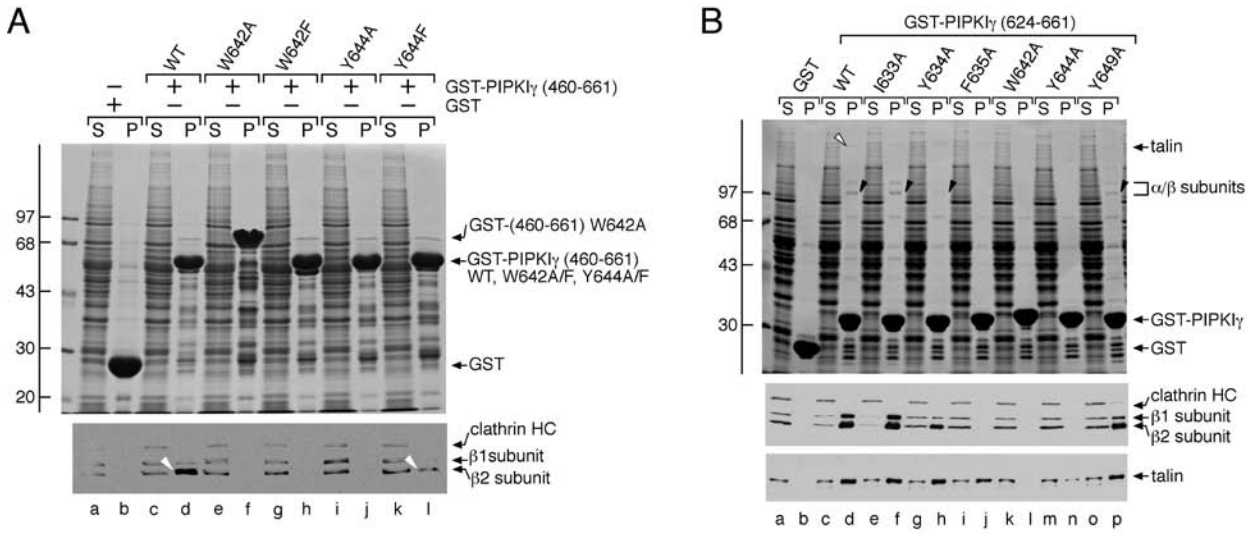

Figure 2.13: Delineation of key anchor residues that mediate PIPKIγ661 binding to the β2 appendage, continued.

(A) Approximately 250 μg GST (lanes a and b), GST-PIPKIγ (460-661) wild type (WT, lanes c and d), or GST-PIPKIγ (460-661) containing W642A (lanes e and f), W642F (lanes g and h), Y644A (lanes i and j) or Y644F (lanes k and l) mutations immobilized on glutathione-Sepharose was incubated with rat brain cytosol as indicated. After centrifugation, aliquots of ~3.5% of each supernatant (S) and ~10% of each pellet (P) were resolved by SDS-PAGE and either stained with Coomassie blue or transferred to nitrocellulose. A portion of the blot was probed with anti-β1/β2-subunit mAb 100/1 and anti-clathrin heavy chain (HC) mAb TD.1. (B) Approximately 100 μg GST (lanes a and b), GST-PIPKIγ (624-661) wild type (WT, lanes c and d) or GST-PIPKIγ (624-661) containing I633A (lanes e and f), Y634A (lanes g and h), F635A (lanes i and j), W642A (lanes k and l), Y644A (lanes m and n) or Y649A (lanes o and p) mutations immobilized on glutathione-Sepharose was incubated with rat brain cytosol as indicated. After centrifugation, aliquots of ~1.5 supernatant (S) and ~10% of each pellet (P) were resolved by SDS-PAGE and either stained with Coomassie blue or transferred to nitrocellulose. Portions of the blot were probed with anti-β1/β2-subunit mAb 100/1 and anti-clathrin heavy chain (HC) mAb TD.1 or anti-talin mAb 8d4.

efficiently (Figure 2.10A), presumably in part because of the natural Phe-for-Tyr substitution.

The pair of aromatics at the end of the Iγ635 sequence are also important; a double Tyr634 and Phe635 to Ala substitution (YF→AA) in the context of the GST-Iγ (460-661) fusion protein diminishes AP-2 binding to the level seen with just the 26 amino-acid extension of the Iγ661 isoform (data not shown). Separate Y634A and F635A mutations in the GST-PIPKIγ (624-661) fusion backbone reveal that Phe635 is critical while Tyr634 is somewhat less so, as there is still some AP-2 bound to the fusion protein with a Y364A mutation (Figure 2.13B). By contrast, converting Ile633 to Ala does not diminish the binding of AP-2 when compared with the wild-type protein. As seen with the GST-Iγ (460-661) fusions, Trp642 and Tyr644 are vital residues for β subunit engagement. The Y649A switch, located 13 residues after the intersection between the 635 and 661 splice forms, shows that this amino acid also contributes weakly to AP-2 binding. The lack of a bulky aromatic residue equivalent to Tyr649 in the Iγ687 longest-splice isoform, as well as other substitutions, may also contribute to the poor interaction with AP-2. This set of mutations has a different effect on talin binding. Only the W642A and Y644A mutants exhibit greatly diminished binding to cytosolic talin (Figure 2.13B), which is in accord with the mapped talin binding region (see Figure 2.9) (Di Paolo *et al.*, 2002; Ling *et al.*, 2002; Ling *et al.*, 2003) and structural studies of the talin FERM F3 subdomain engaged with PIPKIγ peptide (de Pereda *et al.*, 2005; Kong *et al.*, 2006). Altogether, these data indicate that aromatic residues contribute to β2-sandwich subdomain binding possibly through inserting into complementary hydrophobic surfaces in the appendage. The results also confirm the important role of Tyr644 in AP-2 binding (Bairstow *et al.*, 2006), but argue strongly against the kinase-AP-2 interaction being YXXØ-mediated, because those interactions are critically dependent on the

proximal tyrosine that cannot be replaced functionally by phenylalanine (Collawn *et al.*, 1990; Jadot *et al.*, 1992).

2.3.9 Clathrin is displaced from the AP-2 β2 appendage by PIPKIγ661

An additional endocytic coat protein that binds to the sandwich subdomain of the AP-2 β2 appendage is the clathrin heavy chain (Owen *et al.*, 2000; Edeling *et al.*, 2006a; Knuehl *et al.*, 2006; Keyel *et al.*, 2008). Rather than utilizing a short unstructured interaction motif to contact the β2 appendage, the clathrin heavy chain interaction surface is located within the distal leg (Knuehl *et al.*, 2006), comprised of repeating antiparallel α-helices in a solenoid-type fold (ter Haar *et al.*, 1998; Ybe *et al.*, 1999). Although clathrin is a functional trimer, we nevertheless examined whether PIPKIγ661 and clathrin compete for a common binding surface on the β2 appendage. Supplementing whole cytosol with a PIPKIγ 624-661 polypeptide interferes with clathrin binding to immobilized GST-β2 appendage in a dose-dependent manner (Figure 2.14A). The peptide competitor also abolishes endogenous PIPKIγ661 and AP180 binding, but leaves epsin 1 still attached to the β2 appendage, further arguing that it binds to the sandwich subdomain. By contrast, adding a Iγ 624-661 peptide containing a W642A substitution has a weak, if any effect on clathrin, PIPKIγ661 or AP180 binding (Figure 2.14A).

If clathrin engagement by the larger β2 subunit hinge + appendage domains is followed under the same conditions, the triskelia bind much more avidly to the immobilized GST-β2 fragment (Figure 2.14B, compare lanes f and j). The Iγ 624-661 peptide now competes with clathrin only weakly (Figure 2.14B, compare lanes j and l). Yet the added excess peptide does effectively compete PIPKIγ and AP180 off the β2 hinge + appendage,

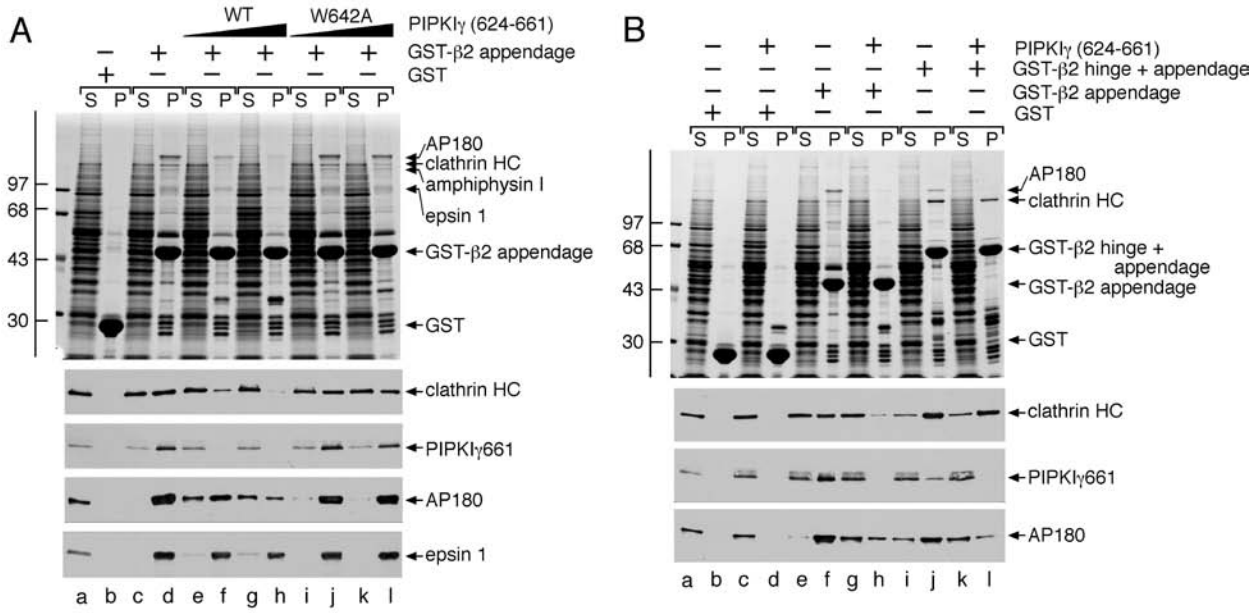

Figure 2.14: Mutually exclusive engagement of the β2 appendage sandwich by either PIPKIγ661 or clathrin.

(A) Approximately 100 μg GST (lanes a and b) or GST-β2 appendage (lanes c-l) immobilized on glutathione-Sepharose was incubated with rat brain cytosol alone (lanes a-d) or cytosol supplemented with 46 μM wild type (lanes e and f) or W642A (lanes i and j) PIPKIγ (624-661) peptide or 139 μM wild type (lanes g and h) or W642A (lanes k and l) PIPKIγ (624-661) peptide. After centrifugation, aliquots of ~1.5% of each supernatant (S) and ~10% of each washed pellet (P) were resolved by SDS-PAGE and either stained with Coomassie blue or transferred to nitrocellulose. Portions of the blots were probed with anti-clathrin heavy chain (HC) mAb TD.1, anti-PIPKIγ mAb clone 12, anti-AP180 mAb clone 34 or affinity-purified anti-epsin 1 antibodies. Notice that although epsin 1 binding to the β2 appendage is affected by the addition of the PIPKIγ peptide, particularly at the highest concentration, the sandwich-binding partners are clearly much more sensitive to the competitor. (B) Approximately 100 μg GST (lanes a-d), GST-β2 appendage (lanes e-h) or GST-β2 hinge + appendage (lanes i-l) immobilized on glutathione-Sepharose was incubated with rat brain cytosol alone (lanes a, b, e, f, i and j) or rat brain cytosol supplemented with 113 μM PIPKIγ (624-661) polypeptide (lanes c, d, g, h, k and l). After centrifugation, aliquots of ~1.5% of each supernatant (S) and ~10% of each washed pellet (P) were resolved by SDS-PAGE and either stained with Coomassie blue or transferred to nitrocellulose. Portions of the blots were probed with anti-clathrin heavy chain (HC) mAb TD.1, anti-PIPKIγ mAb clone 12, or anti-AP180 mAb clone 34.

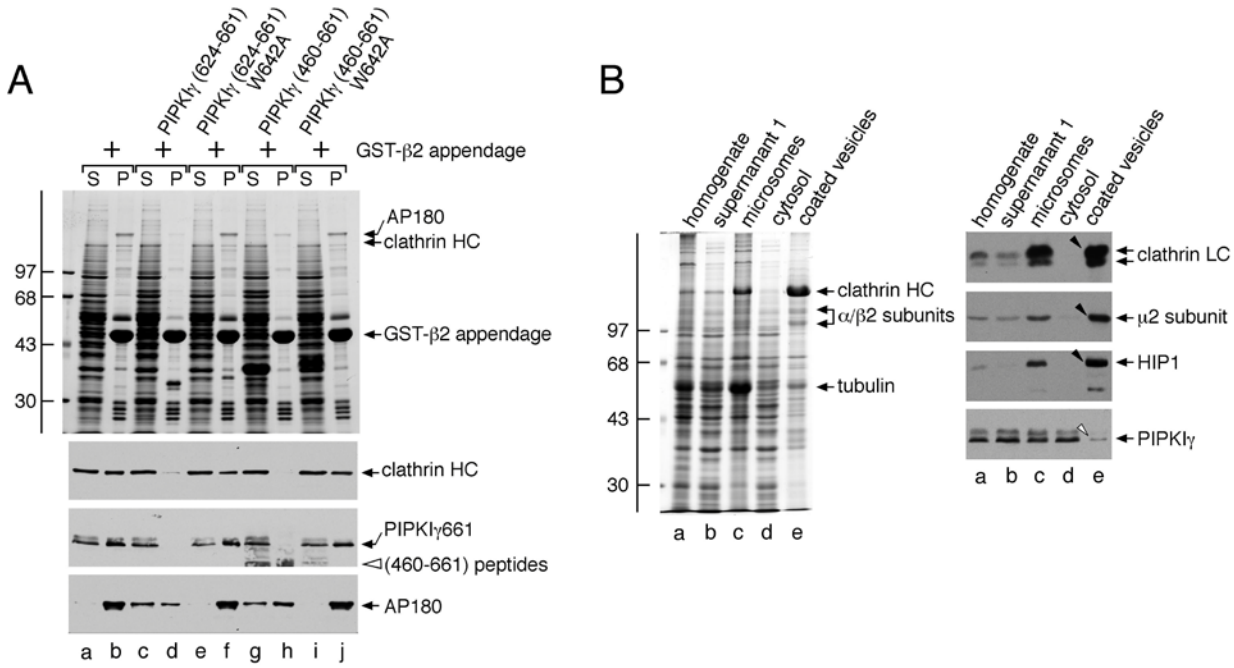

Figure 2.15: Mutually exclusive engagement of the β2 appendage sandwich by either PIPKIγ661 or clathrin, continued.

(A) Approximately 100 μg GST-β2 appendage immobilized on glutathione-Sepharose was incubated with rat brain cytosol alone (lanes a and b) or cytosol supplemented with 113 μM wild type (lanes c and d) or W642A (lanes e and f) PIPKIγ (624-661) polypeptide or 113 μM wild type (lanes g and h) or W642A (lanes i and j) PIPKIγ (460-661) polypeptide. After centrifugation, aliquots of ~1.5% of each supernatant (S) and ~10% of each washed pellet (P) were resolved by SDS-PAGE and either stained with Coomassie blue or transferred to nitrocellulose. Portions of the blots were probed with anti-clathrin heavy chain (HC) mAb TD.1, anti-PIPKIγ mAb clone 12, or anti-AP180 mAb clone 34. (B) Fractions (20 μg) from a preparation of rat brain clathrin-coated vesicles were resolved by SDS-PAGE and either stained with Coomassie blue or transferred to nitrocellulose. Portions of the blots were probed with anti-clathrin light chain (LC) mAb Cl57.3, anti-μ2 subunit serum, affinity-purified anti-HIP1 antibodies, or anti-PIPKIγ mAb clone 12. Only the relevant portions are shown. Note the strong enrichment of clathrin, AP-2 and HIP1 (arrowheads) but exclusion PIPKIγ (open arrowhead) in the coated-vesicle fraction.

however (Figure 2.9B, compare lanes j and l). This selectively refractory behavior is because the extra β2 hinge region contains additional clathrin binding determinants that contact the N-terminal β-propeller of the clathrin heavy chain (Gallusser and Kirchhausen, 1993; Owen *et al.*, 2000; ter Haar *et al.*, 2000). The additional points of contact increase the apparent affinity of clathrin for the β2 chain versus PIPKIγ661 or eps15 (Cupers *et al.*, 1998; Edeling *et al.*, 2006a). Thus, the AP-2 β2 subunit binds more tightly to multivalent clathrin trimers than monovalent PIPKIγ661.

Like the PIPKIγ 624-661 segment, the whole C-terminal Iγ 460-661 polypeptide also interferes with clathrin binding in the presence of cytosol, while the W642A mutant does not (Figure 2.15A). A corollary of these results is that clathrin engagement could displace prebound PIPKIγ661 from AP-2 as the lattice assembly process progresses toward the deeply invaginated state. Circumstantial evidence for this contention comes from the marked de-enrichment of PIPKIγ661 in preparations of rat brain clathrin-coated vesicles (Figure 2.15B) (Wenk *et al.*, 2001). These results imply that the temporal residence of PIPKIγ661 at the bud site may be determined by the extent of clathrin lattice polymerization.

2.4 DISCUSSION

Phosphoinositides are biologically useful signaling molecules in part because they fail to transfer rapidly between different membrane compartments in the absence of vesicular transport. These phospholipids can rapidly move laterally within the plane of the membrane. Bound to PtdIns(4,5)P_2, the diffusion coefficient of the PLCδ1 PH domain (Brough *et al.*, 2005; Hammond

et al., 2009) approximates that of lipid alone within the plasma membrane bilayer (Yaradanakul and Hilgemann, 2007; Golebiewska *et al.*, 2008); this could impact the action of PtdIns(4,5)P_2 at discrete membrane patches on the cell surface. In addition, the inositol-lipid head group can be rapidly remodeled upon delivery to a new organelle, or even while within a forming coated bud or membrane-bounded transport vesicle. This plasticity of the head group, coupled with vectorial membrane flow, allows for differentially phosphorylated PtdIns*P*s to play critical regulatory roles along the secretory and endosomal pathways. Here, we demonstrate that the PIPKIγ661 isoform binds physically to the sandwich subdomain of the AP-2 β2 subunit appendage. This interaction allows for the 5-kinase to be strategically positioned during clathrin-coat assembly and to augment PtdIns(4,5)P_2 production focally. A precedent for this type of localized regulation already exists; the talin FERM domain engages the longer-splice isoforms of PIPKIγ (using a sequence that overlaps the β2-appendage interaction motif), and this association coordinates PtdIns(4,5)P_2 production at focal adhesion sites (Di Paolo *et al.*, 2002; Ling *et al.*, 2002).

In eukaryotes, alternative splicing can increase genomic complexity and diversity. The organization of the C-terminal splice sites allows the synthesis of three distinct PIPKIγ variants: one (PIPKIγ687) can bind selectively to talin via the C-terminal extension, one (PIPKIγ661) to both talin and AP-2, and one (PIPKIγ635) to neither protein. This flexibility could impart importantly different biological functions to each isoform (Mao *et al.*, 2009). An additional level of regulation can fine-tune this variation as phosphorylation of Ser645 impedes AP-2 (Figure 2.5; (Nakano-Kobayashi *et al.*, 2007)) and talin (Lee *et al.*, 2005) binding, while Tyr644 (Tyr649 in the human isoform) phosphorylation enhances the association with talin (Ling *et al.*, 2003; Lee *et al.*, 2005; Kong *et al.*, 2006). Intriguingly, Tyr634 is also subject to phosphorylation in

response to growth factors (Sun *et al.*, 2007b). In the brain, PIPKIγ661 is the major isoform at the presynaptic plasma membrane (Wenk *et al.*, 2001; Di Paolo *et al.*, 2004) suggesting that the endocytic function of the kinase is paramount in this tissue.

We mapped the AP-2 interaction motif in PIPKIγ to a more expansive sequence than those typically recognized by the α appendage (DP[FW], FXDXF and WXX[FW]X$[DE]_n$) or even the platform site on the β2 appendage ($[DE]_nX_{1-2}$FXX[FL]XXXR). The sequence differs too from the ^{721}SFGDGFADF region of murine eps15 that also binds to the β2 sandwich subdomain (Schmid *et al.*, 2006). A co-crystal with the β2 appendage shows the eps15 sequence tract forms a tight turn that depends critically on the central Gly for proper positioning of the three Phe side chains (Schmid *et al.*, 2006). Because of the lack of a Gly within β2 binding region of PIPKIγ661, and the altered spacing of the aromatic residues (Figure 2.12A), it seems unlikely that the kinase and eps15 engage the β2 sandwich site in precisely the same manner. Yet, the strict selectivity of PIPKIγ661 for the sandwich subdomain makes the binding to AP-2 subject to interference by clathrin, which can occupy the same interaction site (Edeling *et al.*, 2006a; Keyel *et al.*, 2008). More important is that in the context of the assembled polyhedral lattice, the clathrin heavy chains project a profusion of terminal domains down into the interior of the assemblage (ter Haar *et al.*, 1998; Edeling *et al.*, 2006a). In our view, this high density of clathrin coupled with the capability of the β2 chain of AP-2 to engage the clathrin heavy chain through at least two binding sites, will strongly favor AP-2 associations with clathrin in regions of extensively assembled coat. In fact, in biochemical assays eps15, which also binds to the AP-2 β2 appendage sandwich (Edeling *et al.*, 2006a; Schmid *et al.*, 2006) but not to clathrin, is displaced from AP-2 by polymerizing clathrin (Cupers *et al.*, 1998). Accordingly, eps15 is restricted to the outer edge of clathrin lattices on the cell surface (Tebar *et al.*, 1996; Edeling *et*

al., 2006a). We propose that this hierarchical binding phenomenon offers a mechanism for temporal and spatial control of PtdIns(4,5)P_2 formation as a function of the extent of polymerized clathrin lattice.

Coincidence detection is a common theme in the coordinated placement of clathrin-coat components necessary to drive bud progression (Di Paolo and De Camilli, 2006). We therefore cannot rule out that PIPKIγ661 utilizes this by establishing secondary associations with the μ2 subunit of AP-2, either through the YXXØ-interaction surface (Bairstow *et al.*, 2006) or by binding of the catalytic core region to a distinct portion of μ2 (Krauss *et al.*, 2006). Conceivably, these additional contacts could be precisely regulated by phosphorylation, as exposure of the μ2 subunit to accommodate YXXØ sorting signals requires phosphorylation of Thr156 (Olusanya *et al.*, 2001). Perhaps this allows PIPKIγ661 binding to be variably regulated at different points in the coat assembly cycle. However, because PIPKIγ661 is not enriched in clathrin-coated vesicles purified from rat brain (Figure 2.15B; (Wenk *et al.*, 2001), and immunoEM reveals PIPKIγ on synaptic plasma membrane adjacent to, but not within, clathrin-coated buds (Wenk *et al.*, 2001), we favor the β2 appendage as the site most able to manage this spatial positioning of the 5-kinase during clathrin-mediated endocytosis at the nerve terminal. Intriguingly, PIPKIγ661 binds to the AP-2 β2 appendage as well as the β1 subunit of the AP-1 heterotetramer (Nakano-Kobayashi *et al.*, 2007). In this regard, it is interesting that AP-1 is implicated in return of certain integral membrane proteins from the recycling endosome compartment and PtdIns(4,5)P_2 is the necessary phosphoinositide (Crottet *et al.*, 2002). Similar regulation by the clathrin heavy chain and/or possibly eps15 could occur as eps15 is located on endosomes and the TGN (Chi *et al.*, 2008), and the key residues that constitute the interaction surface on the β2 appendage sandwich subdomain are all conserved in the AP-1 β1 chain (Keyel *et al.*, 2008).

The structurally related AP-2 α and β2 appendages contact a rich constellation of binding partners, some of which are common to both but nevertheless engage structurally non-equivalent surfaces on each appendage (Edeling *et al.*, 2006a; Schmid *et al.*, 2006). A major, currently unresolved question is why certain proteins have evolved specific combinations of dissimilar AP-2 (and clathrin) interaction motifs as opposed to utilizing standardized, generic connection elements? Also, given the relatively low affinity of these interactions in general, how does a timed succession of protein occupancies lead to progressive coat assembly without misdirected protein placement or catastrophic entanglement? One explanation is that binding events that occur at different locations upon the appendages utilizing particular peptide motifs generate different functional consequences, enabling the two proximate domains to act in concert to coordinate coat assembly. The coordination of PtdIns*P* metabolism at coated buds seems to be emblematic of this type of regulation. The 5-kinase activity of PIPKIs is stimulated several fold by PtdOH (Jenkins *et al.*, 1994; Ishihara *et al.*, 1998). Clathrin-mediated endocytosis ceases rapidly (<5 min) upon administration of 1-2% 1-butanol to cultured cells, and new lattice assembly is prevented (Boucrot *et al.*, 2006), illustrating the likely involvement of PtdOH in coat assembly and progression. We have shown previously that, *in vitro*, PtdOH can promote limited translocation of AP-2 to biological membranes in the absence of PtdIns(4,5)P_2 synthesis (Arneson *et al.*, 1999). In fact, a positive feedback loop operates as the product of PIPKI activity, PtdIns(4,5)P_2, is a required activator of phospholipase D (PLD) (Figure 5.2) (Arneson *et al.*, 1999; Morris, 2007). Primary alcohols interfere with PLD-catalyzed hydrolysis of phosphatidylcholine (PtdCho) because a phosphatidylalcohol and not PtdOH is produced (Jenkins and Frohman, 2005). An alternative pathway for the generation of PtdOH is through the phosphorylation of DAG by diacylglycerol kinase (DGK; Figure 5.2) (Merida *et al.*, 2008).

Intriguingly, the PH domain-containing type II DGK, DGKδ2, partly colocalizes with clathrin-coated structures and binds directly to AP-2, in this case to the platform subdomain of the α appendage (Kawasaki *et al.*, 2007). Although DGKδ2 is widely expressed, mRNA transcripts for the enzyme are not particularly abundant in brain (Sakane *et al.*, 2002). Therefore, at the synapse, this enzyme may not be recruited to presynaptic coated buds concomitantly with PIPKIγ661. Perhaps in different cell types, PtdIns(4,5)P_2 and PtdOH production at clathrin-coated regions is managed by different enzymes associating with distinct sites on the AP-2 appendages.

Like PIPKIγ, the phosphoinositide polyphosphatase synaptojanin 1 is subject to alternative splicing (Ramjaun and McPherson, 1996). Somewhat unexpectedly, the ubiquitously expressed large-splice isoform, SJ170, is present within clathrin-coated structures at the cell surface throughout the assembly cycle (Perera *et al.*, 2006). SJ170 also associates physically with AP-2 (Haffner *et al.*, 2000; Jha *et al.*, 2004) and, similar to PIPKIγ661, we mapped the principal interaction motif to a WXX[FW]X$[DE]_n$ motif within the C-terminal extension of SJ170 (Jha *et al.*, 2004). This type of interaction motif selectively engages the sandwich subdomain of the AP-2 α appendage (Mishra *et al.*, 2004; Ritter *et al.*, 2004; Walther *et al.*, 2004). Thus, PIPKIγ661, DGKδ2 and SJ170 can all associate directly with AP-2, albeit though different contact sites on the appendages (Figure 5.2). By binding to different surfaces of the α or β2 appendage, the various enzymes that modulate PtdIns*P* metabolism at the growing bud can be subject to different regulatory inputs. Therefore, the α and β2 appendages appear to operate as organizational scaffolds, in part to optimize the regional lipid environment necessary for clathrin-coat formation. Indeed, this seems to be a general requirement for efficient receptor internalization because β-arrestin 2, a CLASP that promotes the uptake of stimulated G protein-

coupled receptors (Lefkowitz and Shenoy, 2005; Marchese *et al.*, 2008), also associates directly with DGK (Nelson *et al.*, 2007). β-arrestin 2 also binds physically to PIPKI in a PtdIns(4,5)P_2-sensitive fashion (Nelson *et al.*, 2008). The ability of other CLASPs to engage PIPKIs is in accord with much data showing that, under certain experimental circumstances, internalization of discrete transmembrane cargo molecules continues in an AP-2 gene-silenced background (Hinrichsen *et al.*, 2003; Motley *et al.*, 2003; Huang *et al.*, 2004; Barriere *et al.*, 2006; Keyel *et al.*, 2006; Maurer and Cooper, 2006; Eden *et al.*, 2007).

2.5 ADDITIONAL DATA

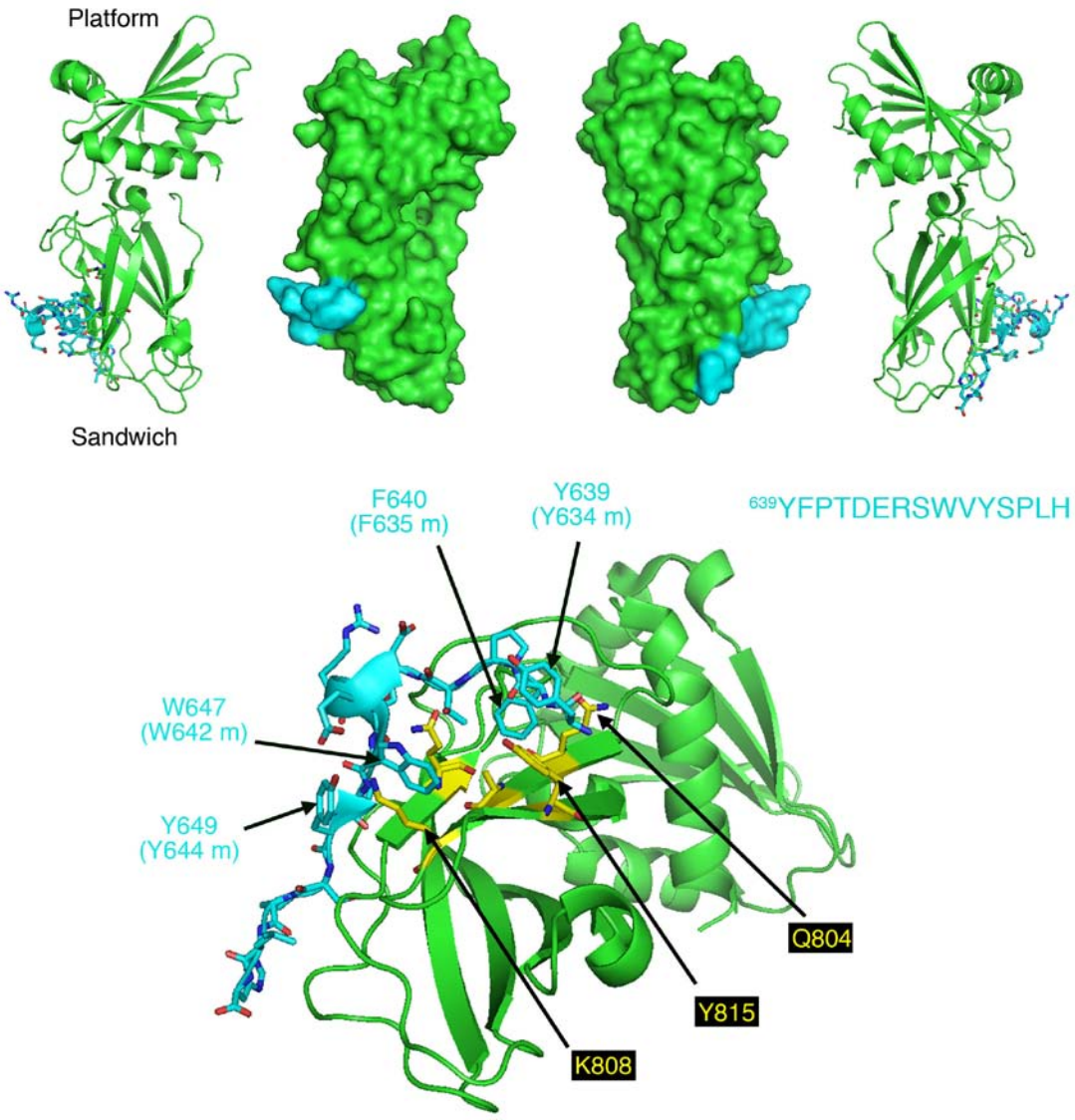

Figure 2.16: Crystal structure of AP-2 β2 appendage in complex with the human PIPKIγ668 C terminus.

Ribbon and space-filling models of human AP-2 β2 appendage (green) and human PIPKIγ668 C terminal peptide (blue) in complex (Protein Data Bank code 3H1Z). The key PIPKIγ668 anchoring residues are labeled with the corresponding mouse residues in parentheses. The β2 appendage sandwich binding pocket residues are depicted in yellow and labeled. Structure solved by (Kahlfeldt *et al.*, 2010).

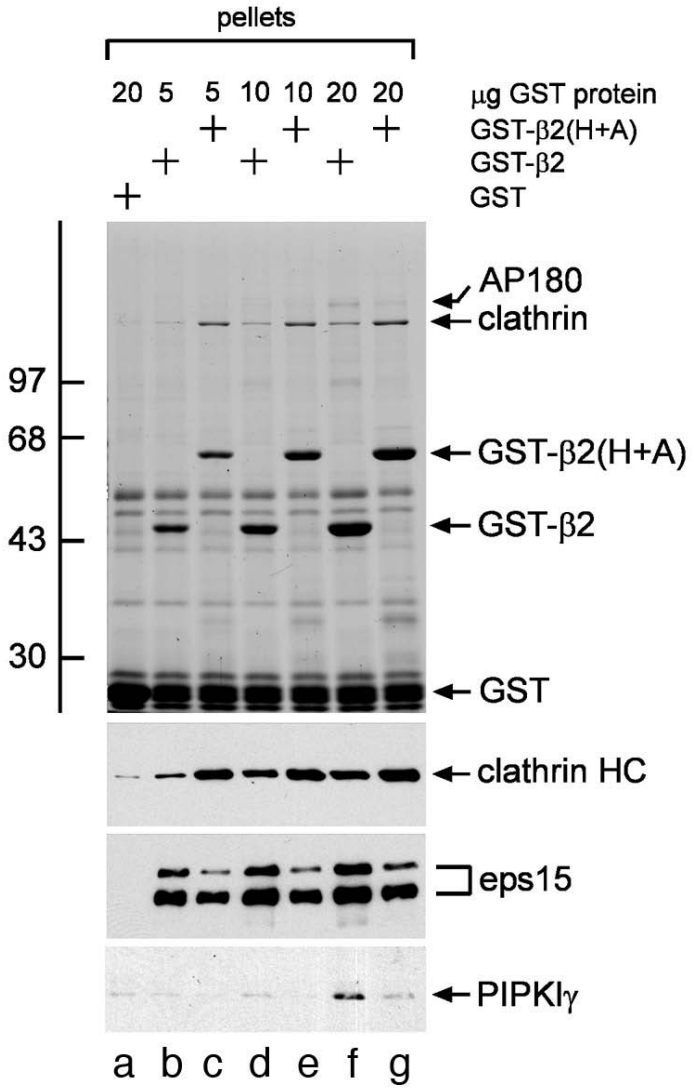

Figure 2.17: Titration of AP-2 β2 appendage sandwich partner binding.
Approximately 5, 10 or 20 μg GST (lane a), GST-β2 appendage (lanes b, d and f) or GST-β2 hinge and appendage (H+A) (lanes c, e and g) were bound to glutathione-Sepharose and incubated with rat brain cytosol. The pellets were washed and resolved by SDS-PAGE and stained with Coomassie Blue (top) or transferred to nitrocellulose and probed with antibodies to clathrin heavy chain (HC) mAb TD.1, affinity purified anti-eps15 rAb or anti-PIPKIγ mAb clone 12 (bottom). Notice the higher apparent affinity of eps15 for β2 appendage over PIPKIγ and the reduced binding of eps15 and increased clathrin binding to the hinge and appendage at lower concentrations (lanes b and c).

3.0 THE AP-2 ADAPTOR β2 APPENDAGE SCAFFOLDS ALTERNATE CARGO ENDOCYTOSIS*

*Portions reprinted from *Molecular Biology of the Cell*, (2008, volume 19, pp. 5309-5326) with permission from The American Society for Cell Biology

3.1 ABSTRACT

The independently-folded appendages of the large α and β2 subunits of the endocytic AP-2 adaptor coordinate proper assembly and operation of endocytic components during clathrin-mediated endocytosis. In addition to binding a variety of adaptors and accessory factors, the β2 subunit binds clathrin and is central to the polymerization of clathrin into a lattice. Though it is clear that clathrin polymerization causes displacement of some β2 appendage binding partners, there has been some dispute as to the precise location of clathrin binding. One proposal is that clathrin binding to the C-terminal β2 appendage platform subdomain displaces adaptors that are retained within assembling vesicles through association with clathrin. β-arrestins are adaptors that recognize G protein-coupled receptors (GPCRs) and target them to clathrin-coated pits through association with the AP-2 β2 appendage platform and clathrin. A β-arrestin 1 mutant, which engages coated structures in the absence of any GPCR stimulation, is

shown to colocalize with β2-YFP and clathrin even in the absence of an operational clathrin-binding sequence. These findings argue against β-arrestin binding to a site upon the β2 appendage platform that is later obstructed by polymerized clathrin. Also, the Type Iγ phosphatidylinositol phosphate kinase (PIPKIγ) binds to the AP-2 β2 appendage sandwich subdomain and the focal adhesion protein talin and expressed PIPKIγ is only found to colocalize with talin in non-neuronal cells. This could indicate that the β2 appendage sandwich subdomains in assembled clathrin lattices are obstructed by clathrin. These results are in agreement with a model in which clathrin assembles by binding the AP-2 β2 appendage sandwich subdomain.

3.2 INTRODUCTION

Clathrin-mediated endocytosis is a process through which many nutrient and signaling receptors, ion channels, and even pathogens, are internalized from the cell surface and delivered to endosomes. The process requires the fine coordination of cargo selection, membrane invagination, and actin dynamics (Conner and Schmid, 2003; Robinson, 2004; Edeling *et al.*, 2006b; Kaksonen *et al.*, 2006). At the plasma membrane, these diverse processes are managed, in part, by the AP-2 heterotetramer. The brick-like AP-2 core is composed of a small σ2 subunit, the cargo-selective μ2 subunit, along with the N-terminal trunks of two large chains, the α- and β2 subunits (Collins *et al.*, 2002). Projecting off both α- and β2-subunit trunks, via flexible hinges, are bilobal appendages that contain binding sites for clathrin and numerous other endocytic proteins (Robinson, 2004; Edeling *et al.*, 2006b; Schmid and McMahon, 2007).

The four assembled subunits permit AP-2 to coordinate various aspects of clathrin-coat formation. The plasma membrane-enriched lipid phosphatidylinositol 4,5-bisphosphate (PtdIns(4,5)P_2) is engaged by both the α- and μ2 subunits (Gaidarov and Keen, 1999; Höning *et al.*, 2005). YXXØ-type sorting signals (as found in the transferrin receptor) are bound directly by the μ2 subunit (Ohno *et al.*, 1995) while [DE]XXXL[LIM] dileucine signals are recognized by a functional hemicomplex of the α and σ2 subunit (Janvier *et al.*, 2003; Coleman *et al.*, 2005; Chaudhuri *et al.*, 2007). Various assembly protein and clathrin associations are established through the α- and β2 appendages (Wang *et al.*, 1995; McPherson and Ritter, 2005; Traub, 2005; Edeling *et al.*, 2006b; Schmid and McMahon, 2007). The αappendage has two interaction surfaces, one each upon the platform and sandwich subdomains. The platform site can bind to DP[WF] and FXDXF interaction motifs (Brett *et al.*, 2002; Praefcke *et al.*, 2004), while the sandwich site engages the WXX[FW]X_n[DE] motif (Mishra *et al.*, 2004; Praefcke *et al.*, 2004; Ritter *et al.*, 2004; Walther *et al.*, 2004). These short interaction sequences are typically positioned within tracts of intrinsically unstructured polypeptide, and proteins bearing the former class of motifs are typically involved in cargo selection and lattice polymerization. Proteins bearing the latter set generally include regulatory proteins such as AAK1, cyclin G-dependent kinase (GAK) and the phosphoinositide polyphosphatase synaptojanin 1 (Jha *et al.*, 2004; Praefcke *et al.*, 2004; Walther *et al.*, 2004). Some of the regulatory proteins, like synaptojanin 1, also contain platform binding sites, potentially allowing them to compete previously bound clathrin-associated sorting proteins (CLASPs) off AP-2 (Mishra *et al.*, 2004; Praefcke *et al.*, 2004). Thus, the α appendage regulates the temporal organization of the developing clathrin lattice through binding sites that permit the recruitment of first lattice assembly and cargo

selective factors, followed by regulatory proteins that control bud formation and likely promote release of proteins from AP-2 once their role in endocytosis is complete.

Similar to the α appendage, the structurally related β2 appendage also contains two interaction surfaces, one analogous to the α appendage-platform site, and one positioned on the opposite side from the cognate a appendage-sandwich site (Edeling *et al.*, 2006a; Schmid *et al.*, 2006). The contact sites on the β2 appendage do not appear to control accessory proteins in precisely the same manner as the hierarchical α appendage-binding sites. Biochemical studies suggest the β2 appendage-platform site is largely dedicated to CLASPs, such as the β-arrestins, which concentrate G protein-coupled receptors (GPCRs) (Kim and Benovic, 2002; Laporte *et al.*, 2002; Milano *et al.*, 2002), the autosomal recessive hypercholesterolemia (ARH) protein, which decodes the FXNPXY-type sorting signal (He *et al.*, 2002; Mishra *et al.*, 2002b), and epsin 1, which recognizes poly/multiubiquitinated cargo (Barriere *et al.*, 2006; Hawryluk *et al.*, 2006). These discrete classes of cargo internalization signal do not bind directly to AP-2. The β2 appendage-sandwich site, along with a type I clathrin box in the β2-hinge, allows AP-2 to polymerize clathrin and regulate eps15 positioning within the assembling lattice (Cupers *et al.*, 1998; Owen *et al.*, 2000; Edeling *et al.*, 2006a), though the β2 appendage-platform site has been suggested to be the clathrin binding site on this appendage (Owen *et al.*, 2000; Schmid *et al.*, 2006). Thus, the β2-subunit contains functionally distinct binding sites that could simultaneously allow privileged access of certain CLASPs to the lattice along with clathrin recruitment. Overall, AP-2 acts as a master adaptor, binding to the plasma membrane, sorting YXXØ- and [DE]XXXL[LIM]-bearing cargo, and coordinating clathrin vesicle formation while simultaneously providing access for alternative types of cargo by scaffolding CLASPs. Accordingly, targeted gene disruption or mutation of AP-2 μ2- or α- subunit genes is

homozygous lethal in mice (Mitsunari *et al.*, 2005), *Drosophila* (Gonzalez-Gaitan and Jackle, 1997) and *C. elegans* (Shim and Lee, 2000).

Structurally, β-arrestins contain an N-terminal bi-lobed arrestin fold that simultaneously binds phosphorylated GPCRs and PtdIns(4,5)P_2, and an unstructured C-terminus containing a type I clathrin box and the β2 appendage-binding sequence (Krupnick *et al.*, 1997a; Gaidarov *et al.*, 1999; Laporte *et al.*, 2000; Han *et al.*, 2001). GPCR activation, phosphorylation, and β-arrestin binding is intimately tied to receptor endocytosis because the β2 appendage binding sequence is bound back on the arrestin fold, stabilizing the inactive state, but is released by β-arrestin recognition of phosphorylated GPCR cytosolic loops (Edeling *et al.*, 2006a; Burtey *et al.*, 2007). The consensus β2-binding sequence $[DE]_nX_{1-2}FXX[FL]XXXR$ binds to the β2 platform as well as the β-arrestin core through the anchoring Phe/Arg residues (Edeling *et al.*, 2006a), though an upstream Iso/Val (X_{1-2} position) stabilizes the core interaction and mutation to Ala releases the C-terminus and constitutively targets β-arrestin to preformed clathrin coats (Burtey *et al.*, 2007).

In this study I made use of the constitutively active IV→AA β-arrestin 1 mutant to examine the importance of clathrin binding to maintain β-arrestin within internalizing clathrin-coated structures. I find that that IV→AA β-arrestin 1 is constitutively targeted to clathrin structures at the cell surface in the absence of GPCR stimulation and that its presence there is unaffected by mutation of the clathrin box motif. Furthermore, clathrin box mutants disappear from the cell surface concomitantly with AP-2. The wildtype and clathrin binding deficient IV→AA β-arrestin 1 also mediates downregulation of the angiotensin receptor and colocalizes with angiotensin ligand on endosomes. I also examined the subcellular localization of the AP-2 β2 appendage sandwich subdomain-binding protein PIPKIγ (Chapter 2). Neither full length

PIPKIγ or a truncation mutant harboring the β2 appendage binding site colocalizes with AP-2 *in vivo* though full length PIPKIγ colocalizes with its other binding partner talin. These data support a model where clathrin assembles around the AP-2 β2 appendage sandwich subdomain, blocking this site but leaving the β2 platform subdomain open.

3.3 RESULTS

3.3.1 Clathrin binding surface on the β2 subunit appendage

In addition to engaging ARH and β-arrestins, the β2-subunit appendage also binds physically to clathrin (Owen *et al.*, 2000; Lundmark and Carlsson, 2002; Edeling *et al.*, 2006a; Knuehl *et al.*, 2006; Schmid *et al.*, 2006). Yet the precise molecular basis for this association is currently controversial. There is general agreement that by binding bivalently to the clathrin heavy chain, some β2-subunit partners could be controlled spatiotemporally as the extent of polymerized clathrin lattice increases (Edeling *et al.*, 2006a; Knuehl *et al.*, 2006; Schmid *et al.*, 2006; Schmid and McMahon, 2007; Ungewickell and Hinrichsen, 2007). We recently mapped the clathrin binding surface to a site, including Tyr815, on the N-terminal sandwich subdomain (Edeling *et al.*, 2006a), and our prior results indicate that clathrin binding to the β2-appendage sandwich can displace interaction partners like eps15 and AP180, which bind to the same site. Because clathrin trimers stoichiometrically outnumber AP-1/2 in preparations of biochemically purified clathrin-coated vesicles (Blondeau *et al.*, 2004; Girard *et al.*, 2005), the excess of clathrin heavy chain terminal domains, which project into the interior of the assembled coat (Musacchio *et al.*, 1999;

Edeling *et al.*, 2006b), can bind avidly to AP-2 through the β2 subunit. Indeed, we (Edeling *et al.*, 2006a) and others (Tebar *et al.*, 1996) localize eps15 to only the periphery of clathrin-coated structures. Similar conclusions have been drawn for the mode of engagement of the monomeric GGA adaptor proteins and clathrin, where the C-terminal GAE domain of the GGAs only contains a sandwich subdomain (Knuehl *et al.*, 2006). Since activation of GPCRs leads to the rapid translocation of an activated GPCR·β-arrestin complex to preexisting clathrin-coated structures at the cell surface (Laporte *et al.*, 2000; Santini *et al.*, 2002; Scott *et al.*, 2002) and because ARH (He *et al.*, 2002; Mishra *et al.*, 2002b) and β-arrestins (Kim and Benovic, 2002; Laporte *et al.*, 2002) specifically engage the platform subdomain of the β2 appendage, we proposed that the β2 platform interaction surface represents a relatively privileged binding site (Mishra *et al.*, 2005; Brett and Traub, 2006; Edeling *et al.*, 2006a). Challenging these findings and calling our conclusions "misleading", McMahon and colleagues assert that it is the platform subdomain, and not the sandwich site, that is the location of the second point of contact between the clathrin heavy chain and the β2 (and β1) hinge + appendage (Schmid *et al.*, 2006; Schmid and McMahon, 2007). In this model, clathrin interference dislodges CLASPs like β-arrestin and ARH from the β2 appendage but, because both these proteins also have an adjacent but separate clathrin binding sequence, the proteins would remain associated with assembling clathrin coats despite occupancy of the β2 platform with a distal leg segment of the heavy chain (Schmid *et al.*, 2006; Schmid and McMahon, 2007). This is a chief feature of the "changing hubs" model formulated to account for the vectorial nature of the clathrin coat assembly process (Schmid and McMahon, 2007). Clearly then, these opposing models have importantly different implications for the molecular basis of ARH- and β-arrestin-mediated cargo capture within forming clathrin coats.

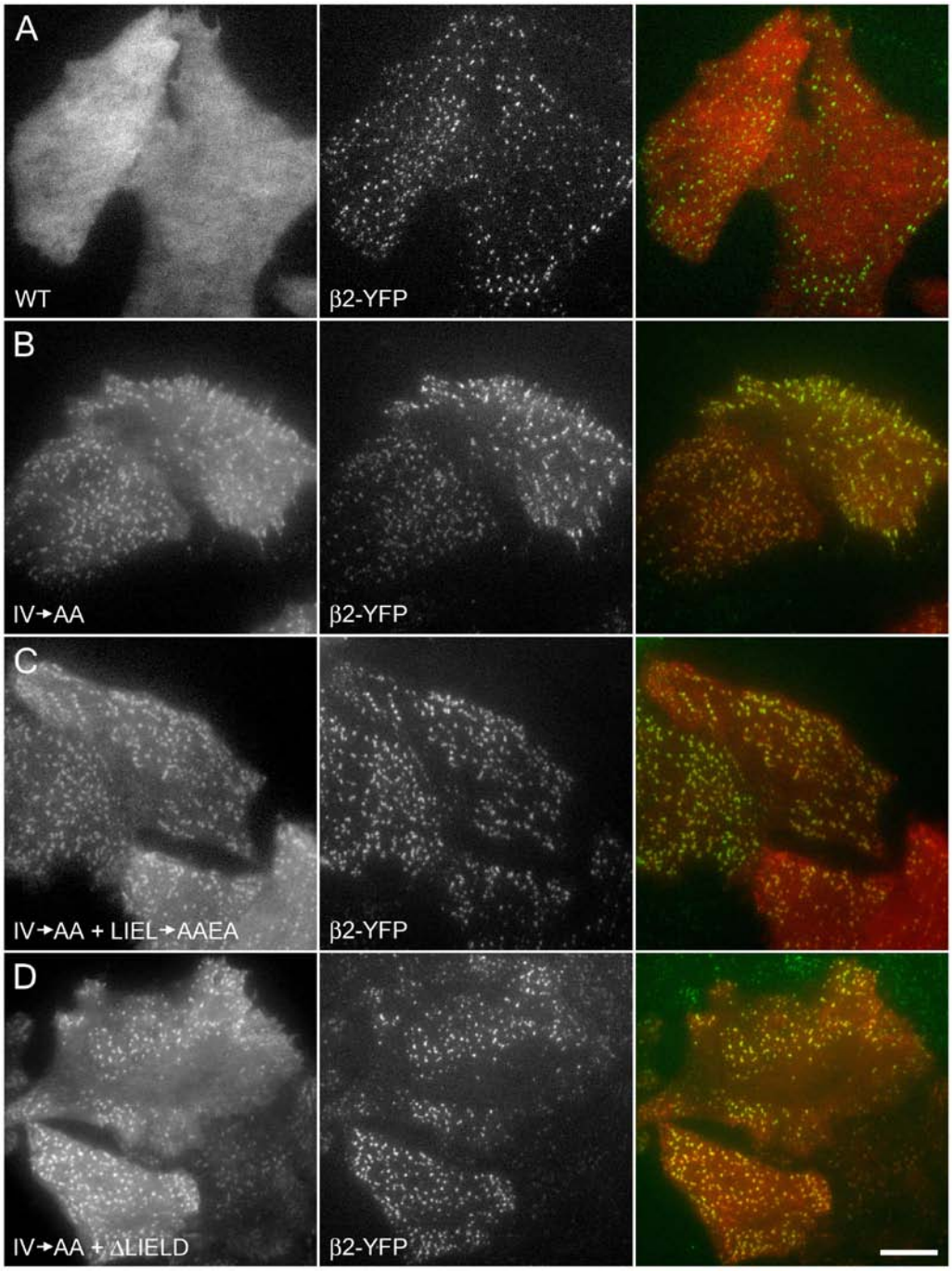

Figure 3.1: Clathrin-binding deficient β-arrestin 1 associates with AP-2.
HeLa SS6 cells stably expressing β2-YFP were transiently transfected with wild type (WT) tdRFP-β-arrestin 1 (A), tdRFP-β-arrestin 1 with the IV→AA activating mutation (B), or tdRFP-β-arrestin 1 (IV→AA) + clathrin box mutation LIEL→AAEA (C) or + clathrin box deletion ΔLIELD (D). Approximately 18 hours post-transfection cells were imaged by TIR-FM to selectively observe the ventral surface. Representative images show tdRFP-β-arrestin 1 (left column), β2-YFP (middle column), and merged (right column) signals. Note that despite a considerable cytosolic pool, there is near complete co-localization of β2-YFP puncta with the tdRFP-β-arrestin 1 (IV→AA) alone or with either clathrin box disruption. Scale bar = 10 μm.

To attempt to distinguish between the two models, we utilized a mutant form of β-arrestin 1. Wild-type β-arrestins remain diffusely cytosolic in the absence of GPCR stimulation (Laporte *et al.,* 2000; Santini *et al.,* 2002; Scott *et al.,* 2002) (Figure 3.1A) by maintaining a basal, inactive conformation. Several closely spaced residues within the C-terminal $[DE]_nX_{1-2}$FXX[FL]XXXR motif interact with the major folded N-terminal region of β-arrestin, rigidifying the protein and attenuating the CLASPs ability to engage the assembling clathrin machinery (Kim and Benovic, 2002; Gurevich and Gurevich, 2004; Edeling *et al.*, 2006a; Burtey *et al.*, 2007). In β-arrestin 1, immediately preceding the proximal Phe388 of the β2 platform binding motif are Ile386 and Val387. Double substitution of these residues to Ala (IV→AA) results in constitutive association of β-arrestin 1 with clathrin-coated structures in the absence of any GPCR activation (Burtey *et al.,* 2007). If β-arrestins only remain associated with surface coated structures by switching to clathrin when assembling clathrin binds the AP-2 β2 subunit appendage, then deletion or mutation of the β-arrestin 1 clathrin box sequence ^{376}LIELD should prevent the IV→AA mutant from colocalizing extensively with clathrin-coated structures at the plasma membrane.

Using TIR-FM to inspect the ventral surface of HeLa SS6 cells stably expressing β2-YFP, we confirm that tdRFP-β-arrestin 1 is soluble while a portion of the IV→AA mutant concentrates at preexisting, β2-subunit positive clathrin-coated structures (Figure 3.1A and B) (Burtey *et al.,* 2007). In the IV→AA background, the colocalization of neither a LIEL→AAEA substitution nor a ΔLIELD mutant with coated structures at the plasma membrane marked by β2-YFP is obviously different from the protein containing an intact clathrin box (Figure 3.1C and D). While 0.6 ± 0.3% of AP-2 structures colocalize with tdRFP-β-arrestin 1, 99.1 ± 0.6% of AP-

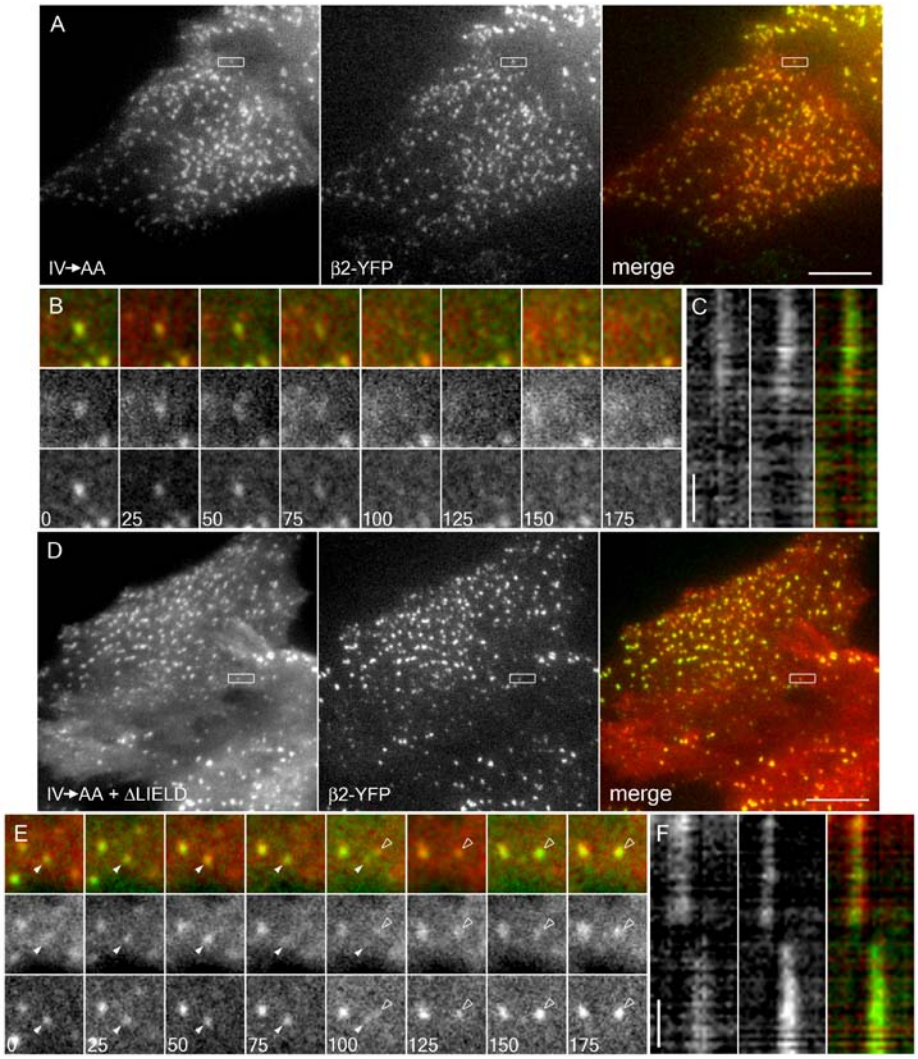

Figure 3.2: Clathrin-binding deficient β-arrestin 1 dynamically associates with AP-2.
HeLa SS6 cells stably expressing β2-YFP were transiently transfected with tdRFP-β-arrestin 1 (IV→AA) (A-C) or tdRFP-β-arrestin 1 (IV→AA+ΔLIELD) (D-F). Approximately 18 hours post-transfection cells were imaged by TIR-FM at one frame every five seconds. (A) Representative frames from the tdRFP-β-arrestin 1 (IV→AA) expressing cells. β-arrestin 1 (left frame) and β2-YFP (middle frame) show extensive co-localization (right frame). (B) A sequence of frames at 25 second intervals shows the simultaneous disappearance of tdRFP-β-arrestin 1 (IV→AA) (middle row) and β2-YFP (bottom row) from the evanescent field. The spot is the same as that boxed in (A). (C) A line drawn along the axis of the box in (A) was used to create a kymograph. tdRFP-β-arrestin 1 IV→AA (left column) and β2-YFP (middle column) leave the evanescent field together (right column). (D) tdRFP-β-arrestin 1 (IV→AA+ΔLIELD) expressing cells likewise show significant overlap with β2-YFP as in (A). (E) The boxed spot in (D) containing tdRFP-β-arrestin 1 (IV→AA+ΔLIELD) (middle row) and β2-YFP (bottom row) disappears from the field (solid arrowhead) at 100 seconds as a second spot containing both proteins appears (open arrowhead). (F) A line drawn along the axis of the box in (D) was used to create a kymograph. tdRFP-β-arrestin 1 (IV→AA+ΔLIELD) (left column) and β2-YFP (middle column) disappear together while the appearance of arrestin in the second spot is slightly preceded by β2-YFP. All horizontal scale bars =10 μm (A, D), while vertical time bars = 60 seconds (C, F).

2-positive spots contain tdRFP-β-arrestin (IV→AA). For the tdRFP-β-arrestin (IV→AA+LIEL→AAEA) and tdRFP-β-arrestin (IV→AA+ΔLIELD) mutants, 95 ± 2% and 89 ± 3% of AP-2 structures contain β-arrestin, respectively.

There are several distinct classes of clathrin-coated structures on the ventral surface of HeLa SS6 cells (Keyel *et al.*, 2004) and the IV→AA β-arrestin 1 mutants localize to all of these. Analysis of the dynamics of *de novo*-forming puncta reveals that, like the tdRFP-β-arrestin 1 (IV→AA) (Figure 3.2A-C), the IV→AA̤ΔLIELD mutant concentrates at, and then disappears with, β2-YFP-tagged AP-2 structures (Figure 3.2D-F). We do not observe earlier loss of the IV→AA̤ΔLIELD tdRFP-β-arrestin 1 mutant from these patches that would indicate failure to switch to a strictly clathrin-dependent mode of association. Very similar results are obtained using BS-C-1 cells stably expressing GFP-tagged clathrin light chain (data not shown), a cell line that exhibits *de novo* coat formation almost exclusively (Ehrlich *et al.*, 2004).

It is important to note that in these experiments, the activation of the β-arrestin 1 (IV→AA) mutant occurs in the absence of any GPCR ligand addition, but HeLa SS6 cells also do express endogenous β-arrestins. While there is currently some doubt that non-visual arrestins oligomerize at physiological concentrations (Hanson *et al.*, 2008a), overexpressed β-arrestins can form multimers (Storez *et al.*, 2005; Milano *et al.*, 2006). Oligomerization requires inositol hexakisphosphate binding and pertains to the soluble form of β-arrestin, as the contact sites for dimer and tetramer assembly are located on the concave surface that engages an activated receptor (Milano *et al.*, 2006; Hanson *et al.*, 2008a; Hanson *et al.*, 2008b). Solution oligomers therefore do not bind to GPCRs, and exposure of the C-terminal region, which couples β-arrestins to the clathrin machinery, destabilizes oligomers (Hanson *et al.*, 2008a). We thus believe it unlikely that hetero-oligomerization with endogenous β-arrestins accounts for the

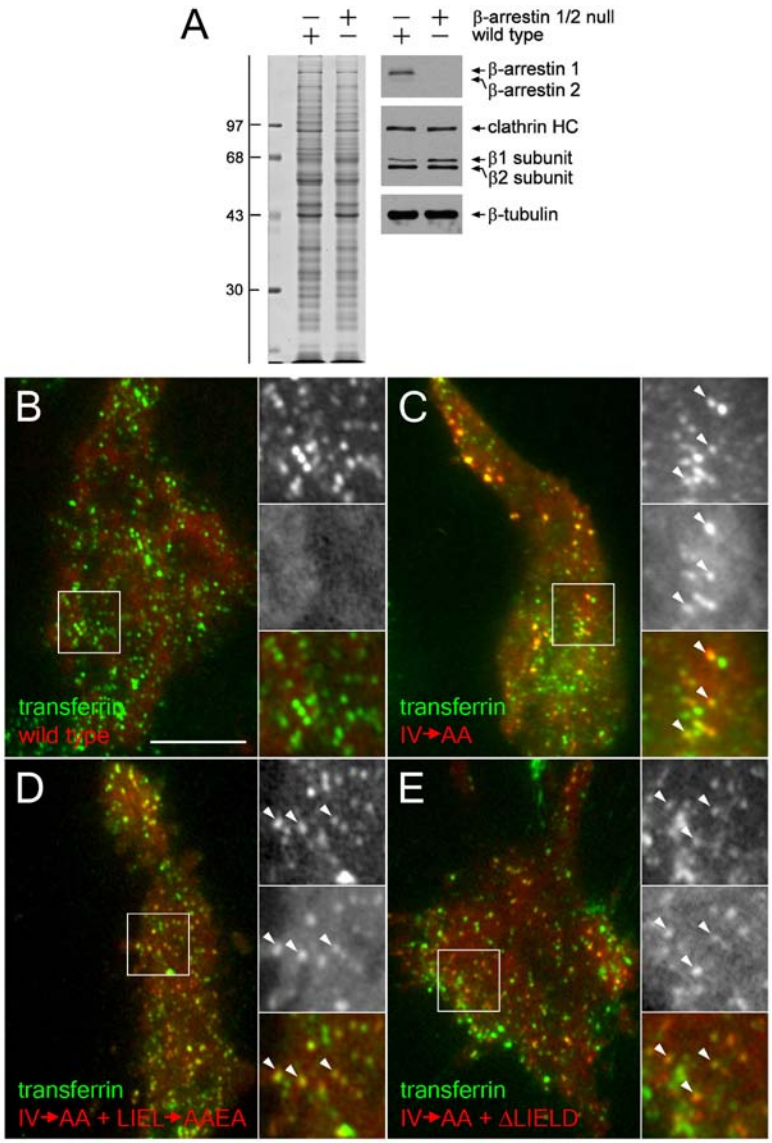

Figure 3.3: Clathrin-binding deficient β-arrestin 1 associates with clathrin-coated structures in the absence of endogenous β-arrestins.

Wild-type and β-arrestin 1/2 null mouse embryonic fibroblasts were lysed and resolved by SDS-PAGE (A, left) and transferred to nitrocellulose (A, right). Portions of the blots were probed with an anti-β-arrestin polyclonal antibody, anti-clathrin HC mAb TD.1 and anti-β1/β2 subunit mAb 100/1, or anti-tubulin mAb E7. Protein size markers noted in kDa. Alternatively, β-arrestin 1/2 null mouse embryonic fibroblasts were transiently transfected with tdRFP-β-arrestin 1 (red) wild type (B), the tdRFP-β-arrestin 1 (IV→AA) activating mutation (C), IV→AA + clathrin box mutation LIEL→AAEA (D), or IV→AA + clathrin box deletion ΔLIELD (E). At 18 hours post-transfection cells were incubated with 25 μg/mL Tf488 (green) on 4°C on ice for one hour to label transferrin receptor in clathrin-coated structures, then rapidly imaged at 17°C by TIR-FM. Under these conditions, transferrin is found both at clathrin coated structures on the cell surface and already in peripheral endosomes. Magnified insets are denoted by white boxes; the IV→AA and IV→AA + clathrin box disruption β-arrestin mutants (middle inset) both co-localize with Tf488 (top inset), as denoted by arrowheads. Scale bar = 10 μm.

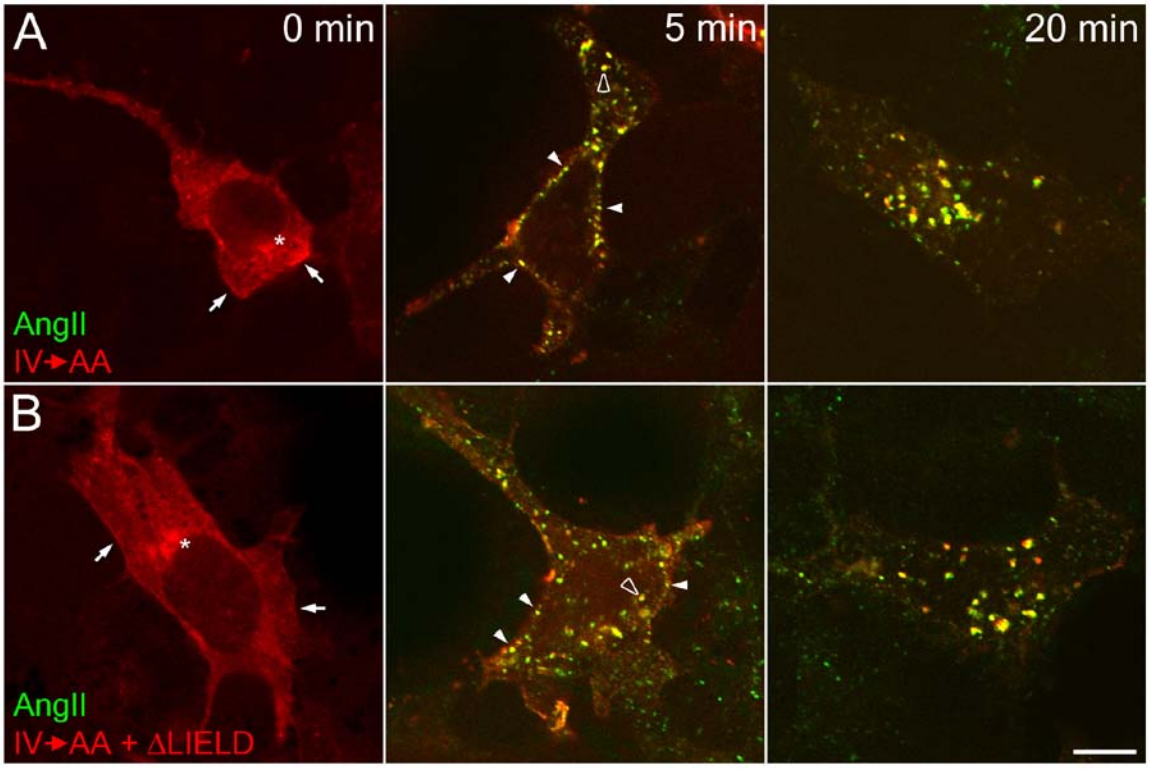

Figure 3.4: Down-regulation of the type 1 angiotensin II receptor by both clathrin-binding deficient β-arrestins.

HEK293 cells stably expressing FLAG-tagged type I angiotensin II receptor were transiently transfected with tdRFP-β-arrestin 1 (IV→AA) (A) or tdRFP-β-arrestin 1 (IV→AA+ΔLIELD) (B). Cells were starved for one hour in starvation medium and then stimulated with 100 nM angiotensin II conjugated to Alexa488 (AngII, green) for 0, 5 or 20 minutes. Cells were washed, fixed, and examined by confocal microscopy. Representative images of medial focal planes are shown. Before stimulation, β-arrestin is largely diffuse in the cytosol but also present at the plasma membrane (arrows) or at a juxtanuclear location (asterisks). After five minutes of stimulation, β-arrestin clusters with angiotensin II at the plasma membrane (closed arrowheads), and on endosomes (open arrowheads). At 20 minutes after stimulation, nearly all β-arrestin and angiotensin II co-localize on larger endosomes. Scale bar = 10 μm.

association of the IV→AA + clathrin box mutants with surface clathrin-coated structures. Supporting this view is that transfection of the tdRFP-β-arrestin 1 (IV→AA) clathrin-binding mutants into β-arrestin 1/2 nullizygous fibroblasts (Kohout *et al.*, 2001) still results in constitutive accumulation of the tagged β-arrestin at membrane puncta that are also positive for surface transferrin (Figure 3.3).

Finally, like the β-arrestin 1 (IV→AA) mutant, the compound (IV→AA+ΔLIELD) mutant translocates rapidly to the surface of angiotensin II-stimulated HEK cells stably expressing the type I angiotensin II receptor (Figure 3.4). At 5 min, both the β-arrestin mutants colocalize with fluorescent angiotensin II at cell-surface patches and peripheral endosomes while, after 20 min, both angiotensin II and β-arrestin 1 (IV→AA+ΔLIELD) are found in larger, juxtanuclear endosomes, typical of a class B GPCR (Hamdan *et al.*, 2007). These results show that deletion of the β-arrestin clathrin box does not have a major negative affect on GPCR downregulation and are fully consistent with a doubly-mutated IV→AA+LIEF→AAEA β-arrestin 2 mutant clustering activated thyrotropin-releasing hormone receptors at AP-2-positive clathrin-coated structures and orchestrating endocytic uptake roughly equivalent to wild-type β-arrestin 2 at 10 min (Burtey *et al.*, 2007). We conclude that β-arrestin switching to a clathrin-dependent mode of association is not an obligate step during the formation of clathrin-coated vesicles, and that the $[DE]_nX_{1\text{-}2}FXX[FL]XXXR$ binding surface upon the platform subdomain of the β2 appendage does represent a privileged interaction site, as it can be rapidly accessed by β-arrestin in the face of ongoing endocytic activity.

3.3.2 Accessibility of the β2 subunit appendage sandwich subdomain

Having shown that binding partners of the AP-2 β2 appendage platform subdomain have privileged access to the growing bud and are not displaced by polymerized clathrin, we sought to show the opposite: that an AP-2 binding partner that solely binds the β2 appendage sandwich domain is displaced as clathrin polymerizes. PIPKIγ is the predominate PtdIns(4)P 5-kinase in the brain and generates PtdIns(4,5)P_2 for compensatory CME at nerve terminals (Wenk *et al.*, 2001; Di Paolo *et al.*, 2004). While its role in CME in non-neuronal cells is unknown, the PIPKIγ661 isoform binds to AP-2 through the β2 appendage sandwich subdomain (Chapter 2 (Thieman *et al.*, 2009)). Its residency at endocytic structures on the cell surface may then be regulated by clathrin. To examine this, HeLa SS6 cells were transfected with monomeric Cherry (mCherry) conjugated PIPKIγ661 and examined by immunofluorescence for AP-2 (Figure 3.5 top). PIPKIγ661 is localized to the plasma membrane as seen by the strong ring of fluorescence at the cell edge from the out of focus side membranes. PIPKIγ661 is found in large and small puncta, however these puncta do not colocalize with AP-2 (Figure 3.5 top). However AP-2 and PIPKIγ661 puncta were often found adjacent to each other (arrowheads). In contrast, another PIPKIγ661 binding partner, the focal adhesion protein talin (Di Paolo *et al.*, 2002; Ling *et al.*, 2002), colocalizes robustly at large and small PIPKIγ661 puncta (Figure 3.5 bottom, arrows). The vicinity of AP-2 structures to the PIPKIγ661 puncta could indicate that these kinase assemblies are excluded from assembling endocytic structures or that PtdIns(4,5)P_2 generated at these talin-positive structures is diffusing and promoting clathrin assembly nearby.

Observation of mCherry-PIPKIγ661 over time in β2-YFP HeLa SS6 cells failed to show enrichment of PIPKIγ661 at the early phases of AP-2 accumulation (data not shown). Similar

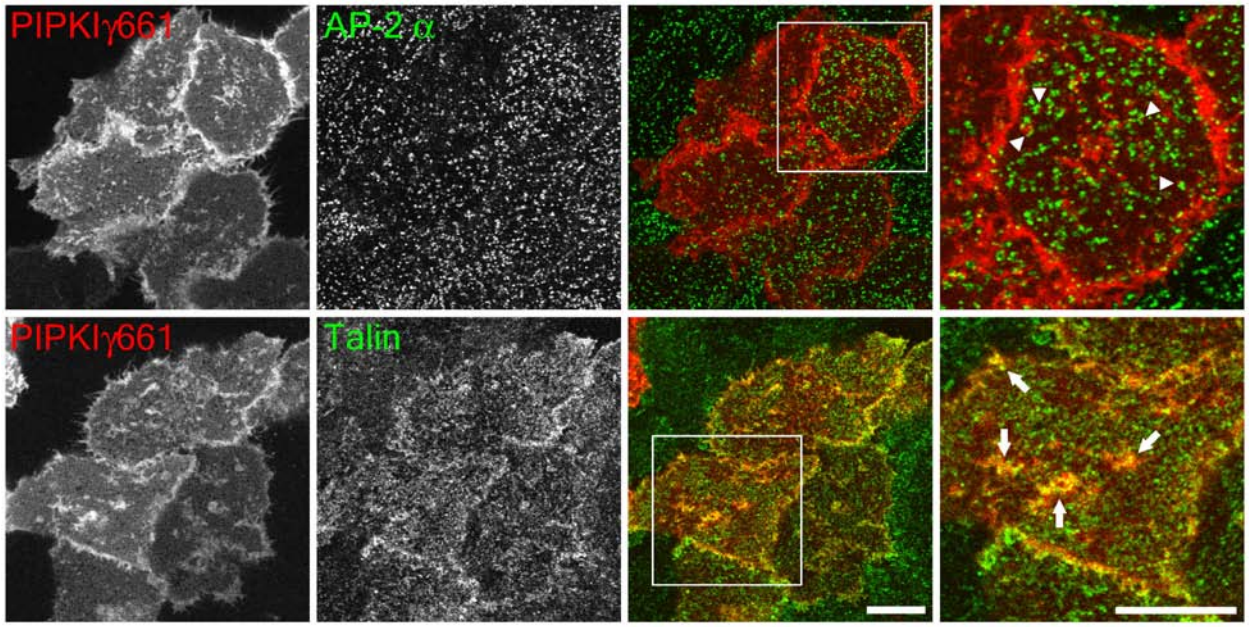

Figure 3.5: PIPKIγ661 localizes adjacent to AP-2 on the ventral surface of HeLa cells.
HeLa SS6 cells were transiently transfected with mCherry-PIPKIγ661 (red) and processed for immunofluorescence at 18 hours post-transfection with monoclonal antibodies against AP-2 α subunit (top) or talin (bottom) (green). The ventral plasma membrane of cells was imaged by confocal microscopy. mCherry-PIPKIγ661 localizes to individual puncta and larger structures that are frequently adjacent to AP-2 (arrowheads). There is extensive colocalization of mCherry-PIPKIγ661 with talin (arrows). Scalebars = 10 μm.

results were obtained when using clathrin light chain-GFP expressing BS-C-1 cells (Ehrlich *et al.*, 2004), or clathrin light chain-GFP expressing CHO cells (Yim *et al.*, 2005), although BS-C-1 and CHO cells did have PIPKIγ661 puncta that may correspond to talin-positive structures (data not shown). As an alternative approach, CCSs in BS-C-1 and CHO cells were depleted and reassembled by incubating cells in 1.5% 1-butanol for a few minutes to inhibit PtdOH production and as a result stimulation of PIPKI followed by washout to reassemble adaptors and clathrin. Staged depletion of PtdIns(4,5)P_2 also failed to recruit PIPKIγ661 to nascent CCSs in these cells. The inability to detect PIPKIγ661 at AP-2 structures even transiently may indicate a greater concentration of binding-competent talin, whose binding sequence in PIPKIγ661 overlaps with the AP-2-binding sequence (de Pereda *et al.*, 2005), or phosphorylation of Ser645, inhibitory for AP-2 binding (Nakano-Kobayashi *et al.*, 2007), by endogenous kinases in these cell lines.

A final possibility is that the PIPKIγ661·AP-2 interaction is of very low affinity. To circumvent this, a double and triple repeat of the AP-2 binding sequence from PIPKIγ661 (residues 630-661) was expressed in frame with mCherry in HeLa cells (Figure 3.6). A single copy of the AP-2 binding tract ((630-661)x1, (Thieman *et al.*, 2009)) failed to colocalize with AP-2 like the full length kinase, but also failed to accumulate in puncta that may have colocalized with talin (Figure 3.5 and 3.6). Expression of GFP-PIPKIγ(460-661) in primary hippocampal neurons did not result in targeting to synaptic boutons any more than a binding-incompetent peptide, despite being able to inhibit FM4-64 uptake (Nakano-Kobayashi *et al.*, 2007). Interestingly, expression of the double ((630-661)x2) or triple ((630-661)x3) binding sequence also resulted in diffuse localization of the mCherry-peptide, but caused an increase in the size of AP-2 structures (Figure 3.7A) and a decrease in the density of AP-2 structures (Figure 3.7B). The triple binding sequence with a critical Trp mutated ((630-661)x3 W642A) had an

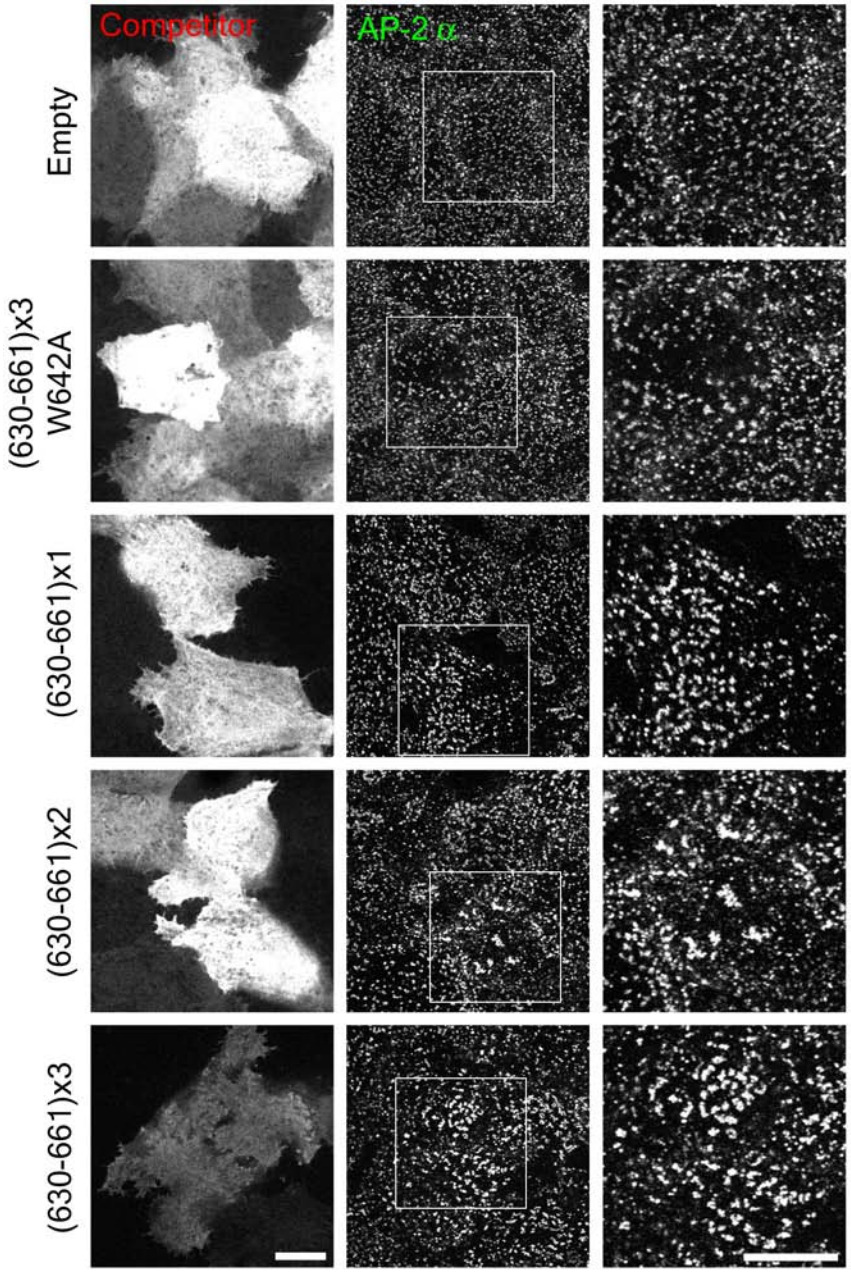

Figure 3.6: Overexpression of the PIPKIγ661 C terminus disrupts the steady-state AP-2 structure morphology.

HeLa SS6 cells were transiently transfected with a plasmid encoding mCherry alone (empty) or with PIPKIγ residues (630-661) as a single (x1), double (x2) or triple (x3) insertion in frame, or as a triple sequence containing the W642A substitution (x3 W642A) (competitor column). At approximately 18 hours post-transfection cells were processed for immunofluorescence with a monoclonal antibody against AP-2 α subunit (middle column). The ventral plasma membrane of cells was imaged by confocal microscopy. Cells expressing (630-661)x2 or x3 display an apparent enlargement of AP-2 puncta. Scale bars = 10 μm.

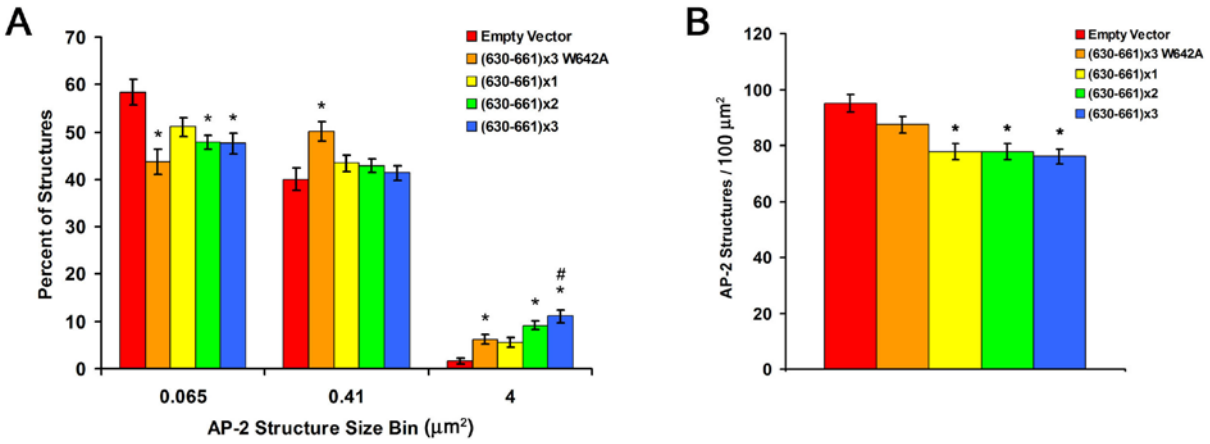

Figure 3.7: Quantitation of AP-2 morphology changes from PIPKIγ661 C terminus overexpression. (A) AP-2 structures on the ventral surface of HeLa cells prepared as in Figure 3.6 were measured for their surface area. Based on the size distribution of the global population of structures three bins were created: 0-0.065 μm^2, 0.065-0.41 μm^2, and 0.41-4 μm^2. In each condition, the percentage of AP-2 structures falling into each bin from 30 cells was averaged. The (630-661)x2 and x3 expression vectors cause an increase in the percentage of AP-2 structures in the large group and decrease in the smallest group. (B) 100 μm^2 square regions encompassing the ventral membrane of cells imaged as in Figure 3.6 were used to measure the number of AP-2 structures and the number from 30 cells was averaged. *, $p<0.05$ relative to empty vector, #, $p<0.05$ relative to x3 W642A. Error bars represent standard error.

intermediary phenotype with increased AP-2 sructure size but relatively normal AP-2 density. An explanation for these results may be that even when present in multiple copies, this AP-2 interaction motif is of sufficiently low enough affinity that it has a high on-off rate. It could still interfere with clathrin binding to the β2 appendage sandwich site on AP-2 and in doing so cause an expansion of AP-2 on the plasma membrane from decreased clathrin-mediated budding.

3.4 DISCUSSION

ARH and the β-arrestins differ significantly from eps15 and several other CLASPs and accessory factors in that they both display only a single AP-2 binding determinant with an absolute selectivity for the platform subdomain of the β2 appendage (Laporte *et al.*, 2000; He *et al.*, 2002; Mishra *et al.*, 2002b). Substantial data attest to the critical and selective importance of the β2 appendage in the initial recruitment of GPCR·β-arrestin complexes to preexisting sites of clathrin assembly. The clathrin box is located within a flexible, unstructured C-terminal loop (Milano *et al.*, 2002), even in the basal β-arrestin conformation. Yet β-arrestins are cytosolic in the absence of GPCR activation (Hamdan *et al.*, 2007) so, although the clathrin box is potentially accessible to the clathrin terminal domain, if the distal $[DE]_nX_{1-2}FXX[FL]XXXR$ sequence is conformationally restrained, β-arrestins fail to associate appreciably with clathrin-coated structures. Similarly, when fused to GFP, the C-terminal region of β-arrestin 2 populates AP-2-positive clathrin structures at the cell surface but this colocalization is completely lost if the $[DE]_nX_{1-2}FXX[FL]XXXR$ sequence is disrupted, even with an intact adjacent clathrin box

(Schmid *et al.*, 2006). Also, the β-arrestin 1 IVF→AAA triple mutant is not colocalized with AP-2 at steady state, despite the conformation relaxation affected by the IV to AA substitution (Burtey *et al.*, 2007). Mutagenic inactivation of the AP-2 binding sequence in β-arrestin 2 still allows translocation of this CLASP to agonist-stimulated GPCRs on the cell surface, but clustering at AP-2-positive puncta is lost, again despite an intact clathrin box (Laporte *et al.*, 2000). Indeed, bioluminescence resonance energy transfer studies show that β-arrestin binding to liganded GPCRs temporally precedes an AP-2 β2 appendage interaction (Hamdan *et al.*, 2007), and that mutation of the interaction surface on the β2 platform subdomain prevents energy transfer to AP-2 (Hamdan *et al.*, 2007). By contrast, even with an inactivating mutation or complete deletion of the clathrin box, β-arrestin 1 still targets to clathrin-coated structures (Figures 3.1 – 3.4). Altogether, this argues strongly that the $[DE]_nX_{1-2}FXX[FL]XXXR$ sequence is the principal determinant governing initial linkage of GPCRs with the endocytic machinery (Laporte *et al.*, 2000).

The binding affinity of ARH (and β-arrestin) for the β2-appendage is greater than its affinity for any other binding partner. ARH binds to the β2-appendage with a K_D of ~1 μM (Mishra *et al.*, 2005), compared with 22 μM for a type I clathrin box LLDLD binding to clathrin (Miele *et al.*, 2004), 10-100 μM for the Shc PTB domain binding to PtdIns(4,5)P_2 (Zhou *et al.*, 1995) and 2-5 μM for various PTB domains binding to FXNPXY peptides (Li *et al.*, 1998; Howell *et al.*, 1999; Stolt *et al.*, 2003; Stolt *et al.*, 2005). In a sequential hub model for clathrin-coated vesicle assembly, it is proposed that AP-2-dependent interactions are diminished as clathrin buds progress toward late-stage events (Schmid *et al.*, 2006; Schmid and McMahon, 2007). In fact, it is conjectured that ARH and β-arrestins only remain associated with deeply invaginated buds by interacting directly with clathrin heavy chains (Schmid *et al.*, 2006). Given

the tenfold difference in binding affinity for the β2 appendage and the clathrin terminal domain, which is also subject to direct competition by numerous other CLASPs and accessory proteins that have tandemly repeated clathrin boxes and are massed at the bud site (Robinson, 2004; Sorkin, 2004; Maldonado-Baez and Wendland, 2006), the biological advantage of moving to an apparently lower affinity association (at the clathrin hub) is not obvious.

The changing hub model was formulated, in part, to account for the inherent directionality of the clathrin-coat assembly process (Schmid *et al.*, 2006; Schmid and McMahon, 2007). Although our view is that CLASPs like ARH and β-arrestin, which associate physically with AP-2 through the β2 appendage, do not necessarily switch to a clathrin-dependent interaction mode in a temporally-defined manner, our observations certainly do not generally invalidate the model, which invokes changing degrees of freedom as a function of ongoing lattice assembly events. Nor do our findings indicate that the clathrin box in β-arrestin is functionally insignificant (Krupnick *et al.*, 1997b; Laporte *et al.*, 2000; Kim and Benovic, 2002; Santini *et al.*, 2002; Garuti *et al.*, 2005). Rather, our data agree with several independent investigations showing the β-arrestin·AP-2 interaction typically initiates clustering of GPCRs into clathrin-coated structures and simply preclude ARH and β-arrestins from the set of potential endocytic factors subject to displacement by assembling clathrin triskelia. Intriguingly, because of the clear functional redundancy between the adaptor β1 and β2 subunits, and because only a single pool of cytosolic clathrin is used to construct all clathrin-coats within the cell, utilization of neither the $[DE]_nX_{1\text{-}2}FXX[FL]XXXR$ motif nor the clathrin box will ensure translocation of β-arrestin or ARH to only those AP-2 and clathrin-containing structures positioned at the cell surface. However, both the β-arrestins (Gaidarov *et al.*, 1999; Milano *et al.*, 2002) and ARH (Mishra *et al.*, 2002b) bind to PtdIns(4,5)P_2, a lipid concentrated in the inner leaflet of the plasma

membrane. The phenomenon of coincidence detection, involving simultaneous contacts with transmembrane cargo receptors, lipids, AP-2 and then clathrin, likely provides the necessary selectivity. The striking translocation of the cytosolic pool of β-arrestin 1 upon angiotensin II application (Figure 3.4) is a graphic demonstration of this avidity-based phenomenon.

PIPKIγ661 specifically binds to the AP-2 β2 appendage sandwich subdomain (Chapter 2 (Thieman *et al.*, 2009)) along with other CLASPs eps15 and AP180 and clathrin itself (Edeling *et al.*, 2006a). Ultrastructural localization of eps15 within clathrin lattices shows it is selectively found at the edge where clathrin is absent or not fully polymerized (Tebar *et al.*, 1996; Edeling *et al.*, 2006a). Therefore clathrin may regulate positioning of sandwich binding partners during assembly. Consistent with this, PIPKIγ661 does not colocalize with AP-2 by confocal microscopy. PIPKIγ661 instead colocalizes with another one of its binding partners talin (Figure 3.5). Talin localizes to focal contacts and activates integrins for inside-out signaling to promote focal adhesion formation (Moser *et al.*, 2009). Talin also recruits PIPKIγ661 to generate PtdIns(4,5)P_2 in a positive feedback loop that promotes recruitment of other focal adhesion proteins including talin (Di Paolo *et al.*, 2002; Ling *et al.*, 2002). This exclusive colocalization of PIPKIγ661 within talin could indicate a higher affinity for the talin binding site. Indeed, the dissociation constant for the PIPKIγ661·talin interaction is ~270 nM (de Pereda *et al.*, 2005) compared with 22 μM for PIPKIγ661·AP-2 β2 (Kahlfeldt *et al.*, 2010). Alternatively, few unoccupied β2 appendages may make detection of PIPKIγ661 at the edge of clathrin lattices difficult to detect. However immunofluorescence for eps15 in HeLa cells clearly shows its colocalization with AP-2 (data not shown, see Chapter 4). Still, AP-2 structures were frequently found adjacent to PIPKIγ661 puncta suggesting some connection (Figure 3.5). Furthermore, although the isolated β2 interaction peptide of PIPKIγ661 did not colocalize with AP-2 or talin,

it undoubtedly caused morphological changes to endocytic structures when present in multiple copies (Figure 3.6). Therefore, the inability to detect fluorescent proteins at clathrin lattices may not indicate their complete absence at these sites in our microscopy setup. These enlarged AP-2 structures may accumulate from reduced endocytic ability as a result of interference of clathrin binding to the β2 sandwich site. Overall, the β2-appendage of AP-2 represents one hub within an intricate web of protein–protein interactions that promotes selective cargo endocytosis by facilitating initial CLASP recruitment.

4.0 THE ENDOCYTIC EFC-DOMAIN PROTEINS FCHO1 AND FCHO2 ARE NON-ESSENTIAL MODULATORS OF CLATHRIN ASSEMBLY

4.1 ABSTRACT

The precise mechanistic basis for clathrin coat initiation at discrete sites on the plasma membrane is uncertain although phosphatidylinositol 4,5-bisphosphate (PtdIns(4,5)P_2) plays a key role. We find the PtdIns(4,5)P_2-binding FCHO1/2 proteins appear as pioneer components at clathrin bud sites, often preceding clathrin deposition. Although HeLa cells produce mRNA transcripts encoding FCHO1 and FCHO2, only FCHO2 is detectable in endocytic clathrin-coated structures at steady state. RNAi-mediated depletion of FCHO2 in HeLa cells reduces, but does not eliminate, the number of clathrin-coated structures at the cell surface and slows, but does not prevent, cargo internalization. The remaining clathrin-coated structures appear aggregated or expanded. Simultaneous silencing of both FCHO1 and FCHO2 with siRNAs results in an analogous phenotype. This extent of large clathrin plaque expansion and/or clustering is infrequent in the control or mock-RNAi-silenced HeLa cells but prominent in MCF-7 cells. Expressed FCHO2 can reduce the size of endocytic structures in both cell lines. The regular size and distribution of surface AP-2- and clathrin-positive puncta is reconstituted in FCHO2-depleted HeLa cells by synchronous expression of either FCHO1 or FCHO2. Together, our data indicate that FCHO1/2 are early coat components with somewhat overlapping functions that play

a significant, albeit non-essential, role in clathrin coat operation. There appears to be several parallel routes to sustain functional clathrin-mediated endocytosis.

4.2 INTRODUCTION

Intracellular compartmentalization is a defining feature of all eukaryotic cells. The evolution of different internal compartments allowed specialization of biosynthetic and catabolic reactions within compositionally distinct, physically discrete subcellular organelles. Yet most membrane-bounded compartments depend on continual contact with other intracellular compartments to ensure proper long-term functioning. Exchange between different organelles typically relies on small, short-lived, tubulovesicular transport carriers, which generally cluster appropriate transmembrane protein cargo molecules and regulatory fusion factors into incipient buds while concurrently preventing efficient conveyance of inappropriate membrane components from the donor compartment (Bonifacino and Glick, 2004). A necessary intermediate in the budding process involves the deformation of an often planar or spherical donor membrane into a perpendicularly oriented cylindrical projection (Zimmerberg and Kozlov, 2005). Due to the universal importance of this membrane restructuring process, several structurally distinct families of soluble proteins can translocate to a bud site to couple membrane bending with vesicular transport. For example, along the endocytic pathway, the BAR (Bin1/amphiphysin/Rvs) domain proteins amphiphysin, endophilin (Ringstad *et al.*, 1999) and sorting nexin 9 (Soulet *et al.*, 2005; Taylor *et al.*, 2011) participate in clathrin-mediated endocytosis. The BAR-PH (pleckstrin homology) domain protein APPL1 (Li *et al.*, 2007; Zhu *et al.*, 2007) is positioned on very early peripheral endosomes (Erdmann *et al.*, 2007; Schenck *et*

al., 2008; Zoncu *et al.*, 2009; Taylor *et al.*, 2011), while other sorting nexins with a PX (phox)-BAR domain organization are found on maturing sorting endosomes (Cullen, 2008). Two common features of many of these membrane-associated proteins is the presence of a rigid crescent-shaped surface that closely apposes the bilayer and a propensity to oligomerize into rings or spirals. These properties seem to promote the physical forces necessary to constrain the bilayer for local bud restructuring (Zimmerberg and Kozlov, 2005; Frost *et al.*, 2009).

One class of membrane-binding, crescent-shaped endocytic proteins are the EFC (extended FCH (Fes/CIP4 homology)) domain proteins (Suetsugu *et al.*, 2010), which have alternatively been dubbed F-BAR proteins because of the overall structural similarity of the helical bundle EFC and BAR domain fold (Frost *et al.*, 2009). In all known EFC proteins, the EFC domain is positioned near the N terminus forming antiparallel α-helical homodimers but six discrete subfamilies are classified depending upon the presence of other modular domains within the polypeptide chain (Heath and Insall, 2008; Suetsugu *et al.*, 2010). The EFC domain proteins FCHO1 and FCHO2 (FCH only protein 1 and 2) (Katoh, 2004; Henne *et al.*, 2007) are characterized by a C-terminal μ homology domain (μHD), distantly related in primary sequence but with an analogous fold to the cargo-selective μ2 subunit of the heterotetrameric AP-2 clathrin adaptor (Reider *et al.*, 2009). This combination of an EFC domain with a μHD is unique and phylogenetically conserved. Since all other known proteins or protein complexes that contain a μHD (AP-1 to AP-4, COPI and stonin 1/2) handle cargo selection during the formation of transport vesicles (Ohno *et al.*, 1995; Owen and Evans, 1998; McMahon and Mills, 2004; Maritzen *et al.*, 2010), FCHO1/2 are candidate sorting adaptors. Indeed, the *Saccharomyces cerevisiae* orthologue, Syp1p, acts as a sorting adaptor for the transmembrane protein Mid2p at cortical actin patches (Reider *et al.*, 2009; Stimpson *et al.*, 2009), which correspond to clathrin-

dependent sorting stations at the cell surface. Here, we characterize the mammalian FCHO1 and FCHO2 proteins as integral endocytic components.

4.3 RESULTS

4.3.1 FCHO1 and FCHO2 are endocytic components

Human FCHO1 (KIAA0290; located on chromosome 19) and FCHO2 (on chromosome 5) display ~50% overall amino acid identity and a similar domain organization (Figure 4.1A) (Katoh, 2004). These paralogous proteins have orthologues in chordates, arthropods and nematodes (Katoh, 2004), as well as in unicellular eukaryotes (Reider *et al.*, 2009; Stimpson *et al.*, 2009). In the budding yeast *Saccharomyces cerevisiae*, Syp1p has an analogous architecture to FCHO1/2 despite limited (<20%) overall primary sequence identity (Figure 4.1A). Phylogenetic dendrograms (TreeFam TF328986) (Ruan *et al.*, 2008) show that SGIP1 is more closely related to FCHO2 than to FCHO1, but this protein, while containing a modular C-terminal μHD, lacks the folded N-terminal helical EFC domain (Figure 4.1A) (Uezu *et al.*, 2007). RT-PCR analysis with gene-specific primers reveals that both FCHO1 and FCHO2 transcripts can be detected in HeLa cells, although the specific FCHO1 amplicon is weak (Figure 4.1B). The presence of the appropriate FCHO1 PCR product is consistent with full-length cDNA clones (CR597235, CR620485 and CR625849) isolated from HeLa cells, and also with the identification of FCHO1- and FCHO2-derived peptides in proteomic analysis of HeLa cell extracts (www.humanproteinpedia.org) (Beausoleil *et al.*, 2006). Similar PCR products are found in the neuroblastoma-derived SH-SY5Y cell line (Biedler *et al.*, 1978), along with an appropriate

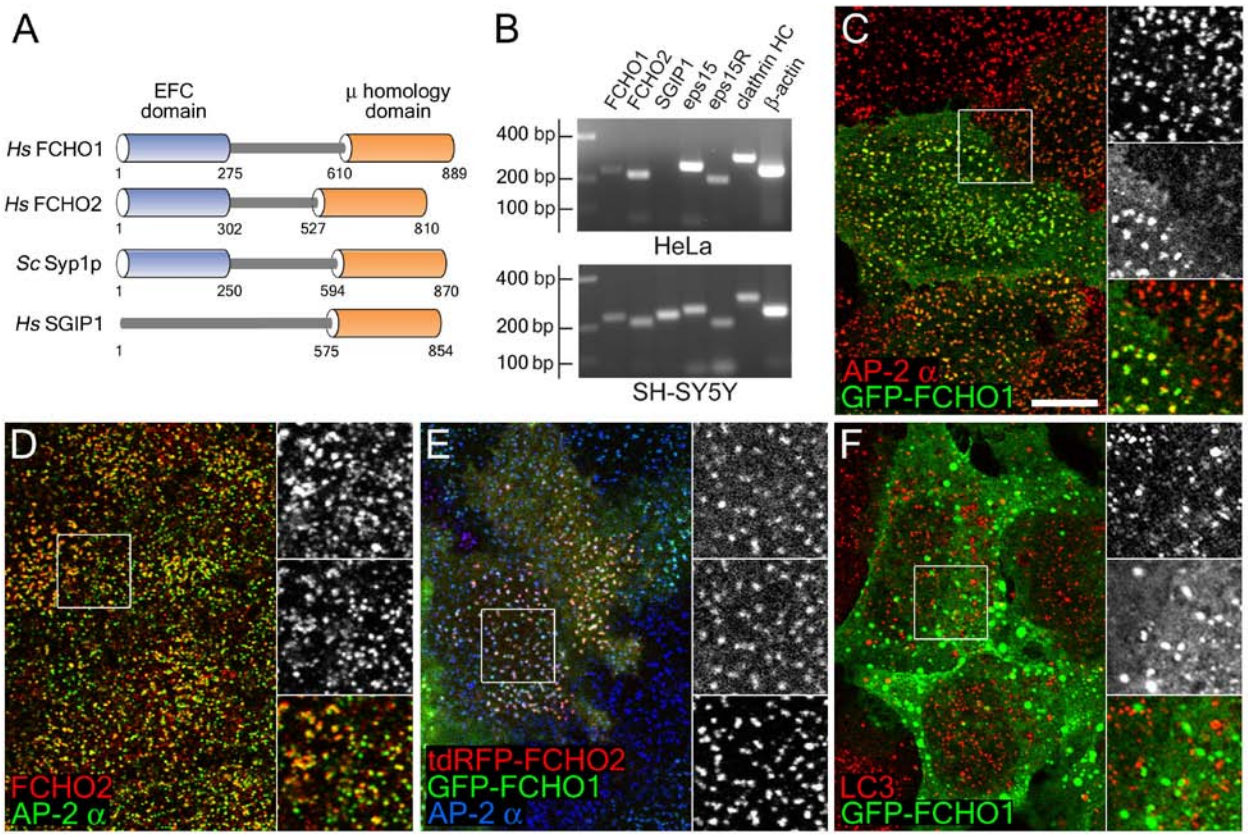

Figure 4.1: FCHO1 and FCHO2 are endocytic proteins.
(A) The muniscin family of *Homo sapiens* FCHO1, FCHO2 and SGIP1 and *Saccharomyces cerevisiae* Syp1p are shown schematically. The EFC domain is displayed in blue and μ homology domain in orange. Approximate domain boundary residue numbers are shown. (B) RT-PCR reactions with primers specific for a variety of endocytic proteins resolved on agarose gels from HeLa cell (top) and SH-SY5Y cell (bottom) lysates. The DNA ladder sizes are indicated at the left. Representative single confocal sections of the ventral membrane of HeLa SS6 cells transfected with GFP-FCHO1 (C,E), tdRFP-FCHO2 (E) or immunolabeled for endogenous FCHO2 (D) and AP-2α (C-E) are shown. (F) A representative medial confocal section of GFP-FCHO1 transfected HeLa SS6 cells immunolabeled for LC3. The vertical order of all insets is the same as the labels. Scalebar, 10μm.

PCR amplicon indicating the presence of the SGIP1 message (Figure 4.1B). Although SGIP1 is reported to be neuron specific (Trevaskis *et al.*, 2005; Uezu *et al.*, 2007), ESTs derived from some non-neuronal tissues are available, the SGIP1 message is evident in SWISS 3T3 cells (Stimpson *et al.*, 2009), and a tryptic peptide from SGIP1 expressed in HeLa cells is reported in the Human Proteinpedia database.

At steady state, both transfected FCHO1 (Reider *et al.*, 2009; Taylor *et al.*, 2011) and SGIP1 (Uezu *et al.*, 2007; Stimpson *et al.*, 2009) colocalize extensively with clathrin-coated structures, unlike several other EFC domain proteins (CIP4/FBP17/PACSIN) implicated in endocytosis (Modregger *et al.*, 2000; Kamioka *et al.*, 2004; Taylor *et al.*, 2011). Consistent with the PCR results, using three different polyclonal antibodies that do recognize transfected FCHO1, we cannot detect endogenous FCHO1 in HeLa cells by either immunoblot or immunofluorescence microscopy (data not shown). However, at low relative levels of expression, ectopic GFP-FCHO1 is found scattered over the ventral surface in both diffraction-limited spots and in larger, long-lived patches positive for the clathrin adaptor AP-2 (Figure 4.1C,E). By contrast, both endogenous (Figure 4.1D) and expressed FCHO2 (Figure 4.1E) colocalize very well with AP-2. Co-expressed GFP-FCHO1 and tdRFP-FCHO2 populate common AP-2-positive puncta at the cell surface (Figure 4.1E). In confocal X-Z projections, transfected FCHO1 or FCHO2 is present at AP-2-positive spots on both the upper and lower membrane surfaces, although enrichment at the ventral side is more marked (Figure 4.2A). At moderate levels of expression, FCHO1 saturates discrete AP-2-positive structures with the exception of those at the periphery and the excess FCHO1 uniformly labels the plasma membrane (Figure 4.1C; middle cell), likely due to the lipid binding properties of the EFC domain (Henne *et al.*, 2007). At the highest levels of overexpression FCHO1 accumulates in

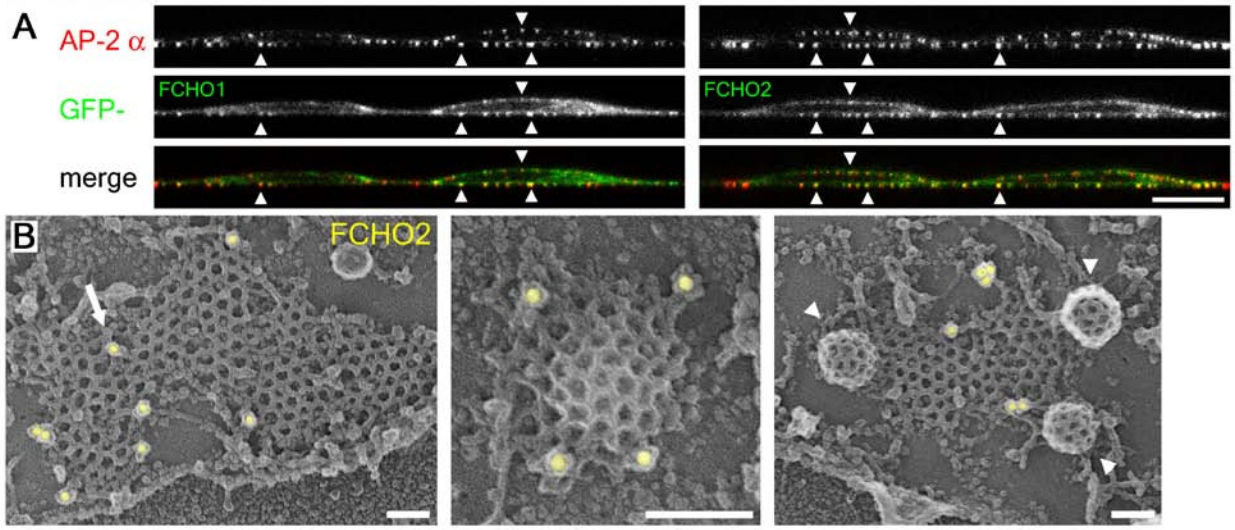

Figure 4.2: FCHO1 and FCHO2 are endocytic proteins, continued.
(A) X-Z projections of HeLa SS6 cells expressing GFP-FCHO1 or GFP-FCHO2 and immunolabeled for AP-2α showing FCHO distribution at the ventral (lower) and dorsal (upper) cell membranes. (B) Deep-etch electron microscopy of the ventral membrane of HeLa SS6 cells with 15-nm immunogold labeling (pseudocolored yellow) for FCHO2. The arrow indicates a region of clathrin lattice discontinuitiy while the arrowheads label deeply invaginated buds. Scalebars, 10μm for (A), 100nm for (B).

larger cytoplasmic puncta, which are not LC3 positive (Figure 4.1F), indicating these are not autophagosome-encapsulated protein aggregates. Some of the core clathrin coat components are not colocalized with these ectopic structures (data not shown). While heavily overexpressed GFP-FCHO1 accumulates at large intracellular foci (Figure 4.1F) (Nakajima *et al.*, 2005), we do not observe specific juxtanuclear localization of the protein at the *trans*-Golgi network (Sakaushi *et al.*, 2007). FCHO1 aggregation appears to be mediated by the μHD with possible contribution from the central unstructured segment as truncation mutants lacking these regions do not form intracellular puncta (data not shown). And unlike GFP-SGIP1-transfected COS-7 cells (Uezu *et al.*, 2007), intracellular tubules emanating from either large or small GFP-FCHO1-labelled membrane structures are rarely observed in fixed HeLa cells (Sakaushi *et al.*, 2007). Even at high relative levels of expression, FCHO2 does not display a similar tendency to form larger aggregates revealing distinct protein biochemistry between FCHO1 and FCHO2.

Endogenous HeLa cell FCHO2 is selectively detected at assembled regions of planar clathrin lattice and rounded *de novo* forming coated buds by immunogold labeling and deep-etch electron microscopy (Figure 4.2B). FCHO2 labeling is discernable principally around the perimeter of these structures on the ventral plasma membrane and only rarely in the center. This spatial dichotomy is not an artifact of poor antibody penetration into the assembled lattice as other coat constituents can be detected throughout the coat by this method (Edeling *et al.*, 2006a; Keyel *et al.*, 2006). In some larger clathrin assemblies, FCHO2 appears to be positioned at geometric discontinuities within the polymeric coat (arrow). The anti-FCHO2 antibodies do not decorate the domed portion of deeply contoured pits (arrowheads).

Like other established clathrin coat constituents, clustered GFP-FCHO1 in low-expressing cells exchanges rapidly ($t_{1/2}$ = 12.8 ± 0.9 sec, average ± standard error, n = 33) with

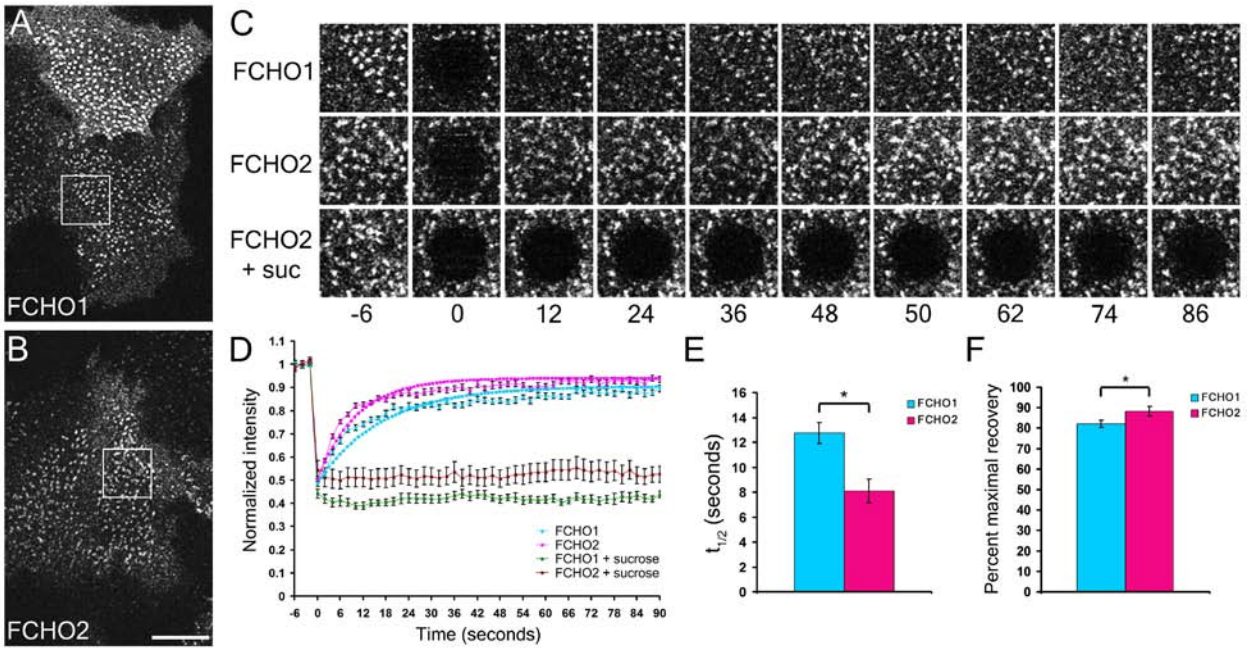

Figure 4.3: Dynamic exchange of FCHO1 and FCHO2 at CCSs.
HeLa SS6 cells transfected with GFP-FCHO1 (A) or GFP-FCHO2 (B) were imaged continuously at 2s/frame and were bleached with a 405nm laser for 2s at time 0 while simultaneously imaging with a 488nm laser (C). (D) The fluorescence intensity of individual FCHO1/2 spots present throughout the experiment were measured and plotted relative to the pre-bleach intensity. Curve-fitting was used to determine the time of half-maximal recovery, $t_{1/2}$ (E), and percent of maximal recovery (F). Asterisk indicates $p<0.05$. Error bars represent standard error. Suc, cells cultured in 0.45M sucrose. Scalebar, 10 μm.

the soluble population in FRAP experiments (Figure 4.3A,C). Interestingly, while GFP-FCHO2 exchanges similarly, it has a significantly faster recovery rate ($t_{1/2}$ = 8.1 ± 0.9 sec, n = 33, $p<0.05$) and greater maximal recovery (88 ± 2% versus 82 ± 2%, $p<0.05$) (Figure 4.3D-F), suggesting that FCHO2 undergoes more rapid exchange with the reserve cytosolic pool and has a larger mobile fraction than FCHO1. In parallel control experiments with 0.45 M extracellular sucrose, which halts clathrin coat protomer exchange activity (Wu *et al.*, 2003; Hoffmann *et al.*, 2010), both FCHO1 and FCHO2 are essentially static. These findings reiterate that FCHO1 and FCHO2 are dynamically interchanging constituents of surface clathrin-coated structures.

4.3.2 Chronology of FCHO1/2 association with endocytic structures

BS-C-1 cells (Hopps *et al.*, 1963) differ from HeLa and most other cultured cells in the conspicuous uniformity of clathrin-coated structures at the cell surface (Ehrlich *et al.*, 2004; Loerke *et al.*, 2009; Saffarian *et al.*, 2009). Still, transfected tdRFP-FCHO1 targets to clathrin-coated structures in BS-C-1 cells (Figure 4.4A), restating that this endocytic protein is not a selective constituent of long-lived clathrin structures as opposed to the *de novo*-forming buds typical of BS-C-1 cells (Saffarian *et al.*, 2009).

To better understand the role of FCHO1 and FCHO2 in clathrin-coated vesicle formation, the temporal properties of individual clathrin-coated structures in FCHO1-expressing cells were examined by total internal reflection fluorescence microscopy (TIR-FM). In BS-C-1 cells stably expressing clathrin light chain-GFP, tdRFP-FCHO1 is present in nearly all clathrin-positive surface structures (94%, Figure 4.4A). FCHO1 (Figure 4.4B, D) or FCHO2 (not shown) is often found preclustered at discrete regions of the plasma membrane prior to clathrin recruitment to these nascent, diffraction-limited bud sites, consistent with previous results (Henne *et al.*, 2010).

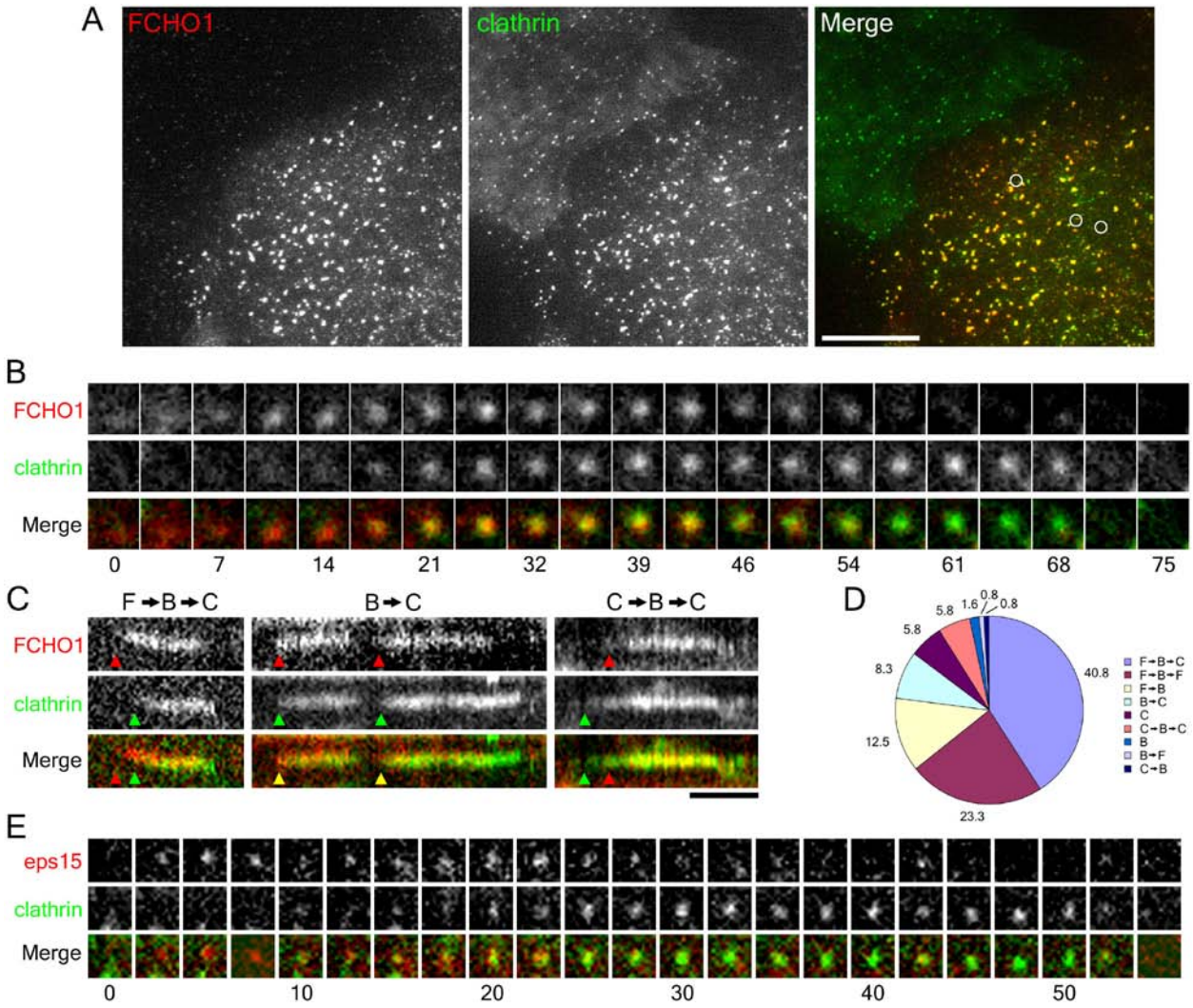

Figure 4.4: FCHO proteins are early components of *de novo* forming CCVs.
BS-C-1 cells stably expressing GFP-clathrin light chain were transfected with tdRFP-FCHO1 (A-C), or tdRFP-eps15 (E) and imaged by TIR-FM. (A) A transfected cell shows extensive colocalization of FCHO1 and clathrin at steady state. (B) The temporal appearance of FCHO1 relative to clathrin at an individual spot is shown. (C) Multiple recruitment profiles for FCHO1 are observed over time as represented by the Y (y-axis)-T (x-axis) kymograph. These spots appeared during image acquisition in the circular regions indicated in (A). 'F' indicates only FCHO1 is present, 'B' indicates both FCHO1 and clathrin are present and 'C' indicates only clathrin is present. (D) The order of appearance/disappearance of FCHO1 and clathrin were manually scored for 120 spots. The percentage of observances for particular profiles using the same nomenclature as in (C) are indicated by numbers on the pie chart. (E) The recruitment of the FCHO1/2 binding partner tdRFP-eps15 to a single clathrin-coated structure is shown. This was the most typical recruitment profile similar to (B) for FCHO1. Numbers below image sequences indicate seconds. Scalebar in A, 10μm. Timebar in C, 1 minute.

Analogous time-resolved TIR-FM imaging of BS-C-1 cells expressing tdRFP-eps15, a physical binding partner of FCHO1 and FCHO2 (Reider *et al.*, 2009; Henne *et al.*, 2010), shows that eps15 is also a pioneer component at emergent bud sites, similarly preceding the arrival of clathrin (Figure 4.4E). This is clearly analogous to the temporal behavior of Syp1p and Ede1p (the yeast eps15 orthologue) at endocytic cortical actin patches (Boettner *et al.*, 2009; Stimpson *et al.*, 2009). Analyzing global translocation of FCHO1 to assembling structures we find a majority (40.8%, Figure 4.4D) exhibit recruitment profiles in which FCHO1 appears prior to clathrin, both proteins then colocalize at the assemblage for some time, and then FCHO1 exits prior to clathrin disappearing from the evanescent field (Figure 4.4B). While various temporal behaviors are observed in BS-C-1 cells, 76.3% of examined structures display early recruitment of FCHO1 and 54.9% show FCHO1 loss prior to clathrin disappearance (Figure 4.3D) (Henne *et al.*, 2010; Taylor *et al.*, 2011). At individual buds, FCHO1 can appear 24 ± 3 seconds (average ± standard error, n = 86) before clathrin and disappear 22 ± 4 seconds (n = 66) prior to clathrin in structures with this behavior. Transfected tdRFP-FCHO2 does not display as noticeable an early arrival profile, perhaps reflecting the faster exchange dynamics.

To verify that the FCHO1-containing clathrin-coated structures are indeed functional, tdRFP-FCHO1 transiently transfected BS-C-1 clathrin light chain-GFP cells were pulsed with fluorescent transferrin while illuminating with TIR-FM (Figure 4.5A). Initially, transferrin is dispersed over the cell surface but quickly binds to clustered transferrin receptors by ~20 seconds. In these image sequences, tdRFP-FCHO1 molecules are already massed at incipient import sites at 10 seconds, while clathrin begins to accumulate around 30 seconds, approximately the same time the transferrin concentrates at the site. The transferrin-positive

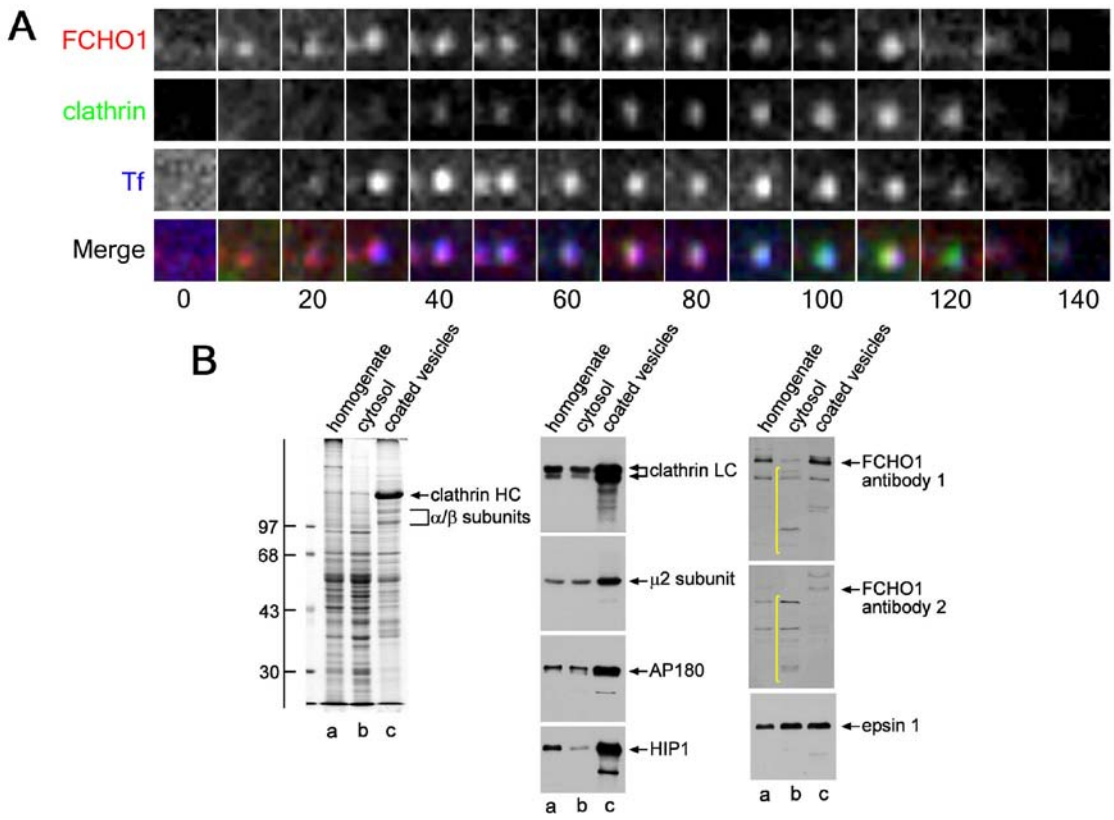

Figure 4.5: FCHO1-containing CCSs are functional and CCVs contain detectable levels of FCHO1. (A) During acquisition of a BS-C-1 GFP-clathrin light chain cell expressing tdRFP-FCHO1, transferrin-Alexa647 (Tf, blue) was added to the media at time point 0 and the progression of an individual clathrin spot is shown. (B) Rat brain fractions (~20 μg) were resolved by SDS-PAGE and stained with Coomassie (left) or transferred to nitrocellulose and probed with antibodies to clathrin and various adaptors (middle and right). Molecular weight marker standards in kiloDaltons are shown. Some FCHO1 degradation products in the cytosol fraction (lane b) are indicated by a yellow bracket. Numbers below image sequences indicate seconds.

clathrin-coated vesicle buds at about 130 seconds while FCHO1 dissipates ~10 seconds earlier. These kinetics of cargo sequestration and vesicle budding clearly indicate that the tdRFP-FCHO1-labelled structures are functional for cargo endocytosis. Our data thus confirm that FCHO1 (and FCHO2) are early arriving pioneer molecules at regions of the plasma membrane destined to become clathrin-coated vesicles (Henne *et al.*, 2010; Taylor *et al.*, 2011).

Because some tdRFP-FCHO1 puncta leave the evanescent field concurrently with punctate clathrin-containing structures (Figure 4.4C,D), we evaluated whether FCHO1 is found in purified clathrin-coated vesicles. The Allen Brain Atlas (www. mouse.brain-map.org) shows extensive FCHO1 RNA message expression in mouse brain by *in situ* hybridization with an antisense riboprobe, and many FCHO1 EST sequences have been obtained from human, mouse and rat brain tissue. In rat brain homogenate, an endogenous ~100-kDa FCHO1 band is identified on immunoblots with two affinity-purified anti-FCHO1 antibodies (Figure 4.5B). Less of the intact form is found in a high-speed cytosolic fraction, but the protein is present in purified clathrin-coated vesicles (Figure 4.4B), albeit not strongly enriched as other endocytic components, like AP180 and Huntington Interacting Protein 1 (HIP1) (Mishra *et al.*, 2001; Blondeau *et al.*, 2004; Thieman *et al.*, 2009), along with AP-2 and clathrin. A striking feature of these immunoblots is the extent of degradation of endogenous FCHO1 in brain cytosolic extracts. Considerable proteolysis is also apparent for full-length FCHO1 transiently expressed in HeLa cells (Figure 4.17); the protein may be subject to rapid proteolytic turnover. FCHO2 is expressed at very low levels in brain and is not found in coated vesicles comparably with FCHO1 (not shown). This agrees with recent findings (Henne *et al.*, 2010) and, along with the differential aggregation of FCHO1 upon forced expression (Figure 4.1F), suggests some separable properties for these apparently redundant paralogues.

4.3.3 FCHO1/2 regulate endocytic structure morphology on the ventral cell surface

Compatible with the low abundance of the FCHO1 transcript and inability to detect endogenous protein, transfecting a pool of FCHO1-targetting siRNA oligonucleotides into HeLa cells has no overt effect on AP-2 distribution (Figure 4.7B), discrepant with recent RNAi results in BS-C-1 cells (Henne *et al.*, 2010). That the siRNA duplexes indeed silence the appropriate mRNA is plainly seen by the dramatic loss of GFP-FCHO1 expression (Figure 4.6A-B). RNAi-mediated suppression of FCHO2 does, by contrast, have a significant effect on coat morphology (Figure 4.7C,E,G). Both ectopic GFP-FCHO2 and endogenous FCHO2 are depleted upon RNAi and the efficiency of protein knockdown is high (Figure 4.6A,C). Similar results are obtained with two independent FCHO2 transcript-targeting siRNAs (Figure 4.7C,E). Despite the dramatic change in endocytic structures on the ventral cell surface, AP-2 positive structures on the dorsal cell surface are minimally affected by FCHO2 knockdown as seen by X-Z projections (Figure 4.7H).

In silenced HeLa cells, an obvious change in the number and positioning of large abutting clathrin plaques occurs at the expense of the diffraction-limited population. In these cells, the average number of AP-2 structures per 100 μm^2 drops from 62 ± 3 in mock cells to 34 ± 2 ($p<0.05$) in FCHO2 knocked-down cells (Figure 4.7I). Coats on the ventral surface become heterogeneous, more clustered and irregular compared with the mock RNAi-treated cells. On average, the AP-2 patches in FCHO2 and FCHO1 + FCHO2 knockdown cells increase in size (Figure 4.7J). The average fluorescence intensity of AP-2 positive clathrin-coated structures >0.2 μm^2 increases by 9% when FCHO2 is extinguished (Figure 4.7C and data not shown). Together, this indicates that more AP-2 molecules are present at these structures. The incidence of >0.6

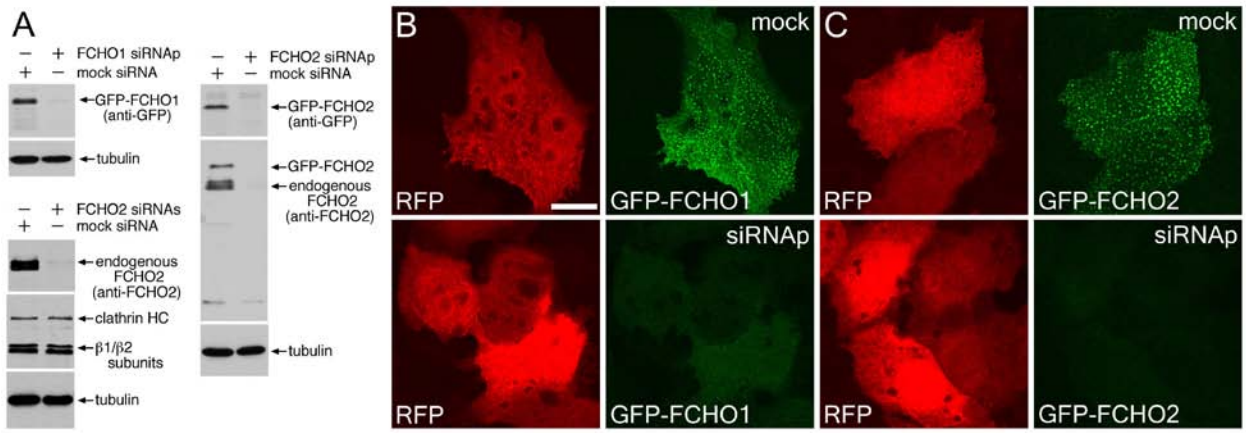

Figure 4.6: RNAi silencing of FCHO1 and FCHO2.
(A) HeLa SS6 cells were treated with two rounds of a mock, single siRNA (siRNAs) or siRNA pool (siRNAp) and cotransfected with GFP-FCHO1 or GFP-FCHO2 on the second round. Cell lysates were resolved by SDS-PAGE, transferred to nitrocellulose, and portions of the blot were probed with anti-GFP, anti-FCHO2, TD.1 anti-clathrin HC and 100/1 anti-AP-1/2 beta1/2, or anti-tubulin antibodies. Alternatively cells grown on coverslips were treated with siRNA by the same method except that they were cotransfected with tdRFP and GFP-FCHO1 (B) or GFP-FCHO2 (C) during the second round of RNAi. Cells were fixed and examined by confocal microscopy. Scale bar, 10 μm.

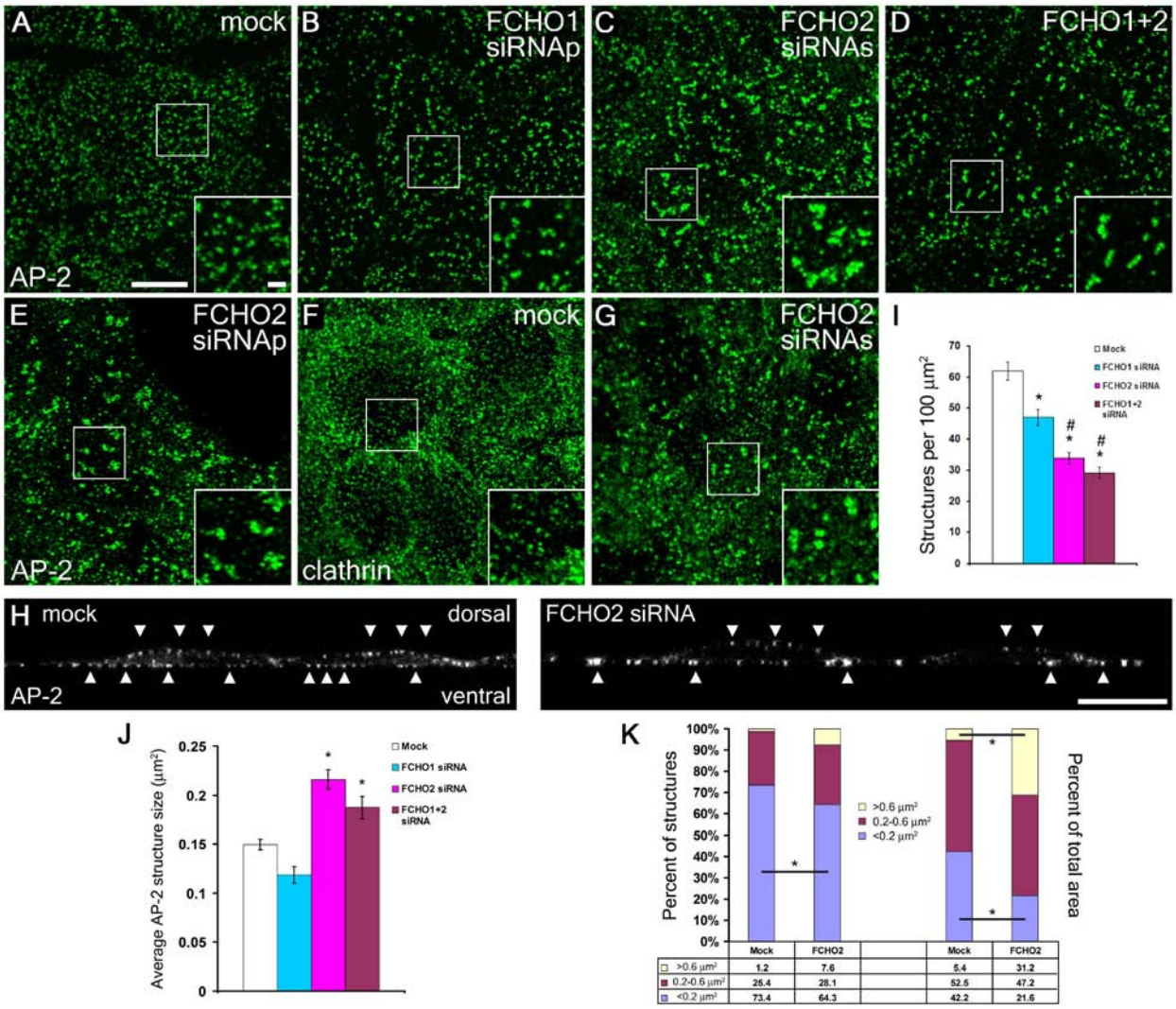

Figure 4.7: FCHO2 regulates CCS morphology.
HeLa SS6 cells were mock-treated (A,F) or transfected with FCHO1 pool (B), FCHO2 single (C,G), or FCHO1+FCHO2 siRNA (D) or FCHO2 pool siRNA (E) and prepared for immunofluorescence with AP.6 anti-AP2 α antibody (A-E) or X22 anti-clathrin heavy chain antibody (F-G). (H) X-Z projections of two mock or FCHO2 siRNA treated cells showing the distribution of AP-2 on dorsal and ventral membranes. (I) Quantitation of the concentration of AP-2 structures per 100 μm^2 in cells treated as in (A-D). Asterisk, $p<0.05$ relative to mock, # $p<0.05$ relative to FCHO1 siRNA, n=30 cells per condition. (J) Average AP-2 structure size in μm^2 in cells treated as in (A-D). Mock (n=1862 spots), FCHO1 (n=1410 spots), FCHO2 (n=1018 spots), FCHO1+2 (n=876 spots). (K) AP-2 structures in mock and FCHO2 siRNA-treated cells were binned into 3 groups: roughly diffraction-limited and small (<0.2 μm^2), medium (0.2-0.6 μm^2), and large (>0.6 μm^2) and compared. The percentage of total AP-2 structures falling into each of the three groups (left) or percent of the total surface area of AP-2 labeling contributed by each bin (right) were compared for mock and FCHO2 siRNA-treated cells. Percentage numbers are given below the graph. Asterisk, $p<0.05$. Error bars represent standard error. Scalebars in A and H 10μm. Scalebar in A inset, 2μm.

μm^2 AP-2 patches increases sixfold (Figure 4.7K left) and, strikingly, these large structures now account for >30% of the assembled AP-2 at the bottom of FCHO2-silenced cells (Figure 4.7K, right). The smallest AP-2 structures, <0.2 μm^2, contribute only half as much of the total area in FCHO2 knockdown cells, a decrease not fully accounted for by the drop in this population (Figure 4.7K, left), implying that these structures are smaller in size as well. Also, there is little difference between FCHO2 or FCHO1 + FCHO2 siRNA-treated cells, affirming a very small pool of functional FCHO1 protein in these cells.

The expanses of AP-2 we observe on the ventral membrane of cells following FCHO1/2 silencing may represent clustering of individual CCSs or dilation of individual clathrin lattices. To try to differentiate between the two we performed deep-etch electron microscopy of adherent HeLa cell ventral membranes. The electron micrographs clearly show that the extent of clathrin polymerization is greater in FCHO2 siRNA treated cells (Figure 4.8). The surface area of individual CCSs is greater in knockdown cells than in mock treated cells. What is more, FCHO2 structure (Henne *et al.*, 2007) and *in vitro* membrane tubulation assays (Henne *et al.*, 2010) suggest that FCHO2 is involved in membrane bending at CCSs, yet we still detect shallow and highly curved clathrin coats. Also, small *de novo* forming clathrin structures are seen in both conditions.

In reciprocal experiments, overexpression of GFP-FCHO1 or GFP-FCHO2 also causes changes in the morphology of endocytic structures on the ventral membrane of HeLa SS6 cells by light microscopy (Figure 4.9A-C). The average size of AP-2 structures is reduced from 0.197 $\pm$ 0.007 μm^2 in GFP expressing cells to 0.114 $\pm$ 0.006 μm^2 in GFP-FCHO1 expressing cells and 0.103 $\pm$ 0.004 μm^2 in GFP-FCHO2 expressing cells (n=45 cells) (Figure 4.9D). The concentration of AP-2 structures also increases from 63 $\pm$ 2 structures per 100 μm^2 in GFP

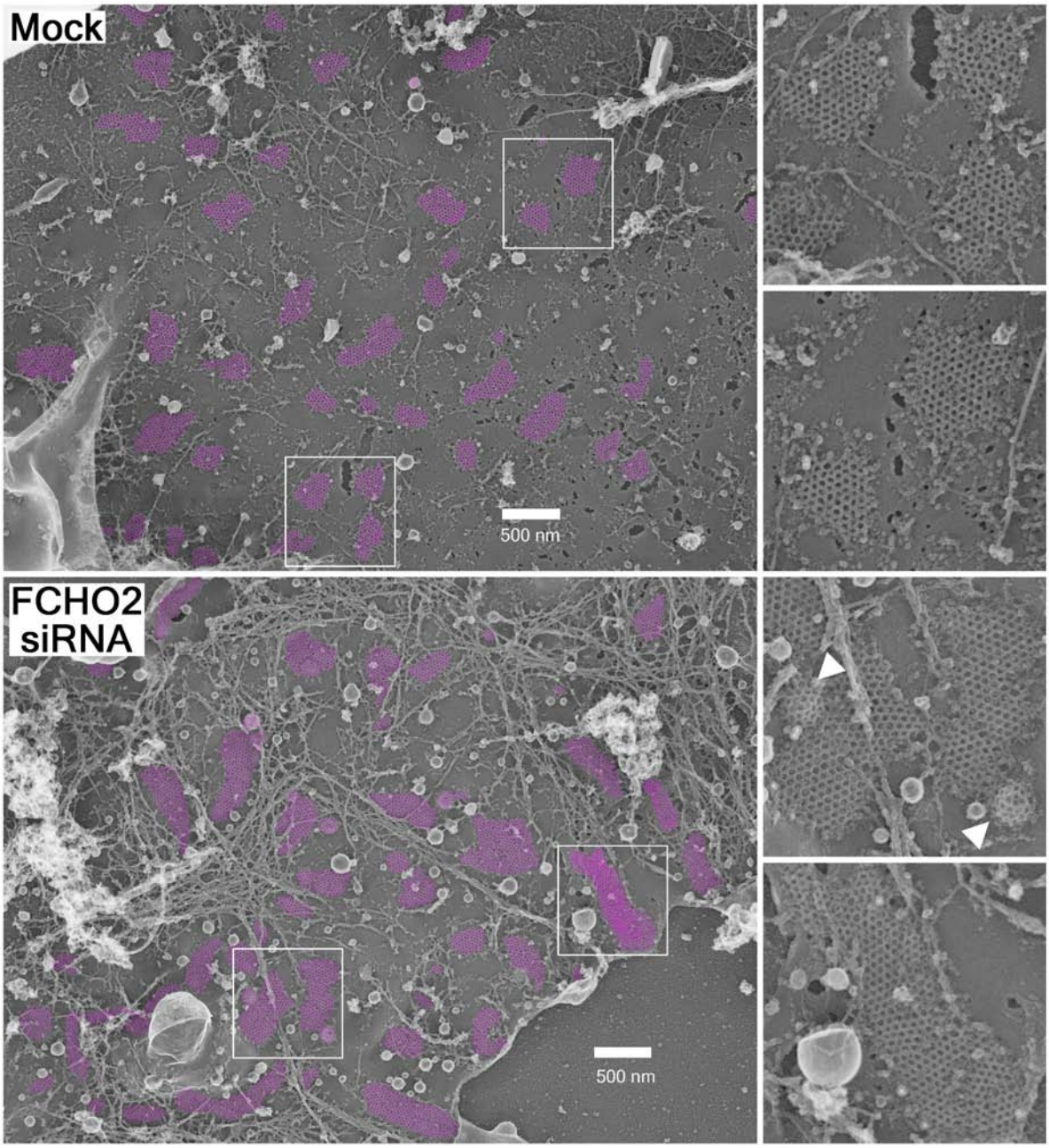

Figure 4.8: FCHO2 silencing causes expansion of ventral CCSs.
HeLa SS6 cells grown on coverglass where mock treated or treated with two rounds of FCHO2 siRNAs. Cells were unroofed by sonication, fixed and processed for deep-etch electron microscopy. CCSs are pseudocolored magenta to demonstrate distribution and size. Boxed areas are magnified on the right. Note the invaginating coats in FCHO2 siRNA-treated cells (arrowheads). Scale bars, 500 nm.

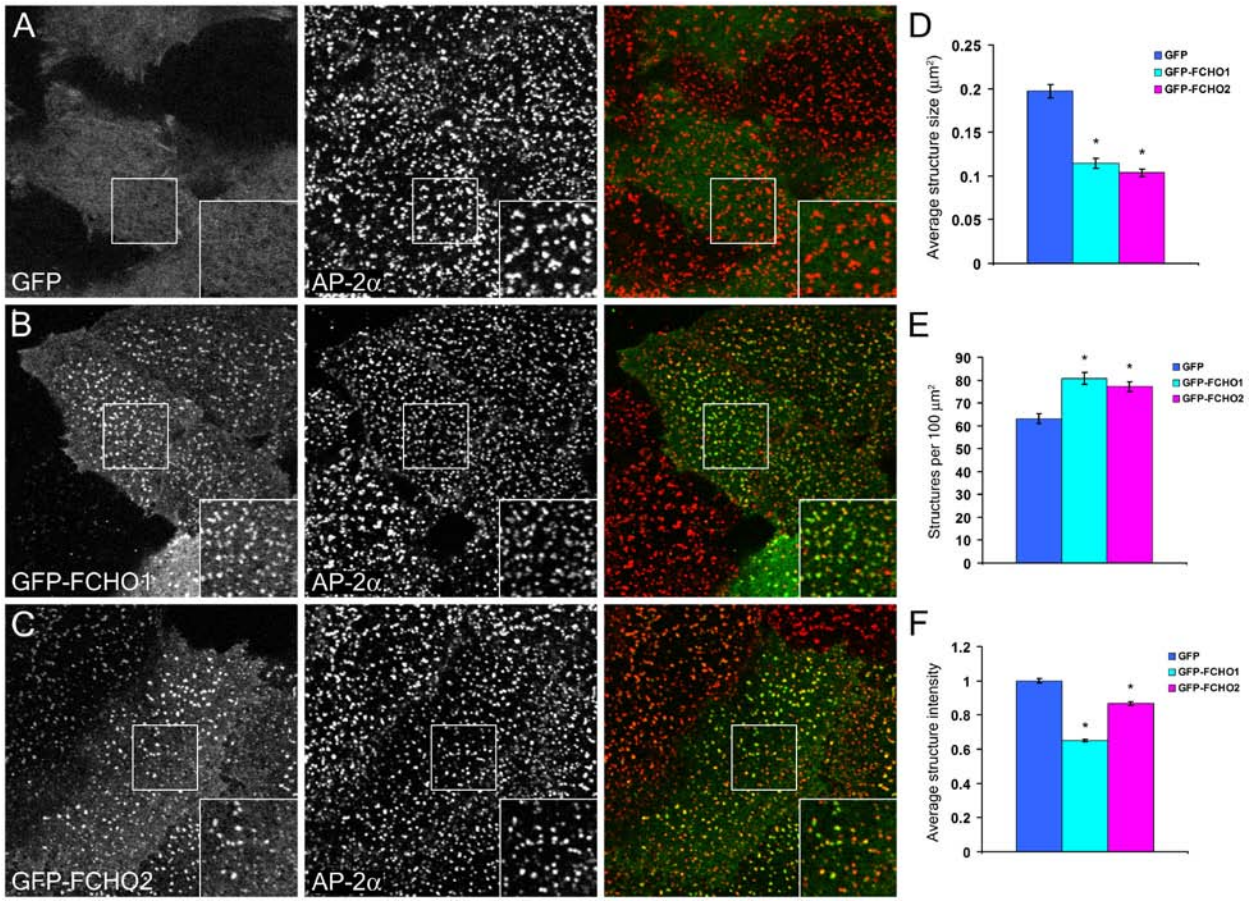

Figure 4.9: FCHO1 and FCHO2 overexpression alters the size and distribution of endocytic structures.

HeLa SS6 cells were transfected with GFP (A), GFP-FCHO1 (B) or GFP-FCHO2 (C) (left panels) and prepared for immunofluorescence for AP-2 α (middle panels). A decrease in the size of AP-2 structures (D) and an increase in the concentration of AP-2 structures (E) is quantified and can be seen as a result of FCHO expression (inset). An apparent decrease in fluorescence intensity (F) is also seen. Error bars represent standard error. Asterisk, $p<0.05$. Scalebar, 10 μm.

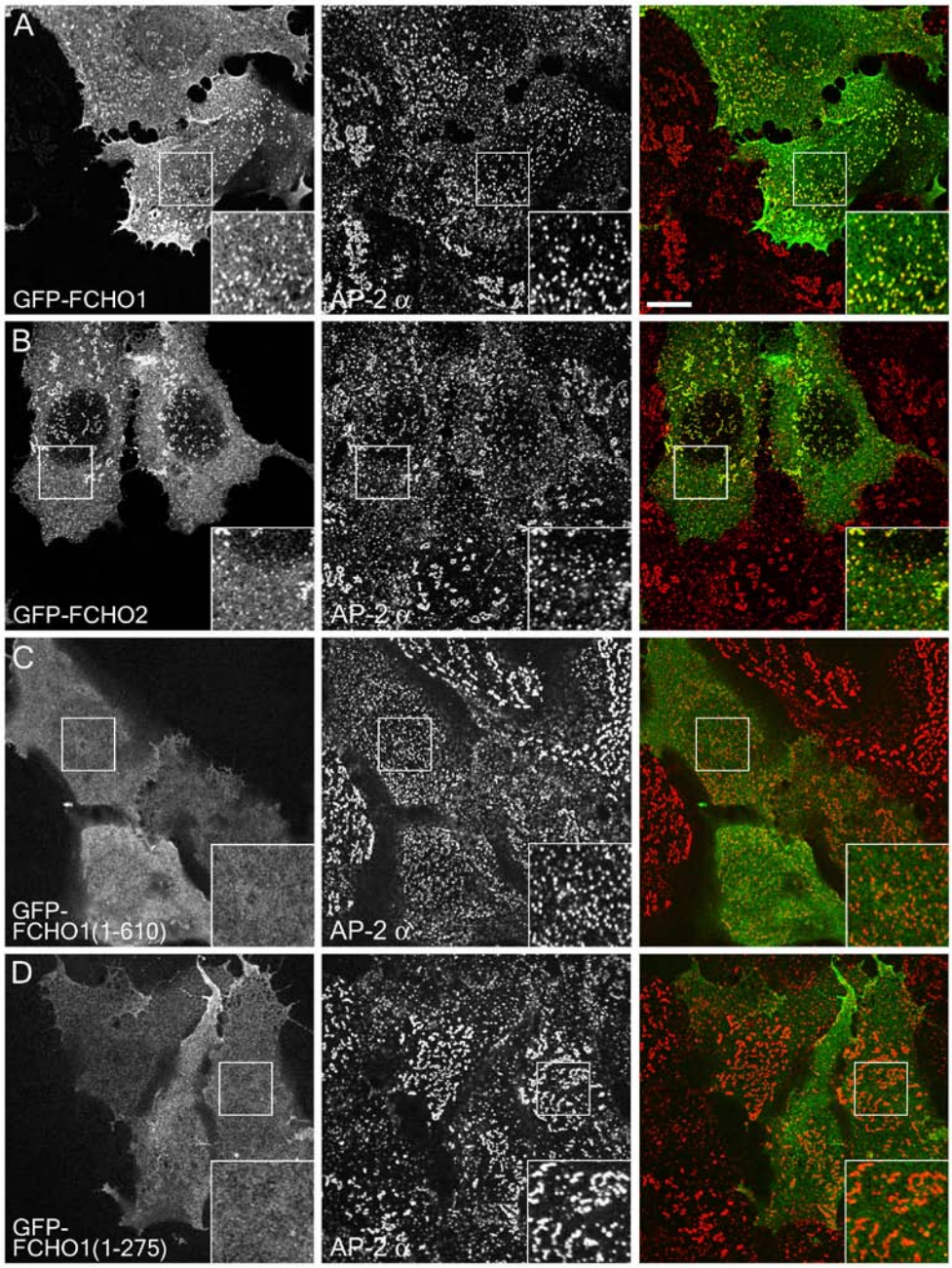

Figure 4.10: FCHO1 and FCHO2 reduce the size of native large CCSs.
MCF-7 cells were transfected with GFP-FCHO1 (A), GFP-FCHO2 (B), GFP-FCHO1(1-610) (C) or GFP-FCHO1(1-275) (D) and prepared for immunofluorescence with antibodies against AP-2 α. GFP-FCHO1 and GFP-FCHO2 colocalize with AP-2 and reduce the size of puncta relative to adjacent untransfected cells. GFP-FCHO1(1-610) causes a similar phenotype but does no colocalize with AP-2 while GFP-FCHO1(1-275) neither changes AP-2 morphology or colocalizes with the structures.

transfected control cells to 81 ± 3 or 77 ± 2 structures per μm^2 in GFP-FCHO1 or FCHO2 expressing cells respectively (Figure 4.9E). The average intensity of structures also falls in FCHO overexpressing cells (Figure 4.9F).

A substantial variability in CCS morphology and dynamic behavior at the plasma membrane of various cultured cell lines exists: this includes the diffraction-limited (<200 nm diameter), *de novo* forming CCSs in BS-C-1 cells (Ehrlich *et al.*, 2004; Loerke *et al.*, 2009), and a combination of *de novo* forming and large (>500 nm), long-lived, non-terminal budding CCS in HeLa (Keyel *et al.*, 2006; Saffarian *et al.*, 2009) and NIH 3T3 cells (Taylor *et al.*, 2011) among others. The breast carcinoma cell line MCF-7 (Soule *et al.*, 1973) displays numerous, AP-2-positive puncta, rings and lines on the ventral plasma membrane that are quite large (Figure 4.10, untransfected cells) when cultured under our conditions. Consistent with the results in HeLa cells but much more marked, GFP-FCHO1 and GFP-FCHO2 expression in these cells resulted in AP-2 structures that were smaller and more uniform in size (Figure 4.10A,B). Overall, FCHO1/2 play an important role in determining the number and size of clathrin-coated structures.

4.3.4 Clathrin-coated structures are dynamic and functional in the absence of FCHO2

Assembled CCSs contain a range of adaptors and accessory factors in addition to AP-2 and clathrin (Traub, 2005) and being an early arriving protein, FCHO2 may influence the positioning of some of these components. Steady-state components of normal endocytic clathrin coats, like eps15, epsin 1 and Dab2 (Keyel *et al.*, 2006), are still present at enlarged lattices in FCHO2-silenced HeLa cells (Figure 4.11). This indicates that although eps15 and eps15R bind directly to the FCHO1/2 μHD (Reider *et al.*, 2009; Henne *et al.*, 2010), this association is not required for

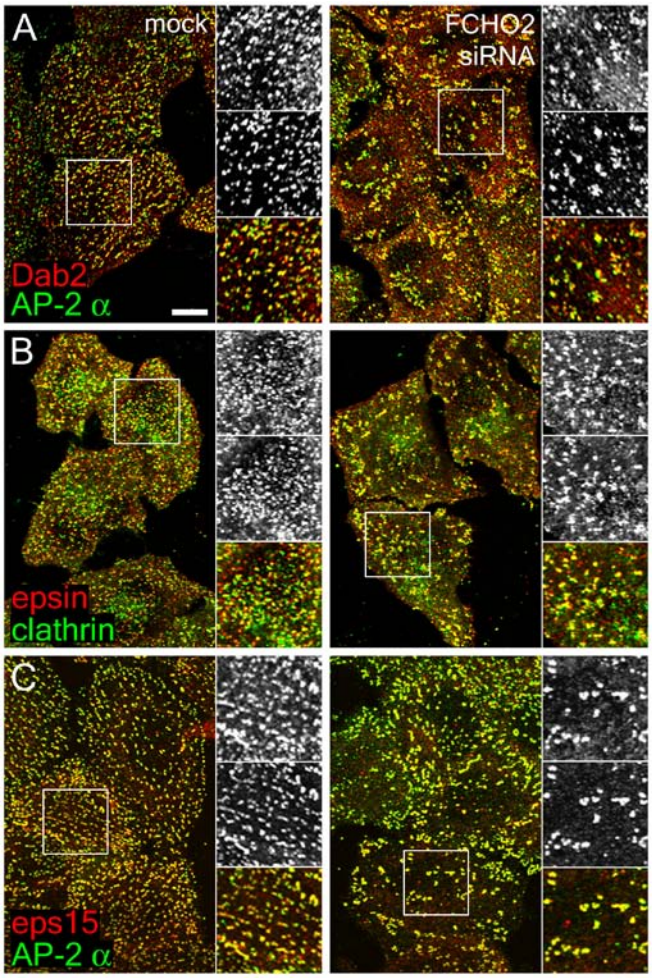

Figure 4.11: Adaptor content of CCSs in FCHO2 silenced cells.
HeLa SS6 cells treated with two rounds of mock or FCHO2 pool siRNA were fixed and labeled with antibodies to Dab2 (A), epsin 1 (B), or eps15 (C) and AP.6 anti-AP2α (A,C) or X22 anti-clathrin heavy chain (B). Scalebar, 10 μm.

placement of eps15/R in surface coats; instead the capability of eps15/R to interact with numerous other endocytic proteins probably assures incorporation into polymerizing lattice devoid of FCHO2. We are unable to replicate the published penetrant FCHO1/2 RNAi phenotype of complete loss of endocytic clathrin coats in BS-C-1 cells (Henne *et al.*, 2010) despite obviously efficient silencing of FCHO2 in the whole cell population (Figure 4.16A,F).

To determine if these enlarged AP-2 patches in HeLa cells are possibly arrested intermediates, we first conducted FRAP experiments with FCHO2 knocked-down cells (Figure 4.12A). In mock-treated cells, AP-2 recovers in bleached zones with a $t_{1/2}$ = 37 ± 6 s (n = 33) (Figure 4.12B, C). This is slower than previously published (Wu *et al.*, 2003; Hinrichsen *et al.*, 2006) and is probably due to the fact that this stable cell line expresses low levels of the β2-YFP subunit that incorporates into <10% of AP-2 molecules at steady state. Depleting FCHO2 does not significantly affect the return rate ($t_{1/2}$ = 42 ± 4 s, n = 33) or the extent of recovery (83 ± 5% compared with 78 ± 5% for mock) (Figure 4.12D). Therefore, the AP-2 in clathrin-coated structures at the surface exchanges with the reserve cytosolic pool at similar rates in either the presence or absence of FCHO2 and can likely rely on the cohort of endocytic proteins at assembled lattices for its targeting.

Next, we examined the lifetime of AP-2 positive structures on the ventral surface of HeLa cells in the presence or absence of FCHO2. HeLa cells differ fundamentally from BS-C-1 cells in that they contain numerous long-lived clathrin-coated structures termed patches or plaques (Maupin and Pollard, 1983; Wu *et al.*, 2003; Keyel *et al.*, 2008; Saffarian *et al.*, 2009) (Figure 4.12E). Ablation of FCHO2 significantly reduces the number of AP-2 spots observed over a 10-min period by ~60% (Figure 4.12E-G); this is largely a result of a drop in the total

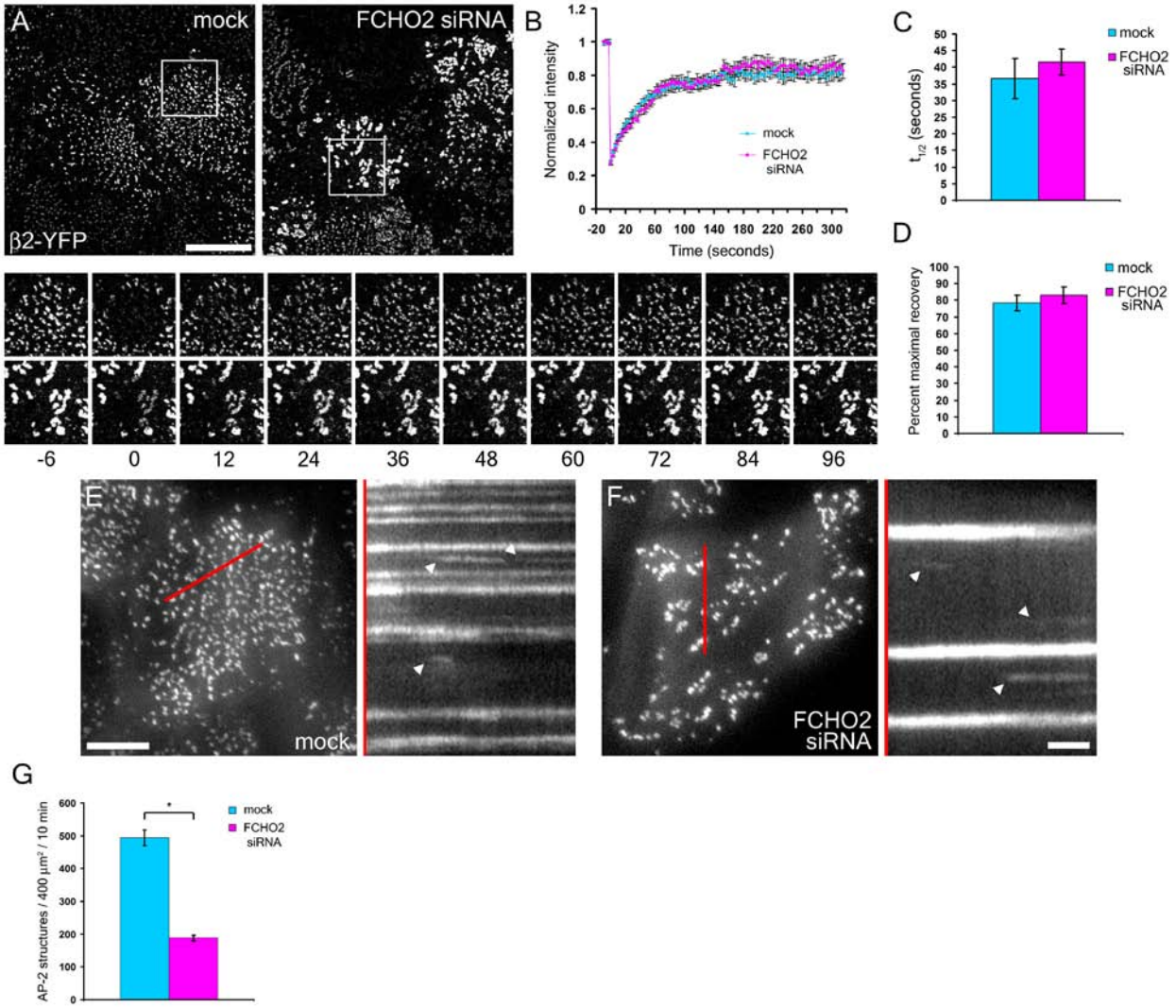

Figure 4.12: Enlarged endocytic structures in FCHO2 knockdown cells have dynamic properties similar to control cells.

(A) HeLa SS6 cells stably expressing AP-2 β2-YFP were mock treated or treated with two rounds of FCHO2 siRNA and imaged by confocal microscopy. At time point zero, a 5 μm circular region was bleached for 2 seconds and imaged continuously. (B) The fluorescence intensity of 33 spots within bleach regions per condition were averaged and plotted relative to pre-bleach intensity. The recovery curves were fitted and used to calculate the time of half-maximal recovery, $t_{1/2}$ (C), and percent of maximal recovery (D). (E-F) HeLa SS6 β2-YFP cells were treated as in (A) and imaged by TIRF microscopy. A three-pixel wide line (red line) was used to create an X-T kymograph from a 10 minute experiment. Both stable assemblies and transient structures (arrowheads) are observed. (G) The total number of AP-2 spots in a 400 μm^2 region over a 10 minute period were averaged for mock and FCHO2 knockdown cells (n=12 cells). Asterisk, $p<0.05$. All error bars represent standard error. Scalebars in A and E, 10 μm. Timebar in F, 3 minutes.

number of structures/μm^2 (see Figure 4.7). However both stable and short-lived endocytic structures are seen in both conditions.

In *S. cerevisiae*, an overt general endocytic defect is not apparent in a *syp1*Δ strain (Reider *et al.*, 2009; Stimpson *et al.*, 2009). Likewise, the essentially normal exchange dynamics, coat lifetimes and CLASP deposition in FCHO2- (and FCHO1 and FCHO2)-depleted cells all suggest that the large clathrin assemblies are likely operational. Indeed, transferrin receptor is found populating AP-2 structures in FCHO2 knockdown cells (Figure 4.13A). Still, a fundamental functional distinction between large clathrin plaques and diffraction-limited clathrin buds has been proposed (Saffarian *et al.*, 2009). The transferrin receptor, a prototypical cargo receptor, is internalized through recognition of a YXXØ-type sorting signal within its cytosolic domain (Jing *et al.*, 1990) by the μ2 subunit of AP-2 (Ohno *et al.*, 1998; Owen and Evans, 1998). The low density lipoprotein (LDL) receptor, by contrast, displays an FXNPXY sorting signal (Chen *et al.*, 1990) recognized by the PTB domain CLASPs Dab2 and ARH (He *et al.*, 2002; Keyel *et al.*, 2006; Maurer and Cooper, 2006). As the FCHO1/2 μHD can bind to Dab2 (Henne *et al.*, 2010), internalization of these two cargo molecules may differ in cells in which FCHO2 is extinguished. Following a 10-min pulse of fluorescently labeled transferrin at 37°C, FCHO2 siRNA-treated HeLa cells show a modest but significant decrease in endocytosis (82 ± 2% the level of mock-treated cells, $p<0.05$, n = 146 cells) (Figure 4.13B,D). Providing FCHO2 knocked-down cells with fluorescently labeled LDL continuously for 20 min at 37°C produces a similar result, with cells internalizing 81 ± 2% the level of mock-treated cells ($p<0.05$, n = 144 cells) (Figure 4.13C,D). These data show that while FCHO2 silenced cells have a grossly altered AP-2 and clathrin distribution, only a subtle effect is observed on bulk endocytosis. In addition,

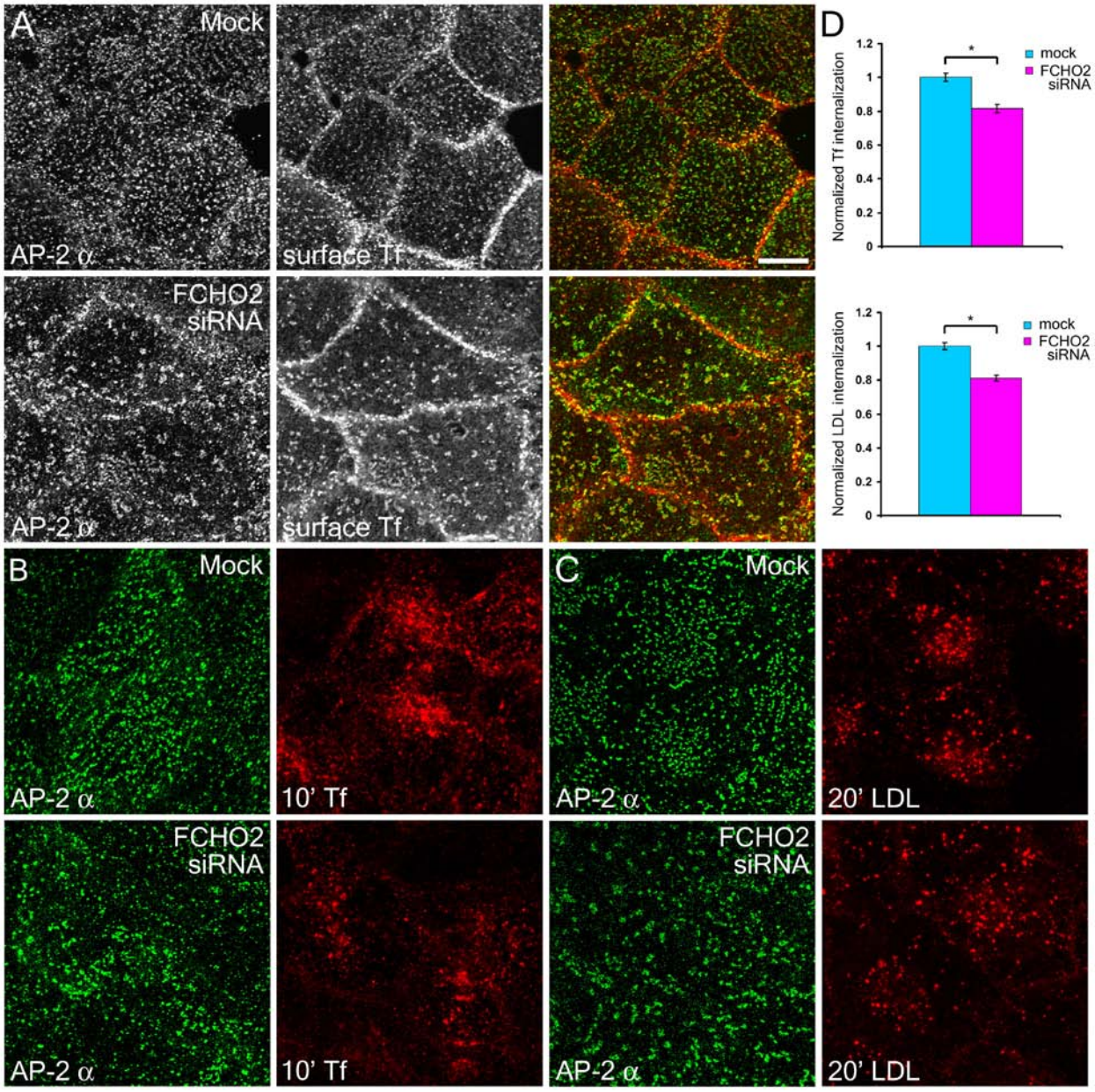

Figure 4.13: Ablation of FCHO2 causes a slight inhibition of endocytosis.
(A) Mock and FCHO2 siRNA-treated HeLa SS6 cells were incubated on ice for one hour with fluorescent transferrin (Tf, red) and then prepared for immunofluorescence of AP-2 (green). Ligand-bound transferrin receptor colocalizes with AP-2 in both conditions. In separate experiments, mock and FCHO2 siRNA-treated HeLa SS6 cells were incubated in the continuous presence of fluorescent Tf for 10 minutes (B) or the continuous presence of fluorescent low density lipoprotein particles (LDL) for 20 minutes (C) at 37°C and then processed for AP-2 immunofluorescence. Representative confocal sections of the ventral cell membrane (AP-2) and maximum Z-projections of the entire cell volume (ligand) are shown. (D) Quantitation shows a ~20% reduction of internalized Tf and LDL following FCHO2 kockdown. Asterisk, $p<0.05$. Error bars represent standard error. Scalebar, 10 μm.

transmembrane cargo recognized by the core adaptor AP-2 and cargo recognized by the CLASPs Dab2 and ARH are equally affected suggesting a general retardation in the kinetics of uptake.

4.3.5 Molecular dissection of FCHO1/2 in its regulation of clathrin-coated structures

The FCHO2 knockdown phenotype in HeLa cells is obtained with two independent siRNA preparations, but to confirm that this is not due to off-target effects, we performed rescue experiments by expressing GFP-FCHO1, tdRFP-FCHO2, or various truncation/chimera constructs (Figures 4.14A and 4.15). Cotransfecting cells with siRNA and GFP produces the typical altered morphology of more sparsely distributed AP-2-positive structures that are larger with brighter apparent fluorescence. By contrast, cotransfection with full-length GFP-FCHO1 or tdRFP-FCHO2 restores the number and more regular size of AP-2 structures (Figures 4.14A and 4.15). Despite a variation in the mouse FCHO2 nucleotides surrounding the siRNA target sequence relative to human FCHO2, this murine transgene is still partially silenced (Figure 4.15). This may explain the lower rescue efficiency observed (Figure 4.14C). These results validate that the morphological phenotype is specific to loss of FCHO2, and that FCHO1 and FCHO2 are functionally redundant in this aspect of their operation.

Tellingly, our failure to abrogate completely clathrin-mediated endocytosis upon FCHO1 + FCHO2 RNAi (Figure 4.16) is not restricted to just HeLa cells. In the human fibrosarcoma cell line HT-1080 (Rasheed *et al.*, 1974) and the breast carcinoma MCF-7 (Soule *et al.*, 1973) fluorescent transferrin is transported from the cell surface to endosomes despite effective silencing of the FCHO2 mRNA and dramatic loss of the protein (Figure 4.16B-F). FCHO1 + 2-silenced HT-1080 cells display a less prominent change in the arrangement of surface clathrin structures than knocked-down HeLa cells but the MCF-7 cells show large clustered clathrin- and

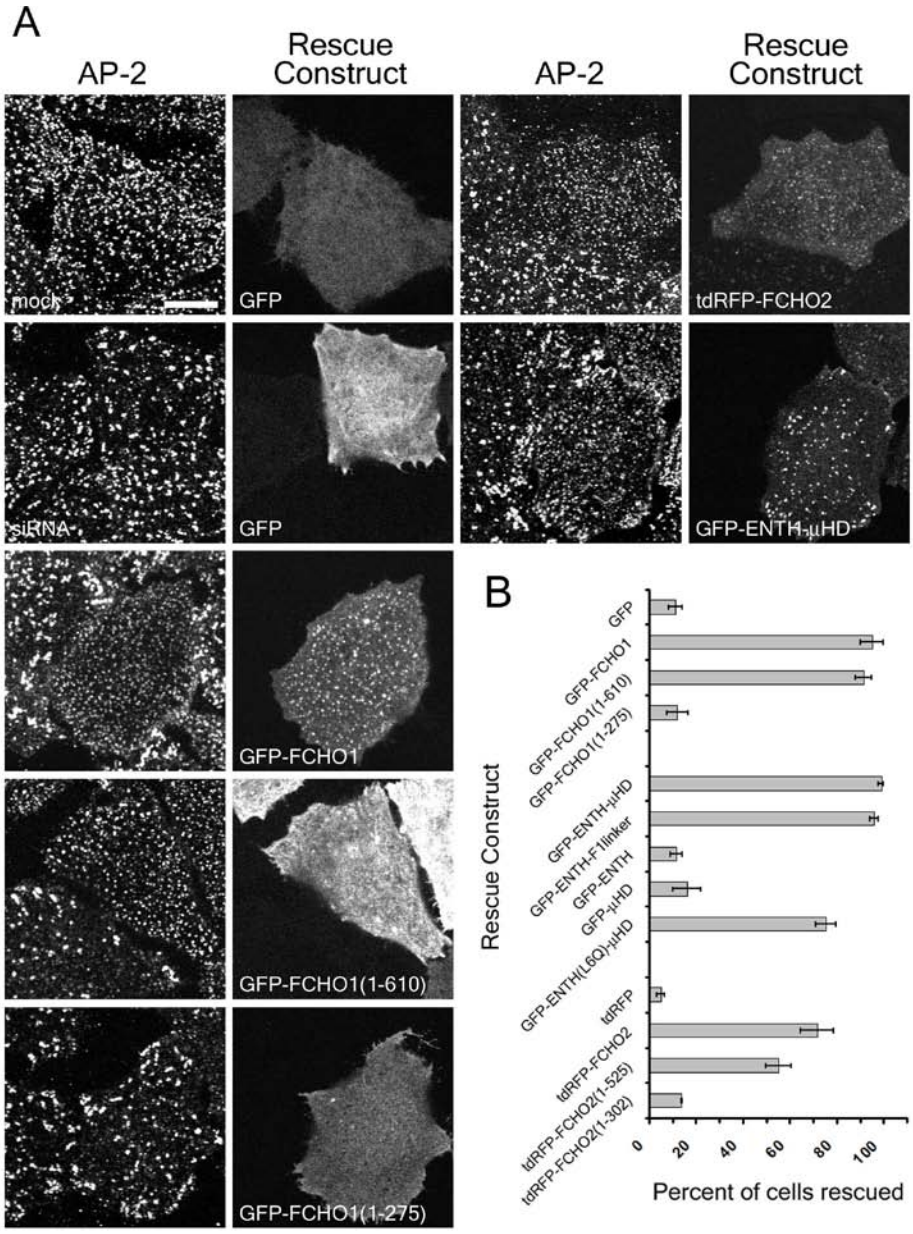

Figure 4.14: Rescue of the FCHO2 knockdown phenotype.
(A) HeLa SS6 cells were treated with two rounds of mock or single FCHO2 siRNA and on the second round were cotransfected with various GFP or tdRFP plasmids. Cells were prepared for immunofluorescence of AP-2 and representative confocal images of the ventral membrane of plasmid expressing cells are shown. (B) Random fields of FCHO2 siRNA-treated and GFP or tdRFP expressing cells were captured and the plasmid was scored for its ability to restore the wildtype distribution of AP-2 as defined by spot concentration and size. Constructs tested include GFP (n=101 cells), GFP-FCHO1 (full length human 1-889, n=68 cells), GFP-FCHO1(1-610) (n=63 cells), GFP-FCHO1(1-275) (n=63 cells), GFP-ENTH-µHD (epsin1 ENTH+FCHO1(276-889), n=81 cells), GFP-ENTH-F1linker (epsin1 ENTH+FCHO1(276-610), n=90 cells), GFP-ENTH (n=72 cells), GFP-µHD (FCHO1(610-889) (n=65 cells), GFP-ENTH(L6Q)-µHD (n= 103 cells), tdRFP (n=59 cells), tdRFP-FCHO2 (full length mouse 1-809, n=96 cells), tdRFP-FCHO2(1-525) (n=95 cells), tdRFP-FCHO2(1-302) (n=64 cells). Error bars represent standard error.

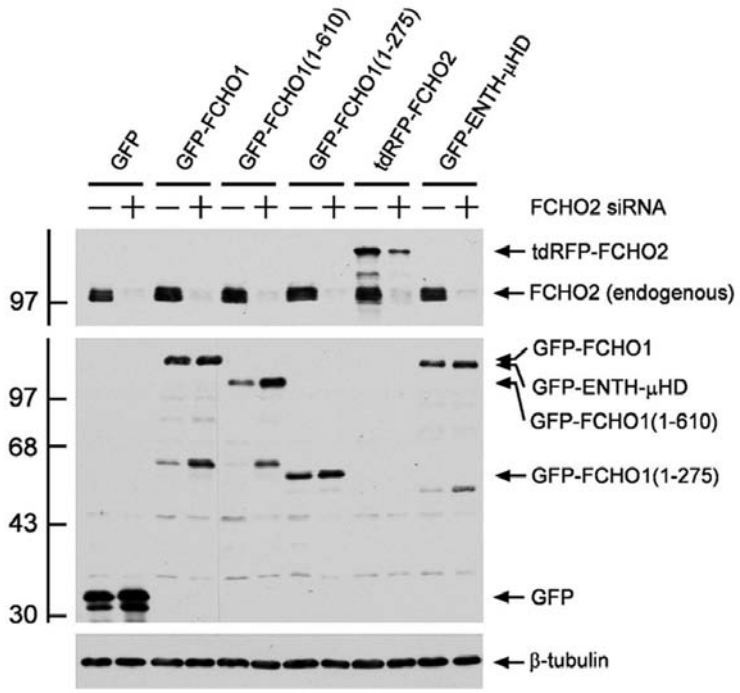

Figure 4.15: Biochemical confirmation of FCHO2 knockdown and rescue.
Cells treated as in Figure 4.14 were lysed in sample buffer and resolved by SDS-PAGE. After transferring to nitrocellulose, portions of the blot were probed with antibodies against FCHO2, GFP, or tubulin. Note the partial silencing of tdRFP-FCHO2. Positions of molecular weight standards (in kDa) are shown on the left.

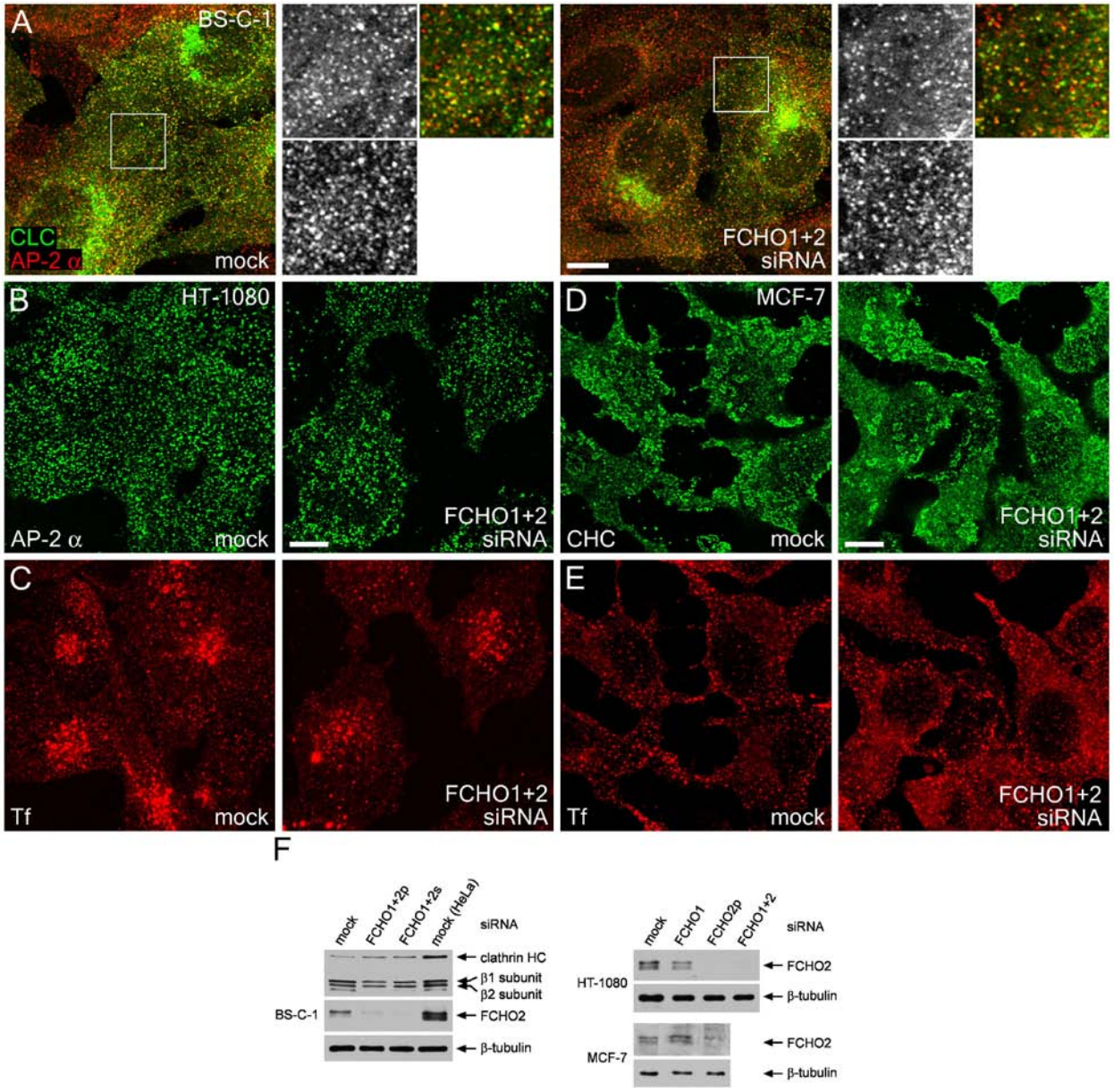

Figure 4.16: Survey of FCHO1/2 knockdown in a variety of mammalian cell lines.
BS-C-1 cells stably expressing GFP-clathrin light chain (CLC) (A), human fibrosarcoma HT-1080 cells (B) and human breast adenocarcinoma MCF-7 cells (D) were mock treated or treated with two rounds of FCHO1 and FCHO2 pool siRNA. HT-1080 (C) and MCF-7 cells (E) were incubated for 10 minutes at 37°C in the continuous presence of 25 μg/mL Tf, washed, and all cells were fixed and prepared for immunofluorescence with antibodies against AP-2 α (A,B) or clathrin heavy chain (D). (F) BS-C-1 GFP-CLC, HT-1080 and MCF-7 cells were treated as above with either FCHO1 and FCHO2 pool siRNA (FCHO1+2p), FCHO1 pool and FCHO2 single siRNA (FCHO1+2s), FCHO1 pool siRNA (FCHO1) or FCHO2 pool siRNA (FCHO2p), lysed in sample buffer and resolved by SDS-PAGE. After transferring to nitrocellulose, portions of the blot were probed with TD.1 anti-clathrin heavy chain, GD/1 anti-AP1/2 β1/β2 subunits, anti-FCHO2, and anti-β-tubulin antibodies.

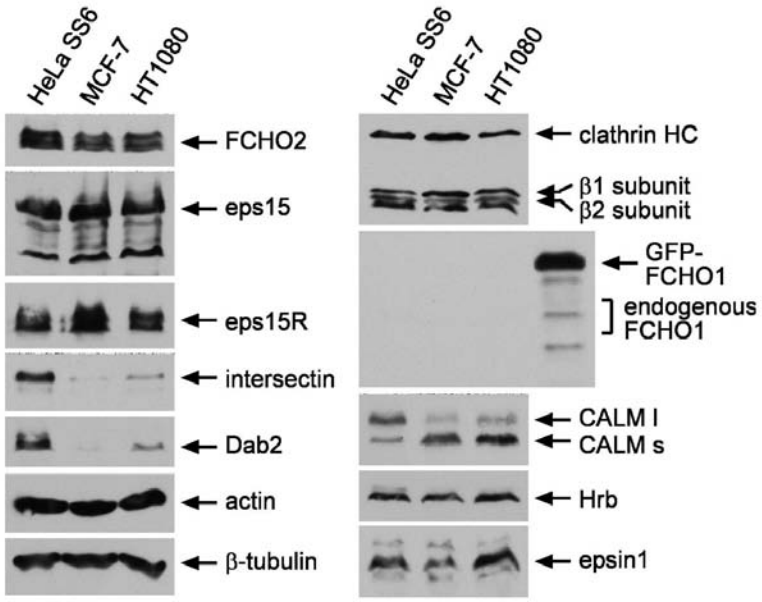

Figure 4.17: Endocytic protein composition of cell lines examined.
Equal concentrations (~70 μg) of untreated HeLa SS6, MCF-7 and HT-1080 lysates were resolved by SDS-PAGE, transferred to nitrocellulose and probed with antibodies against various clathrin coat components. The extra lane in the FCHO1 immunoblot is from HeLa cells transiently transfected with GFP-FCHO1 as a positive control. The bracket is to show where the endogenous FCHO1 band would be expected.

AP-2-positive patches in the absence of FCHO1 + 2 RNAi (Figure 4.16D). Interestingly, this morphological alteration is not due to a lack of expression of FCHO2 protein although it resembles strongly the phenotype that ensues extinguishing these proteins in HeLa cells. A431 squamous carcinoma cells similarly contain large clustered, often ring-like clathrin assemblages on the ventral surface (Hawryluk *et al.*, 2006) and express moderate FCHO2 mRNA transcript levels (www.proteinatlas.org). Dual transfection of MCF-7 cells with FCHO1 and FCHO2 silencing siRNAs does not dramatically alter the morphology of endocytic clathrin structures on the bottom surface of these cells. These results indicate that alone the FCHO1 and/or FCHO2 protein concentration is not the only regulator of clathrin-coated structure aggregation and patch size. I suspect that the relatively mild (HT-1080) or nonexistent (MCF-7) phenotype associated with FCHO1 + 2 knockdown compared with the phenotype in HeLa cells may reflect variations in FCHO1/2 binding partner expression in these cell lines. For instance, in MCF-7, intersectin and Dab2 are barely detectable and in HT-1080 cells they are a fraction of the expression level in HeLa cells (Figure 4.17). In contrast, the levels of FCHO2 and its other binding partners eps15/R are quite similar (Figure 4.17).

The rescue assay allowed us to further probe the structural properties of FCHO1/2 necessary for steady-state endocytic site morphology. While the FCHO1 EFC domain (residues 1-275, Figure 4.1A) alone is not capable of reversing the FCHO2 knockdown phenotype, unexpectedly the EFC and unstructured linker (residues 1-610) do restore cells to a phenotype similar to the normal AP-2 distribution, even though this truncated protein is generally not targeted stably to AP-2 structures at steady state (Figure 4.14). The same is observed for the FCHO2 EFC domain (1-302) and FCHO2 EFC and unstructured linker (1-525) (Figure 4.14B). This suggests that the μHD (residues 610-889 in FCHO1 or 527-810 in FCHO2) plays an

important role in retaining FCHO1/2 at AP-2-positive structures. These data also indicate that a region within the unstructured linker is important for proper maintenance of AP-2/clathrin bud site morphology. In fact, the ability of FCHO1 to reduce the size of large steady-state endocytic structures in MCF-7 cells is also dependent on the unstructured linker but not the μHD (Figure 4.10A,C,D).

This is further exemplified by reconstituting FCHO2-silenced HeLa cells with a chimeric protein composed of the PtdIns(4,5)P_2-binding epsin 1 ENTH (epsin N-terminal homology) domain fused in frame to the unstructured linker and μHD (residues 276-889) of FCHO1 (ENTH-μHD; Figure 4.12A,B). Truncating this construct prior to the μHD still allows rescue of surface clathrin morphology to the same extent (Figure 4.14B). Some evidence suggests that the epsin 1 ENTH domain promotes membrane deformation/tubulation by inserting an amphipathic α helix, ordered around the PtdIns(4,5)P_2 head group, into the bilayer (Ford *et al.*, 2002). If plasma membrane curvature generated by the FCHO1/2 EFC domain is important for the steady-state distribution of AP-2, this property of the ENTH domain could explain the ability of this chimera to rescue. However mutation of Leu6 on the ENTH amphipathic α helix, a residue important for *in vitro* tubulation but not PtdIns(4,5)P_2-rich membrane binding (Ford *et al.*, 2002), did not abrogate rescue of FCHO2 knockdown (GFP-ENTH(L6Q)-μHD, Figure 4.14B). A caveat of these data is that while rescue of morphology is assessed, function is not, such that these ENTH and truncation chimeras may not rescue protein exchange or wild type levels of endocytosis.

4.4 DISCUSSION

FCHO1/2 are early-arriving elements of the endocytic clathrin coat machinery. The steady state positioning of these proteins is a manifestation of the inherent affinities for PtdIns(4,5)P_2, eps15/R, intersectin and Dab2 (Reider *et al.*, 2009; Henne *et al.*, 2010) and, in the case of FCHO1, the AP-2 α appendage (unpublished observation). Unlike other EFC domain proteins tentatively linked to clathrin-mediated endocytosis including Toca1 (Bu *et al.*, 2010), FBP17 (Kamioka *et al.*, 2004), CIP4 (Feng *et al.*, 2010) and PACSINs (Qualmann and Kelly, 2000; Taylor *et al.*, 2011), the muniscins are undoubtedly components that govern the positioning and operation of coated structures. Here we demonstrate that FCHO1 and FCHO2 play a role in determing the number of CCSs in some cell types, regulate the size of flat clathrin lattices on the ventral plasma membrane, and have separable properties from each other that may differentiate their precise functions *in vivo*.

FCHO1/2 are argued to be master levers of CME by remodeling the initial membrane patch and recruiting eps15 and intersectin prior to AP-2 (Henne *et al.*, 2010). Generally, the expression levels of FCHO1/2 do impact the number of CCSs, at least in certain cell types. There was an apparent loss of structures upon FCHO2 knockdown and increase in structures on FCHO1/2 expression in HeLa cells. Also, FCHO1/2 expression in MCF-7 cells appeared to increase the number of endocytic structures perhaps as a result of breaking up the large continuous network of AP-2 staining. However, at most the loss of structures from FCHO2 knockdown was only ~50% and certainly not a complete removal despite complete knockdown. Furthermore we and others (Henne *et al.*, 2010; Taylor *et al.*, 2011) have shown that FCHO1/2 and interacting partner eps15 are clearly early components of *de novo* forming CCSs, often appearing before the onset of AP-2 and clathrin, a behavior not known for any other components

of clathrin assemblies. This positioning is optimal for initiating assembly. While our data do support a clear role in coat initiation, they argue that muniscin-mediated regulation is more complex than a binary actuator of clathrin nucleation.

We believe that FCHO1/2 are not absolutely required for initiation of CME for the following reasons: 1. Depletion of FCHO2 does not alter the ability of AP-2 to exchange with AP-2 molecules in the cytosol (Figure 4.12). In the model proposed earlier (Henne *et al.*, 2010), AP-2 is tethered by FCHO1/2 through eps15/intersectin so that depletion of the FCHO1/2 would certainly hinder AP-2s ability to target to the membrane. In assembled clathrin lattices, other factors present likely allow for exchange. 2. Although the total number of AP-2 structures forming at the surface is reduced in FCHO2 knockdown cells, there are still populations of short and long-lived endocytic structures indicating that FCHO1/2 do not selectively regulate a subset of endocytic structures (Figure 4.12). 3. Endocytosis of transferrin and LDL particles is reduced in knockdown cells, consistent with point 2, but this reduction is modest (~20%) (Figure 4.13 and 4.16). The remaining structures are competent for endocytosis. 4. Invaginating clathrin assemblies are still observed in FCHO2 knockdown cells (Figure 4.8). Clathrin can still stabilize curvature induced by itself or other EFC or BAR domain proteins or possibly by epsin 1. 5. The adaptor content of CCSs is not drastically altered in the absence of FCHO2 (Figure 4.11). 6. A multiparametric high-throughput siRNA screen of proteins to determine their involvement in endocytosis placed FCHO1 and 2 in groups for their role in endosome positioning, not modulation of Tf or EGF endocytosis (Collinet *et al.*, 2010). Endosomes were more peripheral for FCHO2 knockdown similar to what we saw (Figure 4.13), and could be a result of a small reduction in uptake. 7. In yeast, the FCHO1/2 orthologue Syp1p is not required for endocytosis (Stimpson *et al.*, 2009).

An important question is whether or not early sculpting of the bud site by FCHO proteins prior to assembly of clathrin is a prerequisite for clathrin-coated vesicle formation as proposed (Henne *et al.*, 2010)? This obviously pertains more to *de novo* buds on the scale of 100-200 nm diameters than large flat clathrin lattices. In the HeLa SS6 cells we use, knockdown of clathrin results in patches of AP-2 that are invariably flat (Hinrichsen *et al.*, 2006). Presumably FCHO2 is present but is not inducing curvature. In human skin fibroblasts, staged reassembly of clathrin-coated structures by hypotonic shock and recovery followed by deep-etch electron microscopy showed that early clathrin-coated structures are flat and only round up at later time points (Larkin *et al.*, 1986). Finally, rescue experiments with the ENTH-μHD chimera, particularly the amphipathic helix mutant deficient for *in vitro* tubulation, was able to rescue CCS size and placement suggesting that EFC domain-generated membrane curvature was not necessary for steady state morphology of flat clathrin lattices present in these cells. Because it is reasonable to suggest that the ability of FCHO1/2 to promote membrane curvature is regulated by its concentration at bud sites and its oligomeric state, it seems that initially FCHO1 and FCHO2 function primarily in coat assembly rather than for membrane bending but could function in such a role at later stages during their peak concentrations.

A second major finding from this study is that FCHO1 and FCHO2 regulate the size of clathrin assemblies on the ventral membrane of cultured cells. This likely arises from the fact that expressed FCHO1 and FCHO2 are more highly enriched at AP-2 structures on the ventral membrane rather than the dorsal membrane (Figure 4.2A) and FCHO2 knockdown has a greater effect on the distribution and morphology of ventral CCSs (Figure 4.7H). Reduction of FCHO1/2 protein levels increases CCS size in some of the cell types examined reciprocal to the effect on CCS number, while increasing FCHO1/2 expression reduces CCS size. Changes in clathrin

lattice size could happen by either promoting or limiting clathrin polymerization at lattice edges or through increased or decreased non-terminal budding which may occur at the edges of these structures (Rappoport *et al.*, 2004; Traub, 2009; Taylor *et al.*, 2011). Consistent with a role in regulating lattice size, FCHO2 is found at the periphery of *de novo* and long-lived ventral CCSs (Figure 4.2B).

These observations have led us to propose two, not mutually exclusive models. In one model FCHO1 and FCHO2 act as scaffolds to properly arrange pioneer constituents to promote swift polymerization of *de novo* coated buds. As assembly continues, the peripheral ring of FCHO1/2 might allow ordered assembly of AP-2, other CLASPs and regulatory factors in the growing coat coupled to membrane deformation through its EFC domain. At pre-existing clathrin lattices, FCHO1/2 may promote CCV budding from the edges again coupling ordered assembly through eps15/R and intersectin and membrane bending. In the absence of FCHO2, *de novo* buds could still form, but may take longer, hence slowed uptake. Slowed or reduced budding from the edges of long-lived clathrin lattices could yield expanded CCSs if the balance between assembly and removal is skewed. Or moderately slowed uptake may represent the increased diffusion time of transmembrane cargo required to encounter the larger plaques as they are less abundant on the plasma membrane. Conversely, higher concentrations of FCHO1/2 could promote nucleation of more *de novo* structures or promote greater budding from lattices.

FCHO2 is positioned at the edges of flat clathrin-lattices and *de novo* buds (Figure 4.2B) similar to eps15 (Tebar *et al.*, 1996; Edeling *et al.*, 2006a). The interactions of FCHO2 with eps15 and intersectin through the μHD and also the occupancy of the eps15 (Edeling *et al.*, 2006a) and intersectin (Pechstein *et al.*, 2010a) binding sites on the AP-2 β2 appendage sandwich subdomain by assembled clathrin may dictate the positioning of these proteins. At the

edges of the lattices where clathrin assembly is incomplete, eps15 and intersectin could promote AP-2 and clathrin assembly perhaps in concert with FCHO2 induced membrane invagination. Removal of FCHO1/2 and eps15 from *de novo* structures just prior to budding (Figure 4.4 and (Henne *et al.*, 2010), and the absence of detectable levels of FCHO2 on deeply invaginated buds (Figure 4.2B)) could be accomplished by a combination of occupancy of all AP-2 molecules by clathrin with no further AP-2 deposition and membrane curvature of the bud that begins to exceed the intrinsic curvature of the FCHO EFC domain, thus weakening its interaction with the membrane. The fact that FCHO1/2 typically depart from the assemblage before the final budding event could explain how overexpression changes the dynamics of clathrin-coated structures. Increased FCHO1 or -2 concentration by forced expression changes the equilibrium and spots become longer lived and more static in BS-C-1 cells (data not shown). This argues that exit of the majority of FCHO1/2 is required for rapid budding, perhaps because the oligomer must be disassembled.

Yet a precise role of scaffolding assembly early and membrane curvature at a later time is hard to reconcile with the capability of the ENTH-μHD (wildtype and L6Q, membrane bending-deficient), particularly the truncated version of this chimera lacking the μHD (scaffolding deficient), to maintain normal coat morphology and distribution in FCHO2-silenced HeLa cells. Also, invaginating coats are observed at the edges of flat lattices in FCHO2 knockdown cells (Figure 4.8). FCHO1 and FCHO2 could interact with an unidentified protein through the unstructured linker region allowing it to be recruited at lower levels in the absence of the μHD. The identity of such a partner and how this partner contributes to reducing CCS size and increasing CCS number remain to be determined.

In the second model, FCHO1/2, eps15 and intersectin may define the outer perimeter of emerging coated structures. In doing so they could prevent the coalescence and fusion of individual CCSs, maintaining a higher number of more uniform structures. To accomplish this, the putative binding partner of the FCHO1/2 unstructured linker (as the μHD-truncated mutant can substitute) may act to directly or indirectly affect free clathrin triskelion leg availability, preventing or not favoring the anti-parallel engagement of free legs by adjacent lattices. This could be an important role for these proteins as flat clathrin lattices can persist on the plasma membrane for periods greater than 10 minutes (Figure 4.12) (Saffarian *et al.*, 2009). In addition, CCSs may move laterally within the plasma membrane actively on microtubules in some contexts (Rappoport *et al.*, 2003) or experience natural lateral translations during their lifetime at the surface (Loerke *et al.*, 2009). Perhaps through the μHD and eps15/intersectin, FCHO1/2 promote CCS nucleation and at later stages the proposed linker-binding partner regulates adjacent lattice tethering. Reduction of FCHO2 would allow clustering of CCSs and expansion of individual regions of clathrin coats, but in this model it is unclear how overexpression of FCHO1/2 would reduce CCS size. Also while this model explains how ENTH-μHD can rescue the FCHO2 knockdown phenotype because less importance is placed on membrane bending, it cannot account for the μHD truncation mutant's targeting to CCSs. Altogether, while the second model cannot fully explain some of the observations from the rescue experiments, it is better supported by the data.

Because FCHO1/2 is not restricted to diffraction-limited spots in HeLa cells (Figures 4.1 and 4.2) (Henne *et al.*, 2010) and overexpressed FCHO1 and FCHO2 populate the majority of clathrin-coated structures, we do not believe that *de novo* clathrin-coated buds differ from the long-lived, static plaques by selective incorporation of either muniscin. Nor do we believe *de*

novo spots carry the bulk of cargo or represent the major carrier in receptor-mediated endocytosis (Saffarian *et al.*, 2009) as the enlarged CCS in FCHO2-silenced cells are still operational. Reduction by ~50% of the actin-binding endocytic proteins HIP1 and Hip1R in HeLa cells causes the formation of large clathrin assemblies similar to what we find in FCHO1/2-silenced cells, yet Tf internalization is not affected (Engqvist-Goldstein *et al.*, 2004). This demonstrates that altered morphology does not necessarily translate into altered function. Instead, a plausible scenario is that at early assembly times, the precise ratio of FCHO1/2 (and eps15 and intersectin) to AP-2 and clathrin may define whether a diffraction-limited spot or an extensive patch forms. We predict a lower ration of FCHO1/2 and its partners to AP-2, clathrin and epsin would bias the assemblage toward formation of a plaque-like structure. The FCHO1/2 RNAi phenotype in HeLa cells is clearly consistent with this idea.

However the prevailing levels of FCHO2 and adaptors and steady state clathrin morphology in the cell lines examined are not consistent with this idea (Figure 4.16 and 4.17). For instance, MCF-7 cells have the largest CCSs examined and have near undetectable levels of intersectin and Dab2, but HT-1080 cells have uniform and small CCSs but also have very low levels of these two proteins. Normal HeLa cells have a phenotype between these two cell lines yet have higher levels of all FCHO binding partners and in addition endogenous FCHO2 is present at high concentrations at large CCSs in these cells. Instead, FCHO binding partner levels may be more predictive of the sensitivity of a cell line to FCHO1/2 knockdown.

FCHO1/2 control of CCS size is likely more complex. FCHO2 is a phosphoprotein; treatment of HeLa cells with the protein phosphatase inhibitor Calyculin A (Suganuma *et al.*, 1990) causes FCHO2 to migrate more slowly on gels (unpublished observations). Phosphorylation status could either regulate partner binding to the μHD or linker directly or

affect μHD conformation/orientation (Roberts-Galbraith *et al.*, 2010). Another possibility is auto-inhibition. The EFC domain protein Pacsin 1 is auto-inhibited from membrane deformation by binding of its C-terminal SH3 domain back on the EFC domain and this inhibition is relieved by engagement of the SH3 domain by dynamin (Rao *et al.*, 2010). Binding of FCHO1/2 to one of its binding partners could relieve μHD inhibition of EFC binding to the plasma membrane and ensuing curvature generation. It is unknown currently if the μHD can bind to the FCHO EFC domain or linker region.

The last important finding of this study is that FCHO1 and FCHO2 are somewhat redundant but also have some unique properties. Both FCHO1 and FCHO2 are capable of restoring CCS number and size in FCHO2 silenced HeLa cells and have similar effects when overexpressed. Therefore we believe they are both similarly potent in ability to promote nucleation of CCSs and regulate clathrin lattice size. Biochemically these proteins are quite different. FCHO1 is very sensitive to aggregation upon exogenous expression and native and expressed FCHO1 was slightly degraded (Figures 4.1F, 4.5B. 4.17). Considering its ability to aggregate, controlled proteolysis may prevent complications from this byproduct. FCHO1 also makes additional interactions that FCHO2 does not: with AP-2 through the unstructured linker and CALM and HIV-1 Rev binding protein (Hrb) through the μHD (unpublished observations). What is more, FCHO1 recovers more slowly in FRAP experiments perhaps as a result of slower exchange at CCSs from these additional contacts.

The ability to bind CALM and Hrb may impart indirect sorting abilities on FCHO1 as there is evidence these proteins sort SNAREs (Harel *et al.*, 2008; Pryor *et al.*, 2008). Also, while FCHO2 is expressed in all cell lines tested, FCHO1 is not. Tissue specific expression of FCHO1 may be important for cargo sorting. The presence of FCHO1 in purified CCVs is consistent with

a role in cargo sorting and although live-cell experiments show the majority of FCHO1 exiting the evanescent field, trace fluorescence could often be seen until clathrin budding (Figure 4.4). Furthermore, a high-throughput screen for protein-protein interactions in the Transforming Growth Factor β pathway identified an interaction between FCHO1 and Activin receptor-like kinase 2 (Alk2) (Barrios-Rodiles *et al.*, 2005). Alk2 is a Ser/Thr kinase transmembrane receptor involved in gastrulation (Gu *et al.*, 1999), so FCHO1 may act as a CLASP to regulate signaling pathways during development. Future studies will need to determine if FCHO1 and FCHO2 can sort cargo molecules directly similar to Syp1p in yeast (Reider *et al.*, 2009).

In conclusion, FCHO1 and FCHO2 are partially redundant endocytic proteins. They are non-essential regulators of CCS nucleation and actively maintain the morphology of individual CCS. The precise mechanistic details of lattice size regulation remain to be determined as does the identity of the postulated linker-binding partner that is important for this activity. FCHO1/2 are also potential cargo-sorting proteins based on structural and evolutionary evidence and the uptake of various cargo in their absence will remain an intriguing avenue of study.

5.0 CONCLUSIONS

5.1 INTRODUCTION

The field of clathrin-mediated endocytosis is an incredibly rich area of study because of the many participating researchers, the many normal and disease state processes it touches on and its relatively long history, going back to 1964. Yet within the discipline of vesicular traffic, particular aspects of CME, such as the precise mechanism of vesicle nucleation, remain quite unclear when compared with other types of coated vesicles. A partial explanation for this is the apparent near-dizzying array of proteins implicated in endocytosis in mammals that have arisen during the course of evolution and have limited the reach of genetic studies in yeast. Still, multiple concepts of CCV nucleation, some now defunct, have been offered that have helped shape our understanding of this complex process.

This thesis has helped further define the mechanisms by which clathrin-coated structures nucleate on the cell plasma membrane in preparation for endocytosis by clarifying one model and modifying another. Careful biochemical investigation of how the brain-enriched PtdIns(4,5)P_2 generating enzyme PIPKIγ interfaces with the endocytic machinery has identified the binding site on the sandwich subdomain of AP-2 β2 appendage and given rise to a model in which PtdIns(4,5)P_2 generation for vesicle nucleation can be temporally regulated. Also, *in vivo* studies in this thesis have confirmed previous biochemical studies of the AP-2 β2 appendage

platform and sandwich binding sites, showing different levels of accessibility to various binding partners during assembly. The AP-2 β2 appendage binds to clathrin and thus plays an important role in vesicle nucleation as well. Finally, experiments of siRNA-mediated knockdown of the recently identified endocytic proteins FCHO1 and FCHO2 have revealed their involvement in clathrin-coated structure nucleation; they are not absolutely required but may contribute to efficiency and size regulation. My results strengthen the model of PtdIns(4,5)P_2-driven vesicle nucleation for CME but also highlight how multiple pathways might operate in parallel to initiate budding.

5.2 COORDINATION OF LOCALIZED LIPID METABOLISM BY AP-2

5.2.1 Defining the AP-2 β2 subunit appendage sandwich subdomain binding site

The work from Chapter 2 of this thesis along with subsequent studies have greatly helped our understanding of the endocytic accessory factor/adaptor binding sites on the AP-2 β2 appendage. Of the four appendage binding sites, one upon the platform and one upon the sandwich subdomain of both the α and β2 appendages, the β2 sandwich site is the most recently discovered and characterized (Edeling *et al.*, 2006a; Schmid *et al.*, 2006). Yet it also plays a critical role in assembly through binding clathrin (Edeling *et al.*, 2006a) and a variety of other proteins, including PIPKIγ (Chapter 2) (Nakano-Kobayashi *et al.*, 2007). Therefore defining this site will aid in a deeper understanding of assembly during CME and will enable the use of protein-protein interaction data in the future to build predictive, computational models of CCS assembly (Gong *et al.*, 2008).

Using previously identified residues on the AP-2 β2 appendage sandwich subdomain (Edeling *et al.*, 2006a; Schmid *et al.*, 2006) and mutagenesis along with binding assays for interaction with PIPKIγ661, I have confirmed that the sandwich site binding pocket is delimited by residues Gln804, Tyr815, Lys808 and Gln756 in a clockwise circle (see Figure 2.11 and 2.16). I also established that residues Phe635, Trp642 and Tyr644 of the mouse PIPKIγ661 isoform are necessary for binding, similar to other hydrophobic appendage binding motifs. Gratifyingly, my results were subsequently confirmed by the crystal structure of human PIPKIγ668 C-terminal peptide ^{639}**YF**PTDERS**W**V**Y**SPLH^{653} in complex with the β2 appendage (Kahlfeldt *et al.*, 2010). Phe640 (Phe635 in mouse) and Trp647 (Trp642 in mouse) anchor the kinase by inserting into the binding pocket while a short α-helix in the intervening residues positions the side chains (Figure 2.16). Tyr644 stabilizes this interaction through an electrostatic interaction with β2 Lys808.

Eps15 binds to the same site in a similar but different fashion. A co-crystal of the murine eps15 peptide ^{721}S**F**GDG**F**A**DF**STL^{732} with the β2 appendage sandwich domain reveals how Phe722 occupies the same pocket as Phe640 in PIPKIγ and Phe729 inserts into the space for Trp647 of PIPKIγ (Schmid *et al.*, 2006). However Phe726 occupies a shallow pocket unutilized by PIPKIγ and requires a tight turn accommodated by adjacent Gly725. Also, PIPKIγ668 makes additional contacts with its downstream residues ^{650}SPLH^{653} as it wraps around the sandwich subdomain bringing its total interface to 774 Å compared with 395 Å for eps15 (Kahlfeldt *et al.*, 2010). These differences may explain the lower dissociation constant of the PIPKIγ668 peptide (22 μM) (Kahlfeldt *et al.*, 2010) in comparison with eps15 (46 μM) (Schmid *et al.*, 2006), however eps15 has a much higher apparent affinity for β2 appendage in our pull-down assays (Figure 2.17). The entire length of this short eps15 peptide was crystallized (Schmid *et al.*, 2006)

so perhaps additional downstream residues not included in the peptide wrap around the sandwich domain like they do in PIPKIγ or multivalent interactions exist.

A third recent co-crystal of intersectin 1 with the β2 appendage sandwich site reveals the complexity of this binding surface (Pechstein *et al.*, 2010a). Human intersectin 1 ^{847}PNN**W**AD**F**SSTWP^{858} peptide inserts Trp850 into the pocket that accommodates eps15 Phe722 or PIPKIγ Phe640 and Phe853 into the site for eps15 Phe729 or PIPKIγ Trp647. This configuration connects the two aromatic-accepting pockets with the least number of intermediate residues in contrast to the short α-helix of PIPKIγ or tight turn loop of eps15. The unifying theme of these modes of binding are two variably spaced Phe or Trp residues that insert into the two pockets on β2 and additional flanking contacts that stabilize the interaction.

Alignment of eps15 and PIPKIγ661 did not show any significant homology other than the spacing for the distal anchoring Phe and Phe/Trp residues (Figure 2.12). Scanning the C-termini of other AP-2 β2 appendage sandwich partners including AP180, CALM and amphiphysin I/II did reveal some homology to eps15, however (Figure 5.1). These proteins all had at least one sequence in which the first and second anchoring Phe residues of eps15 are conserved in spacing. Also the eps15 Asp724 is conserved in all proteins accept CALM. However these proteins do not have the required Gly in analogous position to eps15 Gly725 that is required to place the adjacent Phe in the middle of a tight turn and they lack the third anchoring Phe at eps15 position 729 (Figure 5.1). Perhaps these proteins are not required to make this tight turn and only utilize two anchoring aromatic residues. Reading the AP180 primary sequence in reverse places a Gly in this position but the position for the third anchoring Phe residue is replaced by Val or Ile. If these sequences really do make up the sandwich binding motif in these proteins, this may explain the higher sensitivity of their binding to mutations in the sandwich sidechains relative to eps15

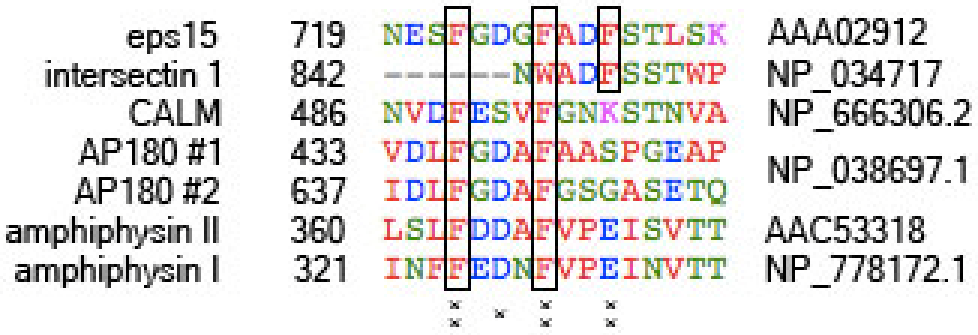

Figure 5.1: Alignment of β2 appendage sandwich subdomain binding proteins.
Primary sequences from mouse endocytic proteins were aligned in ClustalW. Key known (eps15, intersectin) and prospective anchoring residues are boxed. The starting residue numbers and NCBI accession numbers are indicated.

(Edeling *et al.*, 2006a). Alternatively, these proteins could anchor two aromatic residues into the sandwich pocket in a manner similar to PIPKIγ without the need for glycines and a tight loop. Intersectin 1 does align nicely with eps15 but intersectin Trp850 binds to the pocket of β2 that Phe722 of eps15 engages, not the shallow Phe726 pocket as explained above.

The plasticity of the β2 sandwich site in its ability to bind unstructured motifs of different lengths and conformations makes it rather unique among the appendage binding sites. This is especially true in light of the fact that it also binds the structured distal leg of clathrin (Edeling *et al.*, 2006a; Knuehl *et al.*, 2006). Defining a consensus motif for the sandwich subdomain is difficult but may conform to one or more of the following: 1. [F/L]XXGFXDF for eps15 and related sequences (Schmid *et al.*, 2006), 2. FX_nWXY for PIPKIγ and related sequences (Chapter 2), 3. WXXF for intersectin 1 and related sequences (Pechstein *et al.*, 2010a) or 4. FXDXF for other proteins (Figure 5.1), though this is also an α appendage platform binding sequence. Whether these slightly different modes of engaging the β2 appendage sandwich site have

different effects on recruitment of these proteins or their sensitivity to clathrin assembly remain to be determined.

5.2.2 Kinase-mediated PtdIns(4,5)P_2 production for neuronal and somatic cell CME

An important question arising from this thesis dissertation is: does targeting of PIPKIγ661 (668 in humans) to AP-2 for localized PtdIns(4,5)P_2 generation and stimulation of CCS nucleation constitute a general mechanism for endocytosis in all cell types? Genetic studies in mice suggest that PIPKIγ and its PtdIns(4,5)P_2-hydrolyzing counterpart synaptojanin 1 are required for proper CCV generation at the synapse during compensatory endocytosis (Cremona *et al.*, 1999; Wenk *et al.*, 2001; Di Paolo *et al.*, 2004). Indeed, PIPKIγ mRNA and protein is highly expressed in the brain and one or the other can be detected in various other tissues (Ishihara *et al.*, 1998; Wenk *et al.*, 2001; Giudici *et al.*, 2004; Schill and Anderson, 2009; Volpicelli-Daley *et al.*, 2010). However specific detection of the PIPKIγ661 isoform by RT-PCR or Western blot shows that it is restricted to the brain with more moderate expression levels in the heart, lung and perhaps the liver and pancreas but is absent from the gut (Giudici *et al.*, 2004; Schill and Anderson, 2009). An isolated expression pattern is hard to reconcile with a general role in nucleation during CME in somatic cells, nonetheless knockdown of PIPKIγ668 in HeLa cells reduces Tf internalization (Bairstow *et al.*, 2006).

Instead, PIPKIα and PIPKIβ could compensate for CME in tissue where PIPKIγ is low. The mRNA and protein tissue distribution of these proteins is wider (Ishihara *et al.*, 1996; Loijens and Anderson, 1996; Wenk *et al.*, 2001; Volpicelli-Daley *et al.*, 2010). In support of this, forced expression of human PIPKIα and PIPKIβ (PIPKIβ and PIPKIα, respectively in mouse

due to independent discoveries and naming), increases Tf internalization and CCP surface density in HeLa cells while PIPKIγ does not (Padron *et al.*, 2003). Likewise, only knockdown of PIPKIβ reduced Tf internalization. Also, an enzymatically inactive truncated mouse PIPKIβ (mPIPKIβ, or human PIPKIα, hPIPKIα) rescues mutant colony-stimulating factor 1 receptor signaling by stabilizing it at the plasma membrane through dominant-negative inhibition of endocytosis (Davis *et al.*, 1997). In an extension of this, mPIPKIβ expression increased EGFR internalization in NR6 cells (a variant of Swiss 3T3) and trunctated mPIPKIβ blocked EGFR internalization, plasma membrane localization of full-length mPIPKIβ, and reduced clathrin labeling at the membrane (Barbieri *et al.*, 2001). Whether these effects are due to general changes in PtdIns(4,5)P_2 levels in these cell lines, as hPIPKIβ modulation in HeLa cells results in (Padron *et al.*, 2003), or if kinase targeting to CCSs is affected and the mechanism of how this might occur, remain to be determined and are important avenues of study.

Another important factor is the nucleation of CCV from static and long-lived, yet endocytically active CCSs observed in some cultured cell lines (Chapter 4) (Merrifield *et al.*, 2005; Rappoport *et al.*, 2005; Taylor *et al.*, 2011) and isolated primary cells (Bellve *et al.*, 2006). If CCVs can nucleate from the edge of these flat clathrin lattices, the required levels of PtdIns(4,5)P_2 for their assembly may be relaxed. The nucleation potential may come from the adjacent adaptors and clathrin. In this scenario, the prevailing levels of PtdIns(4,5)P_2 on the plasma membrane may be sufficient and targeting of a lipid kinase to these structures unnecessary.

If CME at the synapse and in non-neuronal cells differs in the mode of PtdIns(4,5)P_2 generation used for CCS nucleation, this may reflect the fundamental differences of this process at these two locations. Neuronal CME for compensatory endocytosis during neurotransmission is

a specialized form of endocytosis that must be rapid to maintain organism homeostasis. For instance, the time constant of CME in most synaptic terminals is on the scale of 10-20 seconds (reviewed in (Royle and Lagnado, 2010)) but the productive population of CCSs of cultured somatic cells was measured with a time constant of 87 seconds (Loerke *et al.*, 2009) and intravital imaging of CME in non-neuronal tissue reveals that it may be even slower (Roberto Weigert, personal communication). Neuronal CCV formation also differs structurally as there are numerous brain-specific endocytic proteins including AP180 (CALM homologue), auxilin (GAK homologue) and amphiphysin 1 (Jung and Haucke, 2007) as well as neuron-specific alternatively spliced transcripts for AP-2 α and clathrin light chain (Jackson *et al.*, 1987; Ball *et al.*, 1995). Lastly, the unique combination of cargo such as Syt and the neurotransmitter transporters VMAT2, VAchT and VGLUT1 (Jung and Haucke, 2007) and potentially high cargo concentration if diffusion is limited after SV fusion may also contribute to the speed of clathrin nucleation during CME in neurons. The mechanism of targeting PIPKIγ661 to AP-2 for rapid, localized PtdIns(4,5)P_2 generation and equally rapid negative regulation of coupled clathrin assembly and kinase eviction may be an adaptation to ensure speed and directionality of CME in the brain.

5.2.3 The AP-2 appendages as scaffolds for lipid metabolizing enzymes

The evidence for a role of PtdIns(4,5)P_2 in nucleating and stabilizing CCSs is now incontrovertible. Most of the central adaptors and accessory factors contain modular domains that bind to this lipid and experimentally perturbing PtdIns(4,5)P_2 levels influence the number of CCSs at the plasma membrane of cells in culture. A third line of evidence is the expanding list of

phosphatidylinositol kinases and phosphatases that physically bind to the AP-2 appendages and thus place them appropriately to modify the lipid environment of CCSs (Figure 5.2).

The stage for nucleation is set by PI4K enzymes that generate PtdIns(4)P at the plasma membrane from PtdIns (Vicinanza *et al.*, 2008). In non-neuronal cells, PIPKIα and β likely contribute to global PtdIns(4,5)P_2 at the plasma membrane that can diffuse and participate in CME or they may bind through their kinase core domain to AP-2 μ2 (Krauss *et al.*, 2006) for localized production. In this scenario, the AP-2 core would probably need to undergo a transition from the 'closed' to 'open' state and extend the μ2 C-terminus due to steric constraints for binding (Kahlfeldt *et al.*, 2010) or to position the kinase domain adjacent to its substrate. Therefore if binding the μ2 subunit is functionally relevant, an appreciable level of PtdIns(4,5)P_2 would need to be present initially to stabilize a few molecules of AP-2 to engage the lipid kinase.

In neuronal cells, many endocytic proteins are termed 'dephosphins' because they are phosphorylated under resting conditions by Cdk5 and this evidently prevents physical interaction with partner proteins or activity (Cousin and Robinson, 2001). PIPKIγ661 is a dephosphin and is localized to the presynapse at resting conditions where phosphorylation of Ser645 (mouse residue) (Nakano-Kobayashi *et al.*, 2007) prevents the C-terminal residues (630-661) from engaging the AP-2 β2 appendage sandwich subdomain (Chapter 2). The structural data suggest that an added phosphate group on Ser645 (Ser650 in humans) would prevent hydrogen bonding with the appendage backbone (Kahlfeldt *et al.*, 2010) and weaken the interaction. Following an action potential and Ca^{2+} influx, dephosphins are dephosphorylated by calcineurin (Cousin and Robinson, 2001). Allowing AP-2 to bind PIPKIγ661 stimulates the kinase activity (Nakano-Kobayashi *et al.*, 2007) and is additionally driven by a positive feedback loop of PtdIns(4,5)P_2 stimulation of PLD (Arneson *et al.*, 1999). PLD hydrolyzes the phospholipid PtdCho to the

soluble headgroup choline and membrane-bound PtdOH and this lipid product stimulates PIPKI activity (Jenkins *et al.*, 1994; Ishihara *et al.*, 1998). The positive regulator PtdOH can also be produced by DGKδ when it engages the α appendage platform positioning it at CCSs (Kawasaki *et al.*, 2007). These appendage interactions promote PtdIns(4,5)P_2 generation and stimulate local AP-2 accumulation and clathrin assembly. Interestingly, PtdOH production promotes limited CCS assembly on lysosome membranes *in vitro* even in the absence of ATP (and potential PtdOH-stimulated PtdIns(4,5)P_2 production) (Arneson *et al.*, 1999) and PtdOH specifically influences EGFR and not TfR endocytosis (Antonescu *et al.*, 2010). PtdOH may perform an important unappreciated role in CCS nucleation, perhaps binding a subset of endocytic adaptors or influence membrane biochemistry or curvature. Future research should focus on how PtdOH regulates assembly and specific cargo internalization.

How are positive regulators of nucleation regulated themselves? In *Drosophila*, excessive PtdIns(4,5)P_2 production from overexpression of the PIPKI Skittles inhibits CME of yolk protein endocytosis in a superficially similar fashion to Skittles hypomorphic alleles (Compagnon *et al.*, 2009). Therefore controlled levels of PtdIns(4,5)P_2 are important, not just its production. The activity of PIPKIγ661 appears to be regulated not by phosphorylation directly but through binding its partner proteins AP-2 and talin, a process influenced by PIPKIγ661 phosphorylation status (Di Paolo *et al.*, 2002; Ling *et al.*, 2002; Ling *et al.*, 2003; Nakano-Kobayashi *et al.*, 2007). By controlling PIPKIγ661 binding to these proteins, its localization and activity could be controlled. The requirement for PtdIns(4,5)P_2 at this later assembly stage may decrease as many assembly proteins become concentrated and can assist in recruitment through cooperative actions. This thesis has shown that clathrin binding to the β2 appendage sandwich site causes displacement of PIPKIγ661 and therefore could regulate continued or excessive PtdIns(4,5)P_2

production at CCS (Figure 5.2). In a lysosome clathrin coat recruitment assay, ongoing PtdIns(4,5)P_2 production is not required to allow some clathrin assembly (Arneson *et al.*, 1999), supporting this assertion.Icannot exclude the possibility that PIPKIγ661 could switch to the μ2 subunit following clathrin assembly through the C-terminal YSPL motif (Bairstow *et al.*, 2006) or kinase domain (Krauss *et al.*, 2006). The YSPL motif scheme seems unlikely as I showed that β2·μ2 hemicomplex binding was negligible, and the kinase would have to compete with YXX∅ motif-containing cargo.

The AP-2 appendages also bind directly or indirectly to polyphosphoinositide phosphatases that regulate assembly progression and uncoating (Figure 5.2). The SH2 domain-containing inositol phosphatase 2 (SHIP2) hydrolyzes the C-5 phosphate of PtdIns(3,4,5)P_3 (preferred substrate) and PtdIns(4,5)P_2 at the plasma membrane (Hejna *et al.*, 1995) and knockdown of SHIP2 causes shortening of CCS lifetimes (Nakatsu *et al.*, 2010). SHIP2 is targeted to CCSs by its interaction with intersectin (Nakatsu *et al.*, 2010) and intersectin binds to the α and β2 appendage sandwich subdomains (Pechstein *et al.*, 2010a). Endocytic adaptors can bind PtdIns(3,4,5)P_3 (Rapoport *et al.*, 1997; Itoh *et al.*, 2001) and although under normal circumstances levels of this lipid are low in cells (Wymann and Schneiter, 2008), controlled hydrolysis of this binding surface for adaptors may extend CCS assembly by slightly weakening the assembly to allow appropriate incorporation of cargo and regulatory factors. This may be particularly important in non-neuronal cells where speed is not paramount but producing cargo-laden vesicles is. Interestingly, SHIP2 is recruited to CCSs early in assembly with clathrin but departs the coat before budding (Nakatsu *et al.*, 2010). Intersectin binds to the β2 appendage sandwich subdomain like PIPKIγ661 so that as clathrin assembles, perhaps intersectin's and consequently SHIP2's connections with the endocytic machinery are weakened and its presence

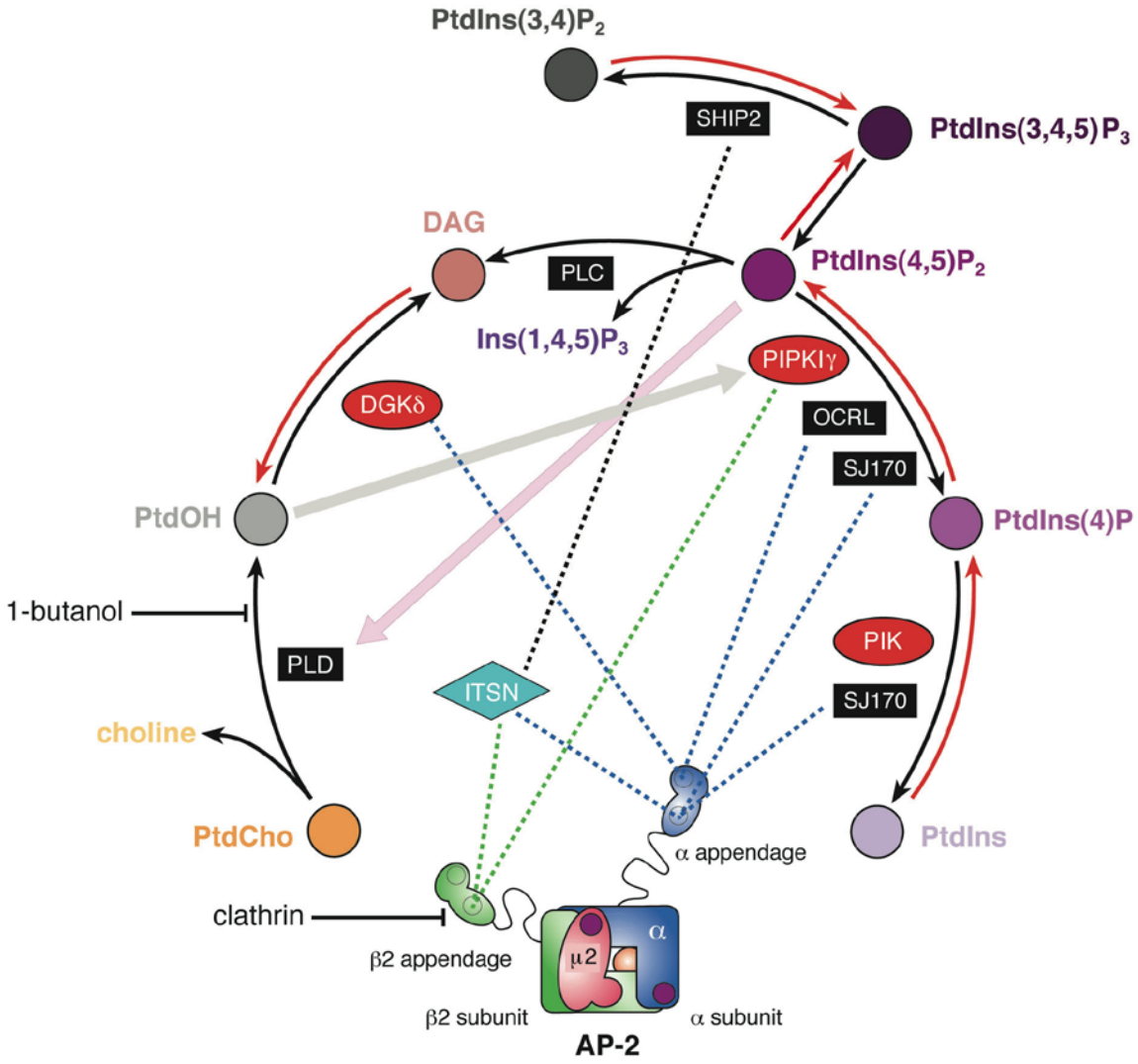

Figure 5.2: Phosphoinositide metabolism at clathrin-coated buds.
Schematic representation of key enzymes responsible for PtdIns(4,5)P_2 synthesis and the mapped interactions with the AP-2 adaptor appendages. The location of the two separate PtdIns(4,5)P_2 binding sites on the AP-2 heterotetramer is indicated with purple spots. Dotted lines represent interactions, solid colored arrows represent stimulation of enzymatic activity. DAG, diacylglycerol; PLD, phospholipase D; PLC, phospholipase C; PIK, phosphatidylinositol 4-kinase; PtdCho, phosphatidylcholine; Ins(1,4,5)P_3, inositol 1,4,5-trisphosphate; PtdIns, phosphatidylinositol; PtdIns(4)P, phosphatidylinositol 4-phosphate; PtdIns(3,4)P_2, phosphatidylinositol 3,4-bisphosphate; PtdIns(3,4,5)P_3, phosphatidylinositol 3,4,5-trisphosphate; ITSN, intersectin; SHIP2, SH2-containing 5'-inositol phosphatase 2; OCRL, Oculocerebral Renal Syndrome of Lowe protein,

reduced. This could allow a brief period in which stabilized PtdIns(3,4,5)P_3 can exert its effect on assembly speed after cargo has been incorporated but prior to fully active phosphatidylinositol hydrolysis for uncoating. However the precise stoichiometries of these lipid species at the nerve terminal or CCSs makes these models only speculative.

Synaptojanin is a phosphatidylinositol polyphosphatase that functions at the later stages of assembly to hydrolyze PtdIns(4,5)P_2 in preparation for removal of adaptors and clathrin. Synaptojanin is alternatively spliced (Ramjaun and McPherson, 1996) as two ubiquitiously expressed isoforms: synaptojanin 145 (SJ145), a brain-enriched isoform containing an α appendage sandwich binding motif (WXXF), and synaptojanin 170 (SJ170), containing α appendage platform (DPF, FXDXF) and an additional sandwich binding motif (WXXF) (Jha *et al.*, 2004; Mishra *et al.*, 2004). Synaptojanin also binds a cohort of other SH3 domain-containing endocytic proteins including endophilin, amphiphysin and intersectin (Cestra *et al.*, 1999). While SJ170 is present at CCS throughout the entire lifecycle, likely resulting from the additional AP-2 contacts, SJ145 is recruited as a burst at budding and probably depends more heavily on binding to its late-stage binding partners endophilin and amphiphysin for its timed recruitment (Perera *et al.*, 2006; Taylor *et al.*, 2011). A recent *in vitro* study suggests membranes of higher curvature stimulate synaptojanin-mediated PtdIns(4,5)P_2 hydrolysis through increased targeting by the BAR domain binding partner endophilin and higher phosphatase activity for PtdIns(4,5)P_2 in highly curved membranes (Chang-Ileto *et al.*, 2011). Combining these data for a molecular description, in non-neuronal cells where the SJ170 isoform predominates, extensive interactions of SJ170 with the AP-2 α appendage place it at CCSs during the entire lifecycle. Low basal activity of SJ170 controls the rate of assembly by dynamically balancing PtdIns(4,5)P_2 levels, similar to the proposed role of SHIP2, but at deeply invaginated buds SJ170 activity is maximal

based on curvature and the presence of BAR domain binding partners. Perhaps SJ170 activity is stimulated through binding its partner proteins. Through binding only to the α appendage (and not the β2 sandwich) and additional contacts with other endocytic proteins, synaptojanin ensures its presence at late stage buds to promote the loosening of adaptor-membrane interactions in preparation for uncoating.

A third phosphoinositide 5-phosphatase, OCRL1, is recruited to CCSs at a late stage just after scission (Erdmann *et al.*, 2007; Taylor *et al.*, 2011). OCRL1 binds to the clathrin terminal domain and also to the AP-2 α appendage via a single platform binding FXDXF motif (Figure 5.2) (Ungewickell *et al.*, 2004). These interactions may contribute to OCRL1's initial recruitment but are soon lost as the vesicle uncoats and it might be maintained on the vesicle by interacting with the early endosome protein APPL1 (Erdmann *et al.*, 2007). While the role of OCRL1 is not well understood it could ensure an early endosome lipid composition of high PtdIns(3)P and low PtdIns(4,5)P_2. The extensive connections of AP-2 with lipid modifying enzymes, particularly three phosphoinositol phosphatases, highlight that phosphoinositide species are carefully monitored and fine-tuned at sites of CME (Sun *et al.*, 2007a).

5.3 THE AP-2 β2 APPENDAGE AS A TEMPORALLY REGULATED ASSEMBLY PLATFORM

It has long been known that assembly of clathrin around the AP-2 β2 subunit causes interference with bound β2 appendage binding partners (Cupers *et al.*, 1998; Owen *et al.*, 2000). This was the basis of the 'changing hubs' model in which early in assembly the AP-2 appendages constitute

the primary hub, coordinating numerous interactions with accessory factors. As clathrin assembles, the clathrin terminal domains begin to outnumber the molecules of AP-2 and become the primary hub, causing a migration of endocytic proteins. This migration is facilitated by a displacement of a subset (β2 appendage platform binding partners) of proteins from the β2 appendage by competition from clathrin (Schmid *et al.*, 2006; Schmid and McMahon, 2007). In particular, because β-arrestin 1 binding to AP-2 β2 and clathrin was shown to be mutually exclusive in pull down assays and increased binding of clathrin (not present in excess) to the AP-2 β2 appendage and hinge slightly reduced bound β-arrestin 1 in similar assays, it was concluded that β-arrestin 1 was maintained within CCVs through its interaction with clathrin after changing hubs (Schmid *et al.*, 2006). This intriguing, albeit not well supported, model is one possible explanation for how forming CCSs can organize their many connections and form in an ordered, vectorial progression.

In Chapters 2 and 3 of this thesis I have presented data in support of an alternate model: clathrin assembly causes displacement of AP-2 β2 appendage sandwich subdomain partners while platform binding proteins including, β-arrestin 1, are unaffected. For some proteins such as amphiphysin I/II and AP180, their residency within forming CCVs could be maintained by their additional binding to AP-2 α appendage or to the clathrin terminal domain (Edeling *et al.*, 2006a). Another, eps15, is lost from mature areas of assembly where clathrin is completely polymerized and is found only at the lattice edges where unoccupied AP-2 molecules reside (Tebar *et al.*, 1996; Edeling *et al.*, 2006a). Paradoxically, eps15 also binds to the α appendage through numerous DPF motifs in its C-terminus (Benmerah *et al.*, 1996) yet is displaced from purified AP-2 when assembled into clathrin cages *in vitro* (Cupers *et al.*, 1998). Partners of the α appendage are not subject to this regulation; epsin 1 (a β2 platform and α platform binder) and

Dab2 (α platform binder) are not removed from CCSs assembled on liposomes (Mishra *et al.*, 2002a). PIPKIγ661 does not bind clathrin or the α appendage directly and would be expected to depart the lattice or relocate to the edge like eps15 where it could generate PtdIns(4,5)P_2 to stabilize assembly. A corollary to this is that while the α appendage does not bind clathrin and does not appear to be significantly affected by clathrin binding to the β2 appendage, one or more displacement mechanisms may operate on this appendage during the CCS lifecycle. AAK1, the kinase that phosphorylates AP-2 μ2 and promotes the open conformation, is displaced from the α appendage by the Rab5 GEF hRME-6 in a process that prepares the vesicle for uncoating by destabilizing AP-2 and begins the transition to an early endosome environment (Semerdjieva *et al.*, 2008).

To contrast this, I find that cargo-independent, activated β-arrestin 1 remains associated with CCSs throughout their lifetime whether it can bind to clathrin or not. These β-arrestin mutant proteins can also mediate the downregulation of the angiotensin receptor. If β-arrestin was lost from AP-2 as clathrin assembles and it could not bind clathrin, it should be lost from the forming vesicle because the sorting CLASP does not contact the core coat components. Furthermore in Chapter 2, the platform protein epsin 1 was not affected by sandwich targeting competitive peptides that affect clathrin binding to the β2 appendage in pull down experiments. Therefore the β2 platform proteins β-arrestins, ARH and epsin 1 constitute a privileged set of β2 appendage proteins that are not subject to interference by clathrin. This makes intuitive sense: why would the clathrin machinery want to temporarily displace proteins that incorporate cargo into the budding vesicle, forcing them to engage clathrin? At deeply invaginated buds, lateral diffusion of the adaptor-cargo pair could be slight but at small, shallow assemblies there is no guarantee that the adaptor-cargo complex will be recaptured. The ‘changing hubs’ model also

invokes the idea of using small irreversible steps, such as replacing lower affinity interactions with higher affinity interactions, to drive the reaction in one direction. However, for β-arrestin 1 a switch from binding the β2 appendage platform to binding the clathrin terminal domain involves switching from a higher affinity (~2 μM (Edeling *et al.*, 2006a; Schmid *et al.*, 2006)) to a lower affinity (22 μM (Miele *et al.*, 2004)) interaction.

With the exception of PIPKIγ661, partners of the AP-2 β2 appendage sandwich site such as AP180, CALM, eps15 and amphiphysin I/II (Edeling *et al.*, 2006a) are structural in nature (although CALM and AP180 may sort cargo as well (Harel *et al.*, 2008)). Causing dislocation of such proteins is much more likely to have an effect on the general architecture and dynamics of the forming CCV. An attractive idea is that reducing the contacts of tentative nucleation proteins eps15 and intersectin 1 (Chapter 4) (Henne *et al.*, 2010) with AP-2 through clathrin polymerization may be a way to segregate the nucleation phase from the assembly phase and this could turn out to be a necessary transition in the vectorial formation of CCVs. In support of this, mass spectrometry analysis of isolated CCVs failed to detect eps15 or intersectin in CCVs from brain (Blondeau *et al.*, 2004) or HeLa cells (Borner *et al.*, 2006) and hepatic CCVs were de-enriched in eps15 based on the low number of identified peptides (Girard *et al.*, 2005).

5.4 CLATHRIN-COATED STRUCTURE NUCLEATION THROUGH FCHO PROTEINS

The concept of a dedicated protein(s) at the plasma membrane to direct recruitment of AP-2 and clathrin for nucleating CCSs is not a new idea. Early models favored the cytosolic tails of cargo molecules (Pearse and Crowther, 1987), Syt (Zhang *et al.*, 1994) or Arf6 GTPase (Paleotti *et al.*,

2005) as the ‘docking complex’. While these intregral membrane or myristoylated protein nucleators have fallen out of favor more recently, the soluble EFC domain proteins FCHO1 and FCHO2 have emerged as playing an important role in nucleating CCSs (this thesis and (Henne *et al.*, 2010)).

A provocative model has been put forth in which FCHO1 and FCHO2 are pioneer components of CCSs that bind to eps15, eps15R, intersectin 1 and intersectin 2 and use these intermediate proteins to recruit AP-2 to regions of assembly (Henne *et al.*, 2010). AP-2 then binds and recruits its other partners including clathrin. Work presented in this thesis both support and reject pieces of this new model. FCHO1 and -2 and their partner eps15 are undoubtedly early components of CCSs in cells where *de novo* forming buds predominate. FCHO1/2 also participate in CCS nucleation in some cell types because modulating their cellular levels similarly affects the number of CCSs. Yet never did I observe a complete loss of CCSs in the absence of FCHO1 and/or FCHO2 in any cell type examined. It follows that unlike PtdIns(4,5)P_2, the presence of FCHO1/2 and its accessory factors for recruitment of AP-2 to sites of endocytosis is not a prerequisite for CME. Therefore backup mechanisms must operate to ensure that CCSs form and perhaps multiple parallel pathways help ensure ongoing operation of the critical process of endocytosis.

FCHO1 and FCHO2 possess properties that distinguish them from many of the other clathrin-associated proteins involved in endocytosis. Most of the CME proteins bind directly to AP-2 and/or clathrin (and some to PtdIns(4,5)P_2 and cargo molecules) (Traub, 2005, 2011). Notable exceptions are dynamin and actin that bind to each other and their own cohort of adaptors and these adaptors link them to AP-2 and/or clathrin. This positioning likely separates their functions spatially and temporally from the assembly machinery. While FCHO1 can bind to

AP-2 (unpublished observations), FCHO1/2 also primarily bind indirectly to AP-2 (but not clathrin) through adaptors such as eps15/R and intersectin 1/2 (Reider *et al.*, 2009; Henne *et al.*, 2010). Also, FCHO1 in particular is beginning to resemble AP-2 in that it contains an unstructured region connecting a folded globular domain, the μHD, that coordinates multiple interactions with eps15, eps15R, intersectin 1, intersectin 2, Dab2 (Henne *et al.*, 2010), CALM and Hrb (unpublished observations). This module may be important for maintaining CCS number and size in specific tissues or cell lines. Additionally, this module may account for the internalization of AP-2-independent cargo in AP-2 RNAi HeLa cells (Barriere *et al.*, 2006; Keyel *et al.*, 2006; Maurer and Cooper, 2006).

Experiments in this thesis have highlighted an interesting connection between the CCS nucleation-associated proteins FCHO1/2 and the size of flat clathrin lattices or plaques observed on the ventral membrane of some adherent cells in culture. A handful of studies have shed light on how these AP-2 and clathrin assemblies may expand laterally. Overexpression of the long isoform of Dab2 (mouse p96 or rat p86) induces enlarged CCSs in NIH 3T3 cells (Morris and Cooper, 2001) and COS7 and HeLa cells (Chetrit *et al.*, 2009). In BS-C-1 cells, expression of a chimeric receptor containing the LDLR cytosolic domain along with Dab2 is necessary to induce so-called giant CCSs that cover a majority of the ventral plasma membrane (Mettlen *et al.*, 2010). The large structures were restricted to the ventral membrane unless a membrane-targeted myristoylated Dab2 was expressed alone suggesting the Dab2 cargo (LDLR chimeric receptor and/or others) promoted large clathrin assemblies specifically on the ventral membrane.

Intriguingly, Dab2 recognizes NPXY motifs within β-integrins and promotes their endocytosis for focal adhesion disassembly (Eto *et al.*, 2008; Chao and Kunz, 2009; Ezratty *et al.*, 2009; Teckchandani *et al.*, 2009). Primary osteoclasts (Akisaka *et al.*, 2003) and HeLa cells

(Maupin and Pollard, 1983) contain extensive flat clathrin assemblies at regions of the ventral membrane closely apposed to the substrate (12 nm) and frequently adjacent to focal contacts (10 nm substrate-membrane spacing) (Maupin and Pollard, 1983) suggesting these structures are involved in adhesion or regulate adhesive properties. In support of this, myotubes grown in culture contain substrate-bound integrins that cluster in focal adhesions and CCSs, and the CCSs can be competed from the integrins by NPXY motif-containing peptides encoding the integrin cytoplasmic domain (De Deyne *et al.*, 1998). High concentrations of integrins could recruit Dab2 and, as a consequence, AP-2 and clathrin. Perhaps then cargo plays an important role in large, flat CCSs generation. Because FCHO1/2 bind Dab2 through their μHD, FCHO1/2 may regulate large CCSs in cells with specific integrin expression patterns or underlying substrate compositions. The absence of FCHO1/2 could promote unregulated Dab2-mediated assembly.

Circumstantial evidence could implicate actin assembly in modulating the size of large CCs on the ventral surface of adherent cells. Hip1R, a CCV component, simultaneously can bind PtdIns(4,5)P_2, clathrin light chain and filamentous actin (Engqvist-Goldstein *et al.*, 1999). Knockdown of Hip1R in HeLa cells causes stable association of CCSs with actin and enlargement of these CCSs (Engqvist-Goldstein *et al.*, 2004). This results from derepression of the actin nucleation promoting factor (NPF) cortactin (Le Clainche *et al.*, 2007), a Hip1R binding partner. Cortactin can then activate Arp2/3 that promotes branched actin formation. Intriguingly, yeast Syp1p binds to Las17p, the yeast homologue of mammalian WASP, through the linker region between the EFC domain and μHD and negatively regulates its activity (Boettner *et al.*, 2009). Las17p/WASP act as actin NPFs for Arp2/3, similar to cortactin. Therefore if the Syp1p-Las17p interaction is conserved in a vertebrate FCHO-WASP interaction, FCHO1/2 knockdown could result in unregulated branched actin formation. How this could

result in large CCSs, such as in the absence of Hip1R, is unclear. Perhaps actin polymerization at flat clathrin lattices, as opposed to invaginating buds with an inward trajectory, could push these assemblies into each other or somehow promote clathrin polymerization at the edges. Such an interaction could explain my results where the μHD-truncated FCHO1/2 can rescue CCS morphology in FCHO2 knockdown cells. Though our lab has been unable to detect an FCHO-WASP interaction by GST pulldown assays, this may be a weak interaction that warrants further investigation.

What exactly are FCHO1/2 doing at bud sites prior to the arrival of AP-2 and how are they clustered in the absence of AP-2? Certainly FCHO1/2 bind PtdIns(4,5)P_2 to target to the plasma membrane (Henne *et al.*, 2010) so that by any proposed mechanism, CCS nucleation requires PtdIns(4,5)P_2. Through a combination of FCHO1/2 oligomerization (Henne *et al.*, 2010) and crosslinking by homodimerization of eps15 (Tebar *et al.*, 1997) and heterodimerization of eps15-intersectin (Koh *et al.*, 2007), clustered patches can form on the membrane. How such nascent assemblies would be prevented from uncontrolled or non-productive deposition remains to be determined. Is the role of these FCHO assemblies to optimize the membrane environment through clustering PtdIns(4,5)P_2 and locally increasing its concentration? Perhaps FCHO1/2 also bind a type I PIPK to generate this lipid. It was proposed that FCHO1/2 initiate sculpting of the bud site (Henne *et al.*, 2010), but the presence of operational flat clathrin lattices in normal HeLa cells appears to lessen this claim. FCHO1/2 may increase the efficiency of recruiting AP-2 to the plasma membrane, but it is hard to imagine an absolute requirement for this step when CCS can be reconstituted on cellular membranes *in vitro* through the addition of purified CCV proteins of which FCHO proteins are de-enriched or of sub-stoichiometric levels (Mahaffey *et al.*, 1989).

In light of the data presented in this thesis, are there multiple pathways that contribute simultaneously to CCS nucleation? A goal in recent years has been to catalog the timing of individual endocytic proteins at CCSs in order to understand the encoded, sequential assembly instructions built into the machinery (Liu *et al.*, 2009; Taylor *et al.*, 2011). This approach will likely yield useful information, however another way to think of CCS nucleation and assembly is as analogous to the energy landscape model of protein folding (Onuchic and Wolynes, 2004). An unfolded protein can assume many different conformations of high entropy, but as it folds it moves down the sides of its folding funnel to its native conformation of lowest free energy and lowest entropy. There are multiple pathways (or sides of the funnel) to reach the same final protein fold. CCSs may form in a similar fashion in which different components could have the ability to contribute at different times. Different cell types also may use slightly different endocytic components and adaptors, yet as adaptors and clathrin triskelion begin to assemble they limit the possible number of subsequent conformations of the forming coated-pit and drive the process forward vectorially. Different tissues may depend to a varying extent on FCHO-mediated or purely PtdIns(4,5)P_2-driven CCS nucleation, though PtdIns(4,5)P_2 will underlie all CCV generation events.

Very little work has focused on the EFC domain proteins FCHO1 and FCHO2 until recently. Future studies will surely tease apart their precise function in nucleation and assembly. Of importance would be knockout studies in mice to see if FCHO1/2 are critical to life such has been done for other endocytic proteins (Wenk *et al.*, 2001; Ferguson *et al.*, 2007; Chen *et al.*, 2009). If FCHO1 is important during development by regulating endocytosis of Alk2, this will likely further our understanding of the process. If FCHO knockout is lethal, embryonic fibroblasts could still be obtained and further studies of CCS nucleation and endocytosis could be

performed in the complete absence of FCHO1/2. This would be a tractable system for further rescue experiments. Synaptosome-derived membrane recruitment assays (Chapter 2) provide another powerful system to examine FCHO1/2 involvement in nucleation. FCHO proteins could be immunodepleted from brain cytosol or exogenous mutant FCHO proteins could be added, particularly FCHO1/2 lacking the μHD. This system will allow examination of assembly prior to the establishment of steady state morphology in siRNA-treated cells.

5.5 CLOSING COMMENTS

In this dissertation, I have helped clarify the sequence of events that give rise to clathrin-coated structures on the plasma membrane. The nucleation phase of clathrin-mediated endocytosis remains one of the least well understood and yet one of the most critical. In its simplest form it involves the lipid PtdIns(4,5)P_2 and the coordinated interaction and recruitment of endocytic adaptors and clathrin to the plasma membrane. In the brain, where a rapid, specialized form of clathrin-mediated endocytosis occurs, PtdIns(4,5)P_2 is generated by PIPKIγ. I have presented a precise molecular description of the requirements for interaction between the C-terminus of PIPKIγ and the clathrin adaptor AP-2 β2 subunit appendage for focal PtdIns(4,5)P_2 production. This interaction is likely critical for rapid PtdIns(4,5)P_2 generation, adaptor recruitment and subsequent clathrin assembly for compensatory endocytosis during neurotransmission. In addition, the binding of PIPKIγ to the sandwich subdomain of the β2 appendage subjects PIPKIγ to displacement from clathrin binding to the same site, effectively limiting activity and preparing the vesicle for uncoating after scission. I also have shown that clathrin binding leaves the other β2 appendage binding site, the platform, unoccupied for the continued engagement of adaptors

such as β-arrestin or ARH. Finally, I have shown that the recently implicated endocytic proteins FCHO1 and FCHO2 are not absolutely required for the nucleation of clathrin-coated structures in cell culture. Instead these proteins are important for maintenance of the steady state distribution of clathrin-coated structure number and size. While other coated vesicle pathways such as COPI (Beck *et al.*, 2009) and COPII (Miller and Barlowe, 2010) are nucleated by GTPases, clathrin-mediated endocytosis may not rely on a proteinaceous nucleating factor which may afford the process more flexibility and tissue-specific specializations.

6.0 MATERIALS AND METHODS

6.1 CHAPTER 2 MATERIALS AND METHODS

6.1.1 DNA constructs

The recombinant proteins consisting of glutathione S-transferase (GST) fused to PIPKIγ (mouse residues 460-635, 460-661, 636-661, 630-661, and 624-661) were generated by polymerase chain reaction (PCR) using a mouse PIPKIγ661 cDNA as a template followed by digestion and ligation into EcoRI/XhoI-cleaved pGEX-4T-1. Point mutations (I633A, Y634A, F635A, W642A, Y644A, Y649A, and S645E) were generated by QuikChange site-directed mutagenesis (Stratagene). The GST-PIPKIγ(460-687) construct was generated by PCR using rat PIPKIγ687 cDNA kindly provided by Robin Irvine (University of Cambridge, Cambridge, UK) as a template followed by digestion and ligation into EcoRI/XhoI-cleaved pGEX-4T-1. A GST-human PIPKIγ668 C-terminal 28 amino acid fusion was generated by PCR utilizing overlapping synthetic oligonucleotides and cloned into pGEX-4T-1. The GST conjugated AP-2 α_C appendage (mouse residues 701-938) (Traub *et al.*, 1999), AP-2 β2 appendage (rat residues 714-951) (Mishra *et al.*, 2005), eps15 (622-736) and a cytosolic portion of the cation-independent mannose 6-phosphate receptor (CI-MPR YSKV, residues 2337-2372) (Doray *et al.*, 2007) have been described previously. The FLAG-tagged AP-2 β2 subunit and μ2 subunit pFastBac Dual

plasmid for baculovirus production was generated as described (Doray *et al.*, 2007). The β2 trunk version was made from the full-length protein by deleting residues 593-951, placing the FLAG epitope after His592. PIPKIγ (630-661) was cloned into EcoRI/BamHI-digested pGBKT7 while AP-2 β2 appendage (rat residues 700-937) was cloned into EcoRI/XhoI-cut pGADT7. Upon confirmation of the sequences, indicated mutations in the β2 appendage were created by QuikChange site-directed mutagenesis (Stratagene). The hexahistidine (His_6) tagged AP-2 β2 hinge and appendage (rat AP-2 β2 residues 592-951) was kindly provided by Tom Kirchhausen (Harvard University, Boston, MA, USA). GST conjugated epsin ENTH domain (rat epsin1 residues 1-163) was described previously (Hawryluk *et al.*, 2006). All clones and mutations were verified by automated dideoxynucleotide sequencing.

6.1.2 Antibodies and immunoblotting

Affinity-purified polyclonal antibody directed against epsin 1 (Drake *et al.*, 2000) and HIP1 (Mishra *et al.*, 2001) were produced in our laboratory by standard procedures. Affinity-purified WI54 peptide antibodies directed against the 26 amino acid insert of PIPKIγ661 have been described (Ling *et al.*, 2002). The anti-clathrin heavy chain monoclonal antibody (mAb) TD.1 was generously provided by Frances Brodsky (UCSF, San Francisco, CA, USA) and the light chain mAb Cl37.3 by Reinhard Jahn. The anti-AP-1/2 β1/β2-subunit mAb 100/1 and rabbit polyclonal anti-eps15 serum were kind gifts of Ernst Ungewickell (Medizinische Hochschule Hannover, Hannover, Germany). The rabbit R11-29 polyclonal anti-AP-2 μ2 subunit serum was a generous gift from Juan Bonifacino (National Institute of Health, Bethesda, MD, USA) while the rabbit polyclonal anti-NECAP antibody was a kind gift of Peter McPherson (McGill

University, Montreal, Quebec, Canada). The anti-PIPKIγ, anti-AP180, and anti-amphiphysinI/II mAbs were purchased from B.D. Transduction Laboratories. The anti-FLAG M1 and M2 and anti-talin mAbs were purchased from Sigma.

Samples were resolved on SDS-PAGE with an altered acrylamide-bis-acrylamide (30:0.4) ratio stock solution. After electrophoresis, proteins were either stained with Coomassie blue or transferred to nitrocellulose in ice-cold 15.6 mM Tris and 120 mM glycine. Blots were usually blocked overnight in 5% skim milk in 10 mM Tris-HCl (pH 7.8), 150 mM NaCl and 0.1% Tween 20 and then portions incubated with primary antibodies as indicated in individual figure legends. After incubation with horseradish peroxidase-conjugated anti-mouse or anti-rabbit immunoglobulin G, immunoreactive bands were visualized with enhanced chemiluminescence.

6.1.3 Protein and tissue extract preparation

GST and various GST fusion proteins were produced in *Escherichia coli* BL21 cells. Bacteria were induced by shifting log-phase cultures (OD_{600} ~0.6) from 37°C to room temperature and then adding isopropyl-1-thio-β-D-galactopyranoside to a final concentration of 100 μM with constant shaking for 3 hours or, in some instances, to 200 μM with constant shaking overnight (~16 hours). The bacteria were recovered by centrifugation at 15,000 x g_{max} at 4°C for 15 min and used immediately or stored at -80°C. Lysis was performed in 50 mM Tris-HCl, pH 7.5, 300 mM NaCl, 0.2% (w/v) Triton X-100, 10 mM β-mercaptoethanol with sonication on ice. Insoluble material was removed by centrifugation at 23,700 x g_{max} at 4°C for 30 min, and then the GST fusions were collected on glutathione-Sepharose. After extensive washing in PBS, GST

fusions were eluted with 25 mM Tris-HCl, pH 8.0, 200 mM NaCl, 10 mM glutathione, 5 mM DTT on ice and dialyzed into PBS, 1 mM DTT before use in binding assays. In some instances, purified fusion proteins were cleaved from the GST with thrombin (GE Biosciences) while still immobilized upon glutathione-Sepharose. Digestion was as recommended by the manufacturer, followed by addition of the irreversible thrombin inhibitor D-Phe-Pro-Arg chloromethyl ketone (Calbiochem) to a final concentration of 25 μM. His_6-β2 hinge + appendage was produced in *E. coli* BL21 (DE3) by induction of log-phase cultures with 1 mM isopropyl 1-thio-β-D-galactopyranoside at room temperature for 3 h. Cleared lysates were incubated with Ni-NTA-agarose, and bound protein was eluted in 50 mM Tris-HCl, pH 7.5, 300 mM NaCl, 200 mM imidazole.

Cytosol was prepared from frozen rat brains (PelFreez) by sequential differential centrifugation after homogenization in 25 mM HEPES-KOH, pH 7.2, 250 mM sucrose, 2 mM EDTA, and 2 mM EGTA supplemented with 1 mM phenylmethylsulfonyl fluoride and Complete (Roche Applied Science) protease inhibitor mixture. The 105,000 x g_{max} supernatant is defined as cytosol and was stored in small aliquots at -80°C. Before use in binding assays, thawed samples of rat brain cytosol were adjusted to 25 mM HEPES-KOH, pH 7.2, 125 mM potassium acetate, 5 mM magnesium acetate, 2 mM EDTA, 2 mM EGTA, and 1 mM DTT (assay buffer) by addition of a 10x stock and then centrifuged at 245,000 x g_{max} (TLA-100.4 rotor) at 4°C for 20 min to remove insoluble particulate material. Lysates from infected Sf9 cells (Doray *et al.*, 2007) were prepared by solubilization of pelleted cells in assay buffer with 0.4% Triton X-100 and supplemented with 1 mM phenylmethylsulfonyl fluoride and Complete (Roche Applied Science) protease inhibitor mixture. After incubation on ice for 15 min, the lysates was sonicated on ice three times for 15 sec and centrifuged at 500 x g_{max}. The supernatants were carefully aspirated

and stored in aliquots at -80°C. Prior to use, thawed Sf9 cell lysates were centrifuged at 125,000 x g_{max} to remove aggregated material. Hemicomplexes were immunoprecipitated from 1 ml of clarified lysate using 35 μl packed anti-FLAG M2 agarose (Sigma) equilibrated in assay buffer lacking DTT. After extensively washing the anti-FLAG agarose, bound proteins were eluted with 200 μg/ml FLAG peptide.

Rat brain clathrin-coated vesicles were prepared exactly as described previously (Mishra *et al.*, 2001). Synaptosomes were prepared from rat brain homogenized in 5 mM HEPES-KOH, pH 7.4, 320 mM sucrose with a Potter-Elvehjem tissue disruptor on ice (Fischer von Mollard *et al.*, 1991). The supernatant from a 2 min 3,000 x g_{max} spin at 4°C was recentrifuged at 13,000 x g_{max} for 12 min, the pellet resuspended in homogenization buffer and again centrifuged at 13,000 x g_{max} for 12 min. The resuspended pellet was layered over a discontinuous gradient of 13%/9%/6% Ficoll 400 in homogenization buffer and centrifuged at 86,600 x g_{max} for 35 min at 4°C. Cream/white-colored synaptosomes were harvested from the 6%/9% and 9%/13% interfaces and concentrated by centrifugation at 27,000 x g_{max} at 4°C for 12.5 min after dilution with homogenization buffer. Tenfold dilution of synaptosomes into ice-cold 5 mM Tris-HCl, pH 8.0 followed by disruption in a Potter-Elvehjem homogenizer was used to generate synaptic plasma membranes. After adjusting the lysed membranes to 1.105 M sucrose, the sample was overlayed with 0.92 M and then 0.32 M sucrose and centrifuged at 60,000 x g_{ave} at 4°C for 60 min. The turbid, white-colored synaptosome plasma membrane-enriched fraction at the 0.92 M/1.105 M interface was collected and concentrated by centrifugation after dilution in 5 mM Tris-HCl, pH 8.0.

6.1.4 Kinase assays and thin layer chromatography

Phosphoinositide synthesis on synaptic membranes was assayed in assay buffer in a final volume of 50 μl, precisely as described previously (Arneson *et al.*, 1999). Briefly, the final concentrations were 0.5 mg/ml for membranes, 5 mg/ml for gel-filtered cytosol, and 500 μM for [γ-^{32}P]ATP (0.5–1 Ci/mmole). Reactions were terminated after 10 min at 37°C by addition of chloroform:methanol:conc. HCl (200:100:0.75), followed by vigorous mixing. After carrier phosphoinositides (50 μg/tube) were added, a biphasic mixture generated by addition of 0.6 M HCl. Samples were centrifuged at 200 x g_{ave} for 5 min, the lower organic phase removed and transferred to a new tube, washed twice with chloroform:methanol:0.6 M HCl (3:48:47) and then dried under a stream of N_2 gas at about 40°C. Dried lipid films were resuspended in chloroform:methanol:H_2O (75:25:1) and spotted onto oxalate-impregnated, heat-activated silica gel HPTLC plates and resolved in chloroform:acetone:methanol:acetic acid:water (160:60:52:48:28). Autoradiographs were quantitiated using ImageJ (Abramoff *et al.*, 2004).

6.1.5 Limited proteolysis

Purified, thrombin-cleaved PIPKIγ (460-635) and PIPKIγ (460-661) (20 μg) were incubated with fivefold serial dilutions of trypsin (Worthington Biochemical Corp.) in 50 mM Tris, pH 8.0, 150 mM NaCl, 5 mM $CaCl_2$, and 1 mM DTT at 37°C for 1 hour. Proteolysis was stopped by addition of 95°C 2x sample buffer and 10% of each reaction was analyzed by SDS-PAGE.

6.1.6 Binding assays

Typically, 100-250 μg of GST or GST fusion proteins were first immobilized upon ~25 μL of packed glutathione-Sepharose by incubation at 4°C for 1 h with continuous mixing. The Sepharose beads containing the required immobilized proteins were then washed and resuspended to 50 μL in assay buffer. A 250 μL volume of clarified rat brain cytosol was usually added and the tubes incubated at 4°C for 60 min with continuous mixing. For the peptide competition assay, thrombin-cleaved protein was added directly to the assay mixture in the presence of 25 μM D-Phe-Pro-Arg chloromethyl ketone. The glutathione-Sepharose beads were recovered by centrifugation at 10,000 x g_{max} for 1 min, and then an aliquot of each supernatant removed and adjusted to 100 μL with SDS-sample buffer. After washing the Sepharose pellets four times each with ~1.5 mL of ice-cold PBS by centrifugation, the supernatants were aspirated, and each pellet resuspended in SDS-sample buffer up to ~80 μL. Unless otherwise noted, 10 μL aliquots, corresponding to approximately 1.5% of each supernatant and 12.5% of each pellet, were analyzed.

For direct interaction assays between His_6-β2 hinge + appendage and GST fusion proteins, typically 5 μg His_6-tagged protein was bound to 5 μL packed Ni-NTA-agarose in 20mM HEPES-HCl, pH 7.5, 20 mM imidazole, 120 mM potassium acetate, 0.1% (w/v) Triton X-100 and 0.1 mg/mL Bovine Serum Albumin (BSA) (binding buffer) for 1 h at 4°C with continuous mixing. After washing, immobilized proteins were incubated with 25 μg GST or GST fusion proteins in a 300 μL volume for 1 h at 4°C with continuous mixing. Proteins were recovered by centrifugation at 10,000 x g_{max} for 1 min. An aliquot of each supernatant was removed and adjusted to 100 μL with sample buffer. Pellets were washed in ~1.5 mL ice-cold

binding buffer without BSA by centrifugation, the supernatants were aspirated, and each pellet was resuspended in SDS-sample buffer up to ~40 μL. Unless otherwise noted 10 μL aliquots, corresponding to approximately 2.5% of each supernatant and 25% of each pellet, were analyzed.

6.1.7 Circular dichroism

Appropriate GST fusion proteins immobilized on glutathione –Sepharose were incubated with thrombin and the soluble fraction dialyzed into 25 mM potassium phosphate, pH 7.4, 1 mM DTT. Circular dichroism spectra were measured on an AVIV Model 202 Spectrometer. Five (PIPKIγ) or three (ENTH domain) reproducible spectra were obtained from samples of concentrations between 0.09-0.11 mg/ml at 25°C in the near-UV wavelength region (190-280 nm). Spectra were averaged, smoothed (Savitzky and Golay, 1964), and baseline corrected by subtraction of similarly collected, averaged, and smoothed data for buffer alone.

6.1.8 Yeast two hybrid assay

The yeast two-hybrid assay was done utilizing the Matchmaker GAL4 system (Clontech) according the manufacturers protocols. Appropriately transformed *Saccharomyces cerevisiae* strain AH109 was selected first on SD minimal medium plates lacking Leu and Trp. Approximately 11-18 individual clones were selected and then streaked onto SD medium lacking Leu and Trp, on plates without His, Leu, and Trp, or onto plates lacking Ade, His, Leu, and Trp. Clones representative of the growth pattern for the interaction being tested where then

resuspended, normalized by optical density and spotted identically onto dropout plates and yeast grown at 30°C for four days.

6.2 CHAPTER 3 MATERIALS AND METHODS

6.2.1 DNA constructs

The β2-YFP plasmid was a kind gift from Alexander Sorkin (Sorkina *et al.*, 2002). The tdRFP (tandem dimer Tomato)-β-arrestin1 was generated by first replacing EGFP with tdRFP (Shaner *et al.*, 2004) between the NheI and BspE1 restriction sites in pEGFP-C1, followed by insertion of full-length *Bos taurus* β-arrestin 1 between XhoI and SalI sites. The tdRFP-β-arrestin 1 paired I386A and V387A (IV→AA) constitutively-active mutant, and the clathrin box ^{376}LIEL→AAEA mutation or clathrin-box-deleted ΔLIELD were all generated using QuikChange Mutagenesis (Stratagene). The monomeric Cherry (mCherry)-PIPKIγ661 plasmid was kindly provided by Richard Anderson (Sun *et al.*, 2007b) and was generated by inserting mCherry between HindIII and BamHI and PIPKIγ661 between BamHI and XbaI of pcDNA3 (Invitrogen). mCherry-PIPKIγ(630-661) was generated by inserting a BamHI restriction site at residues 628-629 of PIPKIγ, cutting and religating the mCherry-PIPKIγ661 plasmid. The PIPKIγ(630-661) tandem and triplet plasmids were generated by inserting an additional restriction site in front of XbaI of mCherry-PIPKIγ(630-661), amplifying (630-661) with this new site at the 5' end and an XbaI site at the 3' end (with or without a new site prior to XbaI), and ligating this into mCherry-

PIPKIγ(630-661). mCherry-PIPKIγ(630-661)x3 W642A was generated as above starting with W642A in the single repeat.

6.2.2 Antibodies

The anti-β-arrestin polyclonal antibody and anti-Talin monoclonal antibody were purchased from Sigma, the anti-tubulin mAb E7 from the Developmental Studies Hybridoma Bank. The AP-2 α-subunit mAb AP.6 has been described previously (Chin *et al.*, 1989). HRP-conjugated donkey anti-mouse and anti-rabbit were purchased from Jackson Immunologicals. The Alexa Fluor 488 angiotensin II and Alexa Fluor 488 transferrin were obtained from Invitrogen.

6.2.3 Cell culture

HeLa SS6 cells (Elbashir *et al.*, 2001) were cultured at 37°C humidified with 5% CO_2 in DMEM supplemented with 10% fetal calf serum and 2 mM L-glutamine (Invitrogen). A line of HeLa SS6 cells stably expressing β2-YFP was selected in the same medium supplemented with 0.5 mg/ml G-418. Analysis of these cells shows that <10% of cellular AP-2 contains the YFP-tagged β2 subunit. β-arrestin nullizygous mouse embryonic fibroblasts were kindly provided by Robert Lefkowitz (Kohout *et al.*, 2001). Cells were maintained in DMEM supplemented with 10% fetal calf serum and 2 mM L-glutamine. HEK 293 cells stably expressing a FLAG-tagged type I angiotensin II receptor were kindly provided by Stéphane Laporte and cultured in EMEM.

6.2.4 Immunofluorescence

HeLa cells were prepared for immunofluorescence as previously described (Mishra *et al.*, 2005). Alexa 488-labeled angiotensin II (100 nM) was added at 37°C for 5 or 20 min. For imaging of surface transferrin receptor-labeled fibroblasts, 25 μg/mL Tf488 was bound at 4°C for one hour in starvation media. Cells were washed once and imaged at 4°C in starvation media using a temperature-controlled stagemount (Harvard Apparatus).

6.2.5 Microscopy

Images were acquired on an Olympus Fluoview FV1000 as previously described (Keyel *et al.*, 2006). Total internal reflection fluorescence microscopy (TIR-FM) was performed as described previously (Keyel *et al.*, 2004) with some modifications. Images were collected with a thermoelectrically cooled Cascade II 512 camera (Photometrics). Data sets were collected with Metamorph software at ~1 frame/5 seconds. For quantification of colocalization of tdRFP-β-arrestin 1 with AP-2 in β2-YFP-expressing cells, an average of 55 spots/cell in 11-15 individual cells were analyzed.

6.3 CHAPTER 4 MATERIALS AND METHODS

6.3.1 Plasmids and small interfering RNA (siRNA)

The cloning of GFP-FCHO1 was described previously (Reider *et al.*, 2009). To generate GFP-FCHO2, full length human FCHO2 was PCR amplified from cDNA clone 9021067 (Open Biosystems, Huntsville, AL) and inserted into pEGFP-C1 using SalI restriction sites and Cold Fusion Cloning Technology (System Biosciences, Mountain View, CA). The tdRFP-conjugated FCHO2 was constructed by amplifying full length mouse FCHO2 from MGC cDNA clone 6830607 (Open Biosystems, Huntsville, AL) with terminal SalI and NotI sites by PCR. At the same a NotI site was introduced into pEGFP-C1 by site-directed mutagenesis PCR then both vectors were digested with SalI/NotI and ligated. GFP was then replaced with tdRFP between NheI and BspE1. The epsin 1 ENTH domain-FCHO1 chimera (GFP-ENTH-μHD) was created by inserting a SpeI site by site-directed mutagenesis PCR at residues 274/275 of FCHO1 in the GFP-FCHO1 construct. Residues 1-163 of rat epsin 1 were amplified by PCR with terminal EcoRI/SpeI restriction sites and used to replace FCHO1 residues 1-275. The GFP-ENTH-FCHO1 linker was generated by inserting a stop codon at FCHO1 residue 611 of the GFP-ENTH-μHD. The GFP-ENTH plasmid was created by inserting a stop codon at residue 164 of GFP-epsin 1. GFP-eps15 was a kind gift of Pier Di Fiore (Fondazione Instituto FIRC di Oncologia Molecolare, Milan, Italy). To generate tdRFP-eps15, eps15 was amplified and cloned between the XhoI and BamHI restriction sites of tdRFP.

The ON-TARGETplus SMARTpool siRNAs targeting human FCHO1 (L-014114-02-0005) and FCHO2 (L-024508-02-0005) were purchased from Thermo Scientific (Waltham,

MA). The Stealth siRNA targeting base pairs 434-458 of human FCHO2 (HSS151016, sequence CCAAGUGUGUAGAACAGGAGCGUUU) was purchased from Invitrogen.

6.3.2 Antibodies

The anti-FCHO2 polyclonal antibody was a kind gift of Harvey McMahon (Henne *et al.*, 2010). The anti-clathrin heavy chain (CHC) monoclonal antibody (mAb) TD.1 (Nathke *et al.*, 1992), the AP-1/2 β1/β2 subunit mAb 100/1 (Ahle *et al.*, 1988), the AP-2α subunit mAb AP.6 (Chin *et al.*, 1989), rabbit R11-29 anti-AP-2 μ2 subunit serum was kindly provided by Juan Bonifacino (National Institutes of Health, Bethesda, MD (Aguilar *et al.*, 1997)), anti-green fluorescent protein (GFP) polyclonal antibody B5 was generously provided by Phyllis Hanson (Washington University School of Medicine, St. Louis, MO; (Dalal *et al.*, 2004)). The anti-CALM mAb was a kind gift of Jeong-Ah Kim. The anti-tubulin mAb E7 was from the Developmental Studies Hybridoma Bank (University of Iowa, Iowa City, IA). Affinity purified polyclonal antibodies to Dab2 (Mishra *et al.*, 2002a) and epsin (Hawryluk *et al.*, 2006) were generated in the lab by standard procedure. The anti-eps15 affinity purified polyclonal antibody was a kind gift of Ernst Ungewickell (Hanover Medical School, Hanover, Germany). Anti-AP-2α subunit mAb clone 8 and anti-intersectin mAb were obtained from BD Biosciences Transduction Laboratories (Lexington, KY). A rabbit polyclonal antibody against bacterially expressed FCHO1 EFC (1-275) was generated (Pickcell Laboratories, Lelystad, The Netherlands) and affinity purified. The anti-FCHO1 goat polyclonal (P-16), anti-eps15 rabbit polyclonal (C-20), and anti-Hrb goat polyclonal antibodies were purchased from Santa Cruz Biotech. (Santa Cruz, CA). The anti-FCHO1 rabbit polyclonal, anti-eps15R rabbit polyclonal and C4 anti-actin mAb antibodies were purchased from Abcam (Cambridge, MA). The anti-LC3B (D11) monoclonal antibody was

purchased from Cell Signaling Technology (Danvers, MA). Horseradish Peroxidase-conjugated goat anti-rabbit and goat anti-mouse antibodies were purchased from GE Healthcare (Piscataway, NJ). Alexa Fluor 488-, and Alexa Fluor 568-conjugated goat anti-mouse and anti-rabbit secondary antibodies and Transferrin-Alexa Fluor 568 were obtained from Invitrogen. All Western blots were performed as described in Chapter 2 materials and methods.

6.3.3 Cell culture, Transfections and Tissue Preparation

HeLa SS6 cells (Elbashir *et al.*, 2001) were cultured at 37°C humidified with 5% CO_2 in DMEM supplemented with 10% fetal calf serum, 25 mM HEPES pH 7.2 and 2 mM L-glutamine (Invitrogen). SH-SY5Y cells were a kind gift of Charleen Chu (University of Pittsburgh) and were cultured in the same medium. A line of HeLa SS6 cells stably expressing the AP-2 β2 subunit conjugated to yellow fluorescent protein (YFP) was selected in the same medium supplemented with 0.5 mg/ml G-418 (Invitrogen). Analysis of these cells shows that <10% of cellular AP-2 contains the YFP-tagged β2 subunit. BS-C-1 cells stably expressing clathrin light chain (CLC) conjugated to EGFP were a kind gift of Tom Kirchhausen (Harvard University) and were maintained in the same medium supplemented with 0.4 mg/ml G-418. HT-1080 cells were a kind gift of Chuanyue Wu (University of Pittsburgh) and the MCF-7 cells were generously provided by Olivera Finn (University of Pittsburgh). Both of these cell lines were cultured in DMEM supplemented with 10% fetal calf serum, 25 mM HEPES pH 7.2 and 2 mM L-glutamine.

For transient transfections, $1.3x10^5$ cells were plated on coverslips in a 24-well dish or $5x10^4$ (HeLa) or $1.2\ x10^4$ BS-C-1 cells were plated directly on the coverglass of Mat-Tek dishes to yield approximately 60-70% confluency at 24 hs. The next day cells were transfected with 400-500 ng DNA with Lipofectamine 2000 (Invitrogen) according to the manufacturer's

instructions. The cells were prepared for immunofluorescence or imaged live ~18 hs post-transfection. For siRNA-mediated knockdown, $1x10^5$ cells were plated in a 24-well dish on day 1 to yield ~50% confluency the next day. On day 2, the cells were transfected with 100 nM siRNA with Oligofectamine (Invitrogen) according to the manufacturer's instructions. The cells were split to coverslips in 24-well dishes or Mat-Tek dishes on day 3 to yield ~50% confluency the day following. On day 4, the cells were transfected in the same manner with siRNA with or without 100 ng rescue plasmid and the following day cells were imaged live or prepared for immunofluorescence at ~72 hs after the first transfection. Clathrin-coated vesicles were isolated from rat brain as described previously (Mishra *et al.*, 2001).

6.3.4 Immunofluorescence

HeLa SS6 cells were prepared for immunofluorescence as described previously (Mishra *et al.*, 2005). For ligand internalization assays, cells were placed in DMEM supplemented with 25 mM HEPES-KOH, pH 7.2 and 0.5% bovine serum albumin (Starvation Media) for one h at 37°C to unload receptors. Cells were then incubated in the continuous presence of 25 μg/ml transferrin conjugated to Alexa Fluor 568 (Tf-568) (Invitrogen) for 10 mins or 10 μg/ml DiI labeled LDL (DiI-LDL) (Biomedical Technologies, Stoughton, MA) for 20 mins at 37°C. Uptake was stopped by incubating cells on coverslips in ice-cold 0.5 M NaCl and 0.2 N acetate (pH~3) to strip surface ligand for transferrin or ice-cold PBS for LDL. After two additional washes in ice-cold PBS, the cells were fixed in 2% paraformaldehyde and processed for immunofluorescence.

6.3.5 Reverse Transcriptase-Polymerase Chain Reaction (RT-PCR)

RNA was isolated from HeLa SS6 and SH-SY5Y cells by dissolving cells in culture in TRIzol (Invitrogen) followed by chloroform extraction. The aqueous layer was precipitated by isopropanol and resuspended in DEPC water. To generate cDNA, the SuperScript III kit (Invitrogen) was used with 4 μg DNase-treated RNA according to the manufacturer's instructions. PCR of endocytic protein transcripts was performed with Taq polymerase (Genscript, Piscataway, NJ) and the following primers: FCHO1 sense 5'-CTG GCG CTG TGC CAC CTG GAA CT-3', FCHO1 antisense 5'-GTA CTC TCC CTC CGC AGC CGC TC-3', FCHO2 sense 5'-CCC CAG CAA TAT CTA GAC ACA GTC C-3', FCHO2 antisense 5'-TAC AGA AAG AGG AGT TGT GGG CC-3', SGIP1 sense 5'-GAA GTG GCA AGA CCC AGG CGT TCC-3', SGIP1 antisense 5'-GGA GGT GTT CCA GTG GGA AAA GGC C-3', Beta-actin sense 5'-GAG AGG CAT CCT CAC CCT GAA GTA C-3', Beta-actin antisense 5'-GCA CAG CCT GGA TAG CAA CGT ACA T-3', Clathrin heavy chain sense 5'-GGA AGG AGA GTC TCA GCC AGT GAA A-3', Clathrin heavy chain antisense 5'-TAT GTA ACT TCC CTC CAG CTT GGC C-3', eps15 sense 5'-TTG TTG CAG CAA GCG ATT CAG CCA-3', eps15 antisense 5'-AGG GCA GGG TCT TGT TGG AGT TCC-3', eps15R sense 5'-AGC CTC AAC AGC ACA GGG AGC CTG-3', eps15R antisense 5'-AAG GTT CTG GGT GAG GCC CGA GTG-3'. The PCR cycle used was 94°C for 3 min, 94°C for 30 s, 53°C (FCHO2 and clathrin) or 55°C (remainder) for 30 s, 72°C for one min, repeated for 30 cycles, final extension at 72°C for seven mins.

6.3.6 Microscopy

Confocal fluorescence images were collected on an Olympus Fluoview 1000 microscope (Center Valley, PA) as described previously (Keyel *et al.*, 2006), however red fluorophores Alexa Fluor 568 and DiI were excited with a 558 nm laser line of a solid state diode laser. For fluorescence recovery after photobleaching experiments, cells were maintained on the microscope in DMEM supplemented with 10% fetal calf serum and 25 mM HEPES, pH 7.2 at 37°C on MatTek dishes (MatTek Corp., Ashland, MA). Cells were imaged continuously at 2s/frame with a 488 nm line argon laser and 5 μm diameter circular subregions were bleached simultaneously with a 405 nm diode laser at maximum intensity for 2 seconds. Alternatively, cells were incubated for ~20 minutes in 0.45M sucrose containing media prior to imaging.

For TIRF microscopy, cells were imaged on a Nikon Eclipse Ti inverted microscope (Melville, NY) with a 60x 1.49 NA oil immersion objective. GFP was excited with a 488 nm line sapphire solid state diode laser (Coherent Inc., Santa Clara, CA) while the DsRed variant tandem Tomato was excited with a 561 nm solid state diode laser (CrystaLaser, Reno, NV). For three color TIR-FM, transferrin-Alexa647 (Molecular Probes, Carlsbad, CA) was excited with a 638 nm line solid state diode laser (Spectra Physics, Santa Clara, CA). All laser lines were selectively blocked within the laser bench and illumination (both intensity and blanking) was controlled by acousto-optical tunable filters. The excitation angle of incidence was controlled by a motorized TIRF illuminator and adjusted for each excitation wavelength between exposures. In all applications, a Z488/561/638rpc beamsplitter (Chroma Technology Corp., Bellows Falls, VT) was used. Images were collected using a CoolSNAP HQ2 CCD camera (Photometrics, Tucson, AZ). Data sets were acquired using Nikon Elements software. Typically images were collected at 0.3-0.5 Hz.

6.3.7 Image Processing

To quantify the behavior of FCHO1 relative to clathrin and spot lifetimes, random clathrin-positive spots were chosen from the middle frame of data sets (typically around 5 mins) and manually scored for FCHO1 content and order of appearance. To quantify FRAP data, the integrated intensity of individual FCHO1/2 spots or AP-2 beta spots within the bleach region were measured over time and normalize to an adjacent region lacking spots in Metamorph software (Molecular Devices, Dowington, PA). Bleaching and recovery are reported relative to the average of three frames prior to bleaching. The recovery curves from 30 spots were fitted (Graphpad Prism Software) and the recovery and $t_{1/2}$ values were averaged.

Particle tracking to determine lifetimes of AP-2 in FCHO2 knockdown cells was performed in Imaris Software (Bitplane, St. Paul, MN). Data sets were smoothed with a Gaussian filter followed by the use of the Spots module. The spots were estimated at a diameter of 0.5 µm and tracked with a Brownian motion algorithm. A maximum of 0.25 µm lateral movement of spots between frames was permitted and gap filling was used for up to 4 consecutive frames. Only tracks greater than or equal to 2 frames with a mean lateral speed less than 0.1 µm/second were scored. A total of 12 cells were analyzed from each condition. To quantitate AP-2 structure properties, single confocal sections of the ventral cell surface were thresholded in Metamorph and regions were created around each thresholded object. Object size, fluorescence intensity and number were exported to Excel. To quantitate ligand internalization, confocal Z-stacks with 0.6 µm step-size through the entire volume of the cell monolayer were used to create a maximum Z projection. Images were background corrected and the integrated fluorescence intensity from a 14x14 µm region were recorded and averaged.

6.3.8 Electron Microscopy

Adherent plasma membrane from cells treated with FCHO2 siRNA as described above were prepared for rapid-freeze, deep-etch electron microscopy as described previously (Heuser, 2000). Briefly, cells grown on oriented pieces of glass coverslip were disrupted by sonication, fixed in paraformaldehyde, and labeled with anti-FCHO2 rAb and then 15-nm gold-conjugated anti-rabbit antibody before flash freezing in liquid helium (Keyel *et al.*, 2006).

6.3.9 Statistics

In all figures, graphs represent average and error bars represent standard error. P values were determined by Student's t-test or analysis of variance (ANOVA) and Tukey's post-hoc test for multiple groups in SPSS (IBM, Chicago, IL).

BIBLIOGRAPHY

Abe, N., Inoue, T., Galvez, T., Klein, L., and Meyer, T. (2008). Dissecting the role of PtdIns(4,5)P_2 in endocytosis and recycling of the transferrin receptor. J. Cell Sci. *121*, 1488-1494.

Abramoff, M.D., Magelhaes, P.J., and Ram, S.J. (2004). Image processing with ImageJ. Biophotinics Int. *11*, 36-42.

Aguilar, R.C., Ohno, H., Roche, K.W., and Bonifacino, J.S. (1997). Functional domain mapping of the clathrin-associated adaptor medium chains µ1 and µ2. J. Biol. Chem. *272*, 27160-27166.

Ahle, S., Mann, A., Eichelsbacher, U., and Ungewickell, U. (1988). Structural relationships between clathrin assembly proteins from the Golgi and the plasma membrane. EMBO J. *7*, 919-929.

Ahle, S., and Ungewickell, E. (1986). Purification and properties of a new clathrin assembly protein. EMBO J. *5*, 3143-3149.

Akisaka, T., Yoshida, H., Suzuki, R., Shimizu, K., and Takama, K. (2003). Clathrin sheets on the protoplasmic surface of ventral membranes of osteoclasts in culture. J. Electron Microsc. (Tokyo) *52*, 535-543.

Alberts, B., Johnson, A., Lewis, J., Raff, M., Roberts, K., and Walter, P. (2002). Molecular Biology of the Cell. Garland Science: New York.

Anderson, H.A., Chen, Y., and Norkin, L.C. (1996). Bound simian virus 40 translocates to caveolin-enriched membrane domains, and its entry is inhibited by drugs that selectively disrupt caveolae. Molecular biology of the cell *7*, 1825-1834.

Anderson, R.G., Goldstein, J.L., and Brown, M.S. (1977). A mutation that impairs the ability of lipoprotein receptors to localise in coated pits on the cell surface of human fibroblasts. Nature *270*, 695-699.

Antonescu, C.N., Danuser, G., and Schmid, S.L. (2010). Phosphatidic acid plays a regulatory role in clathrin-mediated endocytosis. Molecular biology of the cell *21*, 2944-2952.

Aridor, M., Weissman, J., Bannykh, S., Nuoffer, C., and Balch, W.E. (1998). Cargo selection by the COPII budding machinery during export from the ER. The Journal of cell biology *141*, 61-70.

Arneson, L.S., Kunz, J., Anderson, R.A., and Traub, L.M. (1999). Coupled inositide phosphorylation and phospholipase D activation initiates clathrin-coat assembly on lysosomes. J. Biol. Chem. *274*, 17794-17805.

Bairstow, S.F., Ling, K., Su, X., Firestone, A.J., Carbonara, C., and Anderson, R.A. (2006). Type Iγ661 phosphatidylinositol phosphate kinase directly interacts with AP2 and regulates endocytosis. J. Biol. Chem. *281*, 20632-20642.

Balch, W.E., Dunphy, W.G., Braell, W.A., and Rothman, J.E. (1984a). Reconstitution of the transport of protein between successive compartments of the Golgi measured by the coupled incorporation of N-acetylglucosamine. Cell *39*, 405-416.

Balch, W.E., Glick, B.S., and Rothman, J.E. (1984b). Sequential intermediates in the pathway of intercompartmental transport in a cell-free system. Cell *39*, 525-536.

Ball, C.L., Hunt, S.P., and Robinson, M.S. (1995). Expression and localization of a-adaptin isoforms. J. Cell Sci. *108*, 2865-2875.

Barbieri, M.A., Heath, C.M., Peters, E.M., Wells, A., Davis, J.N., and Stahl, P.D. (2001). Phosphatidylinositol-4-phosphate 5-kinase-1β is essential for epidermal growth factor receptor-mediated endocytosis. J. Biol. Chem. *276*, 47212-47216.

Barlowe, C. (2003). Signals for COPII-dependent export from the ER: what's the ticket out? Trends in cell biology *13*, 295-300.

Barlowe, C., Orci, L., Yeung, T., Hosobuchi, M., Hamamoto, S., Salama, N., Rexach, M.F., Ravazzola, M., Amherdt, M., and Schekman, R. (1994). COPII: a membrane coat formed by Sec proteins that drive vesicle budding from the endoplasmic reticulum. Cell *77*, 895-907.

Barriere, H., Nemes, C., Lechardeur, D., Khan-Mohammad, M., Fruh, K., and Lukacs, G.L. (2006). Molecular basis of Ub-dependent internalization of membrane proteins in mammalian cells. Traffic (Copenhagen, Denmark) *7*, 282-297.

Barrios-Rodiles, M., Brown, K.R., Ozdamar, B., Bose, R., Liu, Z., Donovan, R.S., Shinjo, F., Liu, Y., Dembowy, J., Taylor, I.W., Luga, V., Przulj, N., Robinson, M., Suzuki, H., Hayashizaki, Y., Jurisica, I., and Wrana, J.L. (2005). High-throughput mapping of a dynamic signaling network in mammalian cells. Science (New York, N.Y *307*, 1621-1625.

Beausoleil, S.A., Villen, J., Gerber, S.A., Rush, J., and Gygi, S.P. (2006). A probability-based approach for high-throughput protein phosphorylation analysis and site localization. Nat. Biotechnol. *24*, 1285-1292.

Beck, R., Rawet, M., Wieland, F.T., and Cassel, D. (2009). The COPI system: molecular mechanisms and function. FEBS letters *583*, 2701-2709.

Bellve, K.D., Leonard, D., Standley, C., Lifshitz, L.M., Tuft, R.A., Hayakawa, A., Corvera, S., and Fogarty, K.E. (2006). Plasma membrane domains specialized for clathrin-mediated endocytosis in primary cells. J. Biol. Chem. *281*, 16139-16146.

Benmerah, A., Begue, B., Dautry-Varsat, A., and Cerf-Bensussan, N. (1996). The ear of α-adaptin interacts with the COOH-terminal domain of the eps15 protein. J. Biol. Chem. *271*, 12111-12116.

Biedler, J.L., Roffler-Tarlov, S., Schachner, M., and Freedman, L.S. (1978). Multiple neurotransmitter synthesis by human neuroblastoma cell lines and clones. Cancer Res. *38*, 3751-3757.

Blondeau, F., Ritter, B., Allaire, P.D., Wasiak, S., Girard, M., Hussain, N.K., Angers, A., Legendre-Guillemin, V., Roy, L., Boismenu, D., Kearney, R.E., Bell, A.W., Bergeron, J.J., and McPherson, P.S. (2004). Tandem MS analysis of brain clathrin-coated vesicles reveals their critical involvement in synaptic vesicle recycling. Proc. Natl. Acad. Sci. U S A *101*, 3833-3838.

Boehm, M., and Bonifacino, J.S. (2001). Adaptins: the final recount. Mol. Biol. Cell *12*, 2907-2920.

Boettner, D.R., D'Agostino, J.L., Torres, O.T., Daugherty-Clarke, K., Uygur, A., Reider, A., Wendland, B., Lemmon, S.K., and Goode, B.L. (2009). The F-BAR protein Syp1 negatively regulates WASp-Arp2/3 complex activity during endocytic patch formation. Curr. Biol. *19*, 1979-1987.

Bonifacino, J.S., and Glick, B.S. (2004). The mechanisms of vesicle budding and fusion. Cell *116*, 153-166.

Booth, A.G., and Wilson, M.J. (1981). Human placental coated vesicles contain receptor-bound transferrin. Biochem. J. *196*, 355-362.

Borner, G.H., Harbour, M., Hester, S., Lilley, K.S., and Robinson, M.S. (2006). Comparative proteomics of clathrin-coated vesicles. J. Cell Biol. *175*, 571-578.

Boucrot, E., Saffarian, S., Massol, R., Kirchhausen, T., and Ehrlich, M. (2006). Role of lipids and actin in the formation of clathrin-coated pits. Exp. Cell Res. *312*, 4036-4048.

Braell, W.A., Balch, W.E., Dobbertin, D.C., and Rothman, J.E. (1984). The glycoprotein that is transported between successive compartments of the Golgi in a cell-free system resides in stacks of cisternae. Cell *39*, 511-524.

Brett, T.J., and Traub, L.M. (2006). Molecular structures of coat and coat-associated proteins: function follows form Curr. Opin. Cell Biol. *18*, 395-406.

Brett, T.J., Traub, L.M., and Fremont, D.H. (2002). Accessory protein recruitment motifs in clathrin-mediated endocytosis. Structure (Camb.) *10*, 797-809.

Brough, D., Bhatti, F., and Irvine, R.F. (2005). Mobility of proteins associated with the plasma membrane by interaction with inositol lipids. J. Cell. Sci. *118*, 3019-3025.

Bu, W., Lim, K.B., Yu, Y.H., Chou, A.M., Sudhaharan, T., and Ahmed, S. (2010). Cdc42 interaction with N-WASP and Toca-1 regulates membrane tubulation, vesicle formation and vesicle motility: implications for endocytosis. PloS one *5*, e12153.

Burtey, A., Schmid, E.M., Ford, M.G., Rappoport, J.Z., Scott, M.G., Marullo, S., Simon, S.M., McMahon, H.T., and Benmerah, A. (2007). The conserved isoleucine-valine-phenylalanine motif couples activation state and endocytic functions of β-arrestins. Traffic (Copenhagen, Denmark) *8*, 914–931.

Carvou, N., Norden, A.G., Unwin, R.J., and Cockcroft, S. (2006). Signalling through phospholipase C interferes with clathrin-mediated endocytosis. Cell. Signal. *19*, 42-51.

Cestra, G., Castagnoli, L., Dente, L., Minenkova, O., Petrelli, A., Migone, N., Hoffmuller, U., Schneider-Mergener, J., and Cesareni, G. (1999). The SH3 domains of endophilin and amphiphysin bind to the proline-rich region of synaptojanin 1 at distinct sites that display an unconventional binding specificity. The Journal of biological chemistry *274*, 32001-32007.

Chang-Ileto, B., Frere, S.G., Chan, R.B., Voronov, S.V., Roux, A., and Di Paolo, G. (2011). Synaptojanin 1-mediated PI(4,5)P2 hydrolysis is modulated by membrane curvature and facilitates membrane fission. Developmental cell *20*, 206-218.

Chao, W.T., and Kunz, J. (2009). Focal adhesion disassembly requires clathrin-dependent endocytosis of integrins. FEBS Lett. *583*, 1337-1343.

Chaudhuri, R., Lindwasser, O.W., Smith, W.J., Hurley, J.H., and Bonifacino, J.S. (2007). CD4 Downregulation by HIV-1 Nef is Dependent on Clathrin and Involves a Direct Interaction of Nef with the AP2 Clathrin Adaptor. J. Virol. *81*, 3877-3890.

Chen, H., Fre, S., Slepnev, V.I., Capua, M.R., Takei, K., Butler, M.H., Di Fiore, P.P., and De Camilli, P. (1998). Epsin is an EH-domain-binding protein implicated in clathrin-mediated endocytosis. Nature *394*, 793-797.

Chen, H., Ko, G., Zatti, A., Di Giacomo, G., Liu, L., Raiteri, E., Perucco, E., Collesi, C., Min, W., Zeiss, C., De Camilli, P., and Cremona, O. (2009). Embryonic arrest at midgestation and disruption of Notch signaling produced by the absence of both epsin 1 and epsin 2 in mice. Proc. Natl. Acad. Sci. U S A *106*, 13838-13843.

Chen, W.J., Goldstein, J.L., and Brown, M.S. (1990). NPXY, a sequence often found in cytoplasmic tails, is required for coated pit-mediated internalization of the low density lipoprotein receptor. J. Biol. Chem. *265*, 3116-3123.

Chetrit, D., Ziv, N., and Ehrlich, M. (2009). Dab2 regulates clathrin assembly and cell spreading. Biochem. J. *418*, 701-715.

Chi, S., Cao, H., Chen, J., and McNiven, M. (2008). Eps15 mediates vesicle trafficking from the trans-Golgi network via an interaction with clathrin adaptor AP-1. Mol. Biol. Cell *19*, 3564-3575.

Chin, D.J., Straubinger, R.M., Acton, S., Nathke, I., and Brodsky, F.M. (1989). 100-kDa polypeptides in peripheral clathrin-coated vesicles are required for receptor-mediated endocytosis. Proc. Natl. Acad. Sci. USA *86*, 9289-9293.

Coleman, S.H., Van Damme, N., Day, J.R., Noviello, C.M., Hitchin, D., Madrid, R., Benichou, S., and Guatelli, J.C. (2005). Leucine-specific, functional interactions between human immunodeficiency virus type 1 Nef and adaptor protein complexes. J. Virol. *79*, 2066-2078.

Collawn, J.F., Stangel, M., Kuhn, L.A., Esekogwu, V., Jing, S.Q., Trowbridge, I.S., and Tainer, J.A. (1990). Transferrin receptor internalization sequence YXRF implicates a tight turn as the structural recognition motif for endocytosis. Cell *63*, 1061-1072.

Collinet, C., Stoter, M., Bradshaw, C.R., Samusik, N., Rink, J.C., Kenski, D., Habermann, B., Buchholz, F., Henschel, R., Mueller, M.S., Nagel, W.E., Fava, E., Kalaidzidis, Y., and Zerial, M. (2010). Systems survey of endocytosis by multiparametric image analysis. Nature.

Collins, B.M., McCoy, A.J., Kent, H.M., Evans, P.R., and Owen, D.J. (2002). Molecular architecture and functional model of the endocytic AP2 complex. Cell *109*, 523-535.

Compagnon, J., Gervais, L., Roman, M.S., Chamot, B.O.U.S., and Guichet, A. (2009). Interplay between Rab5 and PtdIns(4,5)P_2 controls early endocytosis in the Drosophila germline. J. Cell Sci. *122*, 25-35.

Conner, S.D., and Schmid, S.L. (2003). Regulated portals of entry into the cell. Nature *422*, 37-44.

Conner, S.D., Schroter, T., and Schmid, S.L. (2003). AAK1 mediated μ2 phosphorylation is stimulated by assembled clathrin. Traffic (Copenhagen, Denmark) *4*, 885-890.

Cousin, M.A., and Robinson, P.J. (2001). The dephosphins: dephosphorylation by calcineurin triggers synaptic vesicle endocytosis. Trends Neurosci. *24*, 659-665.

Cremona, O., and De Camilli, P. (2001). Phosphoinositides in membrane traffic at the synapse. J. Cell Sci. *114*, 1041-1052.

Cremona, O., Di Paolo, G., Wenk, M.R., Luthi, A., Kim, W.T., Takei, K., Daniell, L., Nemoto, Y., Shears, S.B., Flavell, R.A., McCormick, D.A., and De Camilli, P. (1999). Essential role of phosphoinositide metabolism in synaptic vesicle recycling. Cell *99*, 179-188.

Crottet, P., Meyer, D.M., Rohrer, J., and Spiess, M. (2002). ARF1.GTP, tyrosine-based signals, and phosphatidylinositol 4,5-bisphosphate constitute a minimal machinery to recruit the AP-1 clathrin adaptor to membranes. Mol. Biol. Cell *13*, 3672-3682.

Cullen, P.J. (2008). Endosomal sorting and signalling: an emerging role for sorting nexins. Nat. Rev. Mol. Cell. Biol. *9*, 574-582.

Cupers, P., Jadhav, A.P., and Kirchhausen, T. (1998). Assembly of clathrin coats disrupts the association between Eps15 and AP-2 adaptors. J. Biol. Chem. *273*, 1847-1850.

Dalal, S., Rosser, M.F., Cyr, D.M., and Hanson, P.I. (2004). Distinct roles for the AAA ATPases NSF and p97 in the secretory pathway. Mol. Biol. Cell *15*, 637-648.

Davis, J.N., Rock, C.O., Cheng, M., Watson, J.B., Ashmun, R.A., Kirk, H., Kay, R.J., and Roussel, M.F. (1997). Complementation of growth factor receptor-dependent mitogenic signaling by a truncated type I phosphatidylinositol 4-phosphate 5-kinase. Molecular and cellular biology *17*, 7398-7406.

de Beer, T., Hoofnagle, A.N., Enmon, J.L., Bowers, R.C., Yamabhai, M., Kay, B.K., and Overduin, M. (2000). Molecular mechanism of NPF recognition by EH domains. Nat. Struct. Biol. *7*, 1018-1022.

De Deyne, P.G., O'Neill, A., Resneck, W.G., Dmytrenko, G.M., Pumplin, D.W., and Bloch, R.J. (1998). The vitronectin receptor associates with clathrin-coated membrane domains via the cytoplasmic domain of its beta5 subunit. Journal of cell science *111 (Pt 18)*, 2729-2740.

de Pereda, J.M., Wegener, K.L., Santelli, E., Bate, N., Ginsberg, M.H., Critchley, D.R., Campbell, I.D., and Liddington, R.C. (2005). Structural basis for phosphatidylinositol phosphate kinase type Iγ binding to talin at focal adhesions. J. Biol. Chem. *280*, 8381-8386.

Di Paolo, G., and De Camilli, P. (2006). Phosphoinositides in cell regulation and membrane dynamics. Nature *443*, 651-657.

Di Paolo, G., Moskowitz, H.S., Gipson, K., Wenk, M.R., Voronov, S., Obayashi, M., Flavell, R., Fitzsimonds, R.M., Ryan, T.A., and De Camilli, P. (2004). Impaired PtdIns(4,5)P_2 synthesis in nerve terminals produces defects in synaptic vesicle trafficking. Nature *431*, 415-422.

Di Paolo, G., Pellegrini, L., Letinic, K., Cestra, G., Zoncu, R., Voronov, S., Chang, S., Guo, J., Wenk, M.R., and De Camilli, P. (2002). Recruitment and regulation of phosphatidylinositol phosphate kinase type 1γ by the FERM domain of talin. Nature *420*, 85-89.

DiAntonio, A., Parfitt, K.D., and Schwarz, T.L. (1993). Synaptic transmission persists in synaptotagmin mutants of Drosophila. Cell *73*, 1281-1290.

Doherty, G.J., and McMahon, H.T. (2009). Mechanisms of endocytosis. Annu. Rev. Biochem. *78*, 857-902.

Doray, B., Lee, I., Knisely, J., Bu, G., and Kornfeld, S. (2007). The γ/σ1 and α/σ2 hemicomplexes of clathrin adaptors AP-1 and AP-2 harbor the dileucine recognition site. Mol. Biol. Cell *18*, 1887-1896.

Drake, M.T., Downs, M.A., and Traub, L.M. (2000). Epsin binds to clathrin by associating directly with the clathrin-terminal domain: evidence for cooperative binding through two discrete sites. J. Biol. Chem. *275*, 6479-6489.

Edeling, M.A., Mishra, S.K., Keyel, P.A., Steinhauser, A.L., Collins, B.M., Roth, R., Heuser, J.E., Owen, D.J., and Traub, L.M. (2006a). Molecular switches involving the AP-2 β2 appendage regulate endocytic cargo selection and clathrin coat assembly. Dev. Cell *10*, 329-342.

Edeling, M.A., Smith, C., and Owen, D. (2006b). Life of a clathrin coat: insights from clathrin and AP structures. Nat. Rev. Mol. Cell Biol. *7*, 32-44.

Eden, E.R., Sun, X.M., Patel, D.D., and Soutar, A.K. (2007). Adaptor protein Disabled-2 modulates low density lipoprotein (LDL) receptor synthesis in fibroblasts from patients with autosomal recessive hypercholesterolemia. Hum. Mol. Genet. *16*, 2751-2759.

Ehrlich, M., Boll, W., Van Oijen, A., Hariharan, R., Chandran, K., Nibert, M.L., and Kirchhausen, T. (2004). Endocytosis by random initiation and stabilization of clathrin-coated pits. Cell *118*, 591-605.

Eisenberg, E., and Greene, L.E. (2007). Multiple roles of auxilin and hsc70 in clathrin-mediated endocytosis. Traffic (Copenhagen, Denmark) *8*, 640-646.

Elbashir, S.M., Harborth, J., Lendeckel, W., Yalcin, A., Weber, K., and Tuschl, T. (2001). Duplexes of 21-nucleotide RNAs mediate RNA interference in cultured mammalian cells. Nature *411*, 494-498.

Engqvist-Goldstein, A.E., Kessels, M.M., Chopra, V.S., Hayden, M.R., and Drubin, D.G. (1999). An actin-binding protein of the Sla2/Huntingtin interacting protein 1 family is a novel component of clathrin-coated pits and vesicles. J. Cell Biol. *147*, 1503-1518.

Engqvist-Goldstein, A.E., Zhang, C.X., Carreno, S., Barroso, C., Heuser, J.E., and Drubin, D.G. (2004). RNAi-mediated Hip1R silencing results in stable association between the endocytic machinery and the actin assembly machinery. Mol. Biol. Cell *15*, 1666-1676.

Erdmann, K.S., Mao, Y., McCrea, H.J., Zoncu, R., Lee, S., Paradise, S., Modregger, J., Biemesderfer, D., Toomre, D., and De Camilli, P. (2007). A role of the Lowe ryndrome protein OCRL in early steps of the endocytic pathway. Dev. Cell *13*, 377-390.

Eto, D.S., Gordon, H.B., Dhakal, B.K., Jones, T.A., and Mulvey, M.A. (2008). Clathrin, AP-2, and the NPXY-binding subset of alternate endocytic adaptors facilitate FimH-mediated bacterial invasion of host cells. Cell. Microbiol. *10*, 2553-2567.

Ezratty, E.J., Bertaux, C., Marcantonio, E.E., and Gundersen, G.G. (2009). Clathrin mediates integrin endocytosis for focal adhesion disassembly in migrating cells. The Journal of cell biology *187*, 733-747.

Feng, Y., Hartig, S.M., Bechill, J.E., Blanchard, E.G., Caudell, E., and Corey, S.J. (2010). The Cdc42-interacting protein-4 (CIP4) gene knock-out mouse reveals delayed and decreased endocytosis. J. Biol. Chem. *285*, 4348-4354.

Ferguson, S.M., Brasnjo, G., Hayashi, M., Wolfel, M., Collesi, C., Giovedi, S., Raimondi, A., Gong, L.W., Ariel, P., Paradise, S., O'Toole, E., Flavell, R., Cremona, O., Miesenbock, G., Ryan, T.A., and De Camilli, P. (2007). A selective activity-dependent requirement for dynamin 1 in synaptic vesicle endocytosis. Science (New York, N.Y *316*, 570-574.

Ferguson, S.M., Raimondi, A., Paradise, S., Shen, H., Mesaki, K., Ferguson, A., Destaing, O., Ko, G., Takasaki, J., Cremona, O., E, O.T., and De Camilli, P. (2009). Coordinated actions of actin and BAR proteins upstream of dynamin at endocytic clathrin-coated pits. Developmental cell *17*, 811-822.

Fischer von Mollard, G., Sudhof, T.C., and Jahn, R. (1991). A small GTP-binding protein dissociates from synaptic vesicles during exocytosis. Nature *349*, 79-81.

Ford, M.G., Mills, I.G., Peter, B.J., Vallis, Y., Praefcke, G.J., Evans, P.R., and McMahon, H.T. (2002). Curvature of clathrin-coated pits driven by epsin. Nature *419*, 361-366.

Ford, M.G., Pearse, B.M., Higgins, M.K., Vallis, Y., Owen, D.J., Gibson, A., Hopkins, C.R., Evans, P.R., and McMahon, H.T. (2001). Simultaneous binding of PtdIns(4,5)P_2 and clathrin by AP180 in the nucleation of clathrin lattices on membranes. Science (New York, N.Y *291*, 1051-1055.

Fotin, A., Cheng, Y., Sliz, P., Grigorieff, N., Harrison, S.C., Kirchhausen, T., and Walz, T. (2004). Molecular model for a complete clathrin lattice from electron cryomicroscopy. Nature *432*, 573-579.

Friend, D.S., and Farquhar, M.G. (1967). Functions of coated vesicles during protein absorption in the rat vas deference. J. Cell Biol. *35*, 357-376.

Frost, A., Unger, V.M., and De Camilli, P. (2009). The BAR domain superfamily: membrane-molding macromolecules. Cell *137*, 191-196.

Gaidarov, I., and Keen, J.H. (1999). Phosphoinositide-AP-2 interactions required for targeting to plasma membrane clathrin-coated pits. J. Cell Biol. *146*, 755-764.

Gaidarov, I., Krupnick, J.G., Falck, J.R., Benovic, J.L., and Keen, J.H. (1999). Arrestin function in G protein-coupled receptor endocytosis requires phosphoinositide binding. EMBO J. *18*, 871-881.

Galletta, B.J., Mooren, O.L., and Cooper, J.A. (2010). Actin dynamics and endocytosis in yeast and mammals. Current opinion in biotechnology *21*, 604-610.

Gallusser, A., and Kirchhausen, T. (1993). The β1 and the β2 subunits of the AP complexes are the clathrin coat assembly components. EMBO J. *12*, 5237-5244.

Garuti, R., Jones, C., Li, W.P., Michaely, P., Herz, J., Gerard, R.D., Cohen, J.C., and Hobbs, H.H. (2005). The modular adaptor protein autosomal recessive hypercholesterolemia (ARH) promotes low density lipoprotein receptor clustering into clathrin-coated pits. J. Biol. Chem. *280*, 40996-41004.

Girard, M., Allaire, P.D., McPherson, P.S., and Blondeau, F. (2005). Non-stoichiometric relationship between clathrin heavy and light chains revealed by quantitative comparative proteomics of clathrin-coated vesicles from brain and liver. Mol. Cell. Proteomics *4*, 1145-1154.

Giudici, M.L., Emson, P.C., and Irvine, R.F. (2004). A novel neuronal-specific splice variant of Type I phosphatidylinositol 4-phosphate 5-kinase isoform gamma. Biochem. J. *379*, 489-496.

Giudici, M.L., Lee, K., Lim, R., and Irvine, R.F. (2006). The intracellular localisation and mobility of Type Igamma phosphatidylinositol 4P 5-kinase splice variants. FEBS Lett. *580*, 6933-6937.

Golebiewska, U., Nyako, M., Woturski, W., Zaitseva, I., and McLaughlin, S. (2008). Diffusion coefficient of fluorescent phosphatidylinositol 4,5-bisphosphate in the plasma membrane of cells. Mol. Biol. Cell *19*, 1663-1669.

Gong, H., Sengupta, D., Linstedt, A.D., and Schwartz, R. (2008). Simulated de novo assembly of golgi compartments by selective cargo capture during vesicle budding and targeted vesicle fusion. Biophysical journal *95*, 1674-1688.

Gonzalez-Gaitan, M., and Jackle, H. (1997). Role of Drosophila α-adaptin in presynaptic vesicle recycling. Cell *88*, 767-776.

Griffiths, G., Pfeiffer, S., Simons, K., and Matlin, K. (1985). Exit of newly synthesized membrane proteins from the trans cisterna of the Golgi complex to the plasma membrane. The Journal of cell biology *101*, 949-964.

Groves, E., Dart, A.E., Covarelli, V., and Caron, E. (2008). Molecular mechanisms of phagocytic uptake in mammalian cells. Cell Mol Life Sci *65*, 1957-1976.

Gu, Z., Reynolds, E.M., Song, J., Lei, H., Feijen, A., Yu, L., He, W., MacLaughlin, D.T., van den Eijnden-van Raaij, J., Donahoe, P.K., and Li, E. (1999). The type I serine/threonine kinase receptor ActRIA (ALK2) is required for gastrulation of the mouse embryo. Development (Cambridge, England) *126*, 2551-2561.

Gurevich, V.V., and Gurevich, E.V. (2004). The molecular acrobatics of arrestin activation. Trends Pharmacol. Sci. *25*, 105-111.

Haffner, C., Paolo, G.D., Rosenthal, J.A., and de Camilli, P. (2000). Direct interaction of the 170 kDa isoform of synaptojanin 1 with clathrin and with the clathrin adaptor AP-2. Curr. Biol. *10*, 471-474.

Hamdan, F.F., Rochdi, M.D., Breton, B., Fessart, D., Michaud, D.E., Charest, P.G., Laporte, S.A., and Bouvier, M. (2007). Unraveling G protein-coupled receptor endocytosis pathways using real-time monitoring of agonist-promoted interaction between β-arrestins and AP-2. J. Biol. Chem. *282*, 29089-29100.

Hammond, G.R.V., Sim, Y., Lagnado, L., and Irvine, R.F. (2009). Reversible binding and rapid diffusion of proteis in complex with inositol lipids serves to coordinate free movement with spatial infomration. J. Cell Biol. *184*, 297-308.

Han, M., Gurevich, V.V., Vishnivetskiy, S.A., Sigler, P.B., and Schubert, C. (2001). Crystal structure of beta-arrestin at 1.9 A: possible mechanism of receptor binding and membrane Translocation. Structure (Camb) *9*, 869-880.

Hansen, C.G., and Nichols, B.J. (2010). Exploring the caves: cavins, caveolins and caveolae. Trends in cell biology *20*, 177-186.

Hanson, S.M., Dawson, E.S., Francis, D.J., Van Eps, N., Klug, C.S., Hubbell, W.L., Meiler, J., and Gurevich, V.V. (2008a). A model for the solution structure of the rod arrestin tetramer. Structure *16*, 924-934.

Hanson, S.M., Vishnivetskiy, S.A., Hubbell, W.L., and Gurevich, V.V. (2008b). Opposing effects of inositol hexakisphosphate on rod arrestin and arrestin2 self-association. Biochemistry *47*, 1070-1075.

Harel, A., Wu, F., Mattson, M.P., Morris, C.M., and Yao, P.J. (2008). Evidence for CALM in directing VAMP2 trafficking. Traffic (Copenhagen, Denmark) *9*, 417-429.

Harris, T.W., Hartwieg, E., Horvitz, H.R., and Jorgensen, E.M. (2000). Mutations in synaptojanin disrupt synaptic vesicle recycling. J. Cell Biol. *150*, 589-600.

Haucke, V., and De Camilli, P. (1999). AP-2 recruitment to synaptotagmin stimulated by tyrosine-based endocytic motifs. Science (New York, N.Y *285*, 1268-1271.

Haucke, V., Wenk, M.R., Chapman, E.R., Farsad, K., and De Camilli, P. (2000). Dual interaction of synaptotagmin with μ2- and α-adaptin facilitates clathrin-coated pit nucleation. EMBO J. *19*, 6011-6019.

Hawryluk, M.J., Keyel, P.A., Mishra, S.K., Watkins, S.C., Heuser, J.E., and Traub, L.M. (2006). Epsin 1 is a polyubiquitin-selective clathrin-associated sorting protein. Traffic (Copenhagen, Denmark) *7*, 262-281.

He, G., Gupta, S., Yi, M., Michaely, P., Hobbs, H.H., and Cohen, J.C. (2002). ARH is a modular adaptor protein that interacts with the LDL receptor, clathrin and AP-2. J. Biol. Chem. *277*, 44044-44049.

Heath, R.J., and Insall, R.H. (2008). F-BAR domains: multifunctional regulators of membrane curvature. J. Cell Sci. *121*, 1951-1954.

Heck, J.N., Mellman, D.L., Ling, K., Sun, Y., Wagoner, M.P., Schill, N.J., and Anderson, R.A. (2007). A conspicuous connection: structure defines function for the phosphatidylinositol-phosphate kinase family. Crit. Rev. Biochem. Mol. Biol. *42*, 15-39.

Hejna, J.A., Saito, H., Merkens, L.S., Tittle, T.V., Jakobs, P.M., Whitney, M.A., Grompe, M., Friedberg, A.S., and Moses, R.E. (1995). Cloning and characterization of a human cDNA (INPPL1) sharing homology with inositol polyphosphate phosphatases. Genomics *29*, 285-287.

Henne, W.M., Boucrot, E., Meinecke, M., Evergren, E., Vallis, Y., Mittal, R., and McMahon, H.T. (2010). FCHo proteins are nucleators of clathrin-mediated endocytosis. Science (New York, N.Y *328* 1281-1284.

Henne, W.M., Kent, H.M., Ford, M.G., Hegde, B.G., Daumke, O., Butler, P.J., Mittal, R., Langen, R., Evans, P.R., and McMahon, H.T. (2007). Structure and analysis of FCHo2 F-BAR domain: a dimerizing and membrane recruitment module that effects membrane curvature. Structure *15*, 839-852.

Heuser, J. (2000). The production of 'cell cortices' for light and electron microscopy. Traffic (Copenhagen, Denmark) *1*, 545-552.

Heuser, J.E., and Keen, J. (1988). Deep-etch visualization of proteins involved in clathrin assembly. J. Cell Biol. *107*, 877-886.

Hinrichsen, L., Harborth, J., Andrees, L., Weber, K., and Ungewickell, E.J. (2003). Effect of clathrin heavy chain- and α-adaptin specific small interfering RNAs on endocytic accessory proteins and receptor trafficking in HeLa cells. J. Biol. Chem. *278*, 45160-45170.

Hinrichsen, L., Meyerholz, A., Groos, S., and Ungewickell, E.J. (2006). Bending a membrane: How clathrin affects budding. Proc. Nat. Acad. Sci. U S A *103*, 8715-8720.

Hoffmann, A., Dannhauser, P.N., Groos, S., Hinrichsen, L., Curth, U., and Ungewickell, E.J. (2010). A comparison of GFP-tagged clathrin light chains with fluorochromated light chains In vivo and In vitro. Traffic (Copenhagen, Denmark) *11*, 1129–1140.

Höning, S., Ricotta, D., Krauss, M., Spate, K., Spolaore, B., Motley, A., Robinson, M., Robinson, C., Haucke, V., and Owen, D.J. (2005). Phosphatidylinositol-(4,5)-bisphosphate regulates sorting signal recognition by the clathrin-associated adaptor complex AP2. Mol. Cell *18*, 519-531.

Hopps, H.E., Bernheim, B.C., Nisalak, A., Tjio, J.H., and Smadel, J.E. (1963). Biologic characteristics of a continuous kidney cell line derived from the African green monkey. J. Immunol. *91*, 416-424.

Howell, B.W., Lanier, L.M., Frank, R., Gertler, F.B., and Cooper, J.A. (1999). The disabled 1 phosphotyrosine-binding domain binds to the internalization signals of transmembrane glycoproteins and to phospholipids. Mol. Cell Biol. *19*, 5179-5188.

Huang, F., Khvorova, A., Marshall, W., and Sorkin, A. (2004). Analysis of clathrin-mediated endocytosis of epidermal growth factor receptor by RNA interference. J. Biol. Chem. *279*, 16657-16661.

Hurley, J.H., Boura, E., Carlson, L.A., and Rozycki, B. (2010). Membrane budding. Cell *143*, 875-887.

Ishihara, H., Shibasaki, Y., Kizuki, N., Katagiri, H., Yazaki, Y., Asano, T., and Oka, Y. (1996). Cloning of cDNAs encoding two isoforms of 68-kDa type I phosphatidylinositol-4-phosphate 5-kinase. J. Biol. Chem. *271*, 23611-23614.

Ishihara, H., Shibasaki, Y., Kizuki, N., Wada, T., Yazaki, Y., Asano, T., and Oka, Y. (1998). Type I phosphatidylinositol-4-phosphate 5-kinases: cloning of the third isoform and deletion/substitution analysis of members of this novel lipid kinase family. J. Biol. Chem. *273*, 8741-8748.

Itoh, T., Koshiba, S., Kigawa, T., Kikuchi, A., Yokoyama, S., and Takenawa, T. (2001). Role of the ENTH domain in phosphatidylinositol-4,5-bisphosphate binding and endocytosis. Science (New York, N.Y *291*, 1047-1051.

Jackson, A.P., Seow, H.F., Holmes, N., Drickamer, K., and Parham, P. (1987). Clathrin light chains contain brain-specific insertion sequences and a region of homology with intermediate filaments. Nature *326*, 154-159.

Jackson, L.P., Kelly, B.T., McCoy, A.J., Gaffry, T., James, L.C., Collins, B.M., Honing, S., Evans, P.R., and Owen, D.J. (2010). A large-scale conformational change couples membrane recruitment to cargo binding in the AP2 clathrin adaptor complex. Cell *141*, 1220-1229.

Jadot, M., Canfield, W.M., Gregory, W., and Kornfeld, S. (1992). Characterization of the signal for rapid internalization of the bovine mannose 6-phosphate/insulin-like growth factor-II receptor. J. Biol. Chem. *267*, 11069-11077.

Janvier, K., Kato, Y., Boehm, M., Rose, J.R., Martina, J.A., Kim, B.Y., Venkatesan, S., and Bonifacino, J.S. (2003). Recognition of dileucine-based sorting signals from HIV-1 Nef and LIMP-II by the AP-1 γ-σ1 and AP-3 δ-σ3 hemicomplexes. J. Cell Biol. *163*, 1281-1290.

Jenkins, G.H., Fisette, P.L., and Anderson, R.A. (1994). Type I phosphatidylinositol 4-phosphate 5-kinase isoforms are specifically stimulated by phosphatidic acid. J. Biol. Chem. *269*, 11547-11554.

Jenkins, G.M., and Frohman, M.A. (2005). Phospholipase D: a lipid centric review. Cell. Mol. Life Sci. *62*, 2305-2316.

Jha, A., Agostinelli, N.R., Mishra, S.K., Keyel, P.A., Hawryluk, M.J., and Traub, L.M. (2004). A novel AP-2 adaptor interaction motif initially identified in the long-splice isoform of synaptojanin 1, SJ170. J. Biol. Chem. *279*, 2281-2290.

Jing, S.Q., Spencer, T., Miller, K., Hopkins, C., and Trowbridge, I.S. (1990). Role of the human transferrin receptor cytoplasmic domain in endocytosis: localization of a specific signal sequence for internalization. The Journal of cell biology *110*, 283-294.

Jost, M., Simpson, F., Kavran, J.M., Lemmon, M.A., and Schmid, S.L. (1998). Phosphatidylinositol-4,5-bisphosphate is required for endocytic coated vesicle formation. Curr. Biol. *8*, 1399-1402.

Jung, N., and Haucke, V. (2007). Clathrin-mediated endocytosis at synapses. Traffic (Copenhagen, Denmark) *8*, 1129-1136.

Kahlfeldt, N., Vahedi-Faridi, A., Koo, S.J., Schafer, J.G., Krainer, G., Keller, S., Saenger, W., Krauss, M., and Haucke, V. (2010). Molecular basis for association of PIPKIg-p90 with clathrin adaptor AP-2. J. Biol. Chem. *285*, 2734-2749.

Kaksonen, M., Toret, C.P., and Drubin, D.G. (2006). Harnessing actin dynamics for clathrin-mediated endocytosis. Nat. Rev. Mol. Cell Biol. *7*, 404-414.

Kalthoff, C., Alves, J., Urbanke, C., Knorr, R., and Ungewickell, E.J. (2002). Unusual structural organization of the endocytic proteins AP180 and epsin 1. J. Biol. Chem. *277*, 8209-8216.

Kamioka, Y., Fukuhara, S., Sawa, H., Nagashima, K., Masuda, M., Matsuda, M., and Mochizuki, N. (2004). A novel dynamin-associating molecule, formin-binding protein 17, induces tubular membrane invaginations and participates in endocytosis. J. Biol. Chem. *279*, 40091-40099.

Kanaseki, T., and Kadota, K. (1969). THE "VESICLE IN A BASKET". A morphological study of the coated vesicle isolated from the nerve endings of the guinea pig brain, with special reference to the mechanism of membrane movements. J. Cell. Biol. *42*, 202-220.

Katoh, M. (2004). Identification and characterization of human *FCHO2* and mouse *Fcho2* genes *in silico*. Int. J. Mo.l Med. *14*, 327-331.

Kawasaki, T., Kobayashi, T., Ueyama, T., Shirai, Y., and Saito, N. (2007). Regulation of clathrin dependent endocytosis by diacylglycerol kinase delta-importance of kinase activity and binding to AP2α. Biochem. J. *409*, 471-479.

Keen, J.H. (1987). Clathrin assembly proteins: affinity purification and a model for coat assembly. J. Cell Biol. *105*, 1989-1998.

Keen, J.H., Willingham, M.C., and Pastan, I.H. (1979). Clathrin-coated vesicles: isolation, dissociation and factor-dependent reassociation of clathrin baskets. Cell *16*, 303-312.

Kelly, B.T., McCoy, A.J., Spate, K., Miller, S.E., Evans, P.R., Honing, S., and Owen, D.J. (2008). A structural explanation for the binding of endocytic dileucine motifs by the AP2 complex. Nature *456*, 976-979.

Kerr, M.C., and Teasdale, R.D. (2009). Defining macropinocytosis. Traffic (Copenhagen, Denmark) *10*, 364-371.

Keyel, P.A., Mishra, S.K., Roth, R., Heuser, J.E., Watkins, S.C., and Traub, L.M. (2006). A single common portal for clathrin-mediated endocytosis of distinct cargo governed by cargo-selective adaptors. Mol. Biol. Cell *17*, 4300-4317.

Keyel, P.A., Thieman, J.R., Roth, R., Erkan, E., Everett, E.T., Watkins, S.C., and Traub, L.M. (2008). The AP-2 adaptor β2 appendage scaffolds alternate cargo endocytosis. Mol. Biol. Cell *19*, 5309-5326.

Keyel, P.A., Watkins, S.C., and Traub, L.M. (2004). Endocytic adaptor molecules reveal an endosomal population of clathrin by total internal reflection fluorescence microscopy. J. Biol. Chem. *279*, 13190-13204.

Kim, Y.M., and Benovic, J.L. (2002). Differential roles of arrestin-2 interaction with clathrin and adaptor protein 2 in G protein-coupled receptor trafficking. J. Biol. Chem. *277*, 30760-30768.

Kirchhausen, T., Bonifacino, J.S., and Riezman, H. (1997). Linking cargo to vesicle formation: receptor tail interactions with coat proteins. Curr. Opin. Cell Biol. *9*, 488-495.

Kirkham, M., Fujita, A., Chadda, R., Nixon, S.J., Kurzchalia, T.V., Sharma, D.K., Pagano, R.E., Hancock, J.F., Mayor, S., and Parton, R.G. (2005). Ultrastructural identification of uncoated caveolin-independent early endocytic vehicles. J. Cell Biol. *168*, 465-476.

Knuehl, C., Chen, C.Y., Manalo, V., Hwang, P.K., Ota, N., and Brodsky, F.M. (2006). Novel binding sites on clathrin and adaptors regulate distinct aspects of coat assembly. Traffic (Copenhagen, Denmark) *7*, 1688-1700.

Koh, T.W., Korolchuk, V.I., Wairkar, Y.P., Jiao, W., Evergren, E., Pan, H., Zhou, Y., Venken, K.J., Shupliakov, O., Robinson, I.M., O'Kane C, J., and Bellen, H.J. (2007). Eps15 and Dap160 control synaptic vesicle membrane retrieval and synapse development. J. Cell Biol. *178*, 309-322.

Kohout, T.A., Lin, F.S., Perry, S.J., Conner, D.A., and Lefkowitz, R.J. (2001). β-arrestin 1 and 2 differentially regulate heptahelical receptor signaling and trafficking. Proc. Natl. Acad. Sci. U S A *98*, 1601-1606.

Kong, X., Wang, X., Misra, S., and Qin, J. (2006). Structural basis for the phosphorylation-regulated focal adhesion targeting of type Iγ phosphatidylinositol phosphate kinase (PIPKIγ) by talin. J. Mol. Biol. *359*, 47-54.

Krauss, M., and Haucke, V. (2007). Phosphoinositide-metabolizing enzymes at the interface between membrane traffic and cell signalling. EMBO Rep. *8*, 241-246.

Krauss, M., Kukhtina, V., Pechstein, A., and Haucke, V. (2006). Stimulation of phosphatidylinositol kinase type I-mediated phosphatidylinositol (4,5)-bisphosphate synthesis by AP-2μ-cargo complexes. Proc. Natl. Acad. Sci. U S A *103*, 11934-11939.

Krupnick, J.G., Goodman, O.B., Jr., Keen, J.H., and Benovic, J.L. (1997a). Arrestin/clathrin interaction. Localization of the clathrin binding domain of nonvisual arrestins to the carboxy terminus. J. Biol. Chem. *272*, 15011-15016.

Krupnick, J.G., Santini, F., Gagnon, A.W., Keen, J.H., and Benovic, J.L. (1997b). Modulation of the arrestin-clathrin interaction in cells. Characterization of beta-arrestin dominant-negative mutants. J. Biol. Chem. *272*, 32507-32512.

Kunz, J., Wilson, M.P., Kisseleva, M., Hurley, J.H., Majerus, P.W., and Anderson, R.A. (2000). The activation loop of phosphatidylinositol phosphate kinases determines signaling specificity. Mol. Cell *5*, 1-11.

Laporte, S.A., Miller, W.E., Kim, K.M., and Caron, M.G. (2002). β-arrestin/AP-2 interaction in G protein-coupled receptor internalization. Identification of a β-arrestin binding site in β2-adaptin. J. Biol. Chem. *277*, 9247-9254.

Laporte, S.A., Oakley, R.H., Holt, J.A., Barak, L.S., and Caron, M.G. (2000). The interaction of β-arrestin with the AP-2 adaptor is required for the clustering of β_2-adrenergic receptor into clathrin-coated pits. J. Biol. Chem. *275*, 23120-23126.

Larkin, J.M., Donzell, W.C., and Anderson, R.G. (1986). Potassium-dependent assembly of coated pits: new coated pits form as planar clathrin lattices. J. Cell Biol. *103*, 2619-2627.

Lauwers, E., Erpapazoglou, Z., Haguenauer-Tsapis, R., and Andre, B. (2010). The ubiquitin code of yeast permease trafficking. Trends in cell biology *20*, 196-204.

Le Borgne, R., Griffiths, G., and Hoflack, B. (1996). Mannose 6-phosphate receptors and ADP-ribosylation factors cooperate for high affinity interaction of the AP-1 Golgi assembly proteins with membranes. J, Biol. Chem. *271*, 2162-2170.

Le Clainche, C., Pauly, B.S., Zhang, C.X., Engqvist-Goldstein, A.E., Cunningham, K., and Drubin, D.G. (2007). A Hip1R-cortactin complex negatively regulates actin assembly associated with endocytosis. EMBO J., in press.

Le Roy, C., and Wrana, J.L. (2005). Clathrin- and non-clathrin-mediated endocytic regulation of cell signalling. Nat. Rev. Mol. Cell Biol. *6*, 112-126.

Lee, D.W., Wu, X., Eisenberg, E., and Greene, L.E. (2006). Recruitment dynamics of GAK and auxilin to clathrin-coated pits during endocytosis. J. Cell Sci. *119*, 3502-3512.

Lee, S.Y., Voronov, S., Letinic, K., Nairn, A.C., Di Paolo, G., and De Camilli, P. (2005). Regulation of the interaction between PIPKIγ and talin by proline-directed protein kinases. J. Cell Biol. *168*, 789-799.

Lefkowitz, R.J., and Shenoy, S.K. (2005). Transduction of receptor signals by β-arrestins. Science (New York, N.Y *308*, 512-517.

Li, C., Ullrich, B., Zhang, J.Z., Anderson, R.G., Brose, N., and Sudhof, T.C. (1995). Ca(2+)-dependent and -independent activities of neural and non-neural synaptotagmins. Nature *375*, 594-599.

Li, J., Mao, X., Dong, L.Q., Liu, F., and Tong, L. (2007). Crystal structures of the BAR-PH and PTB domains of human APPL1. Structure *15*, 525-533.

Li, S.C., Zwahlen, C., Vincent, S.J., McGlade, C.J., Kay, L.E., Pawson, T., and Forman-Kay, J.D. (1998). Structure of a Numb PTB domain-peptide complex suggests a basis for diverse binding specificity. Nat. Struct. Biol. *5*, 1075-1083.

Ling, K., Doughman, R.L., Firestone, A.J., Bunce, M.W., and Anderson, R.A. (2002). Type Iγ phosphatidylinositol phosphate kinase targets and regulates focal adhesions. Nature *420*, 89-93.

Ling, K., Doughman, R.L., Iyer, V.V., Firestone, A.J., Bairstow, S.F., Mosher, D.F., Schaller, M.D., and Anderson, R.A. (2003). Tyrosine phosphorylation of type Igamma phosphatidylinositol phosphate kinase by Src regulates an integrin-talin switch. J. Cell Biol. *163*, 1339-1349.

Littleton, J.T., Stern, M., Schulze, K., Perin, M., and Bellen, H.J. (1993). Mutational analysis of Drosophila synaptotagmin demonstrates its essential role in Ca(2+)-activated neurotransmitter release. Cell *74*, 1125-1134.

Liu, J., Sun, Y., Drubin, D.G., and Oster, G.F. (2009). The mechanochemistry of endocytosis. PLoS biology *7*, e1000204.

Loerke, D., Mettlen, M., Yarar, D., Jaqaman, K., Jaqaman, H., Danuser, G., and Schmid, S.L. (2009). Cargo and dynamin regulate clathrin-coated pit maturation. PLoS biology *7*, e57.

Loijens, J.C., and Anderson, R.A. (1996). Type I phosphatidylinositol-4-phosphate 5-kinases are distinct members of this novel lipid kinase family. J. Biol. Chem. *271*, 32937-32943.

Lundmark, R., and Carlsson, S.R. (2002). The β-appendages of the four adaptor-protein (AP) complexes: structure and binding properties, and identification of sorting nexin 9 as an accessory protein to AP-2. Biochem. J. *362*, 597-607.

Mahaffey, D.T., Moore, M.S., Brodsky, F.M., and Anderson, R.G.W. (1989). Coat proteins isolated from clathrin coated vesicles can assemble into coated pits. J. Cell Biol. *108*, 1615-1624.

Mahaffey, D.T., Peeler, J.S., Brodsky, F.M., and Anderson, R.G.W. (1990). Clathrin-coated pits contain an integral membrane protein that binds the AP-2 subunit with high affinity. J. Biol. Chem. *265*, 16514-16520.

Maldonado-Baez, L., and Wendland, B. (2006). Endocytic adaptors: recruiters, coordinators and regulators. Trends Cell Biol. *16*, 505-513.

Mao, Y.S., Yamaga, M., Zhu, X., Wei, Y.J., Sun, H.Q., Wang, J., Yun, M., Wang, Y., Di Paolo, G., Bennett, M., Mellman, I., Abrams, C.S., De Camilli, P., Lu, C.Y., and Yin, H.L. (2009). Essential and unique roles of PIP5K-γ and -α in Fcγ receptor-mediated phagocytosis. J. Cell Biol. *184*, 281-296.

Marchese, A., Chen, C., Kim, Y.M., and Benovic, J.L. (2003). The ins and outs of G protein-coupled receptor trafficking. Trends Biochem. Sci. *28*, 369-376.

Marchese, A., Paing, M.M., Temple, B.R., and Trejo, J. (2008). G protein-coupled receptor sorting to endosomes and lysosomes. Annu. Rev. Pharmacol. Toxicol. *48*, 601-629.

Maritzen, T., Podufall, J., and Haucke, V. (2010). Stonins--specialized adaptors for synaptic vesicle recycling and beyond? Traffic (Copenhagen, Denmark) *11*, 8-15.

Maupin, P., and Pollard, T.D. (1983). Improved preservation and staining of HeLa cell actin filaments, clathrin-coated membranes, and other cytoplasmic structures by tannic acid-glutaraldehyde-saponin fixation. J. Cell Biol. *96*, 51-62.

Maurer, M.E., and Cooper, J.A. (2006). The adaptor protein Dab2 sorts LDL receptors into coated pits independently of AP-2 and ARH. J. Cell Sci. *119*, 4235-4246.

Mayor, S., and Pagano, R.E. (2007). Pathways of clathrin-independent endocytosis. Nat. Rev. Mol. Cell Biol. *8*, 603-612.

McMahon, H.T., and Mills, I.G. (2004). COP and clathrin-coated vesicle budding: different pathways, common approaches. Curr. Opin. Cell Biol. *16*, 379-391.

McPherson, P.S., and Ritter, B. (2005). Peptide motifs: building the clathrin machinery. Mol. Neurobiol. *32*, 73-87.

Merida, I., Avila-Flores, A., and Merino, E. (2008). Diacylglycerol kinases: at the hub of cell signalling. Biochem. J. *409*, 1-18.

Merrifield, C.J., Perrais, D., and Zenisek, D. (2005). Coupling between clathrin-coated-pit invagination, cortactin recruitment, and membrane scission observed in live cells. Cell *121*, 593-606.

Mettlen, M., Loerke, D., Yarar, D., Danuser, G., and Schmid, S.L. (2010). Cargo- and adaptor-specific mechanisms regulate clathrin-mediated endocytosis. The Journal of cell biology *188*, 919-933.

Mettlen, M., Pucadyil, T., Ramachandran, R., and Schmid, S.L. (2009). Dissecting dynamin's role in clathrin-mediated endocytosis. Biochemical Society transactions *37*, 1022-1026.

Miele, A.E., Watson, P.J., Evans, P.R., Traub, L.M., and Owen, D.J. (2004). Two distinct interaction motifs in amphiphysin bind two independent sites on the clathrin terminal domain β-propeller. Nat. Struct. Mol. Biol. *11*, 242-248.

Milano, S.K., Kim, Y.M., Stefano, F.P., Benovic, J.L., and Brenner, C. (2006). Nonvisual arrestin oligomerization and cellular localization are regulated by inositol hexakisphosphate binding. J. Biol. Chem. *281*, 9812-9823.

Milano, S.K., Pace, H.C., Kim, Y.M., Brenner, C., and Benovic, J.L. (2002). Scaffolding functions of arrestin-2 revealed by crystal structure and mutagenesis. Biochemistry *41*, 3321-3328.

Miller, E.A., and Barlowe, C. (2010). Regulation of coat assembly--sorting things out at the ER. Current opinion in cell biology *22*, 447-453.

Mishra, S.K., Agostinelli, N.R., Brett, T.J., Mizukami, I., Ross, T.S., and Traub, L.M. (2001). Clathrin- and AP-2-binding sites in HIP1 uncover a general assembly role for endocytic accessory proteins. J. Biol. Chem. *276*, 46230-46236.

Mishra, S.K., Hawryluk, M.J., Brett, T.J., Keyel, P.A., Dupin, A.L., Jha, A., Heuser, J.E., Fremont, D.H., and Traub, L.M. (2004). Dual-engagement regulation of protein interactions with the AP-2 adaptor α appendage. J. Biol. Chem. *279*, 46191-46203.

Mishra, S.K., Keyel, P.A., Edeling, M.A., Owen, D.J., and Traub, L.M. (2005). Functional dissection of an AP-2 b2 appendage-binding sequence within the autosomal recessive hypercholesterolemia (ARH) protein. J. Biol. Chem. *280*, 19270-19280.

Mishra, S.K., Keyel, P.A., Hawryluk, M.J., Agostinelli, N.R., Watkins, S.C., and Traub, L.M. (2002a). Disabled-2 exhibits the properties of a cargo-selective endocytic clathrin adaptor. EMBO J. *21*, 4915-4926.

Mishra, S.K., Watkins, S.C., and Traub, L.M. (2002b). The autosomal recessive hypercholesterolemia (ARH) protein interfaces directly with the clathrin-coat machinery. Proc. Natl. Acad. Sci. U S A *99*, 16099-16104.

Mitsunari, T., Nakatsu, F., Shioda, N., Love, P.E., Grinberg, A., Bonifacino, J.S., and Ohno, H. (2005). Clathrin adaptor AP-2 is essential for early embryonal development. Mol. Cell. Biol. *25*, 9318-9323.

Modregger, J., Ritter, B., Witter, B., Paulsson, M., and Plomann, M. (2000). All three PACSIN isoforms bind to endocytic proteins and inhibit endocytosis. J. Cell Sci. *113*, 4511-4521.

Montagnac, G., de Forges, H., Smythe, E., Gueudry, C., Romao, M., Salamero, J., and Chavrier, P. (2011). Decoupling of Activation and Effector Binding Underlies ARF6 Priming of Fast Endocytic Recycling. Curr Biol *21*, 574-579.

Morris, A.J. (2007). Regulation of phospholipase D activity, membrane targeting and intracellular trafficking by phosphoinositides. Biochem. Soc. Symp. *74*, 247-257.

Morris, S.A., Schroder, S., Plessmann, U., Weber, K., and Ungewickell, E. (1993). Clathrin assembly protein AP180: primary structure, domain organization and identification of a clathrin binding site. EMBO J. *12*, 667-675.

Morris, S.M., and Cooper, J.A. (2001). Disabled-2 colocalizes with the LDLR in clathrin-coated pits and interacts with AP-2. Traffic (Copenhagen, Denmark) *2*, 111-123.

Moser, M., Legate, K.R., Zent, R., and Fassler, R. (2009). The tail of integrins, talin, and kindlins. Science (New York, N.Y *324*, 895-899.

Motley, A., Bright, N.A., Seaman, M.N., and Robinson, M.S. (2003). Clathrin-mediated endocytosis in AP-2-depleted cells. J. Cell Biol. *162*, 909-918.

Motley, A.M., Berg, N., Taylor, M.J., Sahlender, D.A., Hirst, J., Owen, D.J., and Robinson, M.S. (2006). Functional analysis of AP-2 α and μ2 subunits. Mol. Biol. Cell *17*, 5298-5308.

Musacchio, A., Smith, C.J., Roseman, A.M., Harrison, S.C., Kirchhausen, T., and Pearse, B.M. (1999). Functional organization of clathrin in coats: combining electron cryomicroscopy and X-ray crystallography. Mol Cell *3*, 761-770.

Nakajima, D., Saito, K., Yamakawa, H., Kikuno, R.F., Nakayama, M., Ohara, R., Okazaki, N., Koga, H., Nagase, T., and Ohara, O. (2005). Preparation of a set of expression-ready clones of mammalian long cDNAs encoding large proteins by the ORF trap cloning method. DNA Res. *12*, 257-267.

Nakano-Kobayashi, A., Yamazaki, M., Unoki, T., Hongu, T., Murata, C., Taguchi, R., Katada, T., Frohman, M.A., Yokozeki, T., and Kanaho, Y. (2007). Role of activation of PIP5Kγ661 by AP-2 complex in synaptic vesicle endocytosis. EMBO J. *26*, 1105-1116.

Nakatsu, F., and Ohno, H. (2003). Adaptor protein complexes as the key regulators of protein sorting in the post-Golgi network. Cell Struct. Funct. *28*, 419-429.

Nakatsu, F., Perera, R.M., Lucast, L., Zoncu, R., Domin, J., Gertler, F.B., Toomre, D., and De Camilli, P. (2010). The inositol 5-phosphatase SHIP2 regulates endocytic clathrin-coated pit dynamics. J. Cell Biol. *190*, 307-315.

Narkis, G., Ofir, R., Landau, D., Manor, E., Volokita, M., Hershkowitz, R., Elbedour, K., and Birk, O.S. (2007). Lethal contractural syndrome type 3 (LCCS3) is caused by a mutation in PIP5K1C, which encodes PIPKIγ of the phophatidylinsitol pathway. Am. J. Hum. Genet. *81*, 530-539.

Naslavsky, N., Rahajeng, J., Chenavas, S., Sorgen, P.L., and Caplan, S. (2007). EHD1 and Eps15 interact with phosphatidylinositols via their Eps15 homology domains. The Journal of biological chemistry *282*, 16612-16622.

Nathke, I.S., Heuser, J., Lupas, A., Stock, J., Turck, C.W., and Brodsky, F.M. (1992). Folding and trimerization of clathrin subunits at the triskelion hub. Cell *68*, 899-910.

Nelson, C.D., Kovacs, J.J., Nobles, K.N., Whalen, E.J., and Lefkowitz, R.J. (2008). β-Arrestin scaffolding of phosphatidylinositol 4-phosphate 5-kinase Iα promotes agonist-stimulated sequestration of the β2-adrenergic receptor. J. Biol. Chem. *283*, 21093-21101.

Nelson, C.D., Perry, S.J., Regier, D.S., Prescott, S.M., Topham, M.K., and Lefkowitz, R.J. (2007). Targeting of diacylglycerol degradation to M1 muscarinic receptors by β-arrestins. Science (New York, N.Y *315*, 663-666.

Nishimura, T., and Kaibuchi, K. (2007). Numb controls integrin endocytosis for directional cell migration with aPKC and PAR-3. Dev. Cell *13*, 15-28.

Novick, P., Field, C., and Schekman, R. (1980). Identification of 23 complementation groups required for post-translational events in the yeast secretory pathway. Cell *21*, 205-215.

Oh, P., Borgstrom, P., Witkiewicz, H., Li, Y., Borgstrom, B.J., Chrastina, A., Iwata, K., Zinn, K.R., Baldwin, R., Testa, J.E., and Schnitzer, J.E. (2007). Live dynamic imaging of caveolae pumping targeted antibody rapidly and specifically across endothelium in the lung. Nature biotechnology *25*, 327-337.

Ohno, H., Aguilar, R.C., Yeh, D., Taura, D., Saito, T., and Bonifacino, J.S. (1998). The medium subunits of adaptor complexes recognize distinct but overlapping sets of tyrosine-based sorting signals. The Journal of biological chemistry *273*, 25915-25921.

Ohno, H., Stewart, J., Fournier, M.-C., Bosshart, H., Rhee, I., Miyatake, S., Saito, T., Galluser, A., Kirchhausen, T., and Bonifacino, J.S. (1995). Interaction of tyrosine-based sorting signals with clathrin-associated proteins. Science (New York, N.Y *269*, 1872-1875.

Olusanya, O., Andrews, P.D., Swedlow, J.R., and Smythe, E. (2001). Phosphorylation of threonine 156 of the μ2 subunit of the AP2 complex is essential for endocytosis in vitro and in vivo. Curr. Biol. *11*, 896-900.

Onuchic, J.N., and Wolynes, P.G. (2004). Theory of protein folding. Current opinion in structural biology *14*, 70-75.

Orci, L., Carpentier, J.L., Perrelet, A., Anderson, R.G., Goldstein, J.L., and Brown, M.S. (1978). Occurrence of low density lipoprotein receptors within large pits on the surface of human fibroblasts as demonstrated by freeze-etching. Exp. Cell Res. *113*, 1-13.

Orci, L., Glick, B.S., and Rothman, J.E. (1986). A new type of coated vesicular carrier that appears not to contain clathrin: its possible role in protein transport within the Golgi stack. Cell *46*, 171-184.

Orci, L., Ravazzola, M., Amherdt, M., Louvard, D., and Perrelet, A. (1985). Clathrin-immunoreactive sites in the Golgi apparatus are concentrated at the trans pole in polypeptide hormone-secreting cells. Proceedings of the National Academy of Sciences of the United States of America *82*, 5385-5389.

Owen, D.J., and Evans, P.R. (1998). A structural explanation for the recognition of tyrosine-based endocytotic signals. Science (New York, N.Y *282*, 1327-1332.

Owen, D.J., Vallis, Y., Noble, M.E., Hunter, J.B., Dafforn, T.R., Evans, P.R., and McMahon, H.T. (1999). A structural explanation for the binding of multiple ligands by the α-adaptin appendage domain. Cell *97*, 805-815.

Owen, D.J., Vallis, Y., Pearse, B.M., McMahon, H.T., and Evans, P.R. (2000). The structure and function of the β2-adaptin appendage domain. EMBO J. *19*, 4216-4227.

Padron, D., Wang, Y.J., Yamamoto, M., Yin, H., and Roth, M.G. (2003). Phosphatidylinositol phosphate 5-kinase Iβ recruits AP-2 to the plasma membrane and regulates rates of constitutive endocytosis. J. Cell Biol. *162*, 693-701.

Palade, G. (1975). Intracellular aspects of the process of protein synthesis. Science (New York, N.Y *189*, 347-358.

Paleotti, O., Macia, E., Luton, F., Klein, S., Partisani, M., Chardin, P., Kirchhausen, T., and Franco, M. (2005). The small G-protein ARF6GTP recruits the AP-2 adaptor complex to membranes. J. Biol. Chem.

Pang, Z.P., and Sudhof, T.C. (2010). Cell biology of Ca2+-triggered exocytosis. Current opinion in cell biology *22*, 496-505.

Pearse, B.M. (1975). Coated vesicles from pig brain: purification and biochemical characterization. Journal of molecular biology *97*, 93-98.

Pearse, B.M. (1976). Clathrin: a unique protein associated with intracellular transfer of membrane by coated vesicles. Proceedings of the National Academy of Sciences of the United States of America *73*, 1255-1259.

Pearse, B.M., and Crowther, R.A. (1987). Structure and assembly of coated vesicles. Annual review of biophysics and biophysical chemistry *16*, 49-68.

Pechstein, A., Bacetic, J., Vahedi-Faridi, A., Gromova, K., Sundborger, A., Tomlin, N., Krainer, G., Vorontsova, O., Schafer, J.G., Owe, S.G., Cousin, M.A., Saenger, W., Shupliakov, O., and Haucke, V. (2010a). Regulation of synaptic vesicle recycling by complex formation between intersectin 1 and the clathrin adaptor complex AP2. Proc. Natl. Acad. Sci. U S A *107*, 4206-4211.

Pechstein, A., Shupliakov, O., and Haucke, V. (2010b). Intersectin 1: a versatile actor in the synaptic vesicle cycle. Biochemical Society transactions *38*, 181-186.

Peeler, J.S., Donzell, W.C., and Anderson, R.G.W. (1993). The appendage domain of the AP-2 subunit is not required for assembly or invagination of clathrin-coated pits. J. Cell Biol. *120*, 47-54.

Perera, R.M., Zoncu, R., Lucast, L., De Camilli, P., and Toomre, D. (2006). Two synaptojanin 1 isoforms are recruited to clathrin-coated pits at different stages. Proc. Natl. Acad. Sci. U S A *103*, 19332-19337.

Poupart, M.E., Fessart, D., Cotton, M., Laporte, S.A., and Claing, A. (2007). ARF6 regulates angiotensin II type 1 receptor endocytosis by controlling the recruitment of AP-2 and clathrin. Cell. Signal.

Praefcke, G.J., Ford, M.G., Schmid, E.M., Olesen, L.E., Gallop, J.L., Peak-Chew, S.Y., Vallis, Y., Babu, M.M., Mills, I.G., and McMahon, H.T. (2004). Evolving nature of the AP2 α-appendage hub during clathrin-coated vesicle endocytosis. EMBO J. *23*, 4371-4383.

Pryor, P.R., Jackson, L., Gray, S.R., Edeling, M.A., Thompson, A., Sanderson, C.M., Evans, P.R., Owen, D.J., and Luzio, J.P. (2008). Molecular basis for the sorting of the SNARE VAMP7 into endocytic clathrin-coated vesicles by the ArfGAP Hrb. Cell *134*, 817-827.

Qualmann, B., and Kelly, R.B. (2000). Syndapin isoforms participate in receptor-mediated endocytosis and actin organization. J. Cell Biol. *148*, 1047-1062.

Ramjaun, A.R., and McPherson, P.S. (1996). Tissue-specific alternative splicing generates two synaptojanin isoforms with differential membrane binding properties. J. Biol. Chem. *271*, 24856-24861.

Rao, Y., Ma, Q., Vahedi-Faridi, A., Sundborger, A., Pechstein, A., Puchkov, D., Luo, L., Shupliakov, O., Saenger, W., and Haucke, V. (2010). Molecular basis for SH3 domain regulation of F-BAR-mediated membrane deformation. Proceedings of the National Academy of Sciences of the United States of America.

Rapoport, I., Miyazaki, M., Boll, W., Duckworth, B., Cantley, L.C., Shoelson, S., and Kirchhausen, T. (1997). Regulatory interactions in the recognition of endocytic sorting signals by AP-2 complexes. EMBO J. *16*, 2240-2250.

Rappoport, J., Simon, S., and Benmerah, A. (2004). Understanding living clathrin-coated pits. Traffic (Copenhagen, Denmark) *5*, 327-337.

Rappoport, J.Z., Benmerah, A., and Simon, S.M. (2005). Analysis of the AP-2 adaptor complex and cargo during clathrin-mediated endocytosis. Traffic (Copenhagen, Denmark) *6*, 539-547.

Rappoport, J.Z., Taha, B.W., and Simon, S.M. (2003). Movement of plasma-membrane-associated clathrin spots along the microtubule cytoskeleton. Traffic (Copenhagen, Denmark) *4*, 460-467.

Rasheed, S., Nelson-Rees, W.A., Toth, E.M., Arnstein, P., and Gardner, M.B. (1974). Characterization of a newly derived human sarcoma cell line (HT-1080). Cancer *33*, 1027-1033.

Reider, A., Barker, S.L., Mishra, S.K., Im, Y.J., Maldonado-Baez, L., Hurley, J.H., Traub, L.M., and Wendland, B. (2009). Syp1 is a conserved endocytic adaptor that contains domains involved in cargo selection and membrane tubulation. The EMBO journal *28*, 3103-3116.

Reider, A., and Wendland, B. (2011). Endocytic adaptors - social networking at the plasma membrane. Journal of cell science *124*, 1613-1622.

Ricotta, D., Conner, S.D., Schmid, S.L., von Figura, K., and Honing, S. (2002). Phosphorylation of the AP2 μ subunit by AAK1 mediates high affinity binding to membrane protein sorting signals. J. Cell Biol. *156*, 791-795.

Ringstad, N., Gad, H., Low, P., Di Paolo, G., Brodin, L., Shupliakov, O., and De Camilli, P. (1999). Endophilin/SH3p4 is required for the transition from early to late stages in clathrin-mediated synaptic vesicle endocytosis. Neuron *24*, 143-154.

Ritter, B., Denisov, A.Y., Philie, J., Deprez, C., Tung, E.C., Gehring, K., and McPherson, P.S. (2004). Two WXXF-based motifs in NECAPs define the specificity of accessory protein binding to AP-1 and AP-2. EMBO J. *23*, 3701-3710.

Ritter, S.L., and Hall, R.A. (2009). Fine-tuning of GPCR activity by receptor-interacting proteins. Nature reviews *10*, 819-830.

Rizzoli, S.O., and Jahn, R. (2007). Kiss-and-run, collapse and 'readily retrievable' vesicles. Traffic (Copenhagen, Denmark) *8*, 1137-1144.

Roberts-Galbraith, R.H., and Gould, K.L. (2010). Setting the F-BAR: functions and regulation of the F-BAR protein family. Cell cycle (Georgetown, Tex *9*, 4091-4097.

Roberts-Galbraith, R.H., Ohi, M.D., Ballif, B.A., Chen, J.S., McLeod, I., McDonald, W.H., Gygi, S.P., Yates, J.R., 3rd, and Gould, K.L. (2010). Dephosphorylation of F-BAR protein Cdc15 modulates its conformation and stimulates its scaffolding activity at the cell division site. Mol. Cell *39*, 86-99.

Robinson, M.S. (2004). Adaptable adaptors for coated vesicles. Trends Cell Biol. *14*, 167-174.

Rohde, G., Wenzel, D., and Haucke, V. (2002). A phosphatidylinositol (4,5)-bisphosphate binding site within μ2-adaptin regulates clathrin-mediated endocytosis. J. Cell Biol. *158*, 209-214.

Roth, T.F., and Porter, K.R. (1964). Yolk protein uptake in the oocyte of the mosquito *Aedes aegypti*. L. J. Cell Biol. *20*, 313-332.

Royle, S.J., and Lagnado, L. (2010). Clathrin-mediated endocytosis at the synaptic terminal: bridging the gap between physiology and molecules. Traffic (Copenhagen, Denmark) *11*, 1489-1497.

Ruan, J., Li, H., Chen, Z., Coghlan, A., Coin, L.J., Guo, Y., Heriche, J.K., Hu, Y., Kristiansen, K., Li, R., Liu, T., Moses, A., Qin, J., Vang, S., Vilella, A.J., Ureta-Vidal, A., Bolund, L., Wang, J., and Durbin, R. (2008). TreeFam: 2008 Update. Nucleic Acids Res. *36*, D735-740.

Saffarian, S., Cocucci, E., and Kirchhausen, T. (2009). Distinct dynamics of endocytic clathrin-coated pits and coated plaques. PLoS biology *7*, e1000191.

Sakane, F., Imai, S., Yamada, K., Murakami, T., Tsushima, S., and Kanoh, H. (2002). Alternative splicing of the human diacylglycerol kinase delta gene generates two isoforms differing in their expression patterns and in regulatory functions. J. Biol. Chem. *277*, 43519-43526.

Sakaushi, S., Inoue, K., Zushi, H., Senda-Murata, K., Fukada, T., Oka, S., and Sugimoto, K. (2007). Dynamic behavior of FCHO1 revealed by live-cell imaging microscopy: its possible involvement in clathrin-coated vesicle formation. Biosci. Biotechnol. Biochem. *71*, 1764-1768.

Salamero, J., Le Borgne, R., Saudrais, C., Goud, B., and Hoflack, B. (1996). Expression of major histocompatibility complex class II molecules in HeLa cells promotes the recruitment of AP-1 Golgi-specific assembly proteins on Golgi membranes. J. Biol. Chem. *271*, 30318-30321.

Santini, F., Gaidarov, I., and Keen, J.H. (2002). G protein-coupled receptor/arrestin3 modulation of the endocytic machinery. J. Cell Biol. *156*, 665-676.

Santini, F., Marks, M.S., and Keen, J.H. (1998). Endocytic clathrin-coated pit formation is independent of receptor internalization signal levels. Mol. Biol. Cell *9*, 1177-1194.

Savitzky, A., and Golay, M.J.E. (1964). Smoothing and differentiation of data by a simplified least squares procedures. Anal. Chem. *36*, 1627-1639.

Schekman, R., and Novick, P. (2004). 23 genes, 23 years later. Cell *116*, S13-S15.

Schenck, A., Goto-Silva, L., Collinet, C., Rhinn, M., Giner, A., Habermann, B., Brand, M., and Zerial, M. (2008). The endosomal protein Appl1 mediates Akt substrate specificity and cell survival in vertebrate development. Cell *133*, 486-497.

Schill, N.J., and Anderson, R.A. (2009). Two novel phosphatidylinositol-4-phosphate 5-kinase type Igamma splice variants expressed in human cells display distinctive cellular targeting. The Biochemical journal *422*, 473-482.

Schmid, E.M., Ford, M.G., Burtey, A., Praefcke, G.J., Peak Chew, S.Y., Mills, I.G., Benmerah, A., and McMahon, H.T. (2006). Role of the AP2 β-appendage hub in recruiting partners for clathrin coated vesicle assembly. PLoS Biol. *4*, e262.

Schmid, E.M., and McMahon, H.T. (2007). Integrating molecular and network biology to decode endocytosis. Nature *448*, 883-888.

Schubert, W., Frank, P.G., Razani, B., Park, D.S., Chow, C.W., and Lisanti, M.P. (2001). Caveolae-deficient endothelial cells show defects in the uptake and transport of albumin in vivo. The Journal of biological chemistry *276*, 48619-48622.

Scott, M.G., Benmerah, A., Muntaner, O., and Marullo, S. (2002). Recruitment of activated G protein-coupled receptors to pre-existing clathrin-coated pits in living cells. J. Biol. Chem. *277*, 3552-3559.

Semerdjieva, S., Shortt, B., Maxwell, E., Singh, S., Fonarev, P., Hansen, J., Schiavo, G., Grant, B.D., and Smythe, E. (2008). Coordinated regulation of AP2 uncoating from clathrin-coated vesicles by rab5 and hRME-6. J. Cell Biol. *183*, 499-511.

Shaner, N.C., Campbell, R.E., Steinbach, P.A., Giepmans, B.N., Palmer, A.E., and Tsien, R.Y. (2004). Improved monomeric red, orange and yellow fluorescent proteins derived from Discosoma sp. red fluorescent protein. Nat. Biotechnol. *22*, 1567-1572.

Shih, S.C., Katzmann, D.J., Schnell, J.D., Sutanto, M., Emr, S.D., and Hicke, L. (2002). Epsins and Vps27p/Hrs contain ubiquitin-binding domains that function in receptor endocytosis. Nat. Cell Biol. *4*, 389-393.

Shih, W., Galluser, A., and Kirchhausen, T. (1995). A clathrin binding site in the hinge of the β2 chain of the mammalian AP complexes. J. Biol. Chem. *270*, 31083-31090.

Shim, J., and Lee, J. (2000). Molecular genetic analysis of *apm-2* and *aps-2*, genes encoding the medium and small chains of the AP-2 clathrin-associated protein complex in the nematode *Caenorhabditis elegans*. Mol. Cells *10*, 309-316.

Simpson, F., Hussain, N.K., Qualmann, B., Kelly, R.B., Kay, B.K., McPherson, P.S., and Schmid, S.L. (1999). SH3-domain-containing proteins function at distinct steps in clathrin-coated vesicle formation. Nat. Cell Biol. *1*, 119-124.

Sims, J.J., and Cohen, R.E. (2009). Linkage-specific avidity defines the lysine 63-linked polyubiquitin-binding preference of rap80. Mol Cell. *33*, 775-783.

Sinha, B., Koster, D., Ruez, R., Gonnord, P., Bastiani, M., Abankwa, D., Stan, R.V., Butler-Browne, G., Vedie, B., Johannes, L., Morone, N., Parton, R.G., Raposo, G., Sens, P., Lamaze, C., and Nassoy, P. (2011). Cells respond to mechanical stress by rapid disassembly of caveolae. Cell *144*, 402-413.

Slepnev, V.I., Ochoa, G.C., Butler, M.H., and De Camilli, P. (2000). Tandem arrangement of the clathrin and AP-2 binding domains in amphiphysin 1, and disruption of clathrin coat function mediated by amphiphysin fragments comprising these sites. J. Biol. Chem. *275*, 17583-17589.

Smith, S.M., Renden, R., and von Gersdorff, H. (2008). Synaptic vesicle endocytosis: fast and slow modes of membrane retrieval. Trends in neurosciences *31*, 559-568.

Sorkin, A. (2004). Cargo recognition during clathrin-mediated endocytosis: a team effort. Curr. Opin. Cell Biol. *16*, 392-399.

Sorkina, T., Huang, F., Beguinot, L., and Sorkin, A. (2002). Effect of tyrosine kinase inhibitors on clathrin-coated pit recruitment and internalization of epidermal growth factor receptor. J. Biol. Chem. *277*, 27433-27441.

Sorkina, T., Miranda, M., Dionne, K.R., Hoover, B.R., Zahniser, N.R., and Sorkin, A. (2006). RNA interference screen reveals an essential role of Nedd4-2 in dopamine transporter ubiquitination and endocytosis. J. Neurosci. *26*, 8195-8205.

Soule, H.D., Vazguez, J., Long, A., Albert, S., and Brennan, M. (1973). A human cell line from a pleural effusion derived from a breast carcinoma. Journal of the National Cancer Institute *51*, 1409-1416.

Soulet, F., Yarar, D., Leonard, M., and Schmid, S.L. (2005). SNX9 regulates dynamin assembly and is required for efficient clathrin-mediated endocytosis. Mol. Biol. Cell *16*, 2058-2067.

Stamnes, M.A., and Rothman, J.E. (1993). The binding of AP-1 clathrin adaptor particles to Golgi membranes requires ADP-ribosylation factor, a small GTP-binding protein. Cell *73*, 999-1005.

Stefan, C.J., Audhya, A., and Emr, S.D. (2002). The yeast synaptojanin-like proteins control the cellular distribution of phosphatidylinositol (4,5)-bisphosphate. Mol. Biol. Cell *13*, 542-557.

Stimpson, H.E., Toret, C.P., Cheng, A.T., Pauly, B.S., and Drubin, D.G. (2009). Early-arriving Syp1p and Ede1p function in endocytic site placement and formation in budding yeast. Molecular biology of the cell *20*, 4640-4651.

Stolt, P.C., and Bock, H.H. (2006). Modulation of lipoprotein receptor functions by intracellular adaptor proteins. Cell. Signal. *18*, 1560-1571.

Stolt, P.C., Chen, Y., Liu, P., Bock, H.H., Blacklow, S.C., and Herz, J. (2005). Phosphoinositide binding by the disabled-1 PTB domain is necessary for membrane localization and reelin signal transduction. J. Biol. Chem. *280*, 9671-9677.

Stolt, P.C., Jeon, H., Song, H.K., Herz, J., Eck, M.J., and Blacklow, S.C. (2003). Origins of peptide selectivity and phosphoinositide binding revealed by structures of Disabled-1 PTB domain complexes. Structure (Camb) *11*, 569-579.

Storez, H., Scott, M.G., Issafras, H., Burtey, A., Benmerah, A., Muntaner, O., Piolot, T., Tramier, M., Coppey-Moisan, M., Bouvier, M., Labbe-Jullie, C., and Marullo, S. (2005). Homo- and hetero-oligomerization of β-arrestins in living cells. J. Biol. Chem. *280*, 40210-40215.

Suetsugu, S., Toyooka, K., and Senju, Y. (2010). Subcellular membrane curvature mediated by the BAR domain superfamily proteins. Semin. Cell. Dev. Biol. *21*, 340-349.

Suganuma, M., Fujiki, H., Furuya-Suguri, H., Yoshizawa, S., Yasumoto, S., Kato, Y., Fusetani, N., and Sugimura, T. (1990). Calyculin A, an inhibitor of protein phosphatases, a potent tumor promoter on CD-1 mouse skin. Cancer research *50*, 3521-3525.

Sun, Y., Carroll, S., Kaksonen, M., Toshima, J.Y., and Drubin, D.G. (2007a). PtdIns(4,5)P_2 turnover is required for multiple stages during clathrin- and actin-dependent endocytic internalization. J. Cell Biol. *177*, 355-367.

Sun, Y., Ling, K., Wagoner, M.P., and Anderson, R.A. (2007b). Type Iγ phosphatidylinositol phosphate kinase is required for EGF-stimulated directional cell migration. J. Cell Biol. *178*, 297-308.

Takeda, S., Kadowaki, S., Haga, T., Takaesu, H., and Mitaku, S. (2002). Identification of G protein-coupled receptor genes from the human genome sequence. FEBS letters *520*, 97-101.

Taylor, M.J., Perrais, D., and Merrifield, C.J. (2011). A high precision survey of the molecular dynamics of Mammalian clathrin-mediated endocytosis. PLoS biology *9*, e1000604.

Tebar, F., Confalonieri, S., Carter, R.E., Di Fiore, P.P., and Sorkin, A. (1997). Eps15 is constitutively oligomerized due to homophilic interaction of its coiled-coil region. The Journal of biological chemistry *272*, 15413-15418.

Tebar, F., Sorkina, T., Sorkin, A., Ericsson, M., and Kirchhausen, T. (1996). eps15 is a component of clathrin-coated pits and vesicles and is located at the rim of clathrin-coated pits. J. Biol. Chem. *271*, 28727-28730.

Teckchandani, A., Toida, N., Goodchild, J., Henderson, C., Watts, J., Wollschid, B., and Cooper, J.A. (2009). Quantitative proteomics identifies a Dab2/integrin module regulating cell migration.

ter Haar, E., Harrison, S.C., and Kirchhausen, T. (2000). Peptide-in-groove interactions link target proteins to the β propeller of clathrin. Proc. Natl. Acad. Sci. U S A *97*, 1096-1100.

ter Haar, E., Musacchio, A., Harrison, S.C., and Kirchhausen, T. (1998). Atomic structure of clathrin: a β propeller terminal domain joins an α zigzag linker. Cell *95*, 563-573.

Thieman, J.R., Mishra, S.K., Ling, K., Doray, B., Anderson, R.A., and Traub, L.M. (2009). Clathrin regulates the association of PIPKIγ661 with the AP-2 adaptor β2 appendage. J. Biol. Chem. *284*, 13924–13939.

Traub, L.M. (2005). Common principles in clathrin-mediated sorting at the Golgi and the plasma membrane. Biochim. Biophys. Acta *1744*, 415-437.

Traub, L.M. (2009). Tickets to ride: selecting cargo for clathrin-regulated internalization. Nat. Rev. Mol. Cell Biol. *10*, 583-596.

Traub, L.M. (2011). Regarding the amazing choreography of clathrin coats. PLoS biology *9*, e1001037.

Traub, L.M., Downs, M.A., Westrich, J.L., and Fremont, D.H. (1999). Crystal structure of the α appendage of AP-2 reveals a recruitment platform for clathrin-coat assembly. Proc. Natl. Acad. Sci. USA *96*, 8907-8912.

Traub, L.M., Ostrom, J.A., and Kornfeld, S. (1993). Biochemical dissection of AP-1 recruitment onto Golgi membranes. J. Cell Biol. *123*, 561-573.

Trevaskis, J., Walder, K., Foletta, V., Kerr-Bayles, L., McMillan, J., Cooper, A., Lee, S., Bolton, K., Prior, M., Fahey, R., Whitecross, K., Morton, G.J., Schwartz, M.W., and Collier, G.R. (2005). Src

homology 3-domain growth factor receptor-bound 2-like (endophilin) interacting protein 1, a novel neuronal protein that regulates energy balance. Endocrinology *146*, 3757-3764.

Uezu, A., Horiuchi, A., Kanda, K., Kikuchi, N., Umeda, K., Tsujita, K., Suetsugu, S., Araki, N., Yamamoto, H., Takenawa, T., and Nakanishi, H. (2007). SGIP1α is an endocytic protein that directly interacts with phospholipids and Eps15. J. Biol. Chem. *282*, 26481-26489.

Unanue, E.R., Ungewickell, E., and Branton, D. (1981). The binding of clathrin triskelions to membranes from coated vesicles. Cell *26*, 439-446.

Ungewickell, A., Ward, M.E., Ungewickell, E., and Majerus, P.W. (2004). The inositol polyphosphate 5-phosphatase Ocrl associates with endosomes that are partially coated with clathrin. Proc. Natl. Acad. Sci. U S A *101*, 13501-13506.

Ungewickell, E., and Branton, D. (1981). Assembly units of clathrin coats. Nature *289*, 420-422.

Ungewickell, E.J., and Hinrichsen, L. (2007). Endocytosis: clathrin-mediated membrane budding. Curr. Opin. Cell. Biol. *19*, 417-425.

Vallis, Y., Wigge, P., Marks, B., Evans, P.R., and McMahon, H.T. (1999). Importance of the pleckstrin homology domain of dynamin in clathrin- mediated endocytosis. Curr. Biol. *9*, 257-260.

van Rheenen, J., Mulugeta Achame, E., Janssen, H., Calafat, J., and Jalink, K. (2005). PIP_2 signaling in lipid domains: a critical re-evaluation. EMBO J. *24*, 1664-1673.

Varnai, P., Thyagarajan, B., Rohacs, T., and Balla, T. (2006). Rapidly inducible changes in phosphatidylinositol 4,5-bisphosphate levels influence multiple regulatory functions of the lipid in intact living cells. J. Cell Biol. *175*, 377-382.

Vicinanza, M., D'Angelo, G., Di Campli, A., and De Matteis, M.A. (2008). Function and dysfunction of the PI system in membrane trafficking. EMBO J. *27*, 2457-2470.

Virshup, D.M., and Bennett, V. (1988). Clathrin-coated vesicle assembly polypeptides: physical proterties and reconstitution studies with brain membranes. J. Cell Biol. *106*, 39-50.

Volpicelli-Daley, L.A., Lucast, L., Gong, L.W., Liu, L., Sasaki, J., Sasaki, T., Abrams, C.S., Kanaho, Y., and De Camilli, P. (2010). Phosphatidylinositol-4-phosphate 5-kinases and phosphatidylinositol 4,5-bisphosphate synthesis in the brain. The Journal of biological chemistry *285*, 28708-28714.

von Poser, C., Zhang, J.Z., Mineo, C., Ding, W., Ying, Y., Sudhof, T.C., and Anderson, R.G. (2000). Synaptotagmin regulation of coated pit assembly. J. Biol. Chem. *275*, 30916-30924.

Walther, K., Diril, M.K., Jung, N., and Haucke, V. (2004). Functional dissection of the interactions of stonin 2 with the adaptor complex AP-2 and synaptotagmin. Proc. Natl. Acad. Sci. U S A *101*, 964-969.

Wang, L.H., Sudhof, T.C., and Anderson, R.G. (1995). The appendage domain of α-adaptin is a high affinity binding site for dynamin. J. Biol. Chem. *270*, 10079-10083.

Wang, Y., Lian, L., Golden, J.A., Morrisey, E.E., and Abrams, C.S. (2007). PIP5KIγ is required for cardiovascular and neuronal development. Proc. Natl. Acad. Sci. U S A *104*, 11748-11753.

Warren, R.A., Green, F.A., and Enns, C.A. (1997). Saturation of the endocytic pathway for the transferrin receptor does not affect the endocytosis of the epidermal growth factor receptor. J. Biol. Chem. *272*, 2116-2121.

Warren, R.A., Green, F.A., Stenberg, P.E., and Enns, C.A. (1998). Distinct saturable pathways for the endocytosis of different tyrosine motifs. J. Biol. Chem. *273*, 17056-17063.

Waters, M.G., Serafini, T., and Rothman, J.E. (1991). 'Coatomer': a cytosolic protein complex containing subunits of non-clathrin-coated Golgi transport vesicles. Nature *349*, 248-251.

Wendland, B. (2002). Epsins: adaptors in endocytosis? Nat. Rev. Mol. Cell Biol. *3*, 971-977.

Wenk, M.R., Pellegrini, L., Klenchin, V.A., Di Paolo, G., Chang, S., Daniell, L., Arioka, M., Martin, T.F., and De Camilli, P. (2001). PIP kinase Iγ is the major $PI(4,5)P_2$ synthesizing enzyme at the synapse. Neuron *32*, 79-88.

Wu, X., Zhao, X., Puertollano, R., Bonifacino, J.S., Eisenberg, E., and Greene, L.E. (2003). Adaptor and clathrin exchange at the plasma membrane and *trans*-Golgi network. Mol. Biol. Cell *14*, 516-528.

Wymann, M.P., and Schneiter, R. (2008). Lipid signalling in disease. Nature reviews *9*, 162-176.

Yaradanakul, A., and Hilgemann, D.W. (2007). Unrestricted diffusion of exogenous and endogenous PIP_2 in baby hamster kidney and Chinese hamster ovary cell plasmalemma. J. Membr. Biol. *220*, 53-67.

Ybe, J.A., Brodsky, F.M., Hofmann, K., Lin, K., Liu, S.H., Chen, L., Earnest, T.N., Fletterick, R.J., and Hwang, P.K. (1999). Clathrin self-assembly is mediated by a tandemly repeated superhelix. Nature *399*, 371-375.

Yim, Y.I., Scarselletta, S., Zang, F., Wu, X., Lee, D.W., Kang, Y.S., Eisenberg, E., and Greene, L.E. (2005). Exchange of clathrin, AP2 and epsin on clathrin-coated pits in permeabilized tissue culture cells. J. Cell. Sci. *118*, 2405-2413.

Yu, J.W., Mendrola, J.M., Audhya, A., Singh, S., Keleti, D., DeWald, D.B., Murray, D., Emr, S.D., and Lemmon, M.A. (2004). Genome-wide wnalysis of membrane targeting by S. cerevisiae pleckstrin pomology domains. Mol. Cell *13*, 677-688.

Zhang, J.Z., Davletov, B.A., Sudhof, T.C., and Anderson, R.G.W. (1994). Synaptotagmin I is a high affinity receptor for clathrin AP-2: implications for membrane recycling. Cell *78*, 751-760.

Zhou, M.M., Ravichandran, K.S., Olejniczak, E.F., Petros, A.M., Meadows, R.P., Sattler, M., Harlan, J.E., Wade, W.S., Burakoff, S.J., and Fesik, S.W. (1995). Structure and ligand recognition of the phosphotyrosine binding domain of Shc. Nature *378*, 584-592.

Zhu, G., Chen, J., Liu, J., Brunzelle, J.S., Huang, B., Wakeham, N., Terzyan, S., Li, X., Rao, Z., Li, G., and Zhang, X.C. (2007). Structure of the APPL1 BAR-PH domain and characterization of its interaction with Rab5. EMBO J. *26*, 3484-3493.

Zhuo, Y., Ilangovan, U., Schirf, V., Demeler, B., Sousa, R., Hinck, A.P., and Lafer, E.M. (2011). Dynamic interactions between clathrin and locally structured elements in a disordered protein mediate clathrin lattice assembly. Journal of molecular biology *404*, 274-290.

Zimmerberg, J., and Kozlov, M.M. (2005). How proteins produce cellular membrane curvature. Nat. Rev. Mol. Cell Biol. *7*, 9-19.

Zoncu, R., Perera, R.M., Balkin, D.M., Pirruccello, M., Toomre, D., and De Camilli, P. (2009). A phosphoinositide switch controls the maturation and signaling properties of APPL endosomes. Cell *136*, 1110-1121.

Zoncu, R., Perera, R.M., Sebastian, R., Nakatsu, F., Chen, H., Balla, T., Ayala, G., Toomre, D., and De Camilli, P.V. (2007). Loss of endocytic clathrin-coated pits upon acute depletion of phosphatidylinositol 4,5-bisphosphate. Proc. Natl. Acad. Sci. U S A *104*, 3793-3798.